Titanocene-Catalyzed Hydrosilylation of Cyclic Ethers to Stereochemically Enriched *Anti-Markovnikov* Alcohols and Fatty Alcohols

Dissertation

zur

Erlangung des Doktorgrades (Dr. rer. nat.)

der

Mathematisch-Naturwissenschaftlichen Fakultät

der

Rheinischen Friedrich-Wilhelms-Universität Bonn

vorgelegt von

Harie Goli

aus Düren

Bonn, 2026

Angefertigt mit Genehmigung der Mathematisch-Naturwissenschaftlichen Fakultät

der Rheinischen Friedrich-Wilhelms-Universität Bonn

Gutachter/Betreuer: Prof. Dr. Andreas Gansäuer

Gutachter: Prof. Dr. Sigurd Höger

Tag der Promotion: 20.05.2026

Jahr der Veröffentlichung: 2026

Die vorliegende Arbeit wurde in der Zeit von Dezember 2022 bis März 2026 am Kekulé-Institut für Organische Chemie und Biochemie der Rheinischen Friedrich-Wilhelms-Universität Bonn unter der Leitung von Prof. Dr. Andreas Gansäuer angefertigt.

Teile dieser Arbeit wurden bereits veröffentlicht:

Converging Stereodivergent Reactions: Highly Stereoselective Formal *anti-Markovnikov* Addition of H_2O to Mixtures of Olefins

S. Höthker, R. Mika, H. Goli, A. Gansäuer, *Chem. Eur. J.* **2023**, *29*, e202301031, DOI: 10.1002/chem.202301031.

Attenuating Nucleophilicity of Titanocene Hydrides Beyond Steric Effects en Route to Fatty Alcohols

S. Höthker, H. Goli, S. Klare, T. Krebs, J. H. Schacht, *Chem. Eur. J.* **2024**, e202402694, DOI: 10.1002/chem.202402694.

Titanocene-Catalyzed Hydrosilylation of Oxetanes─are Oxetanes the Better Epoxides?

H. Goli, U. Kilic, S. Grimme, Z.-W. Qu, A. Gansäuer, *ACS Catal.* **2026**, *16*, 2628–2635, DOI: 10.1021/acscatal.5c08083.

Table of Contents

1. Introduction

1.1 Development of Sustainable Chemistry

1.1.1 Chemistry – A Double-Edged Sword

Chemistry has been an integral part of daily life for thousands of years. Humans have performed chemical reactions long before the fundamental principles of chemistry were understood. These processes involved using fire to cook food, to create pottery, to produce pigments, and to extract metals from ores (metallurgy), significantly improving the quality of life.[1–5] Over the years, curiosity about the limits of chemistry grew, as evidenced by alchemists who attempted to transmute lead into gold. Although their experiments did not achieve the intended results, they contributed to the development of modern laboratory practice.[6] Around the 18th century, the combination of laboratory techniques, prior discoveries, and rational thinking led to the development of modern chemistry.[6,7]

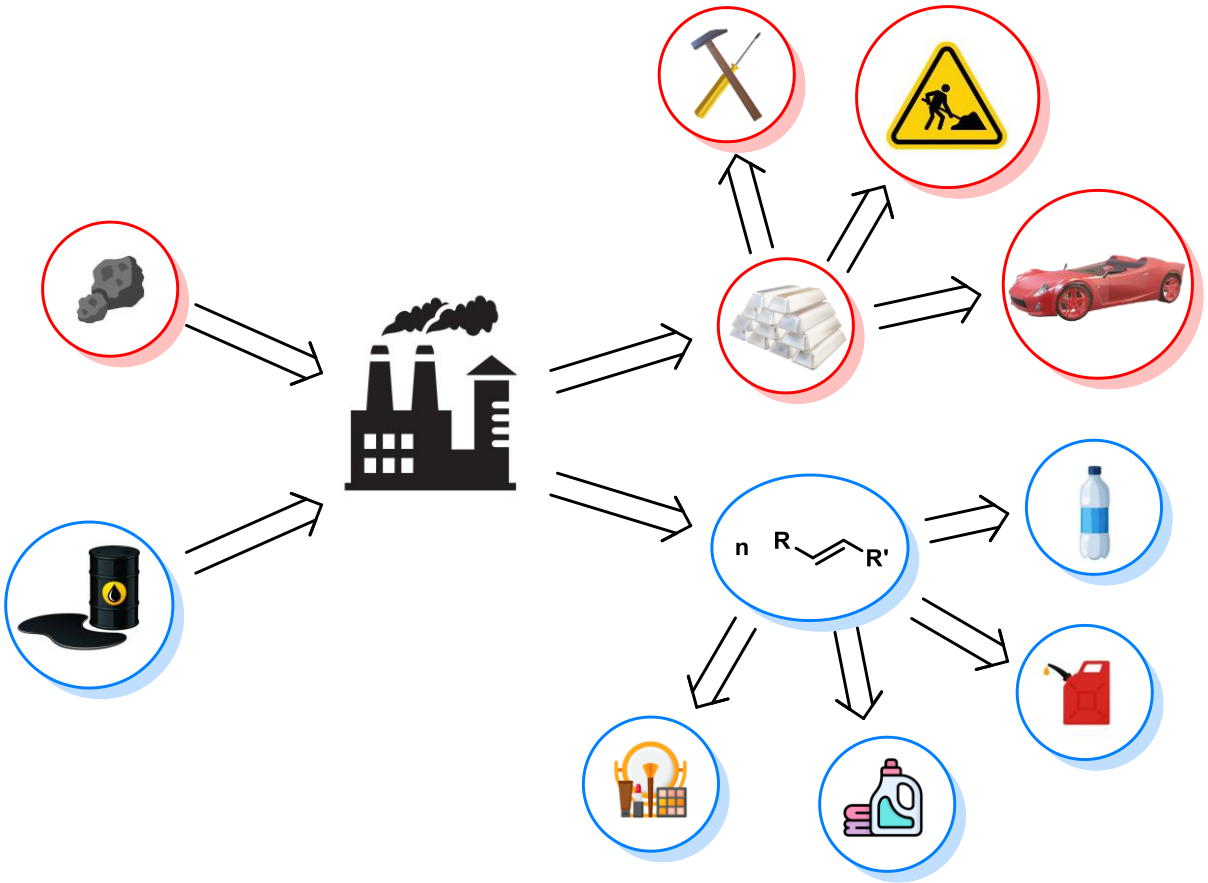

Figure 1: Examples of industrial processes involving chemical transformations to produce numerous essential materials from fossil feedstock.

With the beginning of industrialization, chemical processes could be implemented on an unprecedented large scale. Established chemical transformations, such as the extraction of metals from ores, were intensified. A prime example is the extraction of pig iron from iron ore

in a blast furnace, which can yield up to 10.000 tons per day.[8] The crude iron is subsequently converted into steel, an iron/carbon alloy.[8] This can be used to produce numerous tools,[9] in construction,[10] for automobiles,[11] and for other industrial applications (Figure 1).

Modern chemistry, combined with industrialization, led to the introduction of novel processes that were carried out on a large scale. One notable example is steam cracking, in which petroleum, a mixture of hydrocarbons, is broken down into smaller, often unsaturated, hydrocarbons.[12] These olefins can be further transformed into important plastics,[12] fuel,[12] and fatty alcohols[13] (Figure 1). The latter are precursors of surfactants used in detergents and cosmetic products.[13,14]

While these industrial processes profoundly improved the quality of life, their environmental impact can be devastating. Greenhouse gases and waste generated from chemical manufacturing processes, along with the release of hazardous substances that contaminate soil and water, are significant contributors to climate change.[15,16]

In summary, chemistry can be described as a double-edged sword, as it has both favorable and unfavorable consequences.

1.1.2 The 12 Principles of Green Chemistry

Industrialization, a result of significant progress in science and technology, has boosted the economy, but at the expense of the environment and human health. The damage it has caused over time, as evidenced by the increasing number of man-made environmental hazards such as the formation of ozone holes, led to increased awareness of environmental conservation. In this context, *Anastas* and *Warner* introduced the concept of “green chemistry” along with 12 guiding principles (Figure 2). These guiding principles were invented to counteract environmental degradation.[17,18]

“Prevent waste” refers to minimizing waste generation in order to reduce subsequent disposal, benefiting humans and the environment. “Atom economy” describes the ratio of the incorporation of starting materials into the product. A higher value is favorable, as it results in less waste.[17,18]

“Less hazardous chemical synthesis”, “design safer chemicals”, and “safer solvents and auxiliaries” focus on the toxicity of chemicals used or produced in a process. The ideal reaction should involve non-toxic reactants and solvents that yield benign products. Especially the design of safer chemicals with reduced toxicity while maintaining effectiveness represents a considerable challenge.[17,18]

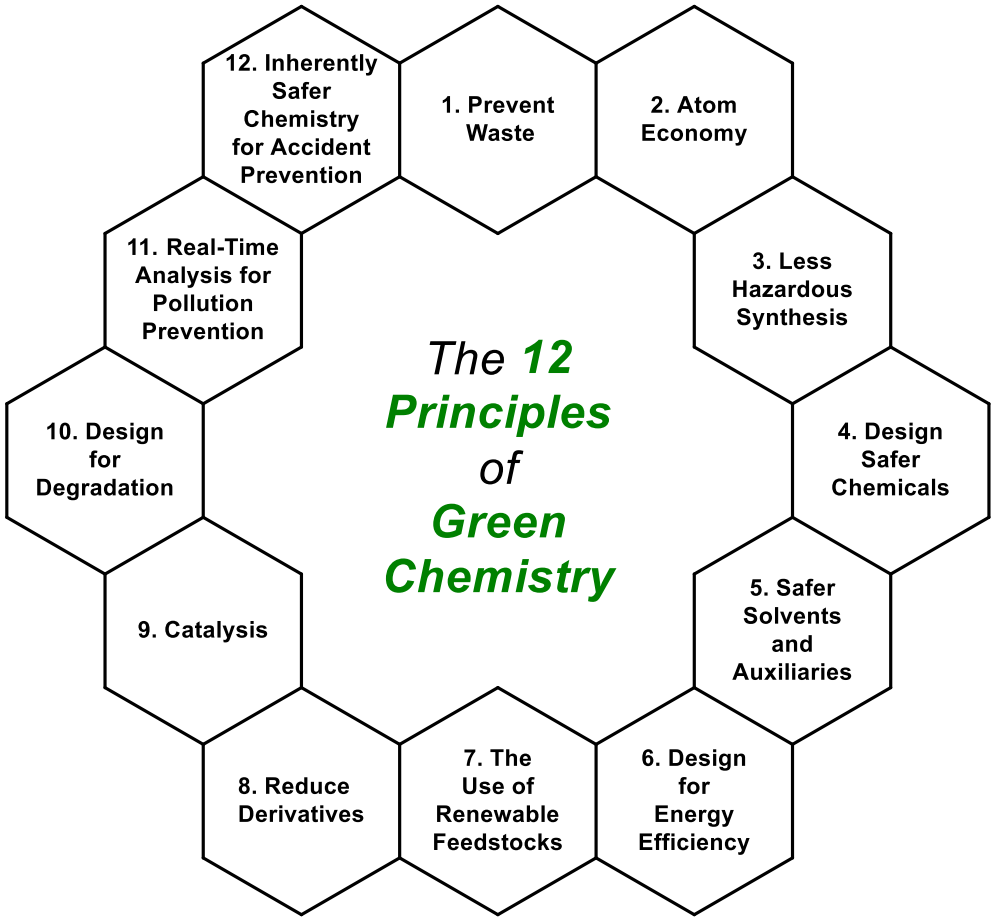

Figure 2: The 12 principles of green chemistry.[17,18]

The best conditions, according to “design for energy efficiency”, are ambient temperature and pressure. Considering the constantly rising costs and the limited supply of fossil fuels,[19] it is also favorable from an economic point of view. Alternatively, “the use of renewable feedstocks” such as solar-, wind-, or hydropower, can be used as an energy source because they are naturally replenished and have much lower environmental impact.[17,18] Importantly, according to this principle, the use of renewable feedstocks is not limited to green energy.[17,18] It also includes the use of chemicals obtained from renewable sources. A prime example is 2-MeTHF, which represents a sustainable alternative to THF, as it can be synthesized from the renewable source levulinic acid.[20]

“Reduce derivatives” suggests synthesizing molecules without unnecessary steps, such as the use of protecting groups or other temporary modifications. “Design for degradation” states that chemicals should break down into environmentally benign compounds after fulfilling their intended purpose, leaving no toxic residues in the environment.[17,18]

“Real-time analysis for pollution prevention” refers to the continuous monitoring of chemical reactions during the process to detect unwanted pollutants immediately and prevent their formation. Without such monitoring, pollutants may only be identified after production, leading

to waste, additional purification steps, and environmental harm. The “inherently safer chemistry for accident prevention” advises substituting chemicals that pose a potential risk with safer ones.[17,18]

“Catalysis” denotes a process that employs recyclable catalytic rather than stoichiometric amounts of reagents. In the following Chapter, this principle will be discussed in more detail owing to its significance in the context of green chemistry.[17,18]

1.2 Definition and Application of Catalysis

1.2.1 Definition and Types of Catalysis

Catalysis represents one of the central pillars of the 12 principles of green chemistry, offering both economic and environmental benefits. In general, catalysis refers to the acceleration of a reaction by the interaction of a substrate with a catalyst *via* an alternative pathway with a lower activation barrier (Figure 3). Catalysts are reactants that are not consumed but regenerated after the product is formed.[21]

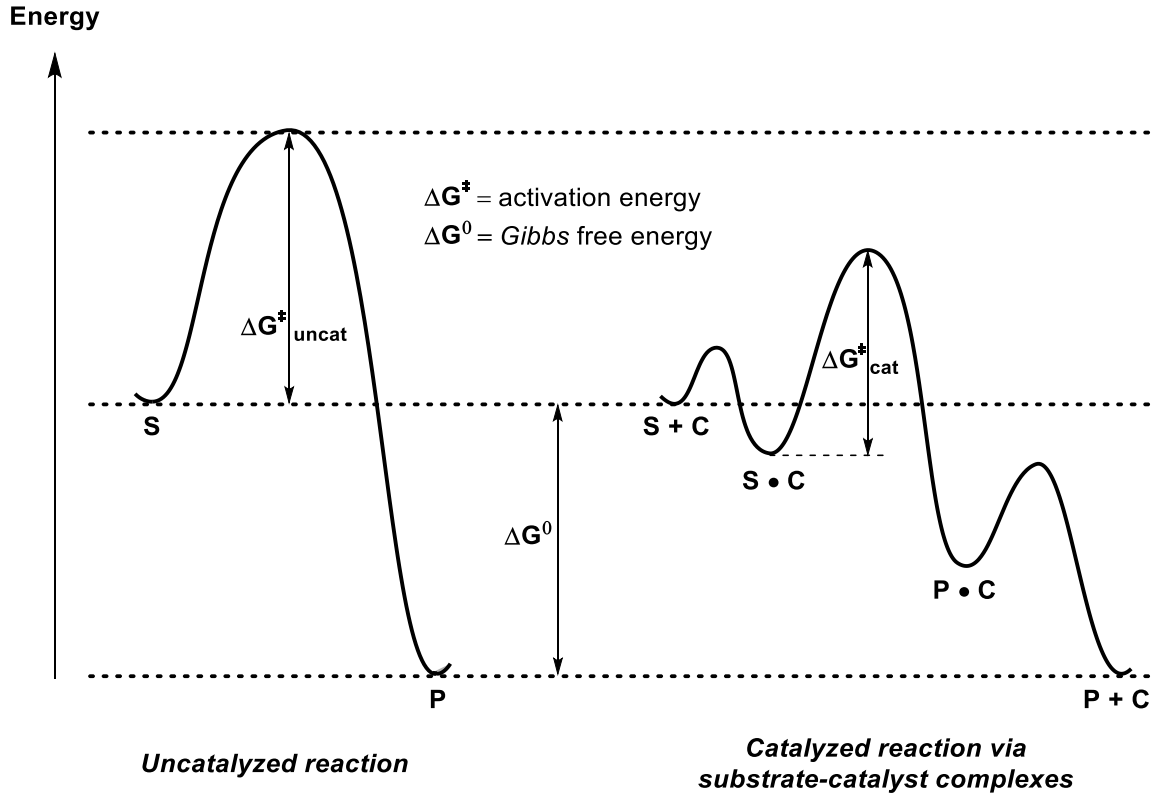

Figure 3: Schematic energy diagram for uncatalyzed vs. catalyzed reactions.[22]

Catalysis is commonly classified into two main types: heterogeneous and homogeneous catalysis. Heterogeneous catalysis occurs on the surface of an insoluble catalyst. The different phases make it easier to purify and recover the catalyst, but the process typically requires higher temperatures and exhibits lower selectivity. In contrast, homogeneous catalysis occurs in solution, making catalyst recovery and purification more challenging. However, the process typically ensues at lower temperatures and offers higher selectivity.[23,24]

1.2.2 Application of Heterogeneous Catalysis

The easier recovery and purification of heterogeneous catalysts make these processes particularly attractive for industrial applications, as the repetitive purchase of expensive

catalysts is avoided. Moreover, the waste production is minimized, leading to an increase in sustainability.[23] Generally, catalysis plays a crucial role in sustainable chemistry, as it is commonly associated with further principles of green chemistry.[25–27] One remarkable example is the synthesis of Ibuprofen®, a frequently used anti-inflammatory compound.[28]

The classical synthesis of Ibuprofen® was developed by *Boots* in 1961 (Scheme 1). This strategy is disadvantageous in terms of green chemistry for multiple reasons. First, it involves stoichiometric amounts of toxic aluminum chloride. Second, it requires six steps to produce the compound. Consequently, several unwanted by-products are generated, increasing the waste and lowering the atom economy. Furthermore, the number of steps affects the energy efficiency, as more energy-demanding steps are employed. Finally, it requires hydroxylamine, an acid (e.g., hydrochloric acid), and sodium ethoxide, all of which are associated with hazardous properties.[28,29]

***Boots* process**

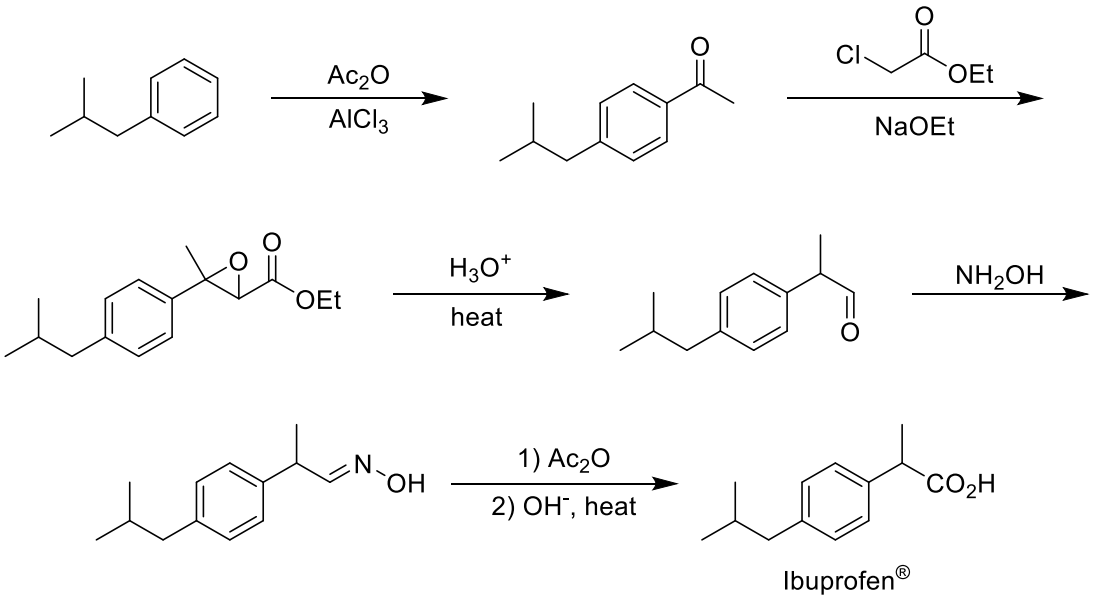

***Boots-Hoechst-Celanese* (BHC) process**

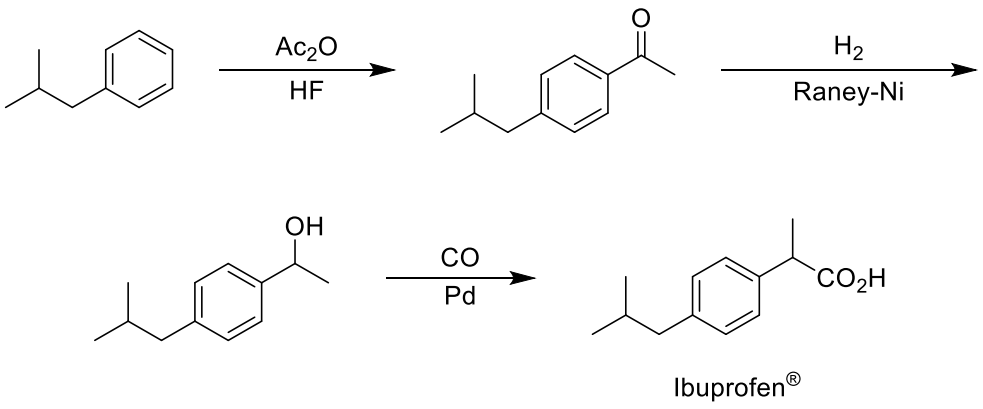

Scheme 1: *Boots* vs. *Boots-Hoechst-Celanese* synthetic route to Ibuprofen®.[28,29]

In 1992, a greener route towards Ibuprofen® was introduced by the *Boots-Hoechst-Celanese* company (Scheme 1). It uses recyclable hydrogen fluoride instead of the toxic aluminum chloride as a catalyst, which additionally serves as the solvent of the reaction. The second and third steps involve heterogeneous catalysts recovered after fulfilling their purpose. Both the hydrogenation and the CO insertion proceed with complete atom economy. The only by-product produced in this process is acetic acid. Owing to its high sustainability, this process won the *Presidential Green Chemistry Challenge Award* in 1997.[28,29]

Another prime example demonstrating the dramatic effect of heterogeneous catalysis on industrial processes is the *Haber-Bosch*-process. This discovery revolutionized global agriculture by providing an efficient route to fertilizers. The *Haber-Bosch* process describes the synthesis of ammonia from nitrogen and hydrogen, typically using magnetite (Fe_3O_4) as the catalyst (Figure 4).[30]

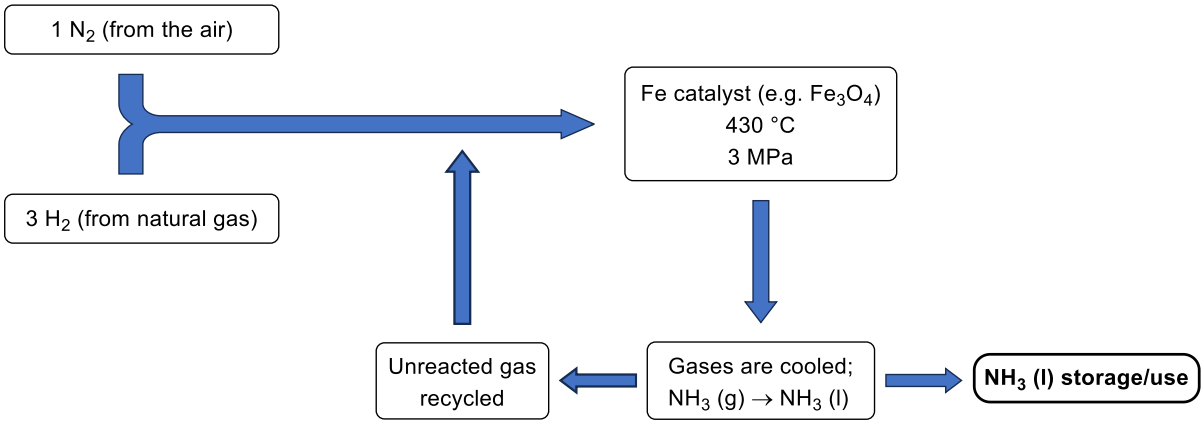

Figure 4: Simplified flow scheme of the *Haber-Bosch* process.[30,31]

Earlier nitrogen fixation reactions, such as the *Frank-Caro* and *Birkeland-Eyde* processes, required large amounts of energy (~1000 °C and ≥3000 °C, respectively) for the activation of molecular nitrogen without a catalyst.[32,33] The use of a heterogeneous catalyst, along with additives, enables the dissociation of N_2 at significantly lower temperatures (430 °C) under high pressure. For this invention, *Haber* and *Bosch* each won the *Nobel* Prize in 1918 and 1931, respectively.[30]

1.2.3 Application of Homogeneous Catalysis

While heterogeneous catalysis is attractive in large-scale processes due to the facile recovery of the catalyst, homogeneous catalysis is crucial for the synthesis of complex molecules such as drugs because it offers superior selectivity.[23,34] Enantioselectivity, or more precisely, chirality, is of significant importance in drug design and development. The purpose of drugs is to target key enzymes, protein-protein interactions, receptor-ligand interactions, or protein-

nucleic acid interactions to weaken the course of the disease. Because the targeted proteins are chiral, the drug's stereochemical information should match to achieve optimal binding affinity. The other enantiomer can exhibit entirely different or no biological activity. Therefore, the exclusive synthesis of the key enantiomer is important.[35] Examples of common drugs that can be prepared *via* homogeneous catalysis are L-DOPA,[36] a medication for treating *Parkinson* disease, and morphine,[37] an analgesic. The catalysts used in such processes commonly contain transition metal centers.[38]

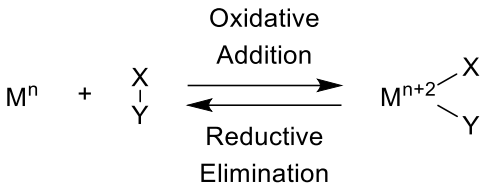

Scheme 2: General process for oxidative addition and reductive elimination *via* a two-electron path.[39]

A wide range of transition-metal-complex-mediated reactions, such as catalytic hydrogenation or coupling reactions, typically proceed *via* oxidative addition and reductive elimination as the fundamental steps (Scheme 2).[40] Two common transition-metal-complex-catalyzed hydrogenations are the asymmetric hydrogenation of olefins according to *Wilkinson*, using a chiral Rh catalyst, and the enantioselective reduction of imines according to *Noyori*, using an enantiopure Ru catalyst.[37,41] The first method was employed in the synthesis of L-DOPA,[36] while the second was applied in a synthetic route to morphine (Scheme 3).[37] Both methods proceed with high enantioselectivity, and *Wilkinson*'s hydrogenation also exhibits complete atom economy. Moreover, the enantioselective hydrogenation by *Noyori* is not limited to imines but can also be applied to olefins,[42] ketones,[43] and *β*-ketoesters.[44]

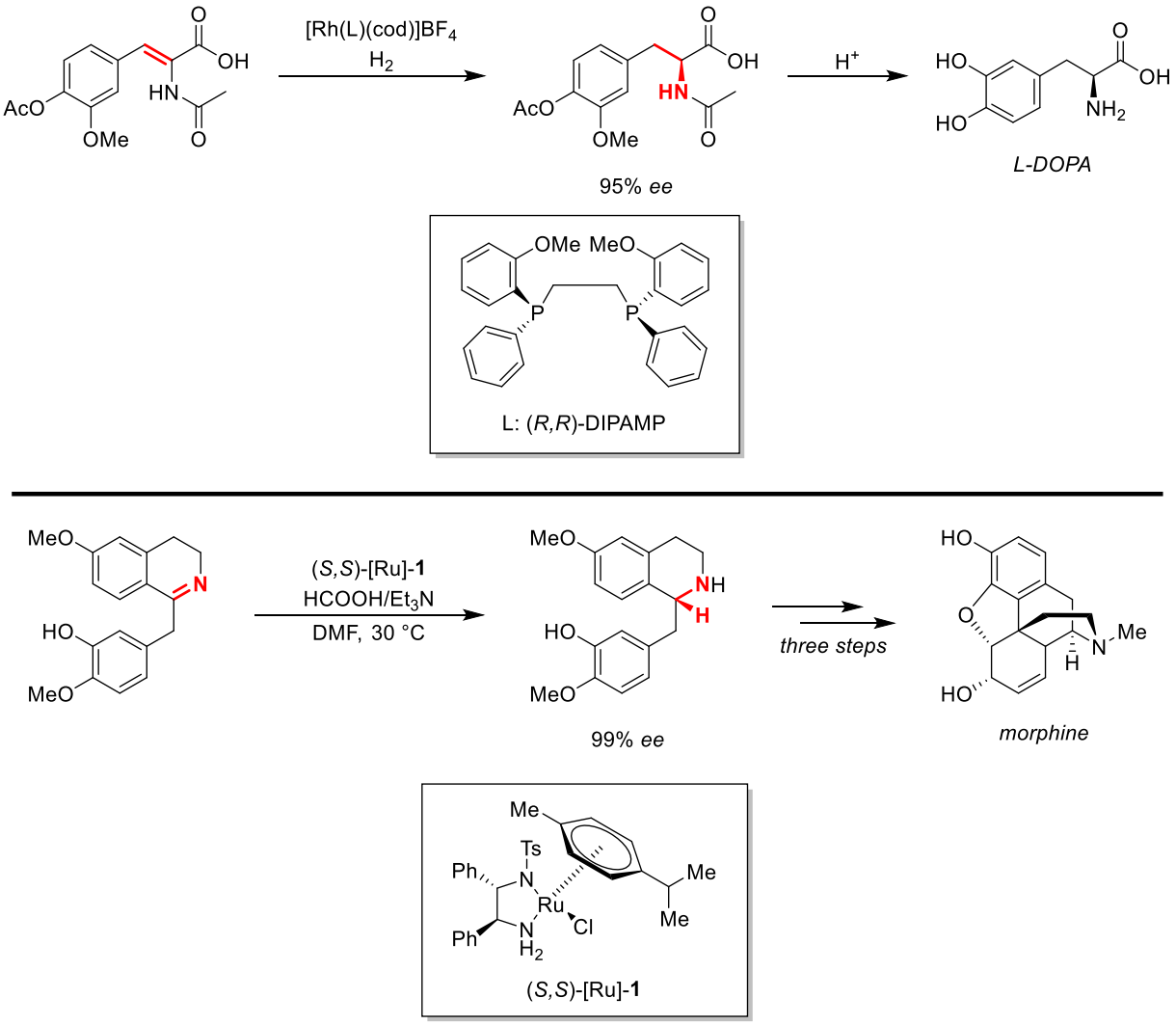

Scheme 3: Asymmetric hydrogenation of an olefin using a Rh-catalyst according to *Wilkinson*, employed in the synthesis of L-DOPA; enantioselective hydrogenation of an imine according to *Noyori*, employed in a synthetic route to morphine.[36,37,45]

Beyond the high selectivity of such processes, homogeneous catalysis allows for altered (Scheme 4, top)[46] or enhanced (Scheme 4, bottom)[47] reactivities through ligand modification. The upper reaction describes the diastereoselective formation of pyrrolidines from acyclic amines *via* Rh-catalyzed intramolecular insertion of nitrogen into a sp^3 C–H bond. The Rh-catalyst bearing *R*-PTAD ligands favors the formation of the *cis*-product, whereas the Rh-catalyst bearing acetoxy (OAc) ligands strongly favors the *trans*-product.[46] In the Ru-catalyzed ring-closing metathesis reaction of an acrylate shown below, [Ru]-**3** affords a significantly higher yield of the corresponding lactone than [Ru]-**2**.[47]

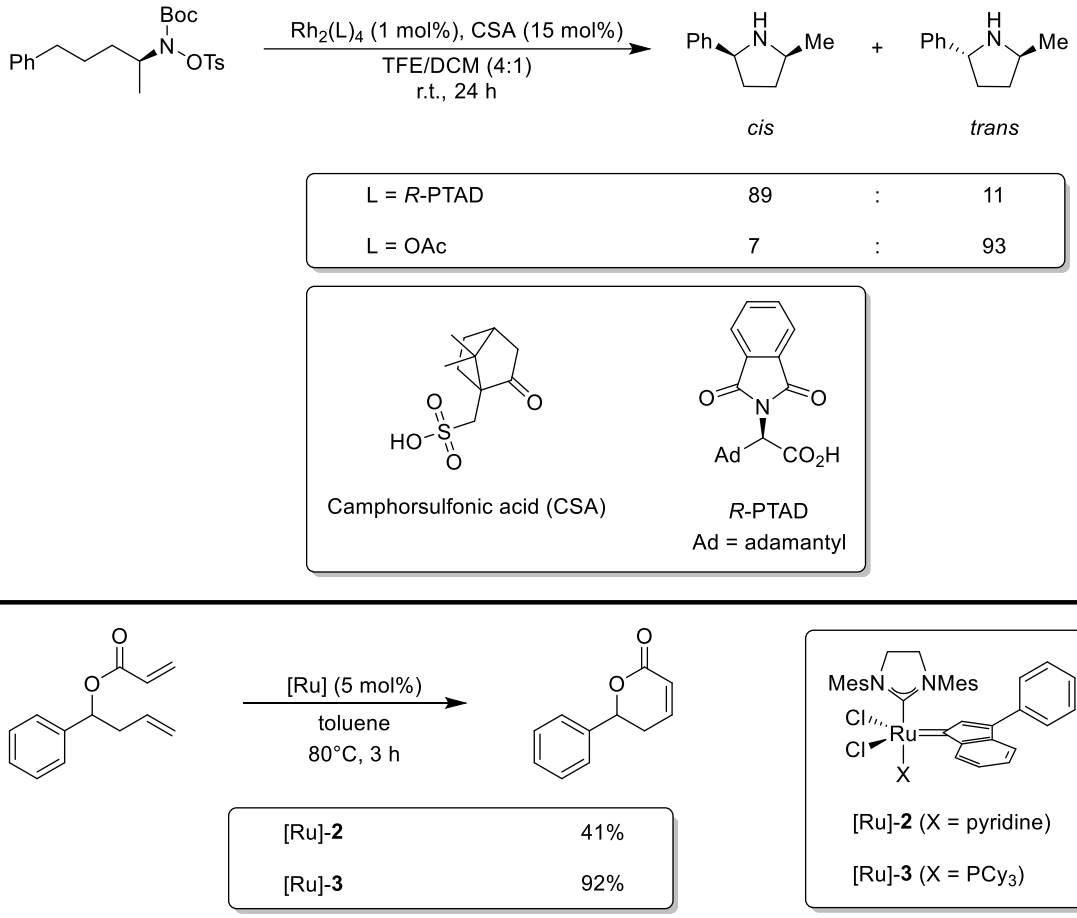

Scheme 4: Rh-catalyzed intramolecular insertion of nitrogen into a sp^3 C–H bond resulting in the diastereoselective formation of pyrrolidines from amines, inversion of diastereoselectivity by modification of the ligand sphere (top);[46] Ru-catalyzed ring closing metathesis reaction of an acrylate towards a lactone, enhancing reactivity by exchange of the pyridine ligand with PCy_3 (bottom).[47]

1.2.4 Noble Metals vs. Abundant Metals

Noble metals, or complexes based on these metals, are frequently employed in transition-metal-catalyzed reactions, such as hydrogenation,[48] coupling,[49] and oxidation[50] reactions. Their widespread use can be attributed to their generally high catalytic activity,[48,50,51] and poisoning resistance.[50] However, the limited abundance of noble metals makes them significantly more expensive than abundant transition metals (Figure 5). Furthermore, noble metal complexes based on Pd or Pt are often more toxic and thus require rigorous removal from the final drug. Therefore, it is of great interest to industry and research to gradually replace precious metals with abundant transition metals in catalytic processes while maintaining efficiency.[52]

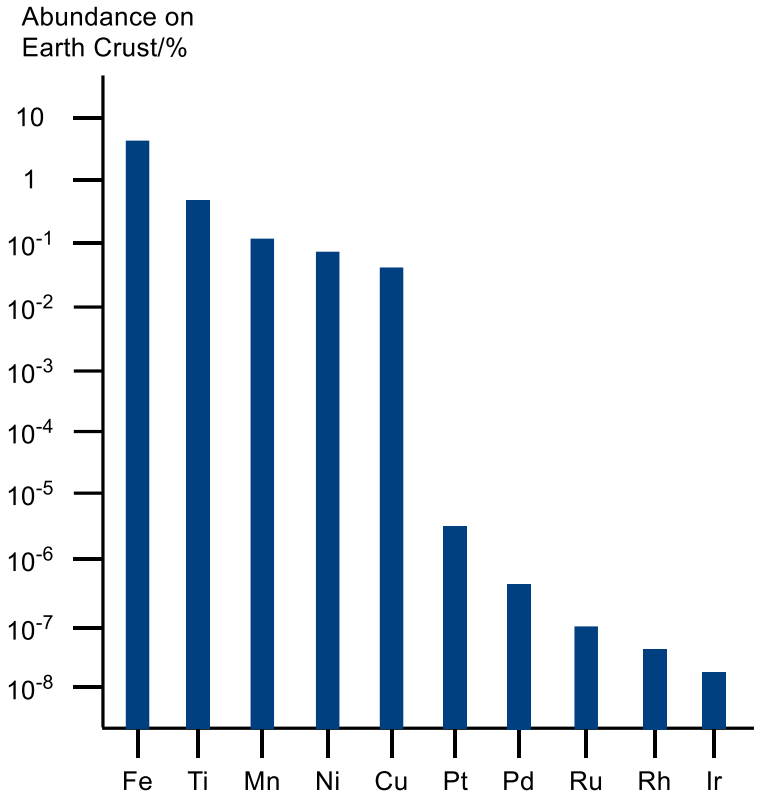

Figure 5: Abundance of selected transition metals in Earth's crust.[53]

The use of iron, the most abundant transition metal,[53] and its complexes were already briefly described (Figures 1 and 4). Therefore, the focus will now be laid on titanium, the second-most abundant transition metal, in the following Chapter.[53]

1.3 The Use of Titanium in Chemistry

The density of titanium and its alloys is approximately 60% lower than that of steel, while they offer high strength and superior corrosion resistance. Furthermore, they operate effectively at high temperatures up to nearly 600 °C. These properties make their use in aeronautics particularly attractive. Considering their additional biocompatibility and non-toxicity, they are also suitable for implants and prosthetics.[54] Aside from the raw metal and its alloys, certain titanium-based compounds, such as the well-known titanium(IV) oxide, are non-toxic as well. Titanium(IV) oxide is widely used as a pigment in paint, food additives, and cosmetics due to its non-toxicity and characteristic white color.[55] Furthermore, it is used as a UV-filter in sunscreen.[56]

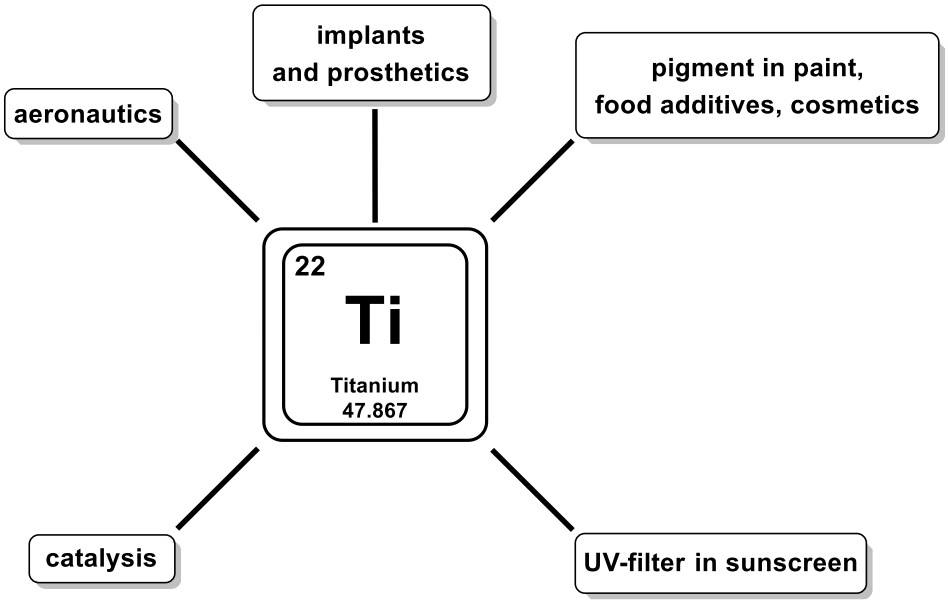

Figure 6: Application of titanium and its alloys and complexes.[54–58]

Titanium-based complexes feature rich redox activity and commonly adopt the oxidation states +III and +IV. As a result, titanium complexes commonly undergo single-electron steps, whereas many other transition metal complexes, such as those of palladium[59] or rhodium,[60] typically undergo two-electron steps.[61] One notable example is the *Ziegler* catalysis (Scheme 5), wherein ethylene is polymerized to polyethylene by using titanium(IV) chloride, and a co-catalyst (e.g., $AlEt_2Cl$).[62,63]

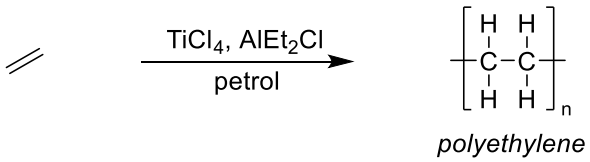

polyethylene

Scheme 5: Polymerization of ethylene.[63]

While this mechanism is not yet fully understood, it is hypothesized that titanium(III) chloride may serve as the active species.[63] This process was a groundbreaking discovery in polymer chemistry,[64] as it is used in the synthesis of several essential plastics, such as polyethylene, which are used for packaging.[65]

In addition to their ability to readily undergo single-electron oxidations or reductions, the strong *Lewis* acidity and high oxophilicity of titanium complexes result in pronounced reactivity toward oxygen-containing functional groups. Consequently, titanium complexes are widely used in radical processes entailing oxygen-containing functional groups.[61]

Radical processes often involve free radicals as the active species. Free radicals are paramagnetic species with at least one unpaired electron, often rendering them highly reactive and unstable.[66] The selectivity of free radical processes cannot be controlled by reagents once the active species has formed. However, processes involving transition-metal-complex-bound radicals enable control over chemo- and stereoselectivity by tuning the ligand environment of the metal reagent or catalyst.[67,68] A prime example showcasing a reagent-controlled, diastereoselective radical reaction is the titanocene-catalyzed pinacol coupling by *Gansäuer et al*.[69] Here, the control arises from the close proximity of the metal complex to the radical, which is generated *via* single-electron transfer (SET).[67,68]

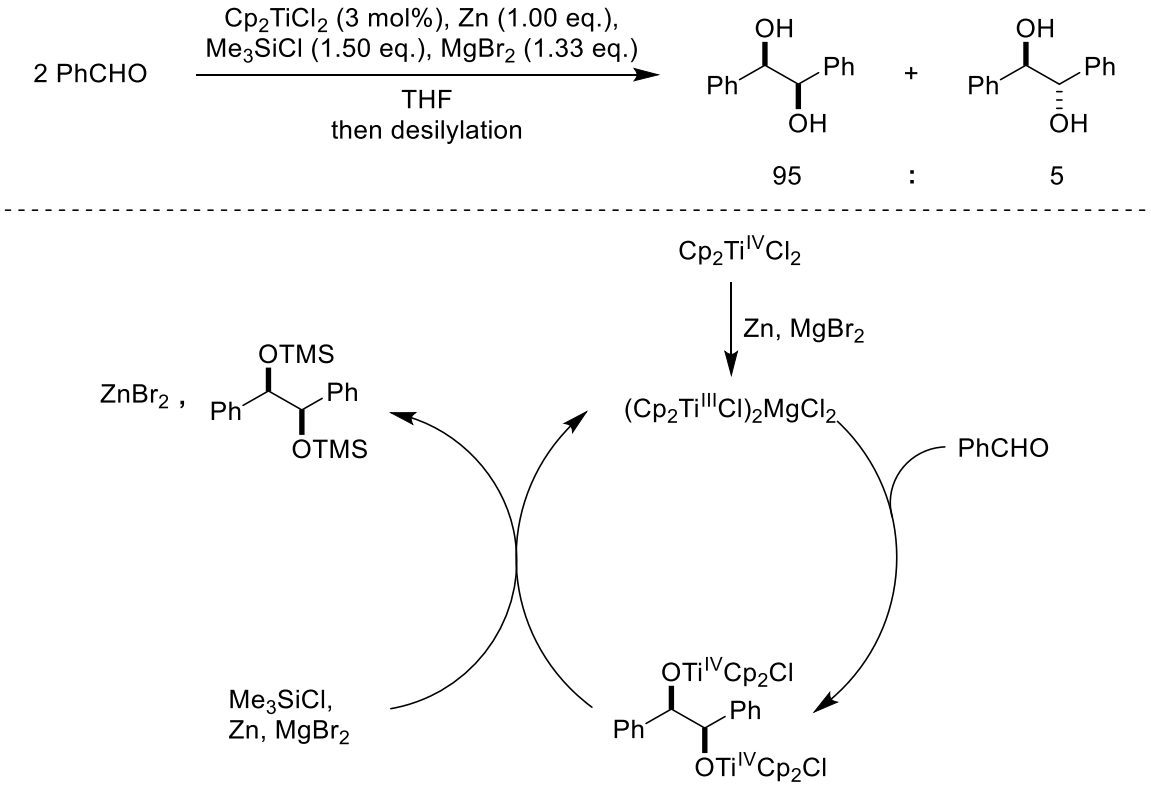

Scheme 6: Proposed mechanism of the titanocene-catalyzed pinacol coupling of benzaldehyde.[69]

Gansäuer et al. proposed a mechanism for the diastereoselective titanocene-catalyzed pinacol coupling shown in Scheme 6. The catalytic cycle is initiated by the generation of the active trinuclear Ti(III)-species by reduction of titanocene dichloride with Zn in the presence of $MgBr_2$. Single electron transfer (SET) from the active species reduces benzaldehyde to the corresponding ketyl radical. *Gansäuer* suggested that the observed diastereoselectivity arises from the binding of two ketyl radicals by the trinuclear titanium-magnesium species (Scheme 7).[69]

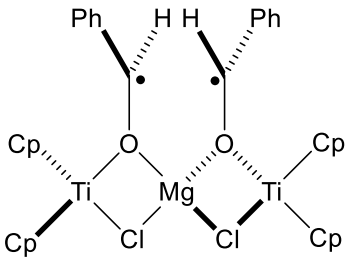

Scheme 7: Possible selectivity-determining intermediate in titanocene-catalyzed pinacol coupling.[69]

The arrangement with minimal steric interaction between the phenyl groups of the two bound ketyl radicals dictates the diastereoselectivity, leading to the formation of a titanium alkoxide. The titanium alkoxide is subsequently cleaved by TMSCl to form the silyl ether and regenerate the active species. Base-promoted deprotection of the silyl ether yields the desired diol with a *d.r.* of 95:5. The trinuclear Ti(III)-species thus controls the diastereoselectivity of the pinacol formation.[69]

Gansäuer et al. continued their studies on reagent-controlled radical reactions, given that the concept was not yet well established in radical chemistry. They switched from carbonyl compounds as radical precursors to epoxides, owing to their reactivity, which renders them attractive for reductive opening *via* SET.[70]

1.4 Definition, Synthesis, and Application of Epoxides

1.4.1 Definition and Synthesis of Epoxides

Epoxides, also known as oxiranes, are three-membered cyclic ethers widely used in organic synthesis due to their high reactivity and versatility as building blocks.[71] Their geometry distorts the bond angles within the ring from the ideal tetrahedral angle of 109.5° to approximately 60° (Figure 7).[72,73] This leads to substantial ring-strain (~27 kcal/mol).[74] The release of this strain upon epoxide opening constitutes a major driving force for their high reactivity.[75]

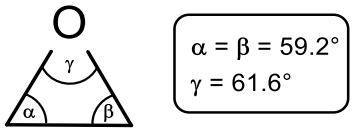

Figure 7: Geometry of ethylene oxide.[72,73]

Oxiranes are readily obtained from olefins, either as a racemic mixture or enantioselectively. Racemic epoxides are widely synthesized *via* the *Prilezhaev* epoxidation using *meta*-chloroperoxybenzoic acid (*m*CPBA) due to its operational simplicity and the reagent's commercial availability.[76,77]

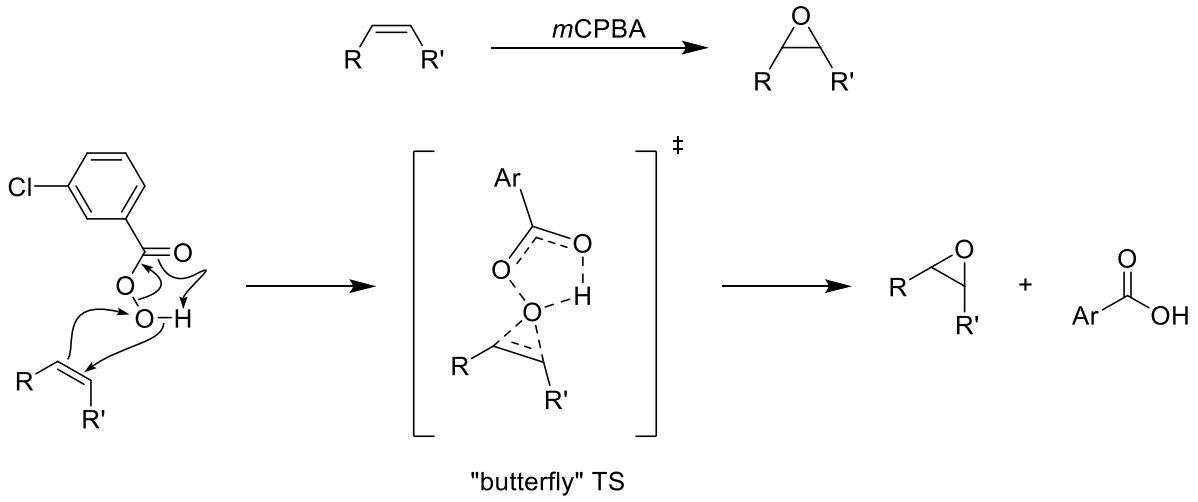

Scheme 8: Mechanism of the *Prilezhaev* epoxidation using *m*CPBA.[76]

The epoxidation proceeds *via* a “butterfly” transition state (TS) in a one-step concerted oxidation, with the olefin acting as the nucleophile and the peracid as the electrophile (Scheme 8).[76]

For their enantioselective preparation, various strategies have been reported. *Sharpless* and *Katsuki* developed the first reliable asymmetric epoxidation method in 1980. They employed titanium(IV) tetraisopropoxide as the catalyst, *tert*-butyl hydroperoxide as the terminal oxidant,

and an enantiomerically pure dialkyl tartrate, such as diethyl tartrate (L-(+)/D-(-)-DET), as a chiral ligand to oxidize allylic alcohols with excellent chemo- and enantioselectivity. The enantioselectivity is directed by the configuration of the chiral ligand. Using L-(+)-DET leads to the oxidation from the bottom face, whereas the use of D-(+)-DET facilitates the addition from the other face (Scheme 9).[78,79] While the method required only catalytic amounts of the Ti-complex and DET for reactive substrates, less reactive olefins necessitated stoichiometric amounts for efficient selective turnover.[78] In 1986, they discovered that the use of 3Å or 4Å molecular sieves substantially improves conversion, reaction time, and enantioselectivity. As a result, only catalytic amounts of the Ti-complex and DET were necessary for every substrate they investigated.[80]

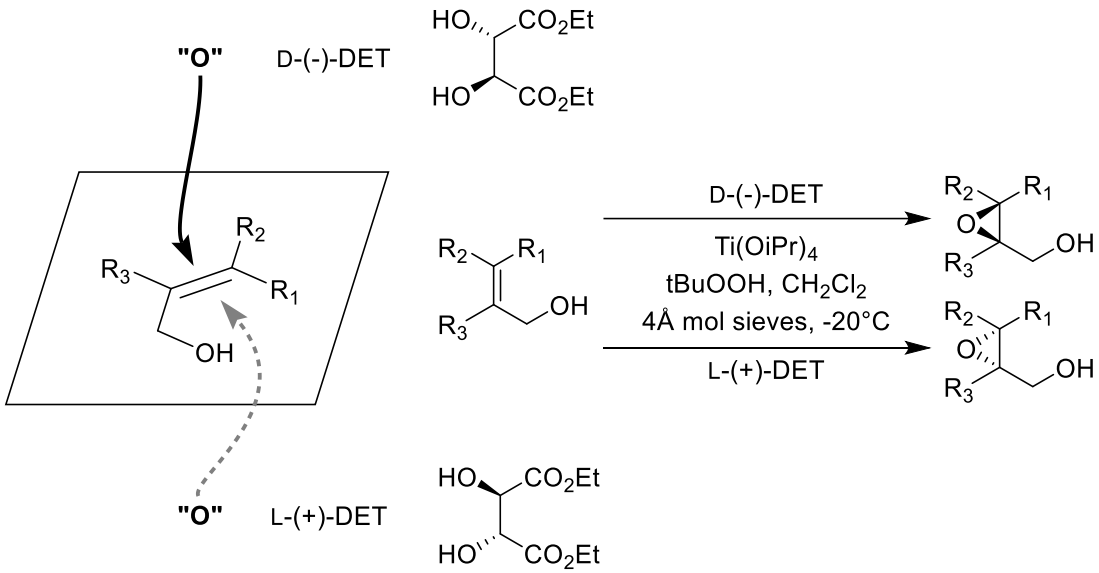

Scheme 9: General scheme for the asymmetric *Sharpless* epoxidation of allylic alcohols.[78,80]

Owing to the commercial availability of the reagents and its operational simplicity, the *Sharpless-Katsuki* epoxidation attracted considerable attention. Nevertheless, its applicability is restricted to allylic alcohols, as the oxidation requires prior coordination of the catalyst to the alcohol group.[78] Generally, the catalytic enantioselective epoxidation of unfunctionalized olefins remained an important challenge in organic chemistry during that time.[81]

Finally, *Jacobsen et al.* developed a method to avoid the use of directing groups in 1990.[81] Inspired by *Kochi et al.*, who employed Mn(III) salen catalysts along with PhIO as the oxidant to synthesize achiral epoxides from olefins,[82] they employed a chiral modification of the catalyst to render this process enantioselective (Scheme 10).[81] Subsequently, *Jacobsen et al.* further modified the catalyst to improve enantioselectivity (Scheme 10) and switched to NaOCl (bleach) as the oxidant due to its commercial availability.[81,83]

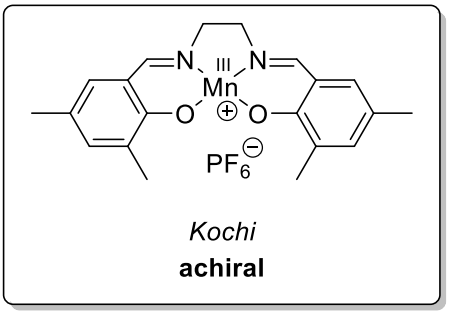

Kochi
achiral

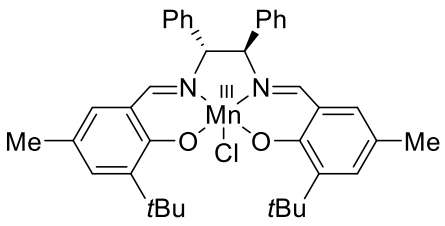

Jacobsen
chiral
1st generation

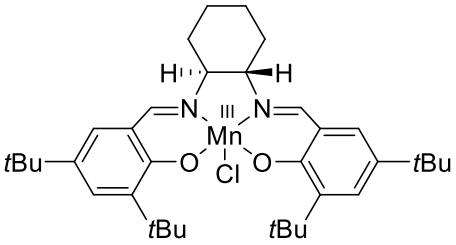

Jacobsen
chiral
2nd generation

Scheme 10: Achiral and chiral modifications of Mn(III) salen complexes by *Kochi* and *Jacobsen*.[82,83]

Furthermore, *Kochi et al.* observed the beneficial effect of an external donor ligand on the epoxidation, as its coordination to the axial site of the metal center improved the reaction rate.[82] Consequently, *Katsuki et al.* investigated its effect on the asymmetric variant of the epoxidation method and noted improved *ee* values.[84]

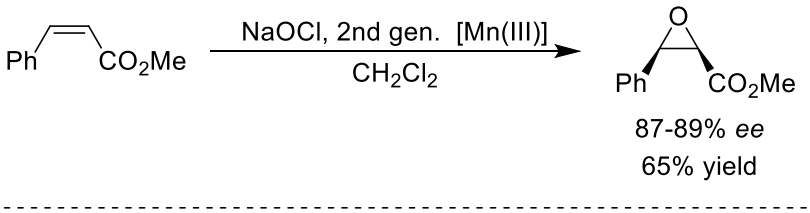

87-89% *ee*
65% yield

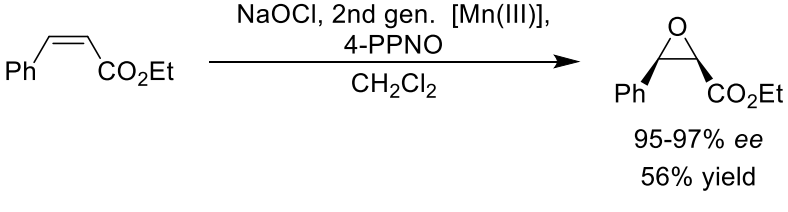

95-97% *ee*
56% yield

Scheme 11: *Jacobsen* epoxidation of structurally similar *cis*-disubstituted alkenes catalyzed by the second gen. Mn-catalyst with (bottom) and without (top) 4-PPNO.[83,85]

Therefore, *Jacobsen et al.* additionally employed donor ligands, such as 4-phenyl-pyridine *N*-oxide (4-PPNO), to further improve enantioselectivity (Scheme 11). Their studies showed that

the donor ligand inhibits catalyst deactivation and suppresses competing unselective *Lewis*-acid-catalyzed addition of the oxidant to the substrate.[85]

It is worth noting that this epoxidation method works best with *cis*-disubstituted alkenes (78–98% *ee*) and worst with *trans*-disubstituted alkenes (20–59% *ee*).[81]

In 1997, *Shi et al.* developed another enantioselective epoxidation method to transform unfunctionalized alkenes. Unlike the *Jacobsen* epoxidation, this method performs better with *trans*-disubstituted and trisubstituted olefins than with *cis*-disubstituted alkenes. The *Shi* epoxidation employs an organic fructose-derived catalyst.[86]

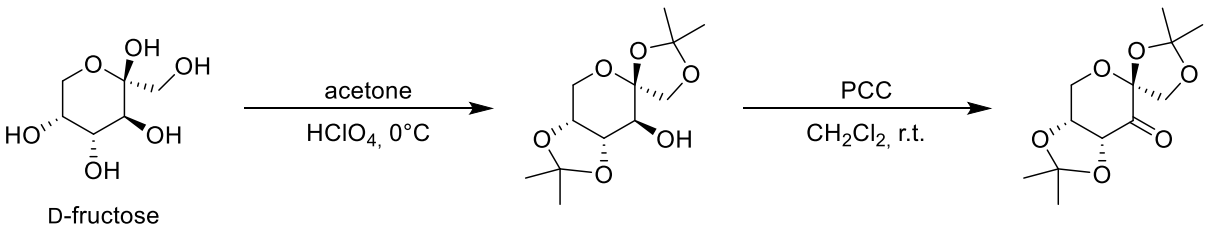

Scheme 12: Synthesis of the *Shi* catalyst from D-Fructose.[86]

The synthesis of the catalyst includes the ketalization and oxidation of the inexpensive D-fructose (Scheme 12).[86]

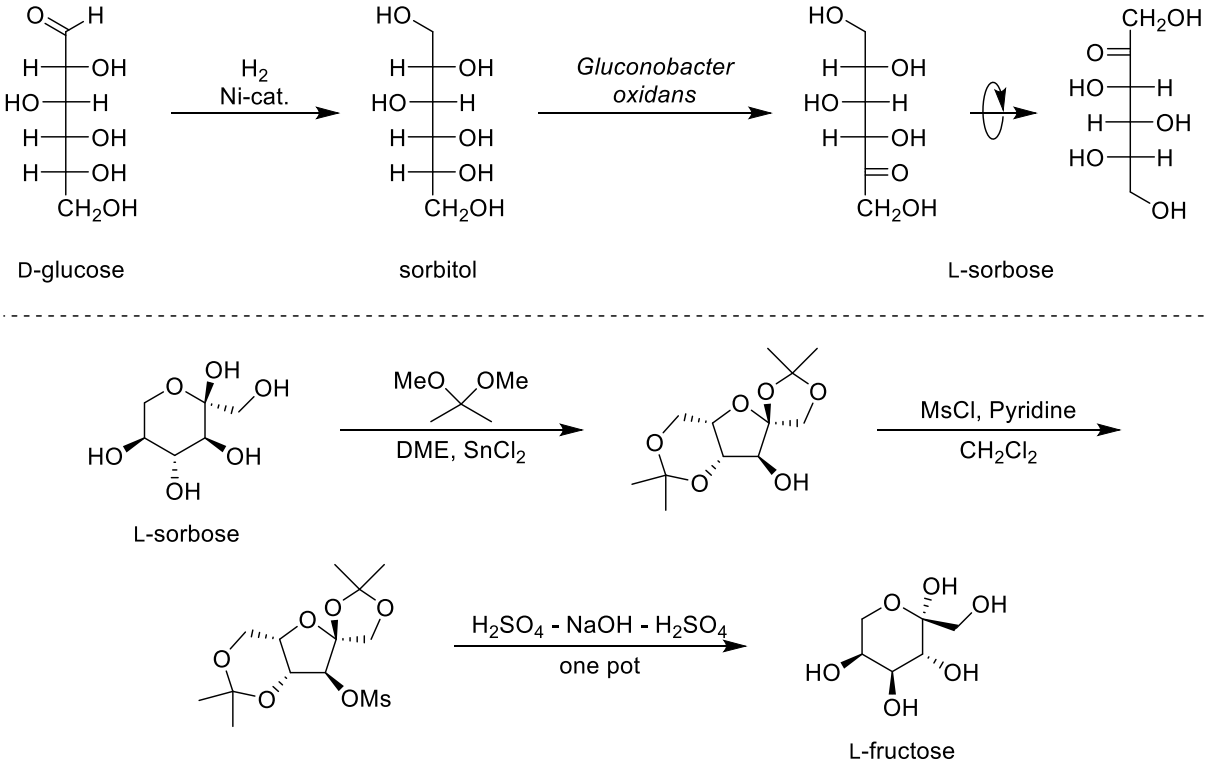

Scheme 13: Synthesis of L-fructose from L-sorbose and extraction of L-sorbose from D-glucose.[86–88]

Analogously, the other enantiomer of the catalyst is accessible from L-fructose, which is synthesized from L-sorbose.[86] Despite being an unnatural sugar, sorbose is commercially available, as it is an intermediate in the industrial synthesis of vitamin C. Sorbose is readily synthesized from D-glucose *via* catalytic hydrogenation followed by enzymatic oxidation (dehydrogenase) of a secondary alcohol by the bacterium *Gluconobacter oxidans*.[87,88] According to the convention of the *Fisher* projection,[89] the most oxidized carbon center points to the top. Hence, the molecule needs to be rotated by 180°. The resulting L-sorbose is then transformed into L-fructose *via* ketalization, mesylation, and a one-pot acid-base treatment (Scheme 13).[86]

Prior to oxidation, the precatalyst is activated by the addition of Oxone® and potassium hydroxide to yield a catalytically active dioxirane. In the following, the mechanism is shown and described for the D-fructose-derived catalyst (Scheme 14).[86]

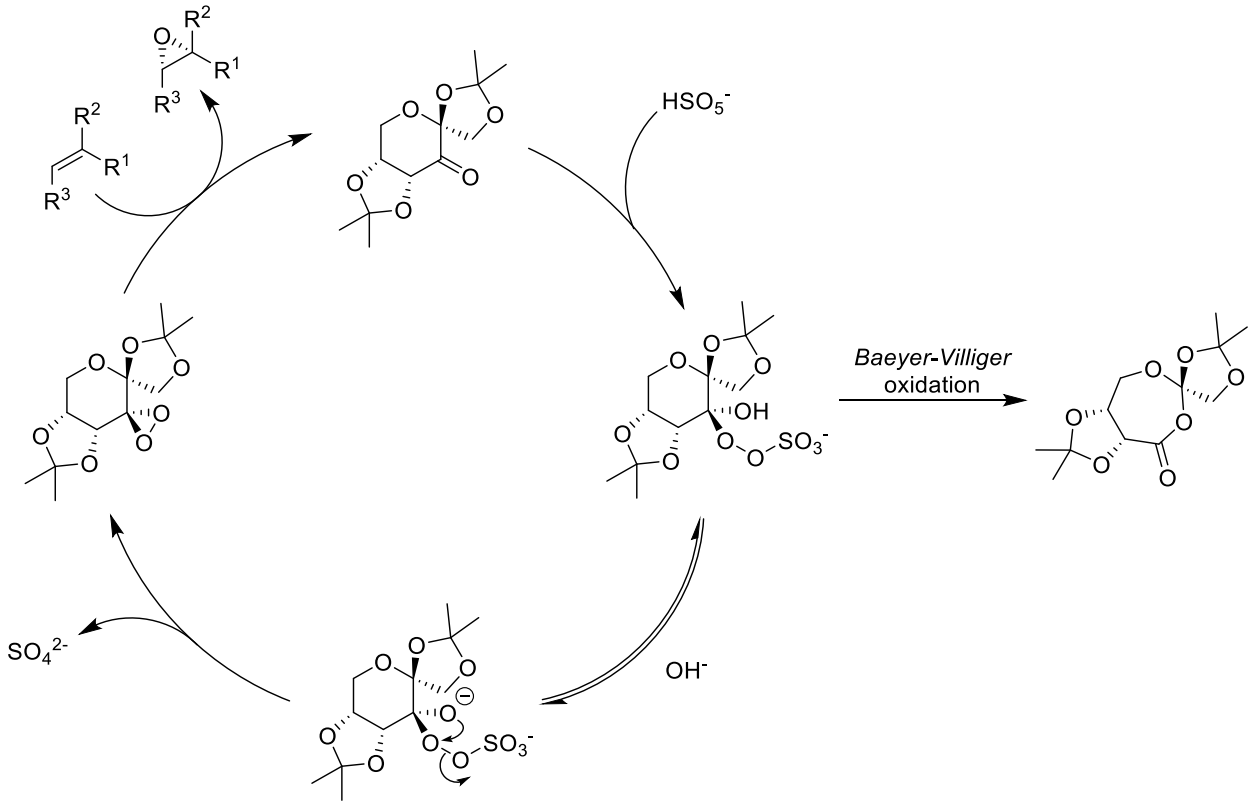

Scheme 14: Postulated mechanism of the *Shi* epoxidation of trisubstituted olefins with the D-fructose-derived catalyst.[86]

Addition of peroxymonosulfate to the ketone group of the catalyst, followed by an intramolecular proton shift to the resulting alkoxide, generates an alcohol. This alcohol undergoes reversible deprotonation by potassium hydroxide to form the corresponding alkoxide. Intramolecular addition of the alkoxide to the adjacent oxygen, accompanied by the displacement of sulfate, yields the active dioxirane. If the reaction is not carried out at a

sufficiently high pH value, the equilibrium of the deprotonation step shifts toward the alcohol. Consequently, the catalyst can decompose *via* an intramolecular *Baeyer-Villiger* oxidation of the alcohol intermediate to give the corresponding deactivated dioxepane (Scheme 14).[86]

Finally, the active dioxirane adds to the olefin, producing the enantiomerically enriched epoxide *via* the favored transition state.[86] A detailed analysis of the possible transition states and the factors governing enantioselectivity will be discussed in Chapter 3.1.

1.4.2 Application of Epoxides in the Synthesis of Alcohols

Epoxides can undergo a wide range of ring-opening reactions (Scheme 15), leading to various functionalized alcohols. Often, epoxide opening proceeds through an S_N2-type nucleophilic substitution, producing *Markovnikov* alcohols. The regioselectivity is kinetically controlled, as the nucleophile approaches the less hindered carbon.[71,90] A further strategy entails the two-electron reduction of epoxides, generating the thermodynamically more stable carbanion, which reacts with an electrophile. This mechanism exhibits the same selectivity as the previous one.[91,92]

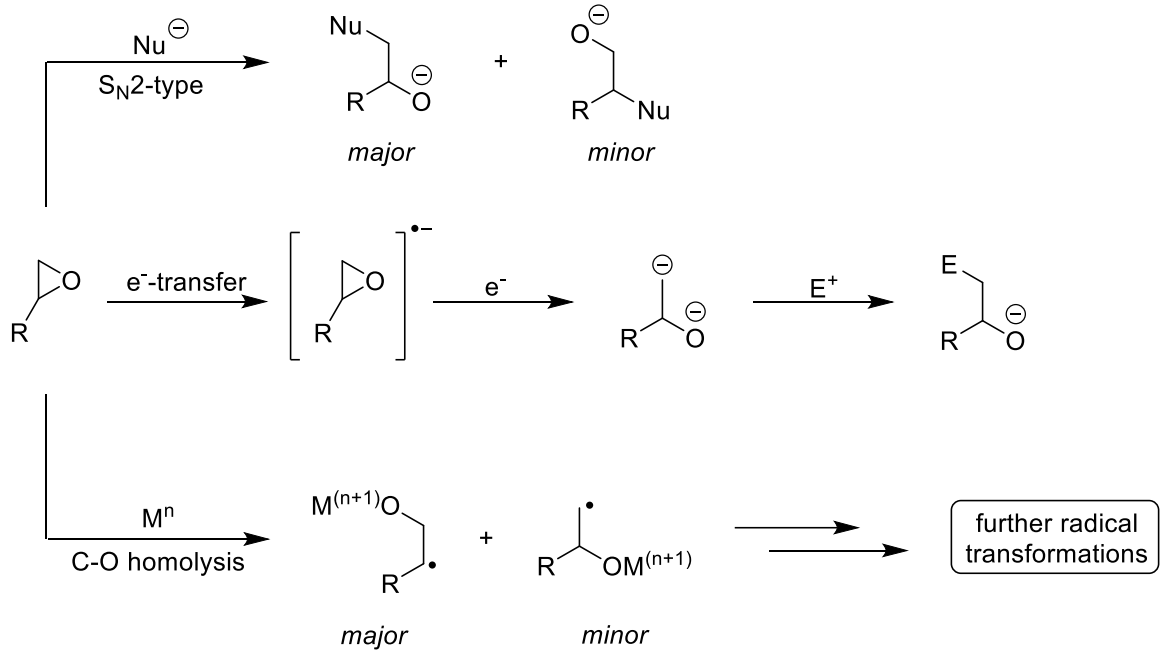

Scheme 15: Three common types of epoxide opening: nucleophilic epoxide opening, two-electron reduction of epoxides, and transition-metal-mediated radical opening of epoxides.[71]

In contrast, the single-electron reduction of epoxides with transition-metal reagents shows the opposite regioselectivity. SET from the transition metal to the epoxide induces homolytic cleavage of the C–O bond, which results in the formation of the thermodynamically more stable radical. The increased stability arises from either hyperconjugation (tertiary > secondary >

primary) or mesomeric stabilization. Subsequently, the intermediate can undergo further radical transformations, including hydrogen atom transfer, to yield the *anti-Markovnikov* alcohol. Given the broad functional group tolerance of radical processes and the mild conditions under which radicals can be generated, the latter constitutes a valuable synthetic tool. Moreover, it affords the alcohol with a regioselectivity opposite to that of classical S_N2-type epoxide opening.[71]

RajanBabu and *Nugent* developed a strategy for accessing *anti-Markovnikov* alcohols based on the single-electron reduction of epoxides with Ti-complexes. They employed commercially available, bench-stable titanocene(IV) dichloride, which was transformed *in situ* into the active Ti(III)-species using Zn (Scheme 16).[71]

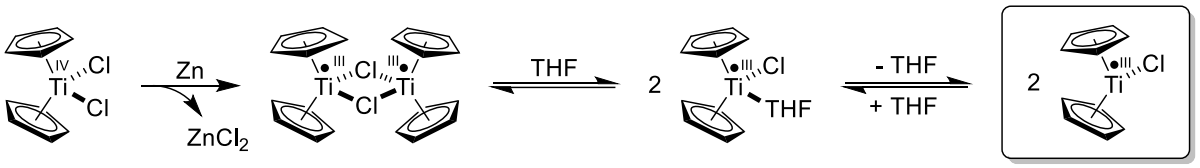

Scheme 16: Zinc-mediated generation of catalytically active Ti(III)-species.[71]

The Ti(III)-species exists as a chloride-bridged dimer due to coordinative unsaturation. However, in the presence of the donor solvent THF, the dimer dissociates to provide the active monomeric species.[71] The binding of the solvent is reversible, resulting in an equilibrium between the dimer, the monomer-solvent complex, and the active species with a vacant coordination site (Scheme 16).

The active species then opens the epoxide *via* single-electron oxidative addition, affording a *β*-titanoxy radical. Hydrogen atom transfer (HAT) using a suitable donor, such as 1,4-cyclohexadiene (1,4-CHD), yields a saturated intermediate, while benzene is formed as a side product. Finally, acidic work-up provides the desired alcohol.[93] However, the *β*-titanoxy radical can be intercepted not only by external trapping agents such as 1,4-CHD but also by a second equivalent of the active species. Subsequent deoxygenation gives the corresponding olefin along with a dimeric titanocene oxide complex (Scheme 17). To suppress the competing deoxygenation, a tenfold excess of the HAT reagent was used. Additionally, the *in situ* prepared solution of titanocene(III) chloride in THF was added dropwise to the epoxide solution, instead of adding the epoxide solution to the titanocene solution. The concentration of the active species was thereby kept at a minimum during the reaction.[71]

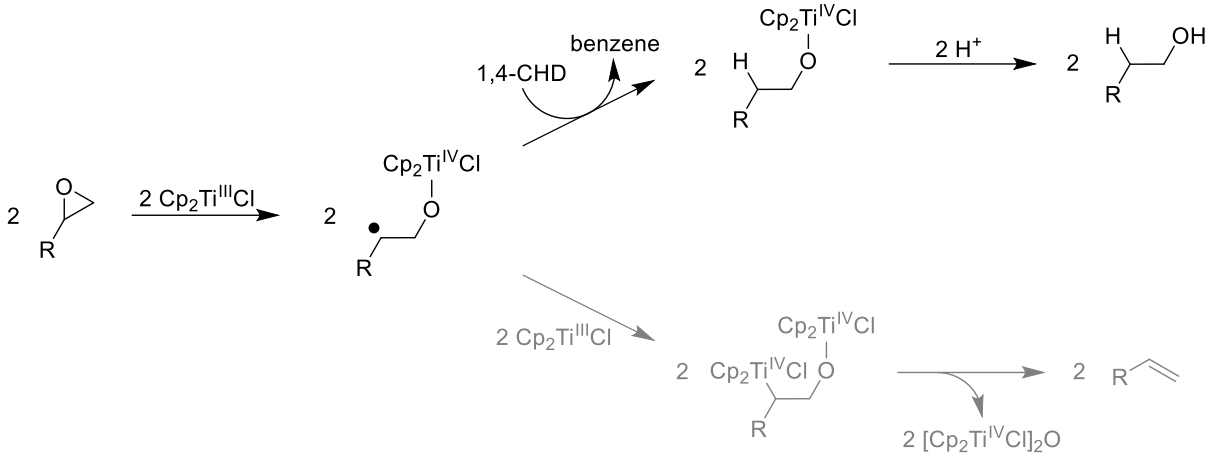

Scheme 17: Mechanism of the titanocene-mediated epoxide reduction and the competing deoxygenation.[93]

Provided that the epoxide is prepared from the corresponding olefin, the overall sequence constitutes a formal hydration of olefins to give *anti-Markovnikov* alcohols.[75] In 1956, *Brown* developed an efficient method for this transformation using stoichiometric amounts of hydroboranes (Scheme 18).[94] As in the radical approach, it proceeds *via* a two-step sequence from alkenes to the respective alcohols. However, it differs in the order of the oxidation and reduction steps. The alkene is reduced by hydroboration, and the resulting organoborane is oxidized with hydrogen peroxide under basic conditions.[75]

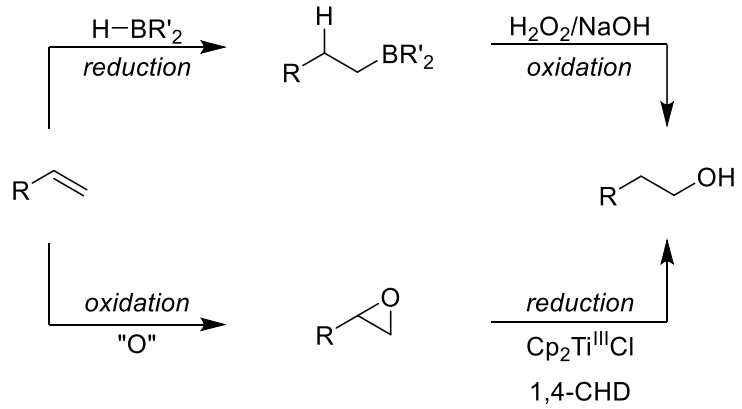

Scheme 18: Comparison of epoxidation/titanocene-mediated epoxide opening sequence to hydroboration/oxidation sequence.[75]

RajanBabu's and *Nugent*'s approach offers a suitable alternative to *Brown*'s hydroboration, as it employs complexes derived from titanium, which is more abundant than boron.[53] However, both methods rely on stoichiometric amounts of the corresponding reagents, which limits their sustainability.[71,94] The *anti-Markovnikov* hydration of olefins is considered one of the greatest challenges in catalysis.[95]

1.5 Titanocene-Catalyzed Epoxide Opening

RajanBabu's and *Nugent*'s approach did not enable catalytic turnover because the titanocene complex remains bound to the alkoxide until the Ti–O bond is cleaved during acidic work-up.[71] *Gansäuer et al.* developed a catalytic method through the addition of a suitable acid prior to the reaction, together with an appropriate reductant. Several requirements had to be met to achieve efficient catalytic turnover: The employed acid must be strong enough to protonate the titanium-oxygen bond, yet weak enough to avoid epoxide opening on its own. Additionally, it must neither oxidize the metal powder nor any active Ti(III)-species. The resulting base must not deactivate any titanium species by coordination. Furthermore, the employed metal powder must rapidly and efficiently reduce titanocene(IV) dichloride to the Ti(III)-species. The generated alcohol should not deactivate any Ti-species. Ultimately, the *Lewis* acid formed during activation should not interfere with the catalytic cycle.[70]

Considering these requirements, the pK_a of the proton donor must be at least three units higher than that of typical alcohols (e.g., MeOH = 15.5) to enable complete protonation. Moreover, the pK_a should not be lower than that of pyridine hydrochloride (5.25), as it is known to open epoxides in chloroform to yield the respective chlorohydrin. The investigation of acids with a pK_a range of 5.25–12.5 revealed 2,4,6-collidine- and 2,6-lutidine-hydrochloride (Scheme 19) to be the most suitable reagents to induce catalytic turnover.[70]

	2,4,6-collidine hydrochloride	*2,6-lutidine hydrochloride*
	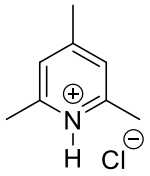	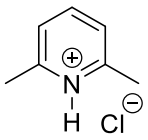
pK_a	7.43	6.65

Scheme 19: pK_a-values of acids used in the titanocene-catalyzed epoxide opening.[70]

Regarding the metal powder, the *Lewis* acidity of the resulting $ZnCl_2$ is high enough to open the epoxide by itself. In contrast, $MnCl_2$ is not *Lewis* acidic enough to trigger this side reaction (Scheme 20).[70]

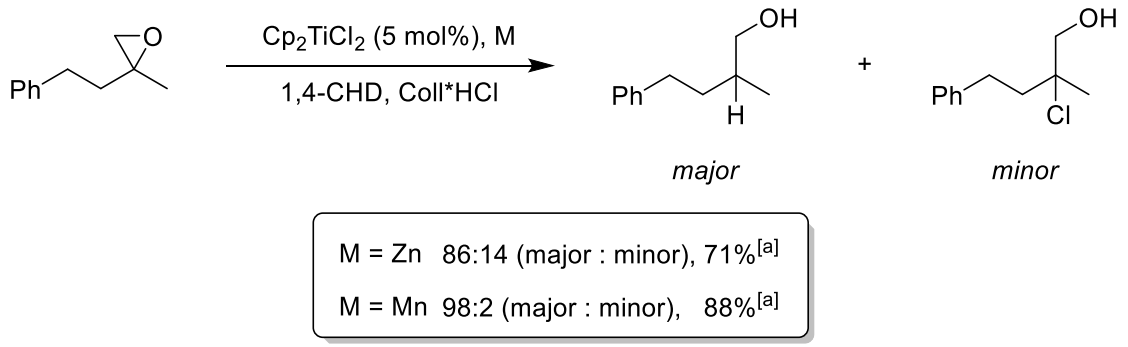

Scheme 20: Impact of the *Lewis* acidity of the activation reagent on the selectivity of the titanocene-catalyzed epoxide opening; [a]isolated yield of major product.[70]

Contrary to the assumptions of *RajanBabu* and *Nugent* that the selectivity of titanocene-mediated C–O homolysis of epoxides is thermodynamically controlled,[71] various results reported by *Gansäuer et al.* suggest a kinetic path.[70] The ring-opening of 1,2-epoxydodecane afforded dodecanol as a 94:6 mixture of 1- and 2-dodecanol. It is worth noting that none of the other examples reported by *Gansäuer et al.* furnished the *Markovnikov* alcohol, even in the case of a trisubstituted epoxide. Furthermore, the thermodynamic path implies an equilibrium between the competing radical intermediates (Scheme 21). According to *Gansäuer*, under thermodynamic control, the equilibrium rate would be affected by the trapping agent. However, in practice, the choice of the trapping agent did not influence the regioselectivity.[70]

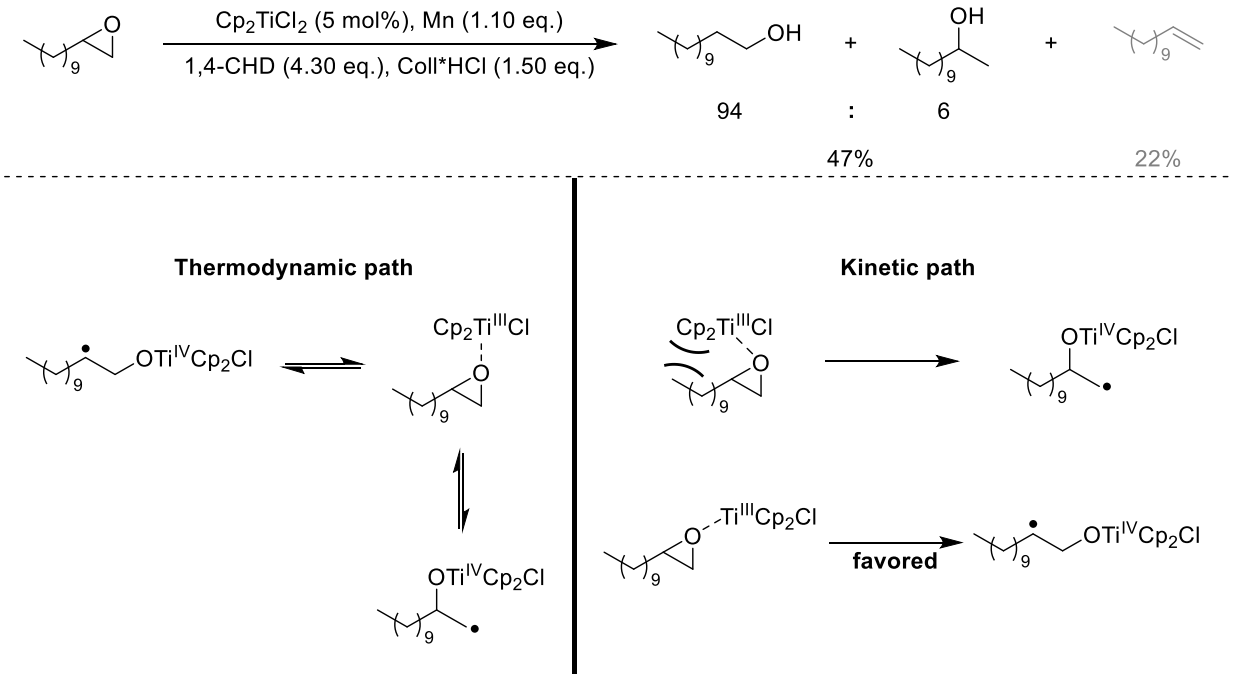

Scheme 21: Possible pathways controlling the regioselectivity of the titanocene-catalyzed opening of 1,2-epoxydodecane.[70]

Consequently, the selectivity is presumably controlled by steric interactions between the catalysts' ligands and the substrates' substituents (Scheme 21).[70] Subsequent density functional theory (DFT) studies confirmed this assumption.[96]

The low steric hindrance induced by the substituents of 1,2-epoxydodecane not only results in a regioisomeric mixture but also facilitates trapping of the *β*-titanoxy radical by another equivalent of $Cp_2Ti(III)Cl$, leading to 22% of deoxygenation product (Scheme 21).[70]

Further studies focusing on the mechanism indicate the presence of an additional active species opening the epoxide. *Daasbjerg et al.* plotted the concentration of Ti(III)-species against time to determine rate constants for the ring-opening by the dimer and monomer. Surprisingly, the rate constant is higher for the opening with the dimer, although the species has no vacant site. Therefore, they proposed the presence of an open dimeric species in the equilibrium (Scheme 22).[97]

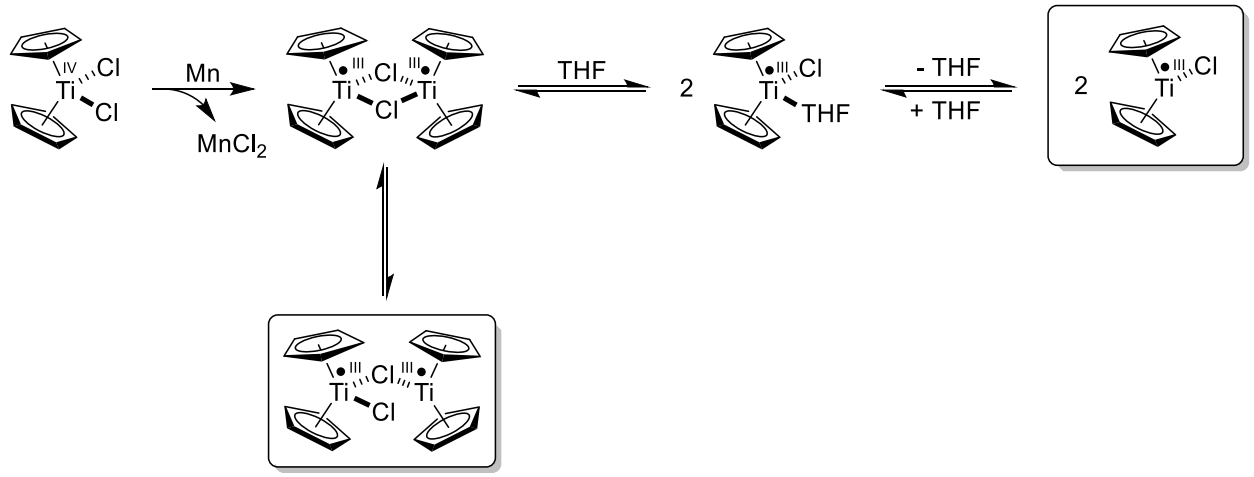

Scheme 22: Equilibrium of the dimer and monomer species resulting from activation.[97,98]

Coll*HCl, which was initially only used as an acid fulfilling the above-listed requirements, displays an additional beneficial effect that *Gansäuer et al.* discovered later. It complexes the monomeric species *via* hydrogen bonding, forming a thermostable resting state (Scheme 23).[99]

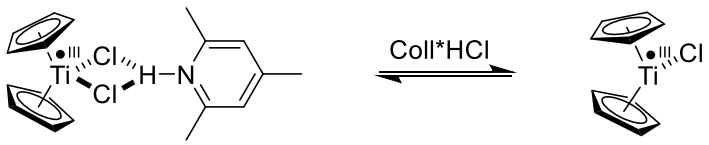

resting state

Scheme 23: Species involved in the opening of epoxides in the presence of Coll*HCl.[98]

Thereby, the formation of thermolabile dimeric species, which result in the degradation of the active species, is suppressed. Consequently, the necessary catalyst loading can be lowered.[99]

Moreover, the monomer is the predominant species in solution, as the equilibrium is shifted towards the monomer in the presence of Coll*HCl.[98]

In light of these findings, the mechanism of the titanocene-catalyzed epoxide opening can be described as follows (Scheme 24).

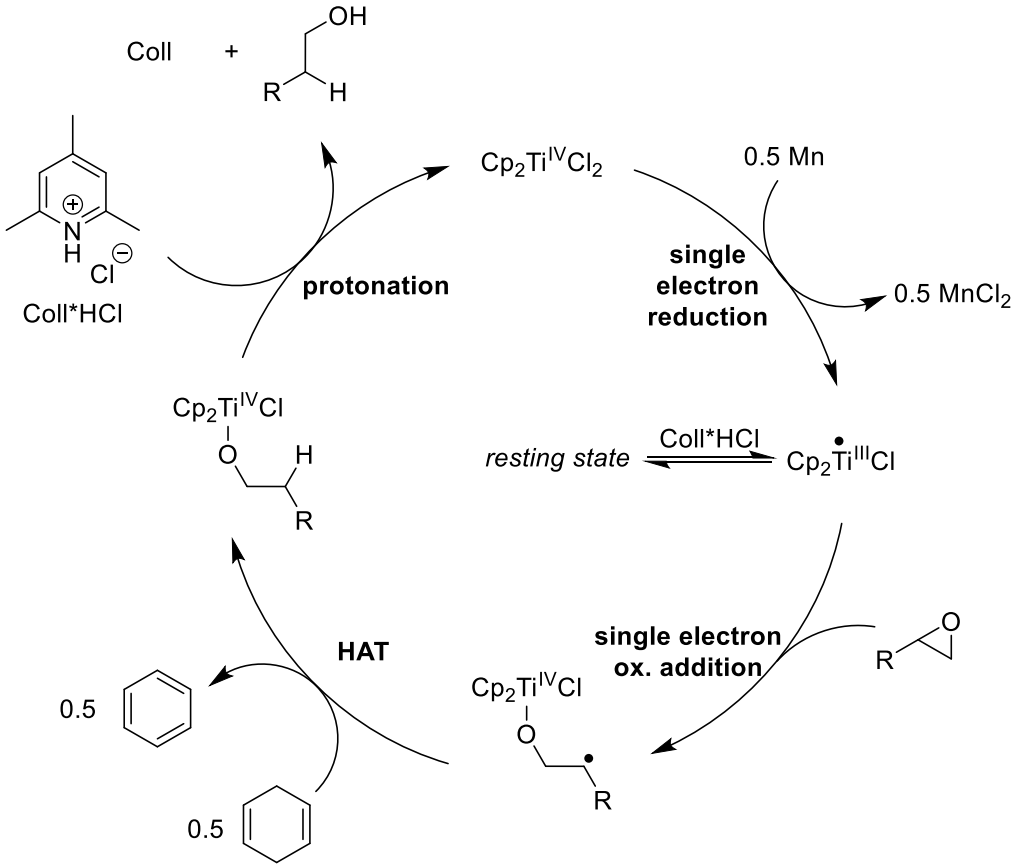

Scheme 24: Catalytic cycle for the titanocene-catalyzed opening of epoxides.[70,98,100]

The catalytic reduction shows comparable functional group tolerance to the stoichiometric system, as esters, ketones, and aromatic ketones do not affect the catalytic cycle. *Gansäuer et al.* demonstrated the tolerance of esters by converting Piv-protected epoxyalcohols into the corresponding *anti-Markovnikov* alcohols in yields of 67–69%. Furthermore, they demonstrated the functional group tolerance of ketones by transforming 2-methyl-2-(2-phenylethyl)oxirane in the presence of the corresponding ketone and acetophenone. In both screening experiments, the ketones did not interfere with the catalytic cycle. Moreover, they subjected epoxides bearing tosylate and chloride groups to their catalytic conditions. Both functional groups, which typically decompose in the presence of highly active reductants such as SmI_2, remained intact.[70]

Except for the opening of 1,2-epoxydodecane, no formation of the deoxygenation product was observed in any other example reported by *Gansäuer et al*. Using only catalytic amounts of titanocene dichloride avoids trapping of the *β*-titanoxy radical by another equivalent of the

active species. Therefore, the required amount of 1,4-CHD could be reduced to four equivalents. In conclusion, the catalytic variant exhibits greater sustainability while maintaining chemoselectivity.[70]

In a later study, *Gansäuer et al.* applied the catalytic system to oxetanes to determine whether comparable efficiency could be achieved, given their apparent structural similarity.[101]

1.6 Properties, Synthesis and Application of Oxetanes

1.6.1 Definition and Reactivity of Oxetanes

Oxetanes represent another class of cyclic ethers and are characterized by their four-membered ring structure. The bond angles within the ring (85–92°) are significantly closer to the ideal tetrahedral angle compared to epoxides (Figure 8). Despite that, their ring strain (~25 kcal/mol) is similar to that of epoxides.[74] Therefore, a comparable reactivity would be expected.

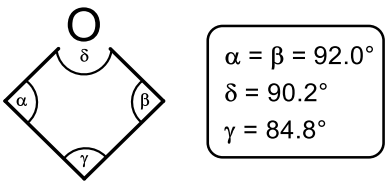

Figure 8: Geometry of trimethylene oxide.[74]

Nonetheless, epoxides display a significantly higher reactivity than oxetanes.[102] This difference in reactivity has been the subject of comprehensive theoretical investigations, wherein the structurally similar cyclopropane and cyclobutane are analyzed. All proposed models share a common feature. They suggest that the valence electrons of cyclopropane are not restricted to individual C–C *σ*-bonds, but delocalize, similar to an aromatic *π*-system. This concept is called *σ*→*π* delocalization.[103]

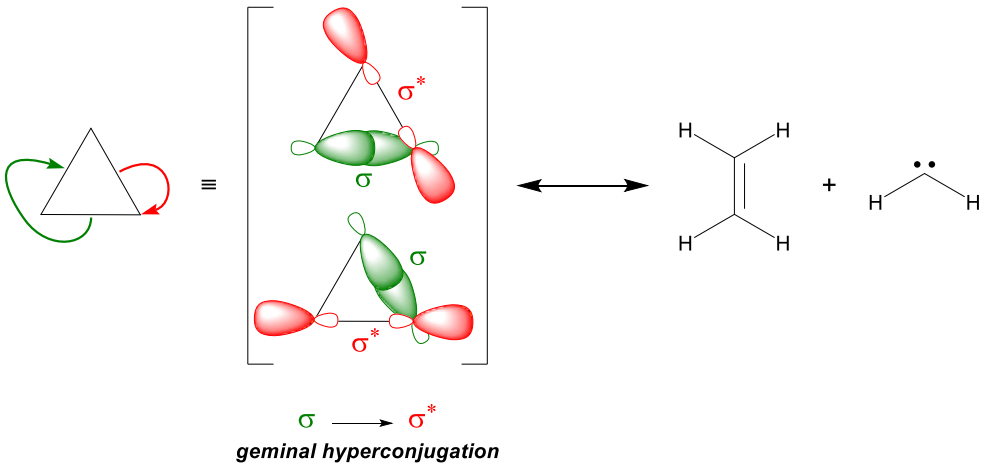

Figure 9: *σ*→*π* delocalization in three-membered rings.[103]

Electrons are delocalized over methylene groups *via* geminal *σ*→*σ** hyperconjugation that is enabled by the p-orbital overlap (Figure 9). The strong distortion of the bond angles within three-membered rings results in significant hyperconjugation. On the contrary, hyperconjugation can be neglected in four-membered rings due to geometry and symmetry

limitations. The higher dipole moment of chlorocyclobutane (2.20 D) with respect to chlorocyclopropane (1.76 D) supports this model.[103]

Sterling et al. proposed that the pronounced delocalization results in earlier, lower transition states, thereby reducing the activation barrier for ring-opening. Their model can be extended to all three- and four-membered rings, such as epoxides and oxetanes.[103] Computational studies determining the activation energy (E_a) for the nucleophilic ring-opening of ethylene oxide and trimethylene oxide by methoxide highlight the impact of electronic delocalization (Scheme 25).[102]

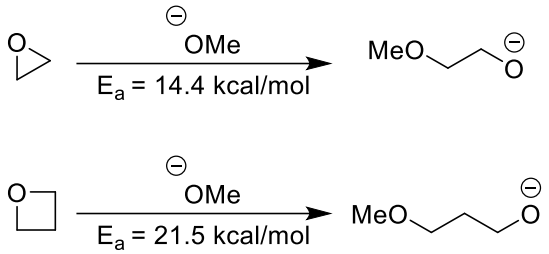

Scheme 25: Activation energies (E_a) for the nucleophilic ring opening of ethylene oxide and trimethylene oxide by methoxide.[102]

The activation energy for the opening of ethylene oxide is 7.1 kcal/mol lower, resulting in a 10^5-fold increase in reactivity.[102,103] Nevertheless, the ring strain of oxetanes provides a sufficient driving force to enable their use as reactive building blocks in ring-opening reactions.[74]

1.6.2 Application of Oxetanes

In analogy to epoxides, oxetanes commonly undergo nucleophilic ring-opening reactions. The high activation barrier for the opening of oxetanes necessitates the addition of *Lewis* acids to facilitate the reaction under mild conditions.[104] Otherwise, the addition of nucleophiles, such as organometallic reagents, requires reflux conditions for efficient turnover (Scheme 26).[105]

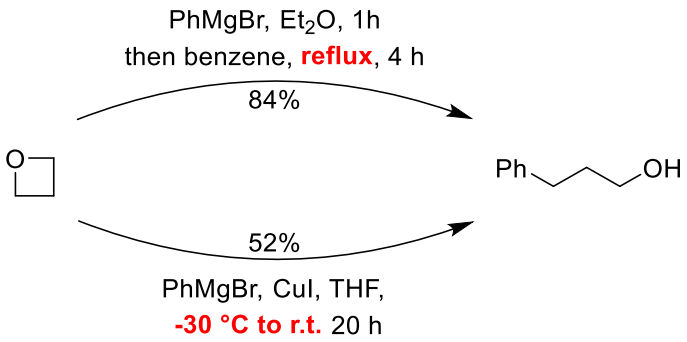

Scheme 26: Impact of *Lewis* acids on the conditions of nucleophilic oxetane opening.[104,105]

Aside from nucleophilic ring-opening reactions, oxetanes are also prone to ring-expansion processes, as demonstrated by the enantioselective Co-catalyzed intramolecular arylation of an aryl oxetane to generate a furane (Scheme 27).[106]

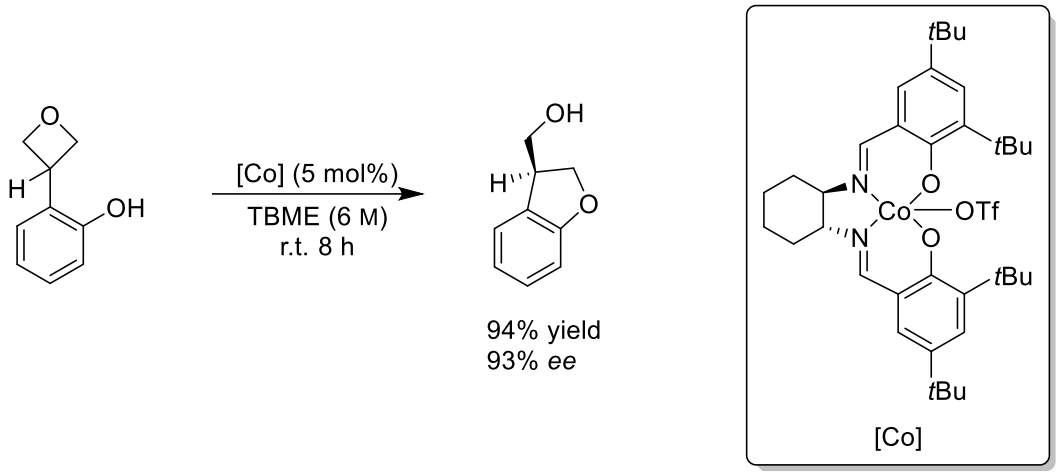

Scheme 27: Co-catalyzed enantioselective intramolecular arylation of an oxetane to access an enantioenriched furane.[106]

Oxetanes can also serve as stable motifs in medicinal chemistry, offering advantageous physicochemical properties. They constitute an efficient substitute for carbonyl groups in drug development, as they possess similar dipole and hydrogen-bonding properties. Oxetanes exhibit superior hydrogen bonding properties among common cyclic ethers. Their propensity for the formation of hydrogen bonds even surpasses that of aliphatic ketones, aldehydes, and esters.[107] Moreover, oxetanes offer greater stability than carbonyl groups. This can be attributed to the electrophilic nature of carbonyl compounds, which makes them more susceptible to enzymatic transformations.[108,109] Additionally, oxetanes are larger, which may be beneficial when a greater volume occupancy enhances binding to the receptor pocket (Figure 10).[110] Another potential benefit is the three-dimensional character of oxetanes, which may enhance aqueous (aq.) solubility and target affinity.[109]

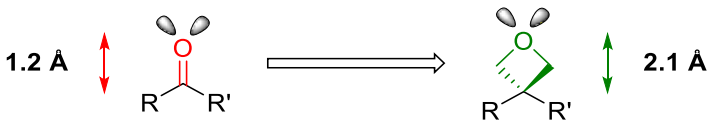

Figure 10: Size differences between carbonyl groups and oxetanes.[74]

Furthermore, their relatively high polarity makes them an attractive replacement for *gem*-dimethyl groups in drug development to increase the aqueous solubility while maintaining bulk. Thereby, the lipophilicity is reduced, which can result in the diminution of metabolic liability (Figure 11).[74]

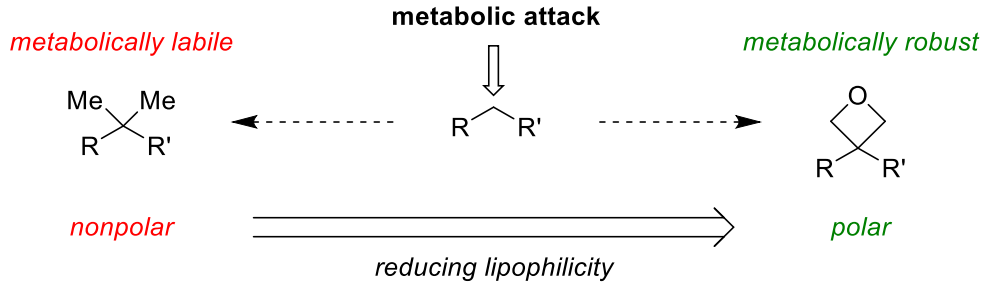

Figure 11: Comparison of *gem*-dimethyl and oxetane properties as motifs in medicinal chemistry.[111]

Several fully synthetic drug candidates comprising an oxetane moiety currently undergo clinical trials. *Crenolanib* is a phase III candidate developed by *AROG Pharmaceuticals*/*Pfizer* for the treatment of various types of cancer, such as acute myeloid leukemia (AML). Another potential drug in the same phase is *Fenebrutinib*, synthesized by *Genentech*, to treat multiple sclerosis (MS) (Scheme 28).[109]

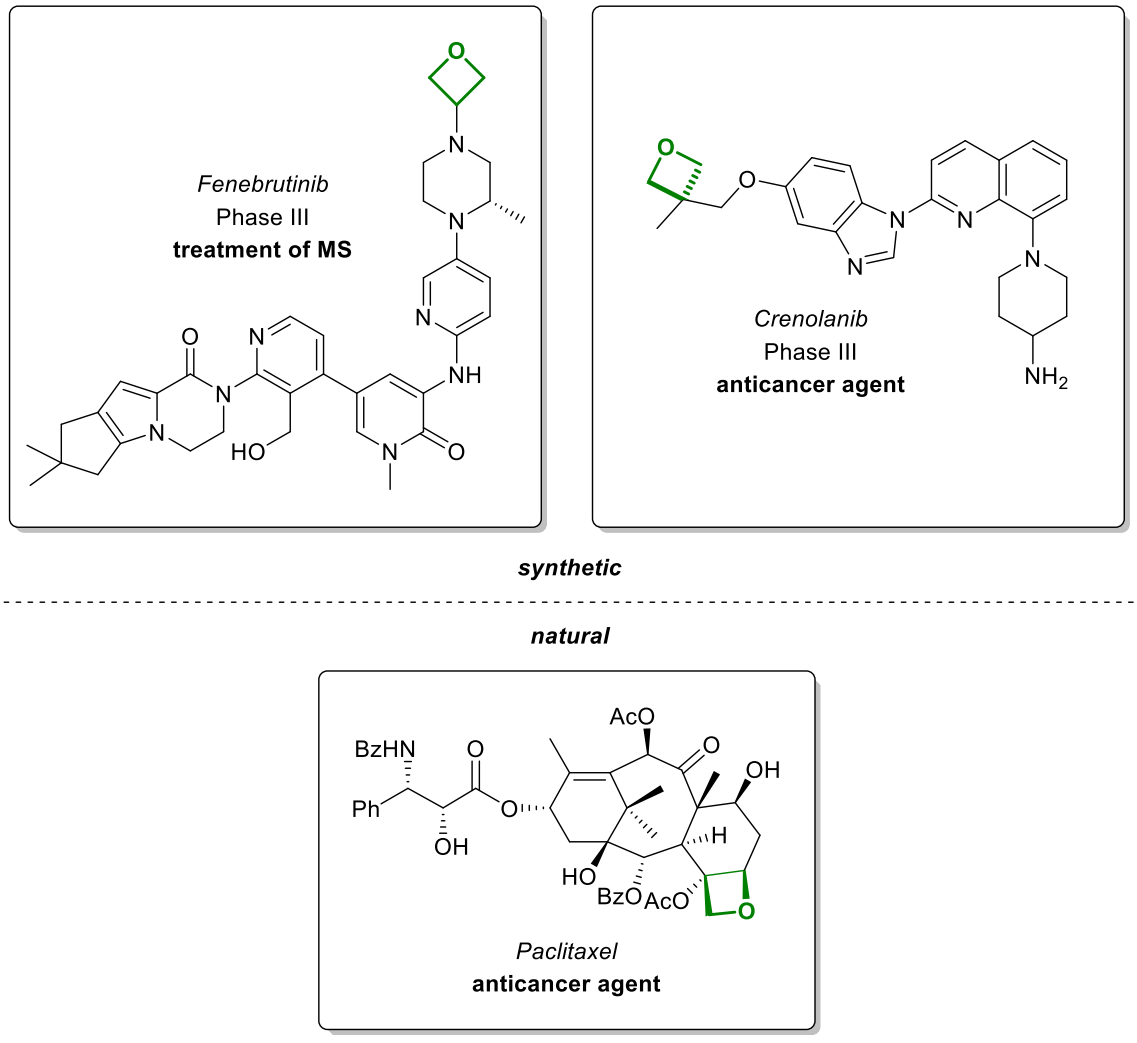

Scheme 28: Natural product with bioactivity (*Paclitaxel*) and fully synthetic drugs in clinical trials phase III (*Fenebrutinib* and *Crenolanib*) containing oxetane scaffold.[109]

A few natural products with biological activity also include oxetane groups. The most prominent example is *Paclitaxel*, which is the first-line drug in the treatment of breast cancer (Scheme 28).[109] Even though the oxetane ring is not strictly required for biological activity, non-oxetane analogues generally show reduced binding affinity and cytotoxicity.[112]

1.6.3 Synthesis of Oxetanes

The contradictory properties of oxetanes as reactive, strained cyclic ethers and as stable motifs with advantageous physicochemical properties, are increasingly exploited in synthetic and medicinal chemistry. Consequently, numerous synthetic strategies for accessing new oxetane derivatives have been developed.[74] Although several routes have been designed, two are most commonly employed. The first is the intramolecular *Williamson* ether synthesis, which entails an etherification of the employed alcohol according to an S_N2 mechanism. The second is [2+2] cycloaddition reactions, such as the photoinduced addition between an aldehyde and an alkene according to *Paternò* and *Büchi* (Scheme 29).[107]

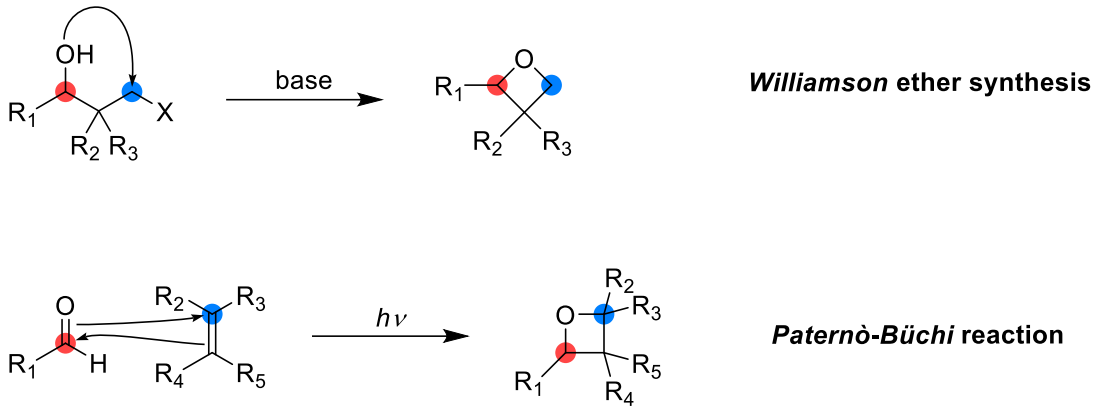

Scheme 29: Two general approaches to synthesize oxetanes.[107]

The intramolecular *Williamson* etherification is one of the most common methods for oxetane synthesis owing to its practicality and versatility.[74,113] However, the yields of this route can be moderate due to the competing *Grob* fragmentation leading to the corresponding olefin and aldehyde, accompanied by the abstraction of the leaving group (X).[114] Moreover, this reaction proceeds *via* a 4-*exo*-*tet* cyclization, which is, in terms of kinetics, the least favoured n-*exo*-*tet* cyclization mode ($n \leq 7$).[115]

The [2+2] cycloaddition reactions, according to *Paternò* and *Büchi*, offer a direct synthesis of highly substituted oxetanes from carbonyl compounds and olefins. This strategy benefits from its high atom economy and versatility. However, its scalability is often limited by the requirement for UV light sources (e.g., Hg or Xe lamps) and dedicated reaction equipment such as quartz vessels.[116–118]

A less common method reported by *Okuma* involves the methylenation of carbonyl groups or epoxides to the corresponding oxetanes *via* the *Corey-Chaykovsky* reaction (Scheme 30). This method offers a straightforward protocol to access the desired oxetanes in high yields under moderately mild conditions. When carbonyl compounds serve as substrates, methylenation proceeds *via* the corresponding epoxide. Methylenation of either the *in situ* formed or directly employed epoxide provides the desired oxetane. Consequently, the *Corey-Chaykovsky* reaction of carbonyl compounds requires at least two equivalents of the reagent (Scheme 30).[119]

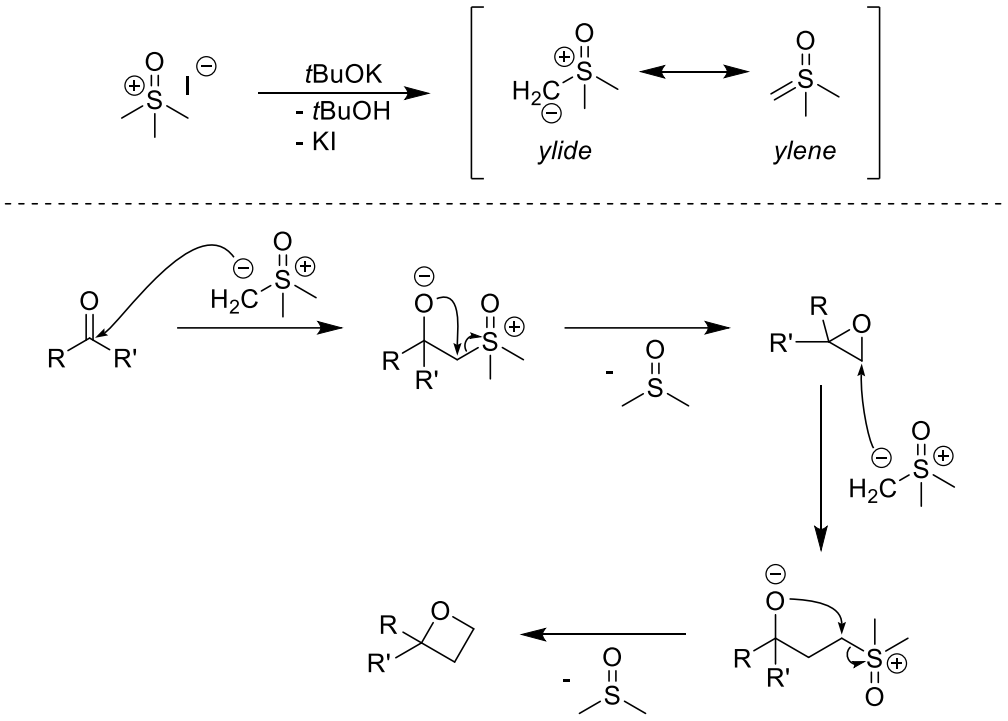

Scheme 30: Mechanism of the *Corey-Chaykovsky* reaction of carbonyl groups.[119]

Trimethylsulfoxonium iodide serves as the methylenation agent, activated by deprotonation. The resulting resonance-stabilized sulfonium ylide adds to the carbonyl group or the less hindered site of the epoxide, affording a zwitterion. Finally, the nucleophilic alkoxide displaces dimethylsulfoxide (DMSO) at the implemented methylene group *via* an intramolecular S_N2 reaction.[119]

By employing chiral epoxides, the resulting oxetanes are obtained with retention of stereochemistry at the higher-substituted carbon (Scheme 31).[120]

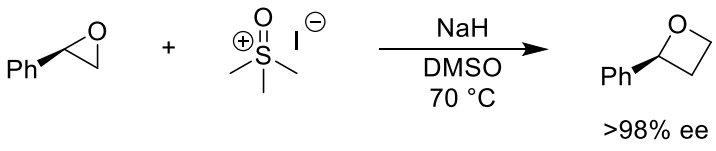

Scheme 31: *Corey-Chaykovsky* reaction of a chiral epoxide.[120]

An earlier approach to enantimerically enriched 2-substituted oxetanes was reported by *Soei et al.* They synthesized these oxetanes from enantiomerically enriched 1,3-halohydrins *via* intramolecular *Williamson* etherification. The substrates were prepared from the corresponding ketones *via* asymmetric hydrogenation using $LiBH_4$ and a chiral ligand (Scheme 32).[121]

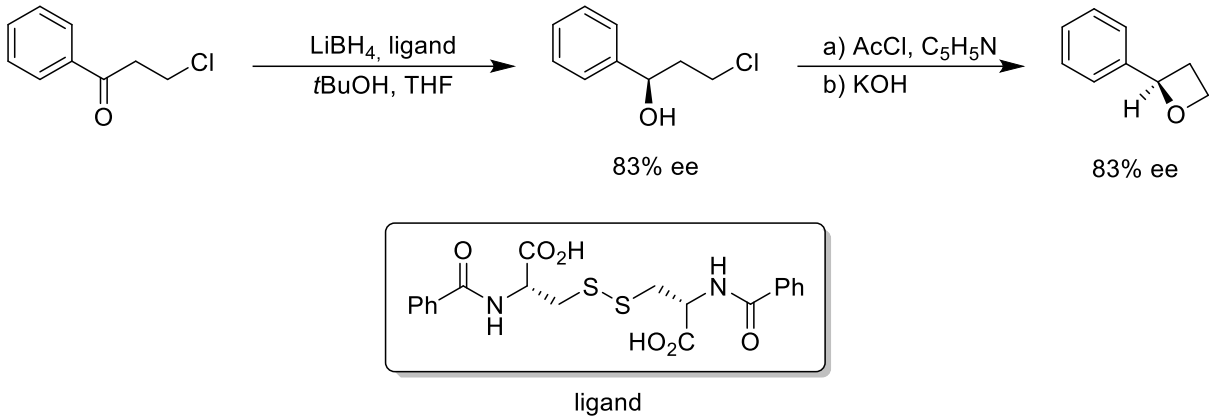

Scheme 32: Asymmetric reduction of a ketone followed by cyclization to the enantiomerically enriched oxetane.[121]

1.7 Titanocene-Catalyzed Oxetane Opening

Gansäuer et al. described the first opening of oxetanes by titanocenes. They investigated the efficiency of reductive oxetane opening using computational and synthetic methods. In analogy to the epoxides, they calculated the TS structures of ring-opening and their corresponding activation energies by DFT. Comparison of the epoxides' and oxetanes' respective activation energies highlights the greater stability of oxetanes.[101]

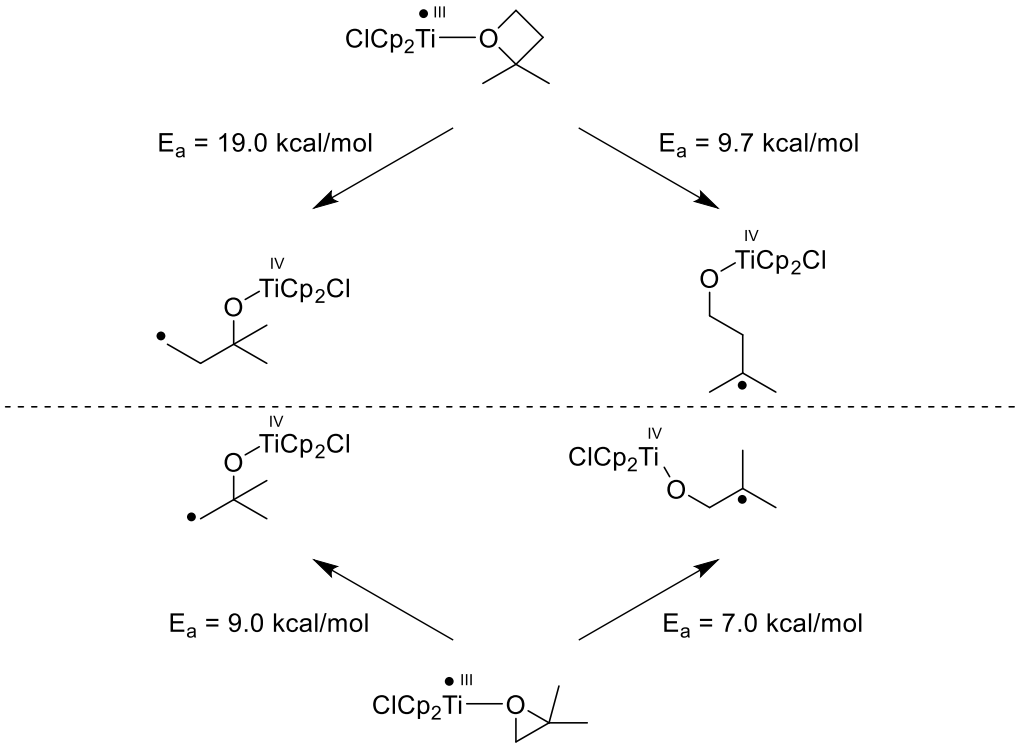

Scheme 33: Activation energies for the titanocene-catalyzed opening of a dimethyl-substituted epoxide and oxetane.[101]

The higher activation barriers for oxetane opening reflect the more pronounced steric interactions between the substrate's substituents and the catalyst. Similar to epoxide opening, the TS of the higher-substituted radical is favored due to electronic and steric factors. Notably, formation of the tertiary *γ*-titanoxy radical is significantly more favorable than that of the corresponding primary radical (Δ = 9.3 kcal/mol). In contrast, the energy difference between the *β*-titanoxy radicals is relatively small (Δ = 2.0 kcal/mol). It should be noted that the relative magnitude of the steric and electronic effects on the transition states of oxetane opening has yet to be quantified. In summary, oxetane opening proceeds at a slower rate yet with greater selectivity than the corresponding reactions with epoxides.[101]

Compared to *β*-titanoxy radicals, *γ*-titanoxy radicals feature an increased distance between the titanocene ligands and the radical center. Consequently, *γ*-titanoxy radicals are not as shielded by the catalyst and behave more like free radicals.[101]

The synthetic investigations of *Gansäuer et al.* primarily focused on benzylic oxetanes, as they require low activation energies (~3.3 kcal/mol) for ring-opening. In the absence of trapping agents, the *γ*-titanoxy radical dimerizes instead of reacting with a second equivalent of the active species (Scheme 34, top). This observation is consistent with a free-radical-type mechanism, as the radicals combine faster than they react with a second equivalent of $Cp_2Ti(III)Cl$.[101]

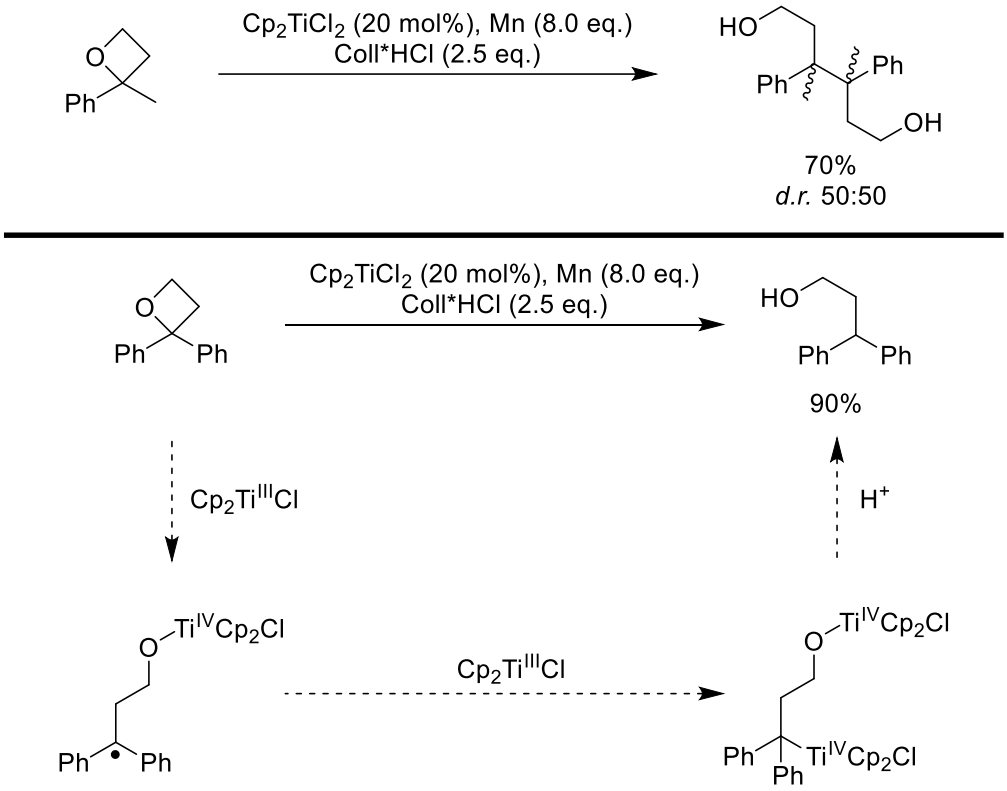

Scheme 34: Titanocene-catalyzed opening of phenyl-substituted oxetanes without the addition of trapping agents.[101]

With sterically more demanding substrates, such as diaryl-substituted oxetanes, dimerization is prevented (Scheme 34, bottom). Instead, the desired alcohols are obtained. They suggested the binding of a second equivalent of the titanocene, followed by protonation of the Ti–C bond.[101]

In the presence of a trapping agent, such as 1,4-CHD, ring-opening of an alkyl-substituted oxetane affords the desired alcohol in moderate yield, along with a low amount of the corresponding homoallylic alcohol (Scheme 35). The formation of the latter is attributed to a competing *β*-hydride elimination resulting from the binding of a second equivalent of the active species (Scheme 35). This occurs even though a tenfold excess of 1,4-CHD, rather than the fourfold excess typically used in the corresponding epoxide opening system, is employed. Presumably, the slow addition of the trapping agent to the “unshielded” *γ*-titanoxy radical promotes the competing *β*-hydride elimination.[101]

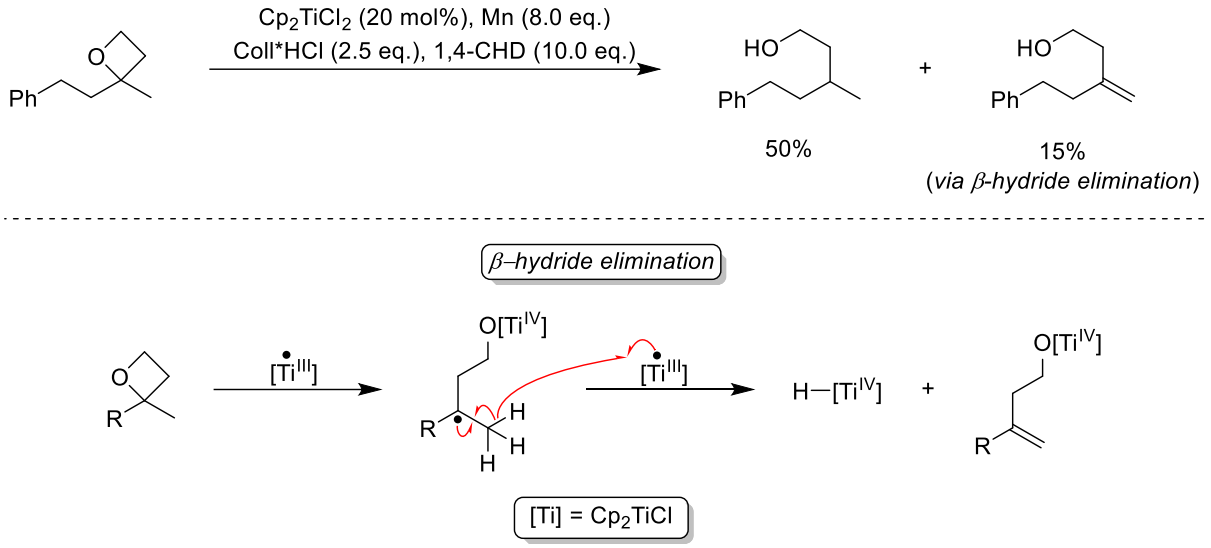

Scheme 35: Titanocene-catalyzed opening of an alkyl-substituted oxetane under similar conditions to typical reductive epoxide opening (top);[101] proposed mechanism of competing *β*-hydride elimination by *Gansäuer et al.* yielding the homoallylic alcohol (bottom).[122]

In conclusion, epoxides outperform oxetanes when this catalytic system is applied, as the reaction proceeds faster and competing side reactions are less prevalent. Nevertheless, regardless of the substrate class, the use of 1,4-CHD imposes intrinsic limitations on the catalytic system, which becomes particularly apparent in the titanocene-catalyzed oxetane opening. Their slow addition to the respective titanoxy radical enables side reactions during the opening of both cyclic ethers (Schemes 20 and 35). Furthermore, the use of 1,4-CHD in large excess reduces the overall sustainability of the system.[70,101] Therefore, *Gansäuer et al.* investigated the use of other external HAT reagents while focusing on the opening of epoxides,[123] which will be discussed in the following Chapter.

1.8 Titanocene-Catalyzed Hydrosilylation of Epoxides

1.8.1 Catalyzed Hydrogen Atom Transfer (CHAT) Reactions from Transition Metal Hydrides

Transition metal hydrides are attractive HAT reagents owing to the relatively low bond dissociation energies of M–H bonds.[124] They can be generated by the reaction of transition metal complexes with molecular hydrogen. *Norton et al*. exploited these properties in radical cyclization reactions using $Cp(CO)_3CrH$ as the catalyst and H_2 as the terminal reductant. Inspired by this work, *Gansäuer et al.* coupled *Norton*'s system with the titanocene-catalyzed opening of epoxides to study the efficiency of catalyzed hydrogen atom transfer (CHAT) reactions (Scheme 36). This cooperative catalytic approach was subsequently evaluated not only with the aforementioned chromium complex, but also with *Wilkinson*'s catalyst ($RhCl(PPh_3)_3$) and *Vaska*'s complex ($IrCl(CO)(PPh_3)_3$).[123]

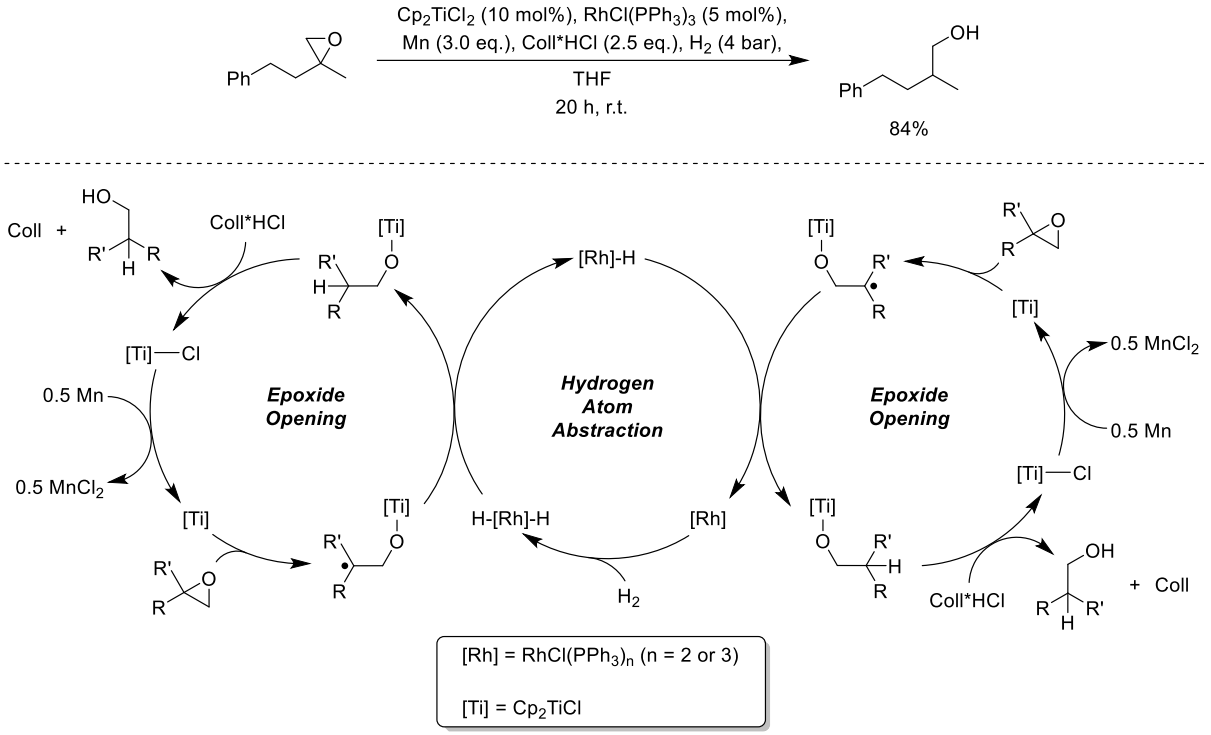

Scheme 36: Cooperative catalysis for sustainable radical reduction of epoxides using H_2.[123,125]

Screening experiments identified *Wilkinson*'s complex as the most effective co-catalyst in combination with high H_2 pressure and manganese as the activating agent for the titanocene catalyst (Scheme 36). Under these conditions, no formation of the side product arising from *β*-hydride elimination was observed.[123]

The cooperative catalysis employs the most environmentally benign and atom-economical HAT reagent, namely molecular hydrogen,[75] thereby avoiding reagents such as 1,4-CHD,

which lead to toxic by-products.[123] However, the use of molecular hydrogen requires activation by a co-catalyst,[123] which increases both cost and waste. The titanocene complex itself is not capable of efficiently activating H_2 to form a titanocene hydride species.[123]

In the context of efficient titanocene hydride formation, *Buchwald et al.* had already demonstrated in the 1990s that silanes can serve as effective terminal HAT reagents in Ti-catalyzed reduction reactions.[126–128] Silanes are sufficiently reactive to generate titanium hydrides from the corresponding titanium alkoxide complexes, in contrast to molecular hydrogen.[126] The higher reactivity is primarily driven by the relatively weak Si–H bond (~90 kcal/mol)[129] and further promoted by the formation of a strong Si–O bond.[130] *Buchwald et al.* used the resulting titanium hydrides, formed *in situ*, in the reduction of ketones,[127] esters,[126] imines,[127] and enamines.[128] The mechanism of the titanium-catalyzed hydrosilylation of ethyl decanoate (Scheme 37) shows that the silane can additionally regenerate the active species due to the formation of a strong Si–O bond.[126]

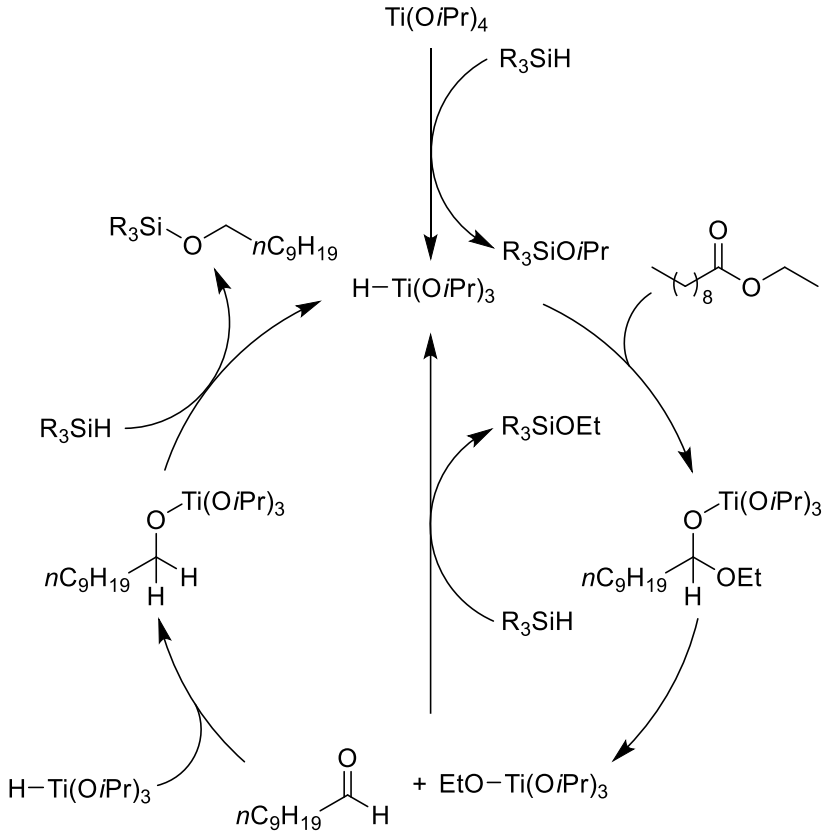

Scheme 37: Catalytic cycle of the titanium-catalyzed hydrosilylation of ethyl decanoate and the subsequently formed corresponding aldehyde.[126]

In addition to their higher reactivity in the formation of titanium(III) hydrides, silanes offer practical advantages over molecular hydrogen. The use of pressurized hydrogen gas requires specialized equipment and safety precautions, whereas many silanes are bench-stable liquids that can be handled under standard laboratory conditions.[75,131–133]

From a resource perspective, silicon is the second-most-abundant element in the Earth's crust,[134] which contributes to the commercial availability of common silanes.[133,135,136] Moreover, silane-based coatings have been described as biodegradable and non-toxic.[137,138]

Overall, silanes are attractive terminal HAT reagents for the generation of titanium hydrides.[126–128] The use of these hydrides is particularly valuable because they act not only as electron transfer (ET) reagents but also as HAT reagents in the titanium-catalyzed hydrosilylation.[126–128]

1.8.2 First Study on the Titanocene-Catalyzed Hydrosilylation of Epoxides

In 2012, *Gansäuer et al.* first applied the titanium-catalyzed hydrosilylation to epoxides. The *in situ* formed titanocene hydrides serve as radical-generating species ***and*** HAT catalysts. Therefore, the reduction of the *β*-titanoxy radical proceeds *via* an ***intramolecular*** HAT process.[131] Consequently, the transfer proceeds significantly faster than in previous systems.[70,123] Analogously to the mechanism shown in Scheme 37,[126] silanes are used as terminal HAT reagents to activate the precatalyst and cleave the Ti–O bond by complex-assisted sigma bond metathesis (*σ*-CAM).[131]

In their first investigation on the titanocene-catalyzed hydrosilylation, *Gansäuer et al.* developed two methods for the reductive opening of epoxides, differing in the choice of the precatalyst. One method employs the dimeric complex $[(Cp_2Ti^{III}OEt)_2]$ as the precatalyst. The active species is generated from the addition of silanes to the corresponding monomer, which is yielded by dissociation of the dimer. While the method gives high yields, handling the precatalyst is tedious due to its sensitivity to water, light, and air. On the other hand, the use of $Cp_2Ti^{IV}(Me)_2$, according to the second method, allows for easier handling, as it is more stable to water and air. However, heating is necessary for reasonable reaction times, and the resulting yields are slightly lower. Furthermore, the precatalyst is sensitive to light, requiring its immediate preparation prior to use.[75,131]

While the exact mechanism of activation of the dimethyl complex remains unclear, two transition states have been proposed for the transformation of the alkoxide complex (Scheme 38).[139–143]

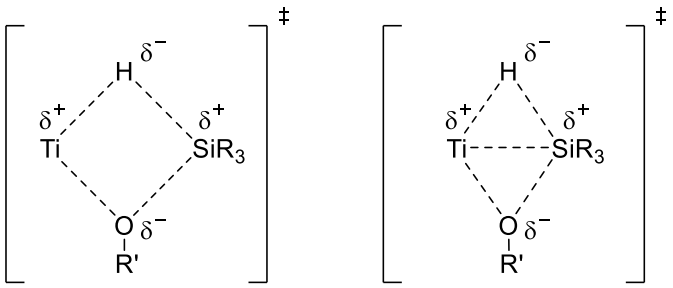

Scheme 38: Proposed transition states of the *σ*-CAM involving $Cp_2Ti^{III}OEt$ and silanes.[139–143]

A square-planar transition state has been assumed first, as the *σ*-CAM resembles a $[2_\sigma+2_\sigma]$-cycloaddition with typically opposing partial charges at the adjacent corners. However, calculations suggested an initial coordination of silane to the titanium and a stabilizing orbital overlap, resulting in a kite-like transition state (Scheme 38).[139–143]

The resulting titanocene hydride opens the epoxide *via* single-electron oxidative addition, affording the *β*-titanoxy radical with the same selectivity that is observed in the previous systems.[70,123] Intramolecular HAT saturates the carbon-centered radical and reduces Ti(IV) to Ti(III). Finally, the addition of silane initiates a *σ*-CAM, yielding a silyl ether and regenerating the active species. Base-promoted desilylation liberates the desired alcohol.[131]

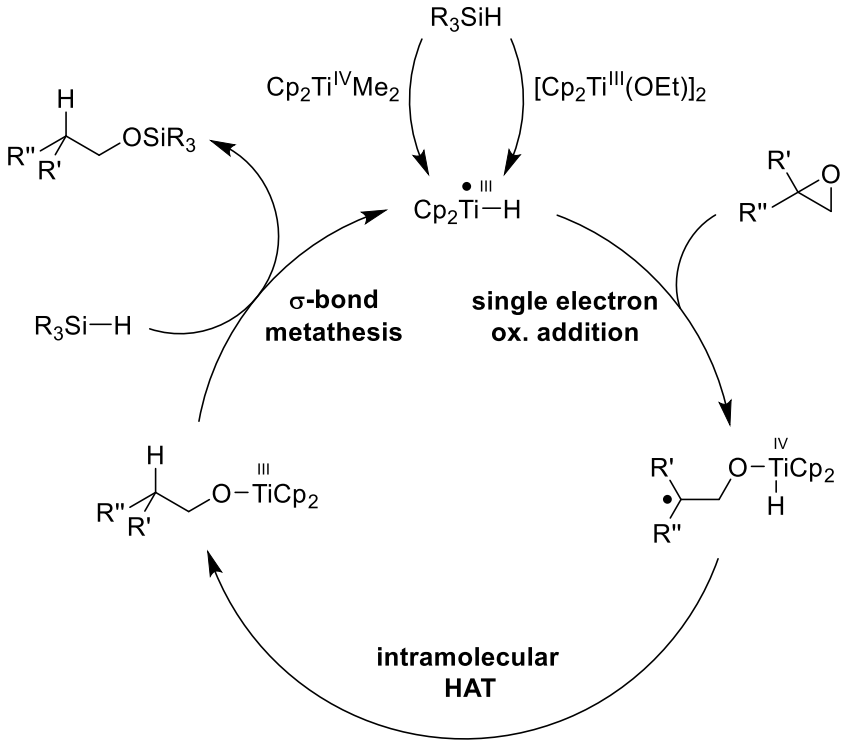

Scheme 39: Mechanism of the titanocene-catalyzed hydrosilylation of epoxides using one of two different precatalysts.[131]

The dual role of silane as both the activation and liberation reagent eliminates the need for Coll*HCl and Mn. Moreover, 1,4-CHD is no longer needed, as the active species also acts as a HAT catalyst. Consequently, the sustainability of the titanocene-catalyzed hydrosilylation of epoxides is significantly higher compared to the first system.[70,131]

The intramolecular nature of the HAT not only obviates the need for an external donor but also enables catalyst-controlled stereoselectivity of radical reduction. For bicyclic epoxides leading to cyclic radicals, a highly selective *syn*-HAT is observed. Computational studies suggest ordered cyclic transition states, with the TS for HAT in a *syn*-fashion being 3.1 kcal/mol lower in energy than the *anti*-selective transition state (Scheme 40, top).[131] Using an external HAT reagent, such as 1,4-CHD, the diastereoselectivity is generally poor, while slightly favoring the opposite diastereomer (Scheme 40, bottom).[131]

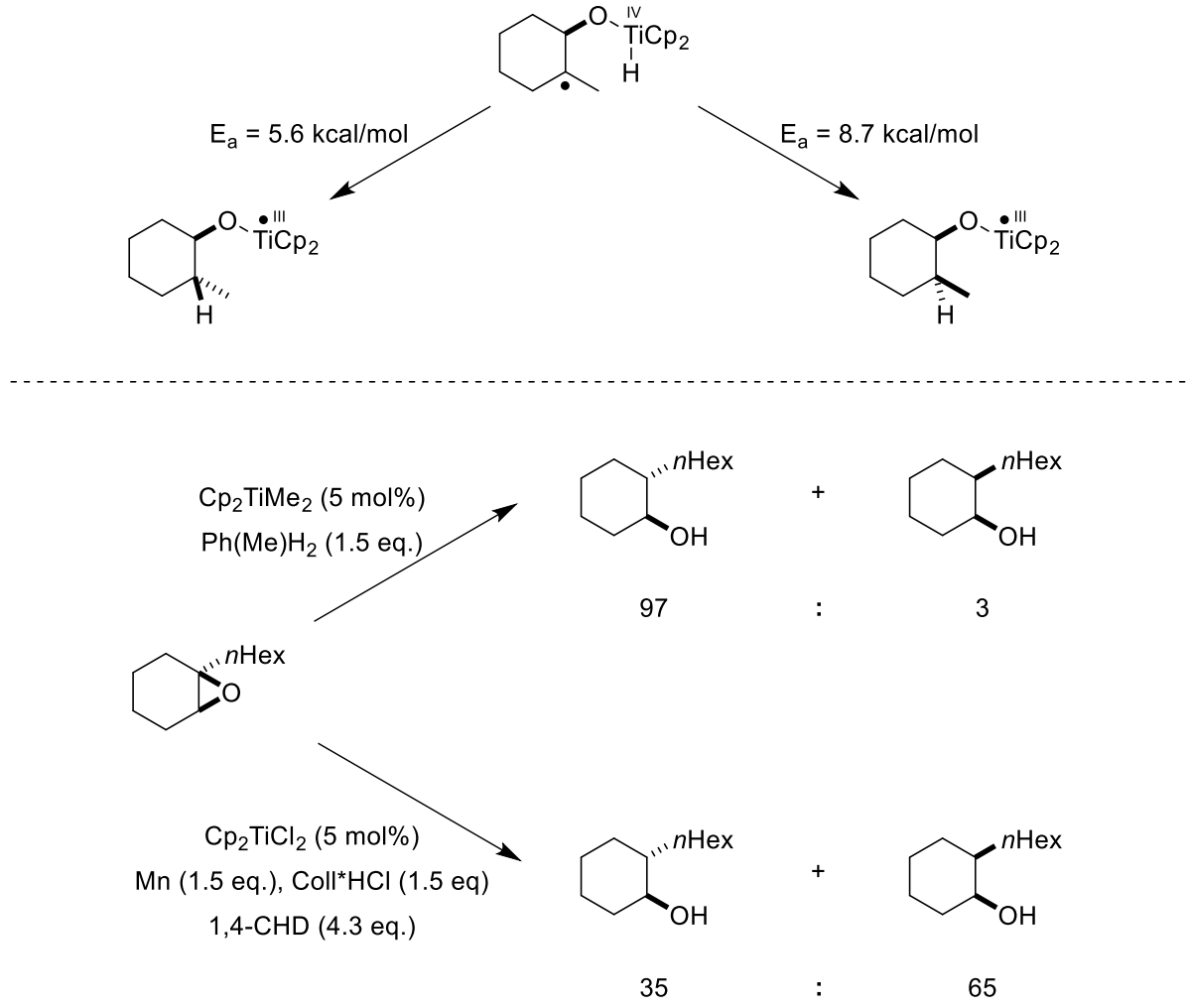

Scheme 40: Origins of diastereoselectivity in the intramolecular HAT reaction of *β*-titanoxy radicals.[131]

The diastereoselective reduction of acyclic radicals affords only moderate selectivity (85:15) when Cp_2TiMe_2 is used as the precatalyst. However, increasing the steric bulk of the ligands

improves the selectivity from 85:15 to 97:3 (Scheme 41). The highest diastereoselectivity is achieved with (tBuC$_5$H$_4$)$_2$TiMe$_2$.[131]

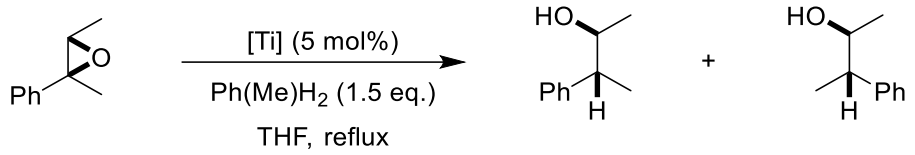

[Ti] = [Cp$_2$TiMe$_2$]	85	:	15
[Ti] = [(cHexC$_5$H$_4$)$_2$TiMe$_2$]	93	:	7
[Ti] = [(tBuC$_5$H$_4$)$_2$TiMe$_2$]	97	:	3

Scheme 41: Impact of various titanocenes on the diastereoselectivity.[131]

Moreover, the reductive opening of a 1:1 *cis*/*trans*-epoxide-mixture demonstrated the diastereoconvergence of the intramolecular HAT, as the *trans*-product was obtained in an identical diastereomeric ratio as observed in the reductive opening of the purely *trans*-substituted epoxide (Scheme 42).[131]

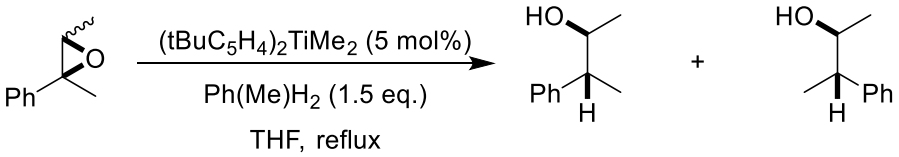

d.r. = 1 : 1 97 : 3

Scheme 42: Titanocene-catalyzed hydrosilylation of a 1:1 *cis*/*trans*-epoxide-mixture.[131]

This finding indicates that the intramolecular HAT is slower than the rotation of the C–C bond adjacent to the radical center after epoxide opening. As a result, the rotation allows for the interconversion of the diastereomeric radicals before the HAT. *Gansäuer et al.* calculated the structures of the two transition states leading to the respective diastereomers of the alcohol (Scheme 43).[131]

Steric interactions between the substituents of the substrate and the ligands of the catalyst dictate the diastereoselectivity according to initial investigations. Bulkier titanocenes induce more pronounced steric interactions in the transition states, enabling improved selectivities. In a recent review concerning the titanocene-catalyzed hydrosilylation, *Höthker* and *Gansäuer* proposed additional steric interactions between the substituents of the substrate, further disfavoring the "*syn*"-*β*-titanoxy radical. A combination of both steric interactions facilitates diastereoconvergence with high selectivity.[75,131]

These results are consistent with the *Hammond*[144] and *Bell-Evans-Polanyi*[145–147] principles. The intramolecular HAT step is exergonic, as the weak Ti–H bond is broken and a strong C–H

bond is formed.[148] According to the *Hammond* principle,[144] the structures of the transition states resemble the reactants in an exergonic process. Hence, following the *Bell-Evans-Polanyi* principle,[145–147] the stability of the rotameric *β*-titanoxy radicals provides an indication of their relative rates in the HAT step. As a result, the major product is formed *via* a *syn*-selective, five-membered transition state from the more stable rotameric *β*-titanoxy radical.[75]

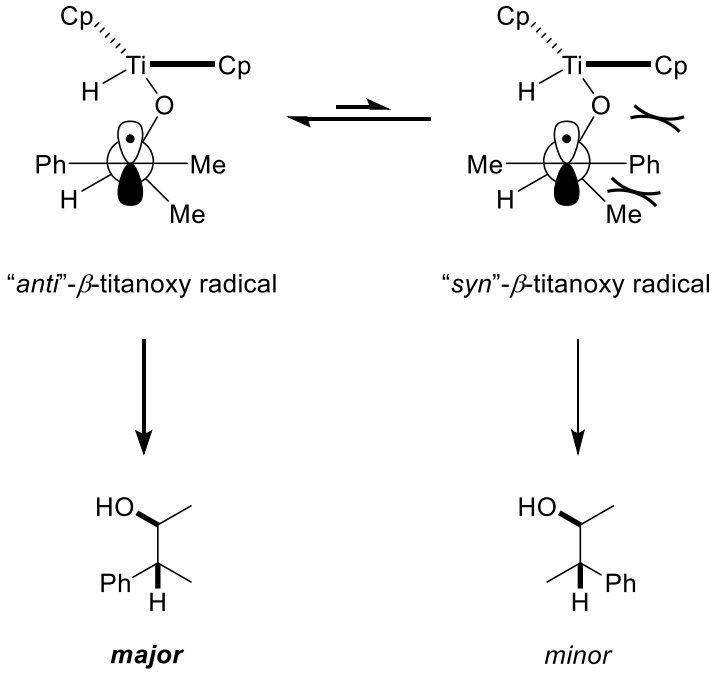

Scheme 43: Interconversion of the transition states of the intramolecular HAT.[75,131]

1.8.3 Second Study on the Titanocene-Catalyzed Hydrosilylation of Epoxides

In their second study on the titanocene-catalyzed hydrosilylation, *Gansäuer et al.* focused on the generation of the active species and reaction kinetics. Their initial approaches relied on sensitive precatalysts to access the reactive titanocene(III) hydride.[75] Moreover, activation of the precatalyst $Cp_2Ti(IV)Me_2$ requires elevated temperatures to achieve reasonable reaction times. Consequently, they searched for more suitable precatalysts.[131,132]

Titanocene(IV) dichloride represents an attractive precatalyst, as it is commercially available and bench-stable.[75] However, a reliable single-electron reduction method is necessary to efficiently generate the active species *in situ*. In this context, *Martin* and *Jellinek* reported in the 1960s that treatment of titanocene(IV) dichloride with two equivalents of allylMgBr affords an η^3-allyl-titanocene(III) complex.[149–151] They postulated a reaction scheme,[151] which can be described as follows: First, a chloride ligand is exchanged by an allyl ligand *via* a salt metathesis reaction while MgX_2 (X = halide) is formed as a by-product. Subsequently, the resulting allyl-titanocene(IV) chloride complex reduces itself to titanocene(III) chloride by

homolysis of the Ti–C bond. This step may be driven by the stability of the resulting allyl radical. Analogously to the first step, the remaining chloride ligand is then exchanged for an allyl ligand, forming a η^3-coordinated titanocene(III) allyl complex. It has been postulated that a sufficiently strong σ-donor solvent can induce a change in hapticity from η^3- to η^1-coordination (Scheme 44).[152]

Building on this strategy, *Gansäuer et al.* generated titanocene(III) hydride from the *in situ* formed η^1-titanocene(III) allyl complex bearing an additional solvent ligand *via* σ-CAM with phenyl silane (Scheme 44).[75] DFT calculations revealed a nearly thermoneutral activation barrier (0.6 kcal/mol) for this transformation. In comparison, the transformation of the previously employed $Cp_2Ti(III)Me$ is exergonic (–4.2 kcal/mol), and the conversion of $Cp_2Ti(III)Ph$ is endergonic (2.5 kcal/mol).[132]

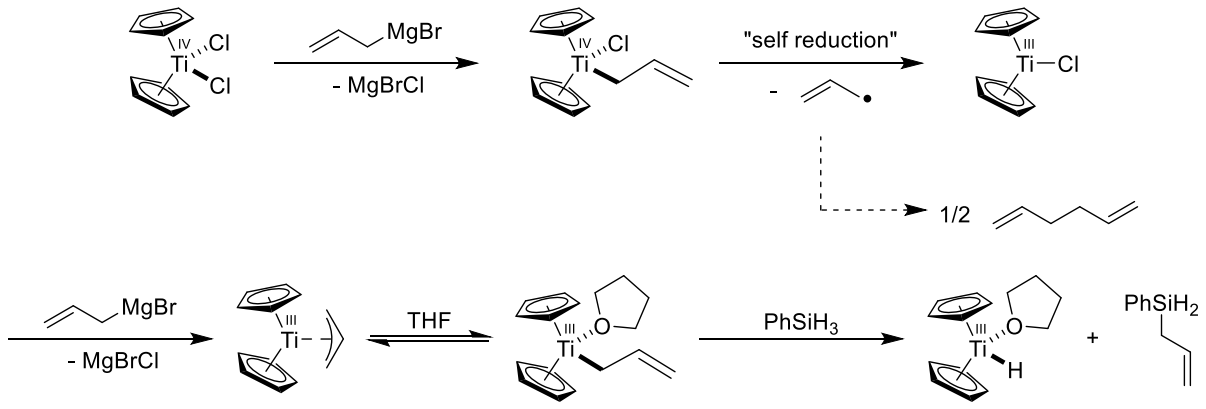

Scheme 44: Mechanism of the “allyl activation” method.[75]

Although the activation of $Cp_2Ti(III)Me$ is energetically favored, the allyl complex is preferred for practical reasons. The allyl-Ti(III)-species is readily generated *in situ* from the bench-stable titanocene(IV) dichloride under mild conditions, whereas $Cp_2Ti(III)Me$ must be prepared from the corresponding light-sensitive precatalyst. Moreover, reactions with Cp_2TiMe_2 often require heating due to the capricious activation.[75,131,132]

After establishing a mild activation protocol from the readily available, bench-stable titanocene dichloride, the ensuing mechanism was elucidated through kinetic and computational studies. “Same excess” experiments demonstrated that $Cp_2Ti(III)H$ barely undergoes inhibition or deactivation over the course of the reaction,[132] whereas, as previously discussed (Chapter 1.5),[99] $Cp_2Ti(III)Cl$ requires complexation with CoII*HCl to prevent deactivation. Kinetic studies on the rate order with respect to the different reactants revealed first-order in the catalyst, zeroth-order in phenyl silane, and inverse first-order in the epoxide. These findings indicate that none of the steps depicted in Scheme 39 constitute the rate-determining step. Therefore, they proposed that a second equivalent of the epoxide binds to the metal-center of the intermediate generated after the intramolecular HAT. The resulting complex is in equilibrium

with the $Cp_2Ti(III)OR$ complex and functions as the resting state of the catalytic cycle (Scheme 45). The return of the resting state to the catalytic cycle is the rate-determining step. Computational studies supported these assumptions, as the opening of epoxides with titanocene(III) alkoxide necessitates around 9 kcal/mol more energy than with titanocene(III) hydride. A screening experiment further demonstrated that no conversion was observed for epoxide opening with titanocene(III) alkoxide.[132]

Considering the “allyl-activation” procedure and the postulated resting state, the catalytic cycle can be described as follows.[132]

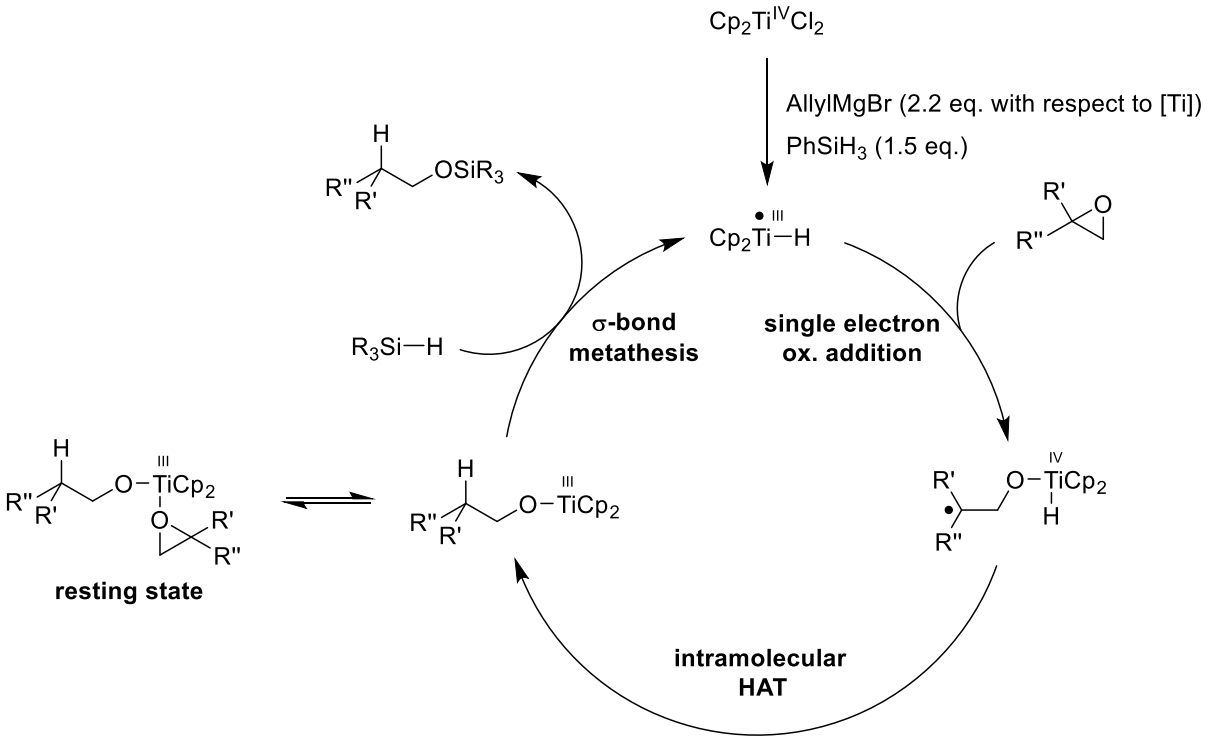

Scheme 45: Mechanism of the titanocene-catalyzed hydrosilylation of epoxides employing the allyl activation method.[132]

1.8.4 Third Study on the Titanocene-Catalyzed Hydrosilylation of Epoxides

In a later study by *Gansäuer et al.*, they selectively incorporated deuterium into the *β*-position of alcohols *via* titanocene-catalyzed deuterosilylation of epoxides with *anti-Markovnikov* selectivity. The deuterosilylation follows the mechanism shown in Scheme 45, with the seemingly slight difference of employing $PhSiD_3$ instead of $PhSiH_3$.[153] Deuteration allows for unique mechanistic insights by analyzing the magnitude and selectivity of deuterium incorporation (DI).[154–157] Moreover, deuteration is an attractive tool in drug synthesis, as deuterated drugs often retain their biochemical potency and selectivity while exhibiting altered metabolic profiles compared to their non-deuterated parent compounds.[158–161] This can be

rationalized by the different reactivities of the C–H and C–D bonds,[158–161] especially in P450 enzyme mediated processes.[161]

Suprisingly, the titanocene-catalyzed deuterosilylation of trisubstituted epoxides provided the respective alcohols with incomplete deuteration (~90%). Furthermore, the DI is affected by the substitution pattern of the epoxide (Scheme 46). This suggests off-cycle isotope scrambling, which occurs faster than epoxide opening.[153]

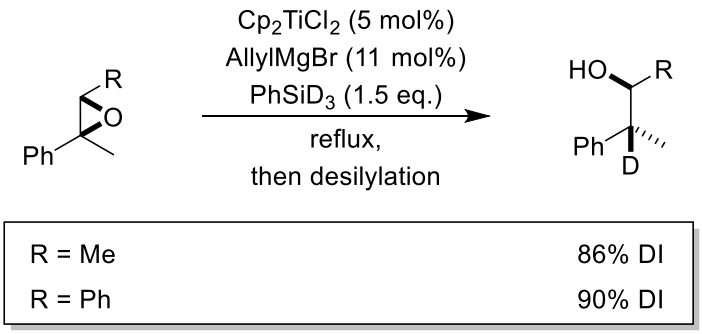

Scheme 46: Impact of substituents on the deuterosilylation of trisubstituted epoxides with respect to DI.[153]

An increase in the catalyst load, which is associated with a higher concentration of the by-products formed during activation, resulted in lower DI. Therefore, they suspected an H–D exchange between the by-products, 1,5-hexadiene or $PhSiH_2$allyl, and the active species. The theory was verified by the deliberate addition of stoichiometric amounts of 1,5-hexadiene, which resulted in an even lower DI. The exchange is realized by deuterometallation of the olefin, followed by *β*-hydride elimination (Scheme 47).[153]

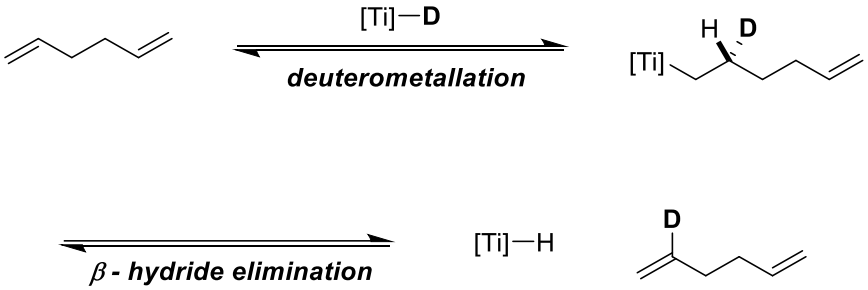

Scheme 47: Mechanism of the H–D exchange between Ti(III)D and 1,5-hexadiene.[153]

To avoid off-cycle isotope scrambling, an activation procedure had to be employed, which does not involve the formation of olefins as by-products. The similar stability of benzylic radicals to allylic radicals prompted them to use benzylMgBr to produce the active species. Indeed, the "benzyl activation" facilitated the formation of alcohols with complete deuteration (98% DI) at the *β*-position, as the by-product bibenzyl lacks olefinic bonds.[153] The mechanism of the "benzyl activation" is analogous to the activation using allylMgBr (Scheme 48).[75] However, the

rate of activation is higher due to the weaker η^3-coordination of the benzyl ligand to the metal center compared to that of an allyl ligand (see Chapter 3.2 for details).[162]

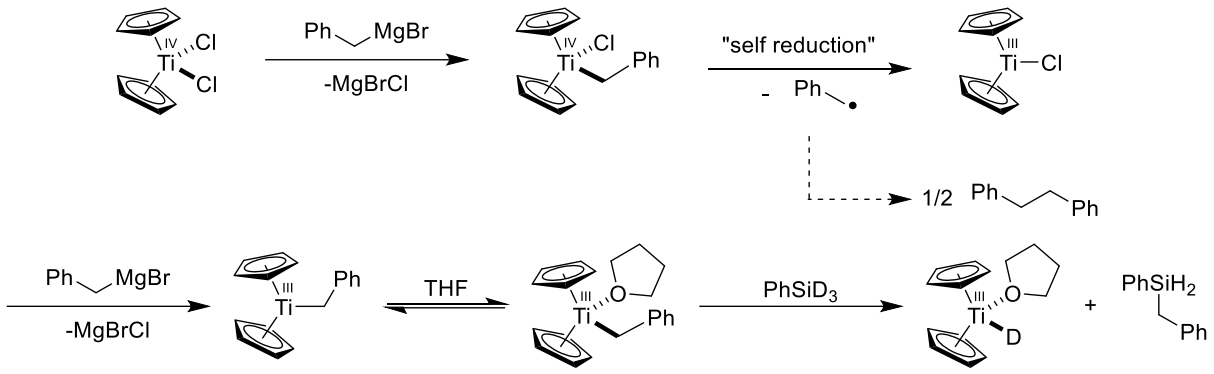

Scheme 48: Mechanism of the benzyl activation of titanocene dichloride.[75]

In addition to the high diastereoselectivity of the titanocene-catalyzed hydrosilylation, the pronounced regioselectivity of the deuterosilylation further proves the radical mechanism of the reaction.[153] A competing pathway involving *Meinwald*-rearrangement and reduction, which yields the *anti-Markovnikov* alcohol *via* an ionic mechanism, can be excluded, as it would give the *α*-deuterated alcohol (Scheme 49).[163,164]

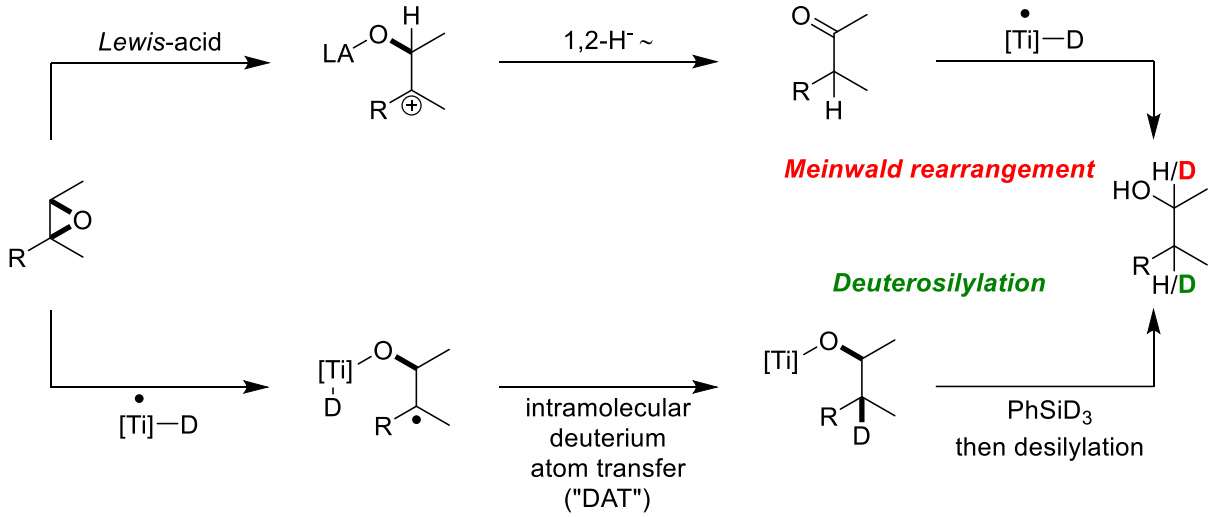

Scheme 49: Regioselectivity of the titanocene-catalyzed deuterosilylation and *Meinwald* rearrangement of trisubstituted epoxides.[153,163–165]

The *Meinwald* rearrangement involves the *Lewis*-acid-catalyzed opening of epoxides, followed by a 1,2-hydride shift. The resulting carbonyl group is reduced by the Ti(III)D-species.[164,165]

1.8.5 Fourth Study on the Titanocene-Catalyzed Hydrosilylation of Epoxides

Further studies of *Gansäuer et al.* focused on the employed silane in the titanocene-catalyzed hydrosilylation of epoxides. The commonly used phenyl silane is relatively expensive and may

yield polymeric by-products that are difficult to remove. Therefore, they investigated various silanes based on cost (Table 1).[133]

Table 1: Prices of silanes used in the titanocene-catalyzed hydrosilylation.[133]

reductant	relative price per mol H
$Ph(Me)SiH_2$	95
$PhSiH_3$	43
Et_3SiH	14
PMHS (13-25 cSt.)	1

Polymethylhydrosiloxane (PMHS) is by far the most cost-efficient silane, as it can be obtained from a by-product of the *Müller-Rochow* process, a key industrial process in the silicone industry (Scheme 50). Furthermore, it is an easy-to-handle, bench-stable, and non-toxic liquid.[133] The use of PMHS would make the hydrosilylation more sustainable, not only owing to its non-toxicity, but also because this industrial "waste product" is effectively recycled.[75]

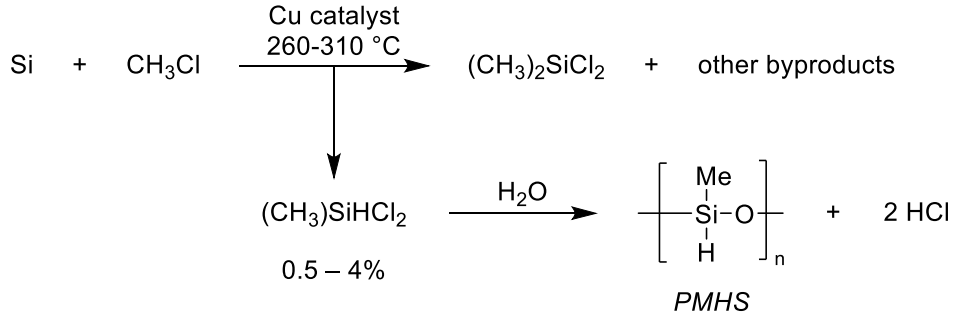

Scheme 50: Formation of PMHS as a by-product of the *Müller-Rochow* process.[166]

Initial experiments showed no formation of titanocene(III) hydride *via* benzyl activation with PMHS.[133] Previous calculations indicated a strongly endergonic *σ*-CAM for the reaction of $Cp_2Ti(III)allyl$ with $(EtO)_3SiH$, whereas the reaction with $PhSiH_3$ is nearly thermoneutral (Chapter 1.8.3).[153] Since PMHS is electronically more similar to $(EtO)_3SiH$ than to $PhSiH_3$, the *σ*-CAM reaction of $Cp_2Ti(III)Bn$ with PMHS is also expected to be endergonic. Thus, they employed substoichiometric amounts (2.5 mol%) of $PhSiH_3$, which served solely to activate the precatalyst. Successful conversion of the epoxide after activation indicates that the driving force of the second *σ*-CAM is sufficient, as the resulting Si–O bond is stronger than a Si–C bond. Nevertheless, the conversion to the desired product is surprisingly low.[133] Previous studies have already shown an increase in selectivity when using 1,4-dioxane as a solvent, as it precipitates the *Lewis* acidic Mg-salts responsible for the *Meinwald* rearrangement.[153] Yet,

using 1,4-dioxane as the sole solvent resulted in a similarly low conversion. However, its use as a cosolvent alongside THF facilitated complete conversion (Scheme 51).[133]

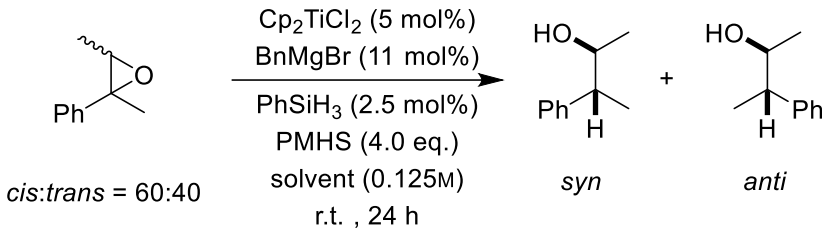

solvent	conversion/%	*d.r.* (*syn*:*anti*)
THF	9	-
1,4-dioxane	12	-
THF:1,4-dioxane (1:1)	**100**	**96:4**

Scheme 51: Solvent screening of the titanocene-catalyzed hydrosilylation using PMHS.[133]

Furthermore, the use of PMHS obviates the need for bulky titanocenes, such as (tBuC$_5$H$_4$)$_2$TiCl$_2$, to achieve high diastereoselectivity. Instead, using commercially available titanocene dichloride is sufficient to yield the desired alcohol in satisfactory diastereomeric excess.[133] *Gansäuer et al.* proposed that coordination of PMHS to the titanocene prior to the intramolecular HAT induces the observed high selectivity (Scheme 52).[133]

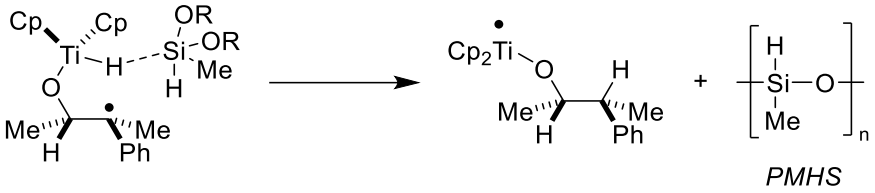

Scheme 52: Coordination of PMHS to the titanocene before the intramolecular HAT.[133]

The catalytic cycle of the titanocene-catalyzed hydrosilylation of epoxides, employing PMHS for the second σ-CAM, is shown below.[75,133]

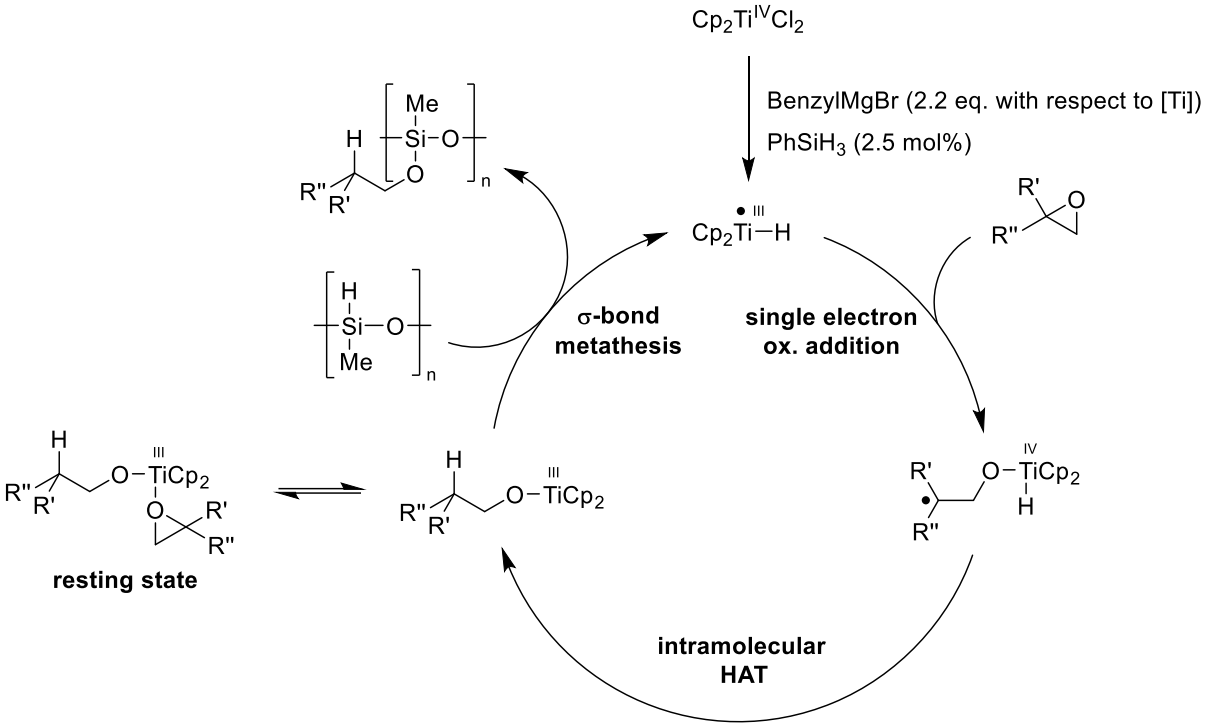

Scheme 53: Catalytic cycle of the titanocene-catalyzed hydrosilylation of epoxides using PMHS.[75,133]

In conclusion, the studies by *Gansäuer et al.* established a sustainable, catalytic, chemo- and stereoselective method for the opening of epoxides to yield *anti-Markovnikov* alcohols.[75]

2. Aim of this Work

This work aims to investigate the titanocene-catalyzed hydrosilylation. In particular, it focuses on combining the catalytic system with a suitable epoxidation method to readily access stereochemically enriched *anti-Markovnikov* alcohols. Moreover, it addresses solutions to the relatively low regioselectivity in the ring opening of monosubstituted, aliphatic epoxides. Finally, it evaluates whether comparable efficiency can be achieved when applied to oxetanes.

The first task involves developing an enantioselective formal addition of H_2O to trisubstituted olefins without the need for the tedious separation of intermediary undesired diastereomers. Previous studies by *Gansäuer et al.* on the titanocene-catalyzed hydrosilylation demonstrated that the intramolecular HAT step sets the stereoinformation at the benzylic position relative to the homobenzylic center independent of the epoxide's relative configuration (Chapter 1.8.2).[131] Therefore, an epoxidation method is necessary that fixes the stereoinformation at the homobenzylic center with high selectivity, regardless of the olefin's geometry (Scheme 54). Moreover, the enantioselective epoxidation method should be applicable to unfunctionalized trisubstituted olefins to provide a general strategy.

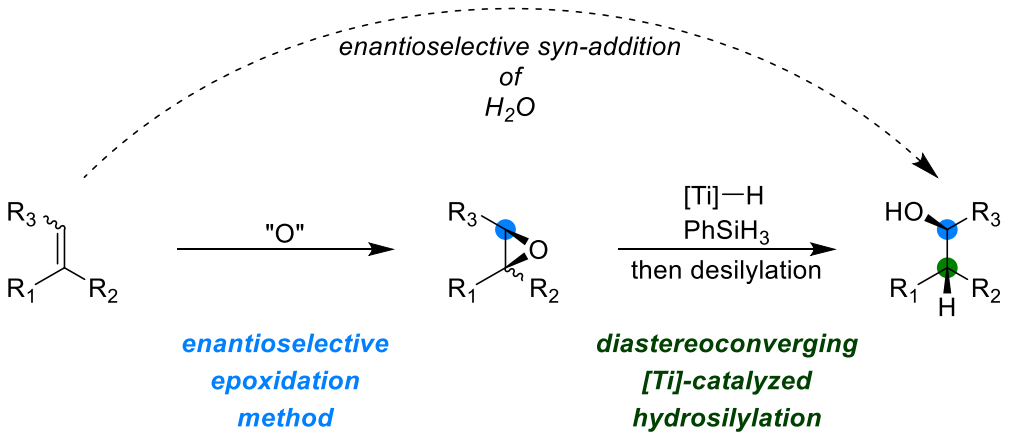

Scheme 54: Diastereo- and enantioselective formal addition of H_2O to olefins by combining an enantioselective epoxidation method with the stereoconverging hydrosilylation.

The second objective focuses on improving the efficiency of the titanocene-catalyzed reductive opening of monosubstituted epoxides. Both systems described in Chapters 1.5 and 1.8 exhibit poor performance in the reductive opening of monosubstituted substrates.[70,131] While the system discussed in Chapter 1.5 provided satisfying regioselectivity (94:6) for the opening of 1,2-epoxydodecane, it generated the desired alcohol with moderate yield (Scheme 21). Furthermore, a minor amount of the deoxygenation product was formed as a by-product (Scheme 21).[70] Employing the titanocene-catalyzed hydrosilylation (see Chapter 1.8.2) improves the sustainability and suppresses the competing deoxygenation. However, the

regioselectivity is reduced (78:22).[131] The design of novel hydrosilylation catalysts could circumvent this issue (Scheme 55).

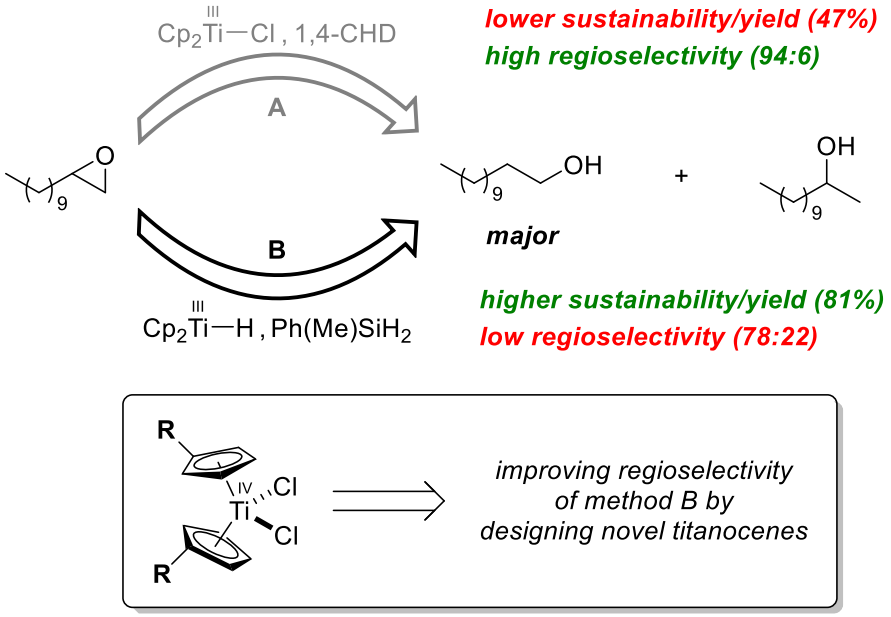

Scheme 55: Properties of two methods for the titanocene-catalyzed reductive opening of epoxides developed by *Gansäuer et al*., design of novel titanocenes to overcome drawbacks of hydrosilylation.[70,131]

The last task deals with the titanocene-catalyzed reductive opening of oxetanes. As described in Chapter 1.7, oxetane opening is less efficient than the corresponding opening of epoxides. The lower performance is reflected in low yields and selectivity. Presumably, the higher activation barrier for ring opening and the slow addition of the trapping agent affect the yields and selectivity.[101]

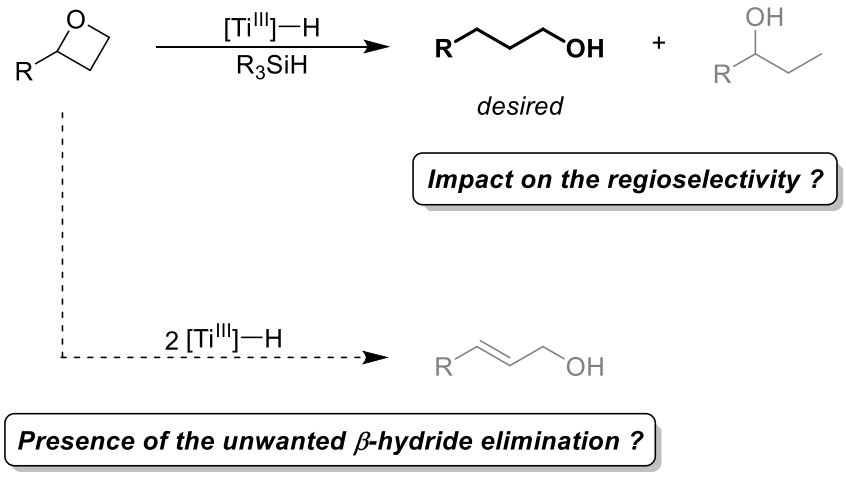

Scheme 56: Impact of titanocene(III) hydride as the active species on the regioselectivity and the reaction selectivity of the titanocene-catalyzed reductive oxetane opening.

Using titanocene(III) hydride instead of titanocene(III) chloride as the active species has been shown to increase the selectivity of the desired radical pathway during epoxide opening.[70,131] Based on this, the hydrosilylation is applied to oxetanes to investigate whether similar improvements can be achieved (Scheme 56).

3. Results and Discussion

3.1 Diastereoconvergent Hydrosilylation of Enantioenriched Epoxides towards Optically Active *Anti-Markovnikov* Alcohols

The preparation of adjacent stereocenters with control over both relative and absolute configuration constitutes a key strategy in natural product synthesis and drug development.[167] In this context, titanocene-catalyzed hydrosilylation combined with a suitable epoxidation method could potentially provide a valuable synthetic approach.

The titanocene-catalyzed hydrosilylation of trisubstituted benzylic epoxides offers a straightforward approach to *anti-Markovnikov* alcohols with relative stereochemical control. This can be attributed to the stereodefining intramolecular HAT step. It sets the stereoinformation at the benzylic position relative to the homobenzylic center, independent of the epoxide's relative configuration.[131] To access *anti-Markovnikov* alcohols, which are diastereomerically ***and*** enantiomerically enriched, an epoxidation method is required that fixes the stereoinformation at the homobenzylic center with high enantioselectivity. Importantly, the enantioselective epoxidation method must afford the same absolute configuration at the less-substituted carbon regardless of the olefin's geometry. To establish a general strategy, the enantioselective epoxidation method should be applicable to unfunctionalized trisubstituted olefins.

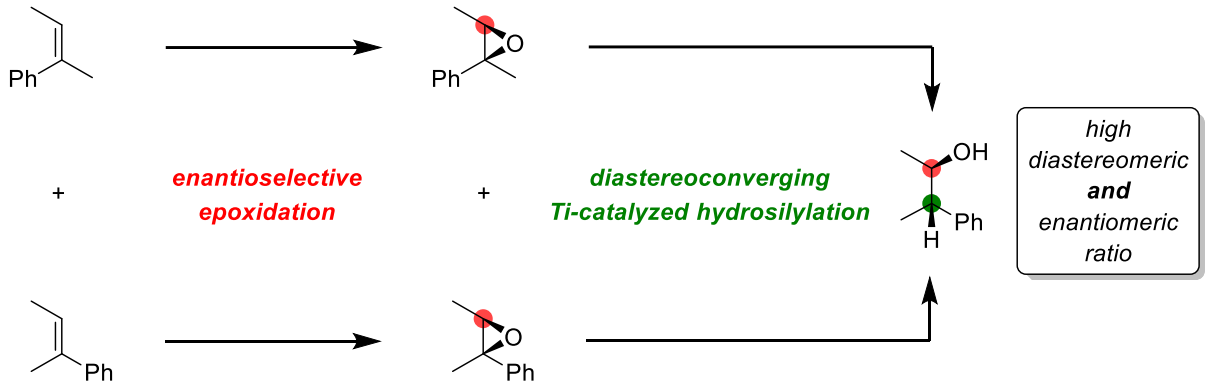

Scheme 57: Two-step sequence from a mixture of trisubstituted olefins to a single isomer of an *anti-Markovnikov* alcohol with high *d.r.* and *e.r.* through enantioselective epoxidation followed by stereoconverging hydrosilylation.

Notably, the diastereomeric olefin mixture does not require tedious prior separation due to the diastereoconvergence of the titanocene-catalyzed hydrosilylation.[131] Consequently, less waste is produced, and a simple *Wittig* olefination[168] from commercially available substrates is sufficient.

To develop a general process, epoxidation reactions requiring a directing group (DG), such as the *Sharpless* epoxidation,[78] are excluded from our investigations (Scheme 58). Strategies,

including the enantioselective synthesis of diols,[169] followed by cyclization[170] reduce the sustainability and efficiency (Scheme 58). Thus, we investigated catalytic asymmetric one-step oxidation reactions suitable for unfunctionalized alkenes, such as the *Jacobsen* and *Shi* epoxidation,[86,171] described in Chapter 1.4.

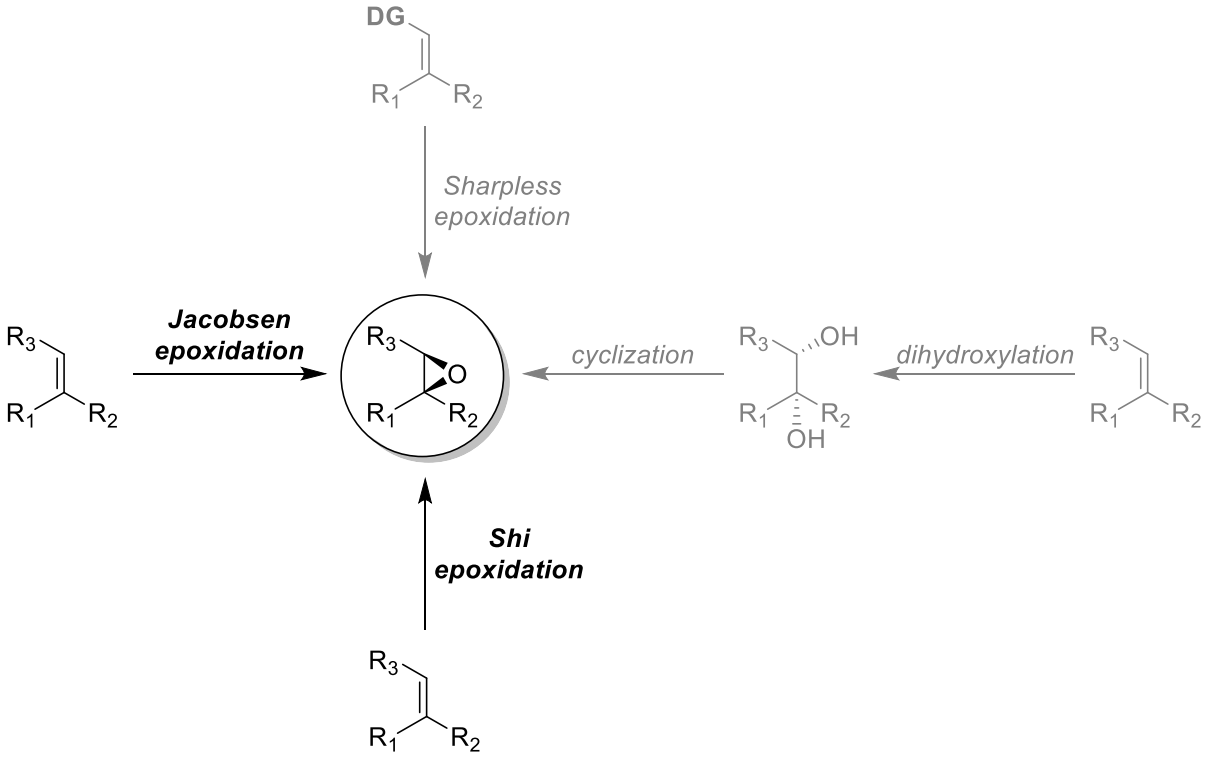

Scheme 58: Different methods to synthesize enantiomerically enriched trisubstituted epoxides; grey-coloured transformations are disfavored for the requirement of directing groups (DG) or inefficiency.[78,86,169,171]

Both methods facilitate efficient stereoselective transformation of unfunctionalized alkenes.[86,171] To determine which method suits our strategy best, both epoxidation reactions will be discussed in more detail, focusing on selectivity and sustainability.

Jacobsen et al. employed their second-generation catalyst (Scheme 10) not only for the transformation of *cis*-disubstituted alkenes, but also for the oxidation of trisubstituted alkenes. They reported high *ee*'s (>90%) for cyclic and bulkier acyclic olefins. The underlying selectivity of these reactions was explained with a simplified model (Scheme 59).[171] Transition state **B** involves pronounced steric interactions between the larger substituent of the less-substituted carbon and the nearly planar ligand plane of the catalyst. In contrast, steric repulsion is avoided in TS-**A** as the hydrogen substituent points towards the plane.[171] The substituents of the higher-substituted carbon are too far from the ligand plane to cause significant steric repulsion. Therefore, their impact on the selectivity is negligible. This model suggests a fixed

configuration at the less-substituted carbon, regardless of the olefin's geometry, whereas the configuration of the other carbon center is governed by the olefin's geometry.

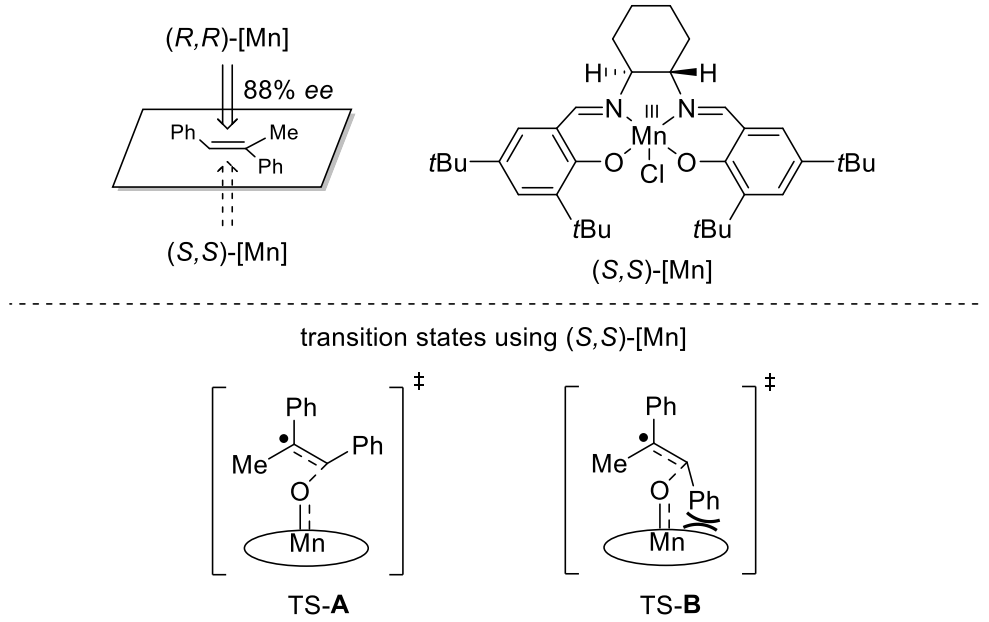

Scheme 59: Transition states of the *Jacobsen* epoxidation of trisubstituted olefins using the second generation (*S,S*)-Mn(III) salen catalyst.[171]

Norrby et al. applied *Jacobsen*'s conditions to the isolated (*E*)- and (Z)-isomer of *α*,*β*-dimethylstyrene using the catalyst shown in Scheme 59. The results supported this model (Scheme 59), as the absolute configuration of the less-substituted carbon was controlled with equal selectivity irrespective of the olefin's geometry. However, the resulting enantiomeric excess was relatively low (71–73%).[172] Presumably, the *Jacobsen* epoxidation of less bulky substrates, such as *α*,*β*-dimethylstyrene, leads to reduced enantioselectivity. Nevertheless, *Höthker* performed the oxidation of *α*,*β*-dimethylstyrene according to *Jacobsen*'s procedure (Scheme 60).[171] Yet, he failed to reproduce the yield shown in the literature, as only 5% conversion was achieved. Due to the difficulty in reproducing the *Jacobsen* epoxidation of *α*,*β*-dimethylstyrene efficiently and the resulting low *ee* according to *Norrby*'s study,[172] the focus was laid on the *Shi* epoxidation.

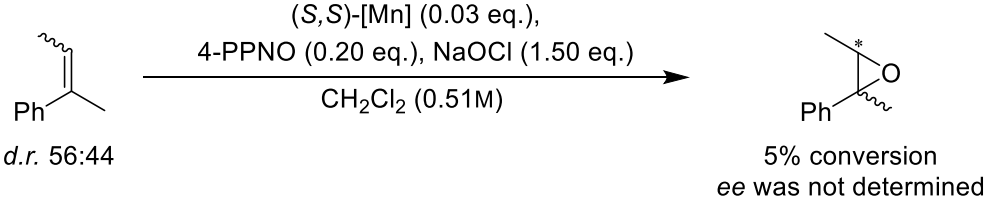

Scheme 60: Attempted *Jacobsen* epoxidation of a diastereomeric mixture of *α*,*β*-dimethylstyrene; performed by *Höthker*.

In contrast to the *Jacobsen* epoxidation, *Shi et al.* reported a high *ee* (96.8%) for the conversion of *α*,*β*-dimethylstyrene.[86] As discussed in Chapter 1.4.1, they used a fructose-derived precatalyst, which is activated *via* the addition of Oxone®. The addition of the active dioxirane to *α*,*β*-dimethylstyrene yielded the epoxide in high enantiomeric excess.[86] To understand the high enantioselectivity, the corresponding transition states will be analyzed. Generally, eight distinct transition states are possible for the addition of the active dioxirane (activation and structure shown in Scheme 14) to the olefin. Half of these represent a planar approach of the dioxirane to the substrate, whereas the remaining four correspond to a spiro-oriented approach (Figure 13). In the planar transition states, the dioxirane group is oriented parallel to the olefin, while in the spiro transition states, it is perpendicular to the alkene. In all cases, the substrate exclusively attacks the dioxirane from the top face, as the bottom face is sterically hindered by one of the acetonide groups (Figure 12).[86]

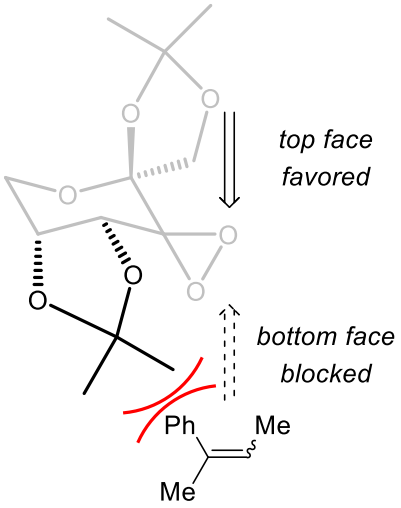

Figure 12: Approach of the trisubstituted olefin to the dioxirane from the top and bottom face; blocked bottom face due to one of the bulky acetonide groups.

The other acetonide group limits the possible orientations of the substrate when it approaches from the top face. Six of the transition states (Planar/Spiro-**A**–**C**) exhibit pronounced steric repulsion between the top face acetonide group and one of the larger moieties (Me or Ph) of the olefin (Figure 13). Only the remaining two transition states (Planar/Spiro-**D**) are sterically favored (Figure 13). In these TS, the smallest residue, hydrogen, points towards the respective acetonide group. Consequently, the selectivity of the oxidation of trisubstituted olefins is primarily controlled by the orientation of the residues at the less-substituted carbon. As a result, both the corresponding (*E*)- and (*Z*)-isomers lead to the same configuration at the less-substituted carbon. On the other hand, the produced configuration at the higher substituted carbon depends on the olefin's geometry.[86]

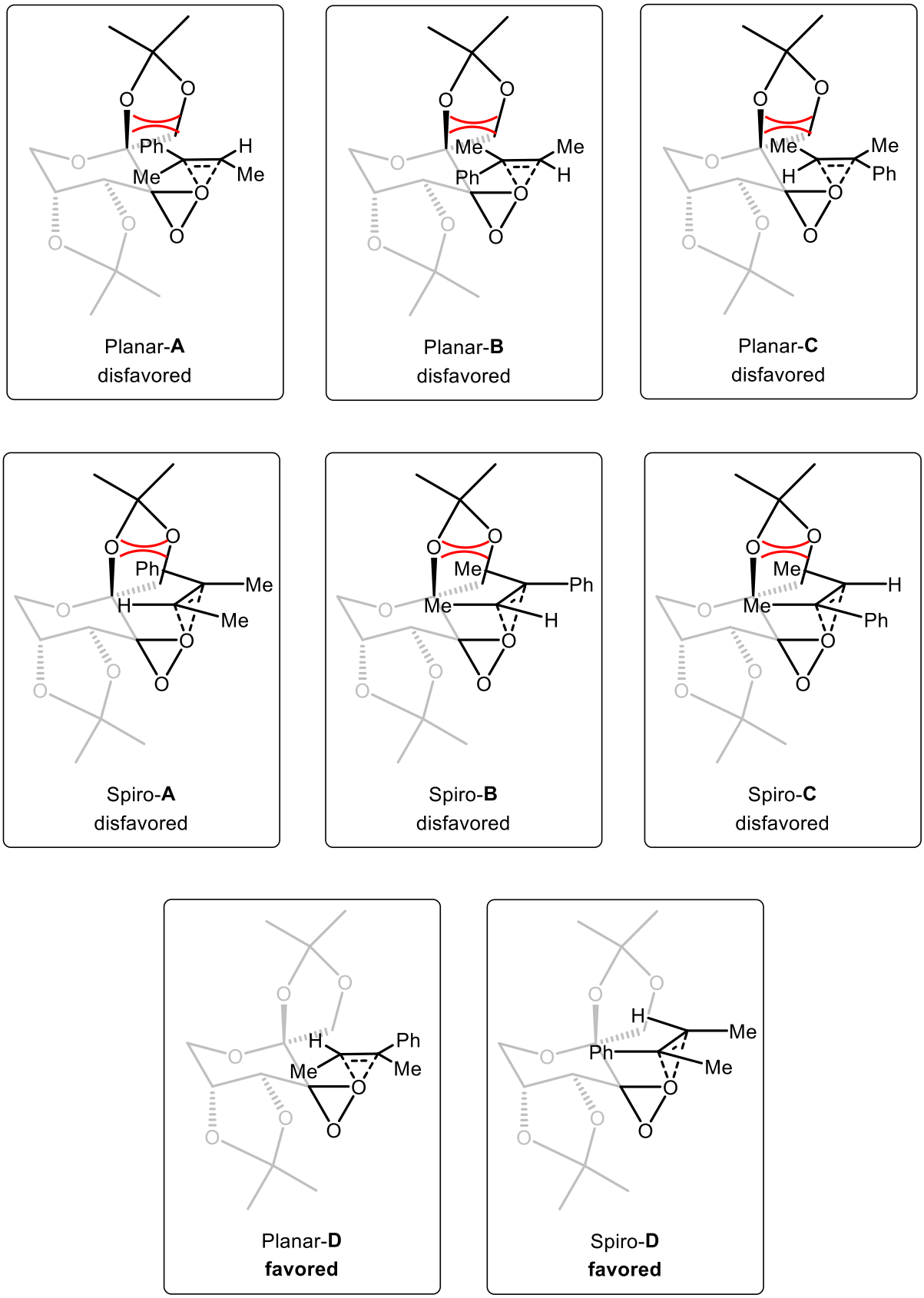

Figure 13: Spiro and planar transition states for the *Shi* epoxidation of (*E*)-*α*,*β*-dimethylstyrene.[86]

To determine whether the planar-**D** or the spiro-**D** transition state is the most favored TS, electronic factors have to be considered. *Bach et al.* proposed stabilizing electronic interactions between the oxygen lone pairs of the dioxirane and the π^* orbital of the olefin. In the planar transition state, the orbital planes are perpendicular to each other. Thus, orbital overlap is not possible. In contrast, for the spiro approach, orbital overlap is possible as they are aligned parallel to each other (Scheme 61).[86,173] Therefore, the spiro TS is assumed to be the favored one according to *Shi*. As a result, the *Shi* epoxidation of (*E*)-*α*,*β*-dimethylstyrene affords the (*R*)-configuration at the less-substituted carbon (Scheme 61).[86]

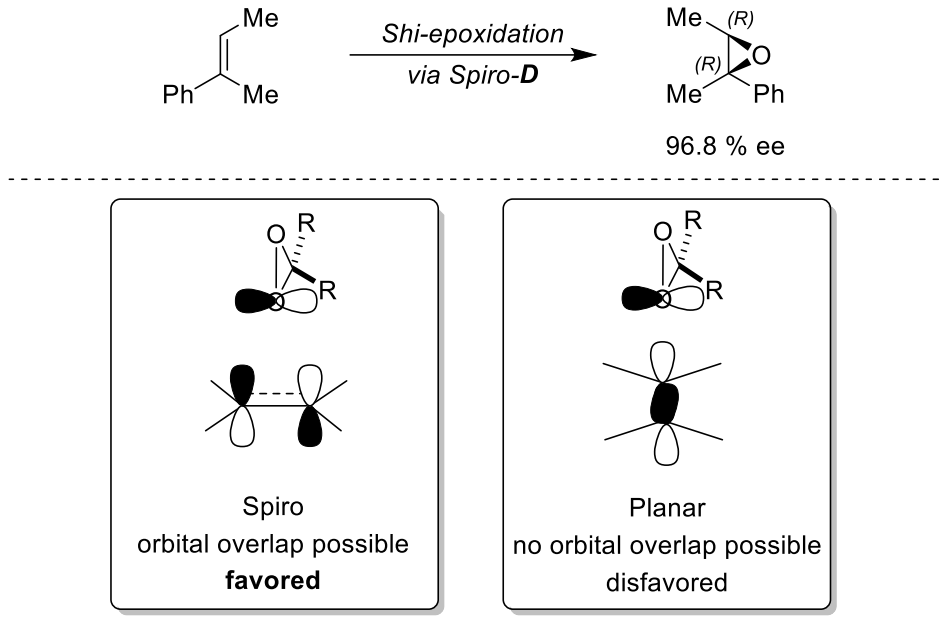

Scheme 61: *Shi* epoxidation of *α*,*β*-dimethylstyrene *via* spiro-**D** and illustration of stabilizing electronic interactions present in spiro-TS in contrast to planar transition states.[86]

In addition to its superior enantioselectivity for the conversion of *α*,*β*-dimethylstyrene, the *Shi* epoxidation relies on a more sustainable catalyst. As outlined in Chapter 1.4.1, the catalyst is readily synthesized from the inexpensive and sustainable D-Fructose (Scheme 12).[86] While a comparable yield was obtained for the first step, reproduction of the literature yield (93%) in the second step was not successful (Table 2). Instead, a yield of 17% was observed by *Höthker*.

Table 2: Screening conditions for the oxidation of alcohol **1** to the *Shi* catalyst **2**.[148,162]

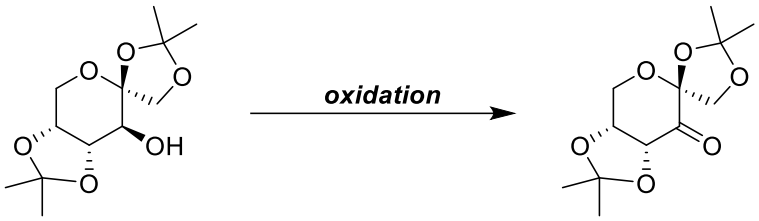

1
(obtained in 45% yield from D-Fructose)

2

oxidation	reagents	solvent	time	temperature	yield
A[a]	PCC (2.7 eq.), 3Å MS	CH_2Cl_2	3 h	r.t.	17%
B[a]	PCC (4.7 eq.), Florisil®	CH_2Cl_2	46 h	r.t.	25%
C[a]	$RuCl_3$ x nH_2O (3 mol%), $BnNEt_3Cl$ (5 mol%), K_2CO_3 (15 mol%), $NaIO_4$ (1.5 eq.)	H_2O, $CHCl_3$	2 h	75 °C	no conversion
D	$RuCl_3$ x H_2O (2 mol%), $BnNEt_3Cl$ (5 mol%), K_2CO_3 (15 mol%), $NaIO_4$ (1.5 eq.)	H_2O, $CHCl_3$	6 h	75 °C	33%
E[a]	PDC (1.4 eq.), HOAc (trace), 3Å MS	CH_2Cl_2	19 h	r.t.	86%

[a]performed by *Höthker*.

Subsequently, he replaced molecular sieves with Florisil® and employed reflux conditions to slightly increase the yield (25%). To further enhance the yield, *Höthker* then applied different conditions[174] similar to those used in the *Ley Griffith*[175] oxidation. However, no conversion was observed when using the [$RuCl_3$ x nH_2O] complex. Within the scope of this work, these conditions were investigated with the monohydrate complex. Gratifyingly, the yield of the oxidation was further increased to 33%. Finally, *Höthker* discovered that the use of pyridinium dichromate (PDC) along with catalytic amounts of acetic acid leads to the best result (86%).[162]

After identifying a potentially suitable epoxidation method and developing a reproducible and high-yielding synthetic route to the respective catalyst, we evaluated the synergy of the titanocene-catalyzed hydrosilylation with the *Shi* epoxidation. For the titanocene-catalyzed hydrosilylation, two methods differing in the choice of the precatalyst, silane, and solvent were investigated. Earlier studies (Scheme 41) already highlighted the beneficial impact of bulkier titanocene catalysts on the diastereoselectivity of the epoxide reduction when using phenyl silanes.[131] Therefore, we used $PhSiH_3$ along with $(t\text{Bu}C_5H_4)_2TiCl_2$ in THF to achieve optimal

diastereoselectivity in method **A**. In method **B**, we employed PMHS and commercially available titanocene dichloride Cp_2TiCl_2 in THF/1,4-dioxane (1:1). The unmodified titanocene dichloride is sufficient for this method to proceed with high diastereoselectivity, as shown by previous results (Scheme 51), due to the coordination of the bulky PMHS to the metal center prior to the intramolecular HAT (Scheme 52).[133]

To evaluate our strategy, we tested it on a diastereomeric mixture of *α*,*β*-dimethylstyrene and the respective isolated (*Z*)-isomer. The substrate was prepared from the corresponding commercially available ketone *via Wittig* olefination.[168] However, only the crucial two steps will be discussed in the following (Scheme 62).

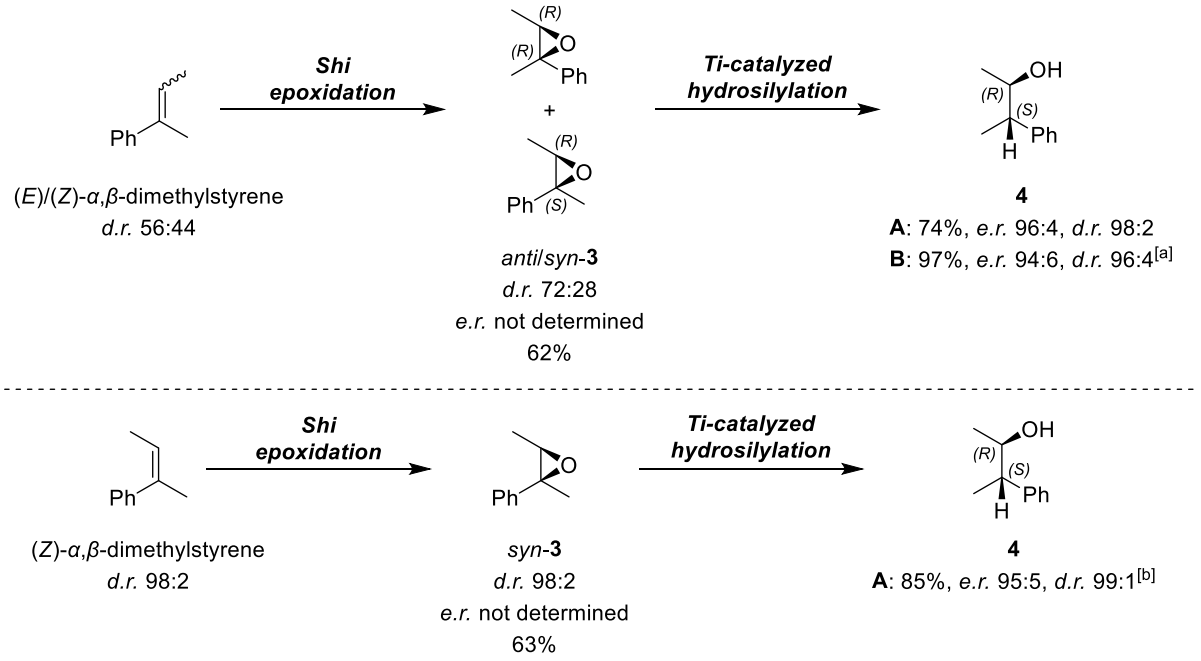

Scheme 62: Application of the *Shi* epoxidation followed by titanocene-catalyzed hydrosilylation on a diastereomeric mixture of *α*,*β*-dimethylstyrene and the isolated (*Z*)-isomer; method **A**: $(t\text{BuC}_5\text{H}_4)_2\text{TiCl}_2$ (5 mol%), BnMgBr(11 mol%), $PhSiH_3$ (1.5 eq.), THF; method **B**: Cp_2TiCl_2 (5 mol%), BnMgBr(11 mol%), $PhSiH_3$ (2.5 mol%), PMHS (4.0 eq.), THF/1,4-dioxane (1:1); [a]performed by *Mika*; [b]performed by *Höthker*.[148]

Gratifyingly, our synthetic route afforded the desired alcohol with similarly high enantio- and diastereoselectivity from both, the diastereomeric mixture and the purely (*Z*)-substituted olefin, thereby validating our concept. This demonstrates that both methods can be combined without affecting each other. The high diastereomeric ratio reflects the diastereoconvergent nature of the epoxide reduction, while the enantiomeric ratio (*e.r.*) proves the high selectivity of the *Shi* epoxidation in establishing the “upper” stereocenter with (*R*)-configuration, independent of the olefin’s geometry. Comparison with the results of the converted isolated isomer confirms the selectivity of the *Shi* epoxidation. Furthermore, both titanocene-catalyzed hydrosilylation

methods provide the alcohol with high diastereoselectivity. It is worth noting that method **B** produces the alcohol with noticeably higher yields.

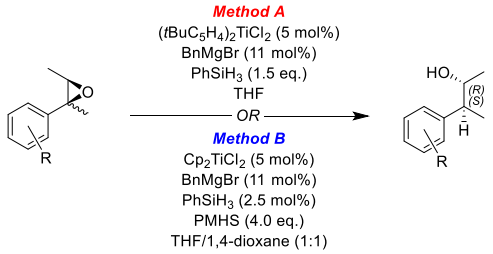

4
A
d.r. substrate 72:28
74%, *d.r.* 98:2, ***e.r.* 96:4**
B
d.r. substrate 72:28[a]
97%, *d.r.* 96:4, ***e.r.* 94:6**

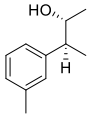

5
A
d.r. substrate 74:26[a]
50%, *d.r.* 96:4, ***e.r.* 98:2**
B
d.r. substrate 74:26
89%, *d.r.* 99:1, ***e.r.* 97:3**

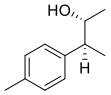

6
A
d.r. substrate 53:47
76%, *d.r.* 98:2, ***e.r.* 95:5**
B
d.r. substrate 53:47
80%, *d.r.* 95:5, ***e.r.* 93:7**

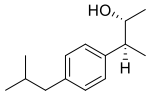

7
A
d.r. substrate 49:51[b]
87%, *d.r.* 97:3, ***e.r.* 96:4**
B
d.r. substrate 49:51[b]
88%, *d.r.* 94:6, ***e.r.* 95:5**

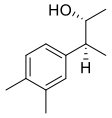

8
A
d.r. substrate 74:26[b]
76%, *d.r.* 96:4, ***e.r.* 96:4**
B
d.r. substrate 74:26[a]
73%, *d.r.* >99:1[c], ***e.r.* 96:4**

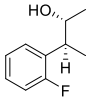

9
A
d.r. substrate 76:24
70%, *d.r.* 98:2, ***e.r.* 96:4**
B
d.r. substrate 76:24
53%, *d.r.* 99:1, ***e.r.* 95:5**

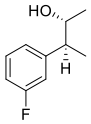

10
A
d.r. substrate 84:16[a]
64%, *d.r.* 95:5, ***e.r.* 98:2**
B
unclean reaction

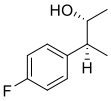

11
A
d.r. substrate 77:23
77%, *d.r.* 97:3, ***e.r.* 96:4**
B
unclean reaction

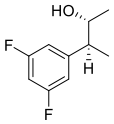

12
A
d.r. substrate 77:23[b]
79%, *d.r.* 97:3, ***e.r.* 98:2**
B
d.r. substrate 77:23[a]
73%, *d.r.* 96:4, ***e.r.* 98:2**

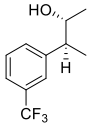

13
A
d.r. substrate 78:22
57%, *d.r.* 99:1, ***e.r.* 98:2**
B
d.r. substrate 78:22
67%, *d.r.* 97:3, ***e.r.* 98:2**

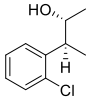

14
A
d.r. substrate 32:68
68%, *d.r.* 93:7, ***e.r.* 96:4**
B
d.r. substrate 32:68
74%, *d.r.* 96:4, ***e.r.* 96:4**

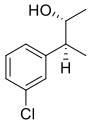

15
A
d.r. substrate 77:23[a]
82%, *d.r.* 97:3, ***e.r.* 98:2**
B
d.r. substrate 77:23[b]
84%, *d.r.* 93:7, ***e.r.* 98:2**

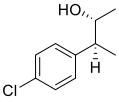

16
A
d.r. substrate 75:25
70%, *d.r.* 98:2, ***e.r.* 97:3**
B
d.r. substrate 75:25
63%, *d.r.* 99:1, ***e.r.* 96:4**

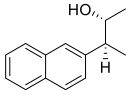

17
A
d.r. substrate 82:18[b]
85%, *d.r.* 97:3, ***e.r.* 96:4**
B
d.r. substrate 82:18[b]
74%, *d.r.* 92:8, ***e.r.* 96:4**

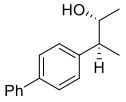

18
A
d.r. substrate 72:28[b]
65%, *d.r.* 97:3, ***e.r.* 96:4**
B
d.r. substrate 72:28[b]
91%, *d.r.* 95:5, ***e.r.* 97:3**

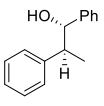

19
A
d.r. substrate 36:64[a]
81%, *d.r.* 96:4, ***e.r.* 95:5**
B
d.r. substrate 44:56[b]
67%, *d.r.* 97:3, ***e.r.* 95.5**

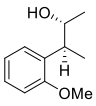

20
A
d.r. substrate 36:64[b]
82%, *d.r.* 97:3, ***e.r.* 97:3**
B
d.r. substrate 36:64[b]
74%, *d.r.* 97:3, ***e.r.* 96:4**

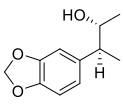

21
A
d.r. substrate 77:23[b]
87%, *d.r.* 96:4, ***e.r.* 93:7**
B
d.r. substrate 77:23[b]
92%, *d.r.* 94:6, ***e.r.* 92:8**

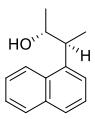

22
A
d.r. substrate 34:55:11[b,d]
82%, *d.r.* 99:1, ***e.r.* 95:5**
B
d.r. substrate 34:55:11[b,d]
83%, *d.r.* 94:6, ***e.r.* 96:4**

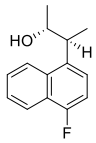

23
A
d.r. substrate 43:48:9[b,d]
81%, *d.r.* >99:1, ***e.r.* 95:5**
B
d.r. substrate 43:48:9[b,d]
81%, *d.r.* 95:5, ***e.r.* 95:5**

Scheme 63: Results for the converging titanocene-catalyzed hydrosilylation of numerous styrene oxide derivatives; diastereomeric ratios of the substrates are shown as *anti*:*syn* ratios; [a]performed by *Mika*; [b]performed by *Höthker*; [c]minor diastereomer separated by flash chromatography; [d]diastereomeric ratio indicated as *anti*:*syn*(1):*syn*(2) ratio.[148]

To determine if this observation was just coincidental or if the more cost-efficient and sustainable method, as outlined in Chapter 1.8.5, is indeed also superior regarding the yields, both methods are applied to numerous other styrene oxide derivatives (Scheme 63).

Independent of the substitution pattern, our “converging-divergence” strategy yields the desired *anti-Markovnikov* alcohols in high diastereomeric and enantiomeric ratios (Scheme 63). While both methods provide the alcohols with a similarly high diastereomeric ratio, differences in the yields become evident. However, no clear winner in terms of yields is observed. Whereas method **B** provides alcohols **4**, **5**, **13**, and **18** with higher yields, method A affords **10**, **11**, **17**, **19**, and **9** with superior yields (Scheme 63). In the case of **10** and **11**, method **B** forms an inseparable allylic alcohol as a side product, as demonstrated by the NMR spectrum of **11** (Figure 14). The allylic alcohol is formed *via* *β*-hydride elimination, analogous to the mechanism shown in Scheme 35. This pathway is likely favored because prior coordination of PMHS to the metal center (Scheme 52) retards the intramolecular HAT step. Nevertheless, for the epoxide reduction according to method **A**, no formation of this side product was observed.

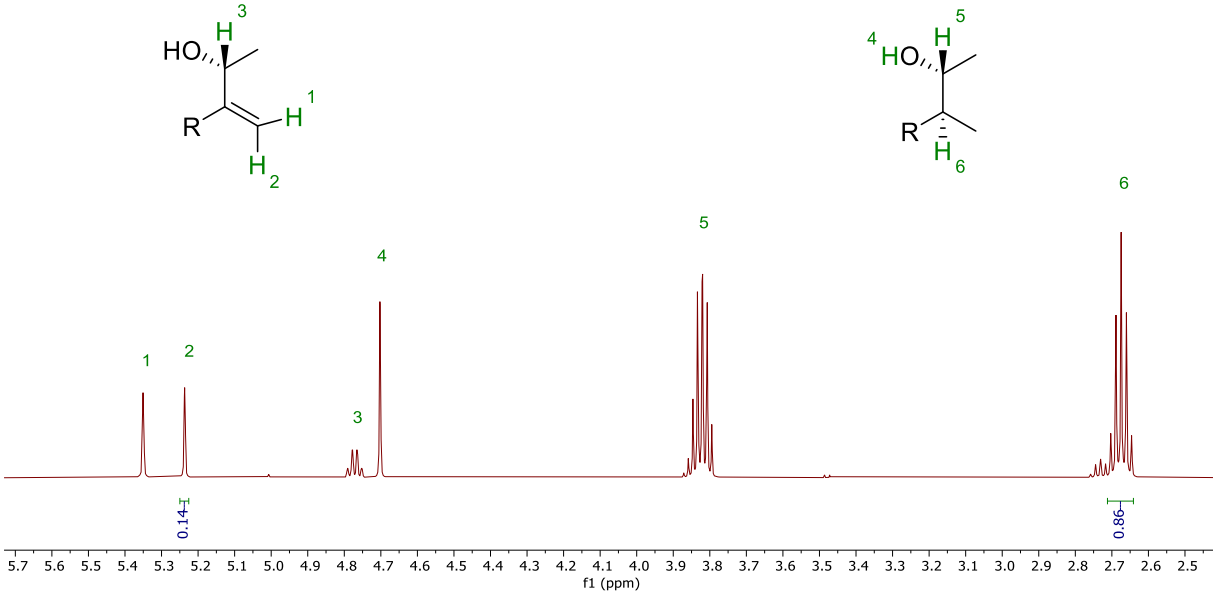

Figure 14: Characteristic signals of alcohol **11** and the corresponding allylic alcohol indicated in the ^{1}H-NMR spectrum.

Thus, the limitations of one method are compensated by the effectiveness of the other. The use of both methods renders this strategy more reliable in providing the alcohols with high yields and selectivity.

The enantiomeric ratios of the epoxides could not be determined, due to commonly observed coelution of enantiomers upon chiral separation using chiral high performance liquid chromatography (HPLC). However, it is fair to assume that high enantiomeric ratios are obtained if the corresponding alcohol is yielded with excellent enantioselectivity. Furthermore, to demonstrate the overall performance of our strategy, only the *e.r.* of the final product is crucial. While the absolute configuration of the alcohols was not determined, their configuration can be confidently assigned based on *Shi*'s and *Gansäuer*'s corresponding transition states.[86,131] The *e.r.* was determined *via Mosher* ester analysis. After transforming the alcohols into the corresponding *Mosher* esters, ^{19}F-NMR spectra were recorded and the signals were integrated to determine the diastereomeric ratios of the *Mosher* esters, from which the *e.r.* was derived. To identify the characteristic signals, we synthesized racemic standards and stacked the NMR spectra, as shown below with alcohol **16**.

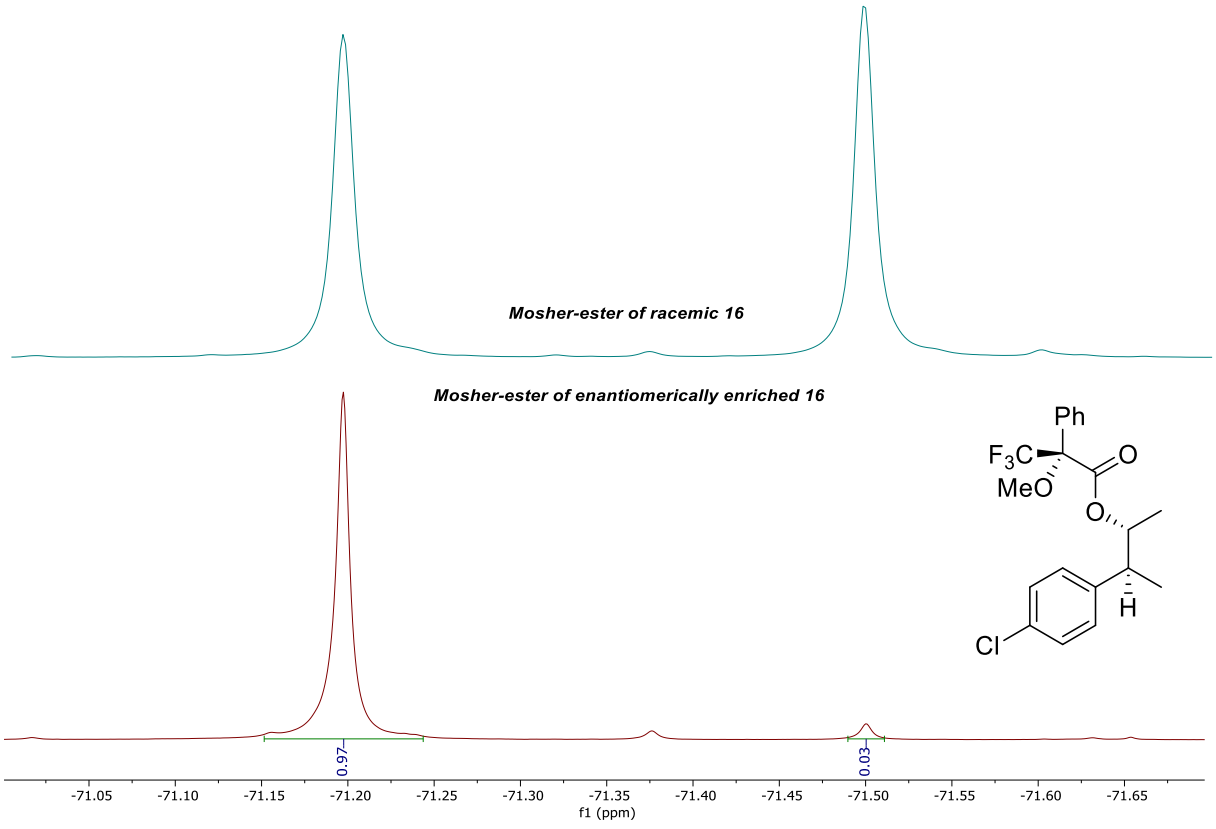

Figure 15: ^{19}F-NMR spectra for the corresponding racemic (top) and enantiomerically enriched (bottom) *Mosher*-esters synthesized from alcohol **16**.

The diastereomeric ratios of the intermediates and products were measured *via* integration of characteristic signals shown in the respective ^{1}H- and ^{13}C-NMR spectra. The *anti*-isomer of the epoxides is typically formed faster than the *syn*-isomer. This is consistent with *Shi*'s studies.[86] A few exceptions have been observed, which require comment.

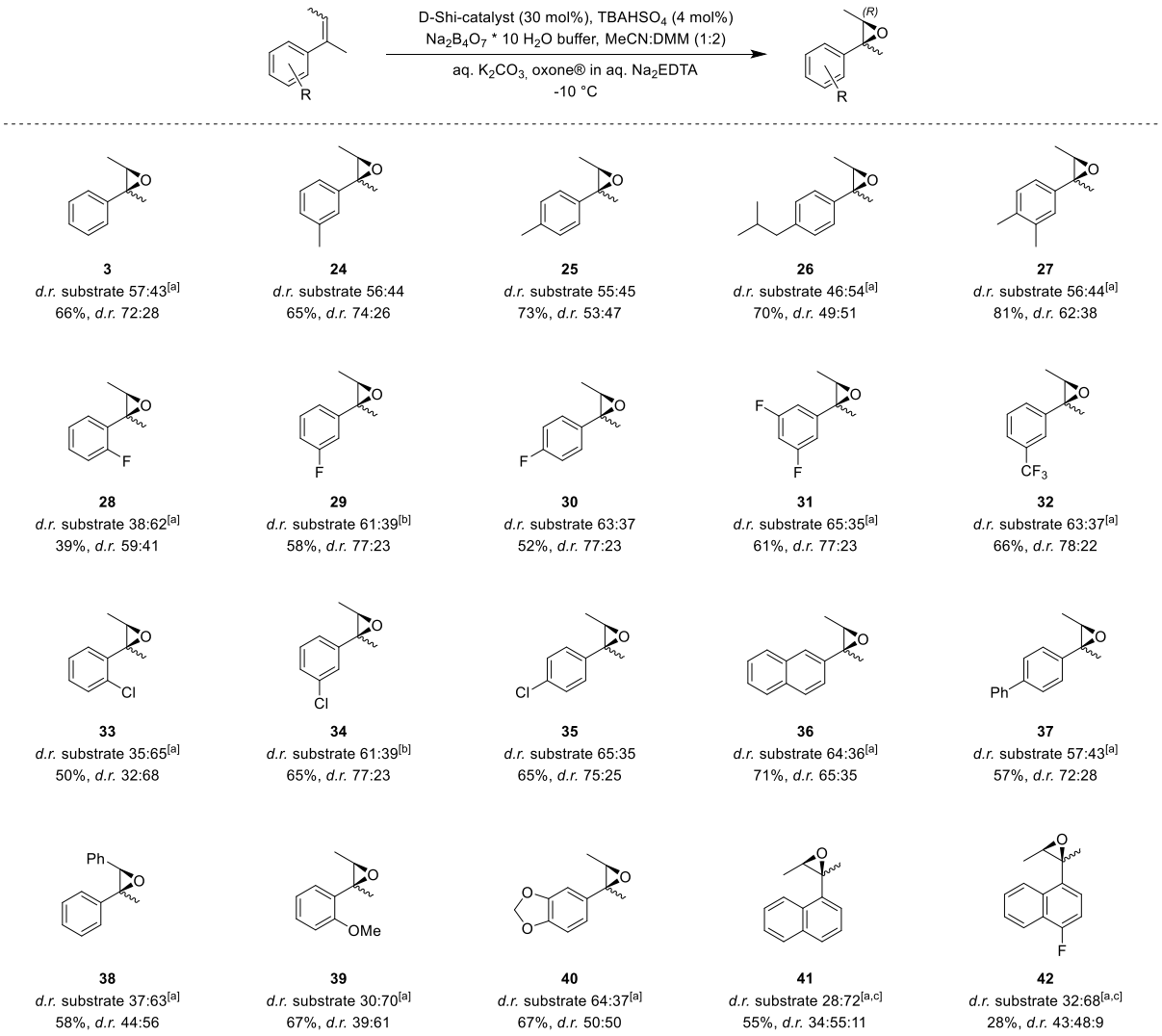

Scheme 64: Results for the *Shi*-epoxidation of the trisubstituted olefins; diastereomeric ratios of the olefins are given as (*E*):(*Z*) and for the epoxides as *anti*:*syn*; [a]*Shi*-epoxidation performed by *Höthker*; [b]*Shi*-epoxidation performed by *Mika*; [c]diastereomeric ratios are given as *anti*:*syn*(1):*syn*(2).[148]

For substrates **33** and **39**, substituents in the *ortho* position presumably increase the steric demand of the phenyl group on the catalyst to such an extent that the *syn*-isomer is favored. The substrates **41** and **42** are particularly noteworthy, as they exist as three distinguishable diastereomers. Initially, it was assumed that these epoxides consisted of only two diastereomers and that the additional signals observed in the NMR spectra arose from impurities. However, independent of the epoxidation method employed (*Matteson*- or *Shi*-epoxidation),[86,176] the same additional signals appeared consistenly. This observation

suggested that an additional chiral element might be responsible for the third set of signals. However, if this hypothesis were correct, the unusual number of observed isomers would raise an important question: why would only three, rather than four, isomers be detected in the NMR spectra? To determine whether the additional signals indeed arise from a further chiral element rather than from impurities, and to investigate the origin of the observed signal pattern, variable-temperature NMR experiments were performed. In order to avoid signals that could interfere with the analysis, ^{19}F-NMR spectra of **42** were recorded.

The measurements between 273 K and 243 K revealed a progressive broadening of the signal at 123.3 ppm. Upon further cooling to 233 K, this signal splits into two (Figure 16). This behavior suggests a temperature-dependent diastereomeric interconversion process, with a coalescence temperature of approximately 243 K. The axis between the epoxide and arene is therefore proposed as the additional chiral element, because this would explain the observed temperature-dependent behavior. Following this assumption, the signal that only begins to split at 233 K corresponds to the isomer with relatively unhindered rotation around this axis. Consequently, the assignment of this signal to a specific isomer remains to be established.

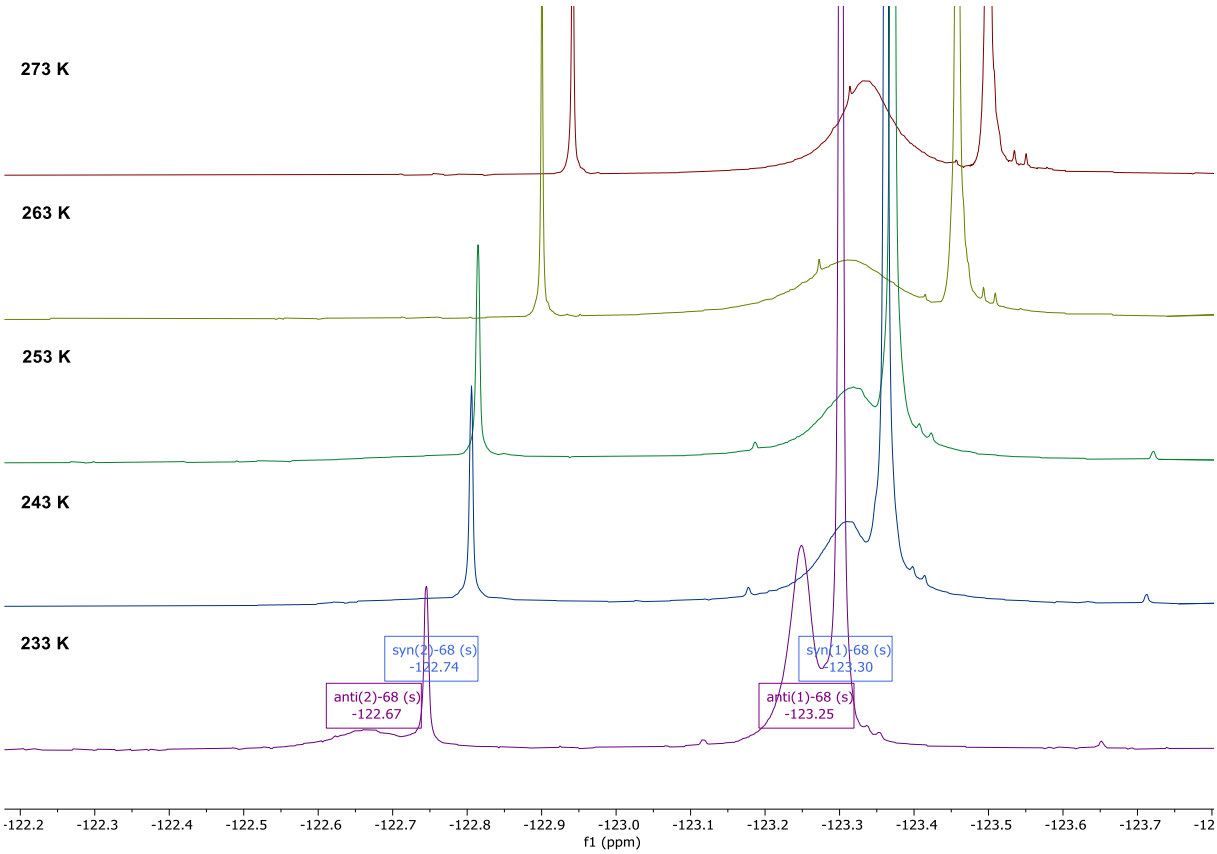

Figure 16: Excerpt of variable temperature ^{19}F-NMR spectra of epoxide **42** at temperatures between 233–273 K in C_6D_5Cl (470 MHz).[148]

To identify this signal, the ^{1}H-NMR spectrum of epoxide **42** was compared with those of the *ortho*-substituted epoxides **33** and **39**, as the annulated ring of epoxide **42** can be considered

analogous to an *ortho*-substituent. The ^{1}H-NMR spectra of **33** and **39** showed an exclusive broadening of the *syn*-isomer signals, indicating more hindered rotation for this diastereomer. Hence, the signal that only begins to split at 233 K can be assigned to the *anti*-isomer. As a result, two *syn*-isomers and only one *anti*-isomer are observed in the spectrum of epoxide **42** at room temperature.

Subsequent measurements between 323 K and 353 K show the broadening of the signal corresponding to the second *syn*-isomer. While well-resolved spectra could not be obtained above this temperature, it is reasonable to assume that the coalescence temperature is slightly above 353 K (Figure 17). Nevertheless, it is surprising that the rotation is not sufficiently fast to allow interconversion of the two *syn*-rotamers, even at 80 °C.

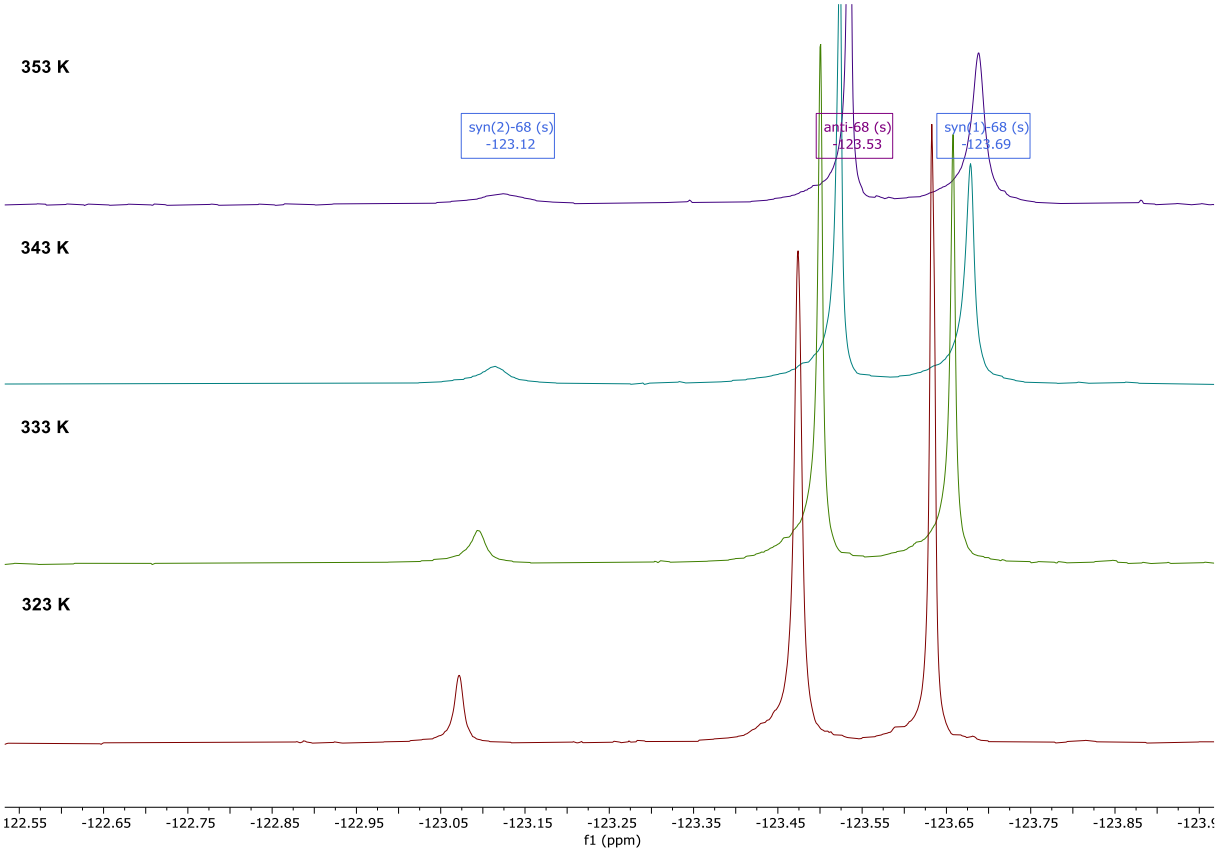

Figure 17: Excerpt of variable temperature ^{19}F-NMR spectra of epoxide **42** at temperatures between 323–353 K in C_6D_5Cl (470 MHz).[148]

To rationalize why the rotation around the axis between the epoxide and arene is more hindered in the *syn*-isomer, the mode of rotation is compared for both isomers (Figure 18). Regardless of the direction of rotation in the *syn*-isomer, both methyl groups experience steric clashes with both “substituents” of the phenyl group simultaneously. In contrast, rotation of the epoxide moiety in the *anti*-isomer can proceed either *via* the sterically more favorable pathway over the hydrogen group or toward the annulated aromatic ring. Furthermore, steric hindrance occurs sequentially, with only one methyl group being sterically hindered at a time during

rotation. Hence, a faster interconversion of the *anti*-rotamers is observed, resulting in the coalescence of the corresponding signals.

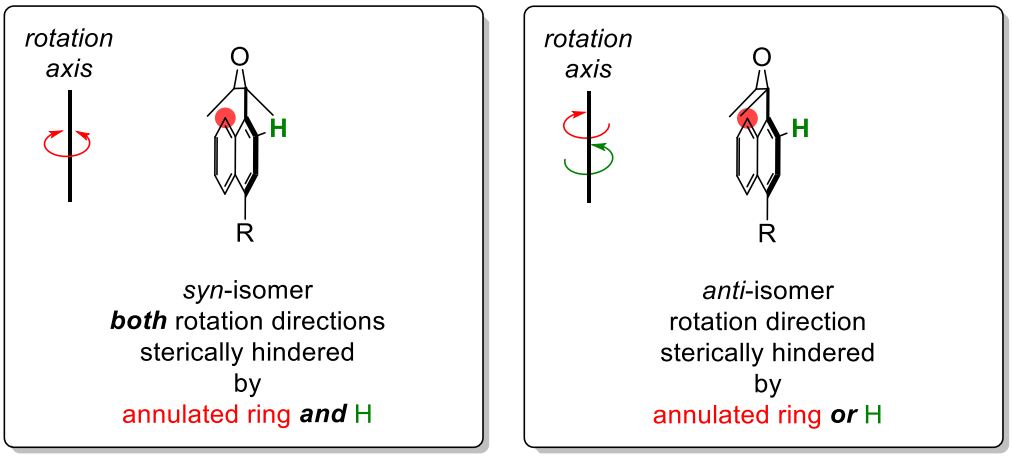

Figure 18: Rotation of the C–C bond between the phenyl and epoxide moiety; comparison of steric hindrance during rotation in the *syn*- and *anti*-isomers.

To quantify the faster rotation in the *anti*-isomer compared to the *syn*-isomer, the corresponding activation barriers have been calculated using the following equations. The differences in chemical shift at their respective coalescence temperatures was determined to be 0.58 ppm for the *anti*-rotamers, and 0.57 ppm for the *syn*-rotamers.

$$k_C = \frac{k_B T}{h} * e^{-\frac{\Delta G^{\ddagger}}{RT}}$$

$$\Delta G^{\ddagger} = -RTln\left(\frac{k_C h}{k_B T}\right)$$

$$with\ k_C = \frac{\pi}{\sqrt{2}} * \Delta\nu \approx\ 2.22 * 470\ MHz * \Delta\delta$$

$k_C = rate\ of\ exchange\ at\ coalescence\ temperature$

$k_B = Boltzmann - constant = 1.381 * 10^{-23} J\ K^{-1}$

$T = absolute\ coalescence\ temperature\ (anti = 243\ K;\ syn = 353\ K)$

$h = Planck\ constant = 6.626 * 10^{-34} J\ s^{-1}$

$\Delta G^{\ddagger} = Energy\ of\ activation\ at\ coalescence\ temperature$

$R = universal\ gas\ constant = 8.314\ J\ K\ mol^{-1}$

$\Delta\nu = difference\ in\ NMR - shift\ in\ Hz = operating\ frequency\ (470\ MHz) *\ \Delta\delta$

$\Delta\delta = difference\ in\ NMR - shift\ in\ ppm$

For the calculation of the activation barrier of the *syn*-isomer, 353 K was used as an estimate for the coalescence temperature, as it should be sufficiently close to the exact value. Taking all of these values into account, the activation barriers were calculated to be 11.0 kcal/mol for the *anti*-isomer and 16.3 kcal/mol for the *syn*-isomer.[148] As expected, the rotational energy barrier of the *anti*-isomer is significantly lower, facilitating the interconversion. Due to the structural similarity of **41**, we assumed comparable results for this epoxide.

Remarkably, even in the presence of three isomers, the following diastereoconverging titanocene-catalyzed hydrosilylation transforms the mixture into a single *anti-Markovnikov* alcohol with high diastereomeric and enantiomeric ratio (Scheme 63).

Furthermore, *Höthker* demonstrated the scalability of this strategy by applying the more sustainable and cost-efficient conditions (method **B**) to epoxide **26** on a 2.5 g scale (Scheme 65).[148] Further transformation *via Parikh-Doering* oxidation and subsequent reductive amination of the ketone provides access to numerous biologically active phenylethylamines, such as the weight loss medication Pentorex® (Scheme 65).[148] Notably, the stereocenter introduced by the titanocene-catalyzed hydrosilylation remains unaffected after oxidation.

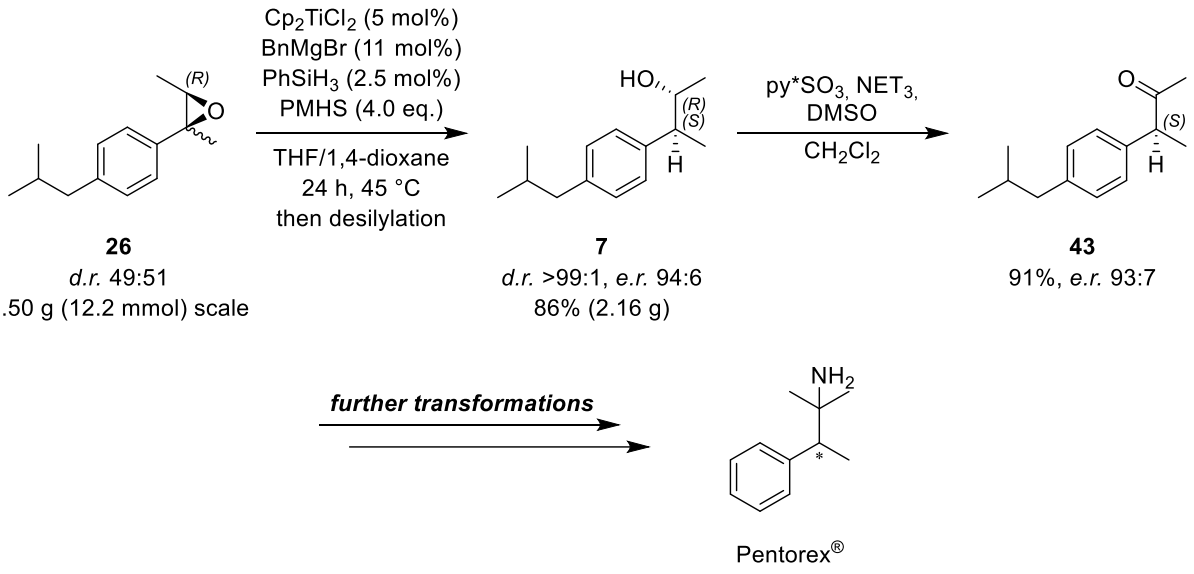

Scheme 65: Large-scale synthesis of the alcohol **7** from the diastereomeric mixture of epoxide **26** *via* stereoconverging titanocene catalyzed hydrosylilation; *Parikh-Doering* oxidation to ketone **43**; both steps performed by *Höthker*; further transformations lead to weight loss medication Pentorex®.[148]

3.2 Designing Electron-Deficient Titanocenes for the Efficient Synthesis of Fatty Alcohols

The ability of titanocene hydrides to transform 1,1-disubstituted,[132] trisubstituted,[131,148] and benzylic[148] epoxides efficiently into *anti-Markovnikov* alcohols has been proven repeatedly, as highlighted in the reductive opening of benzylic trisubstituted epoxides (Scheme 63). For these substrates, radical epoxide opening to the more stabilized radical occurs comparatively fast upon catalyst-binding.[97] Consequently, the hydricity of the active species, which could initiate a nucleophilic pathway toward the undesired *Markovnikov* alcohol, can be neglected. However, initial studies of the titanocene-catalyzed hydrosilylation demonstrated, through the opening of dodecene oxide, that the hydricity of the active species cannot be ruled out in general. Here, a relatively low *r.r.* (78:22) was observed (Scheme 66).[131] This can be attributed to the slower radical opening of monosubstituted epoxides by the active species compared to benzylic trisubstituted or 1,1-disubstituted epoxides, thereby enabling a competing nucleophilic pathway. The slower opening likely results from less pronounced steric interactions between the catalyst's ligands and the epoxide's substituents during complexation.[97]

In contrast, using the previous catalytic system, including an external non-nucleophilic HAT donor (1,4-CHD) in combination with titanocene(III) chloride as the active species, an excellent *r.r.* (94:6) was obtained (Scheme 66).[70] Here, the regioselectivity is controlled solely by the relative stability of the transition states leading to the respective radical intermediates. Nonetheless, the desired alcohol was obtained in low yield due to a competitive deoxygenation reaction towards the respective olefin (Scheme 66).[70]

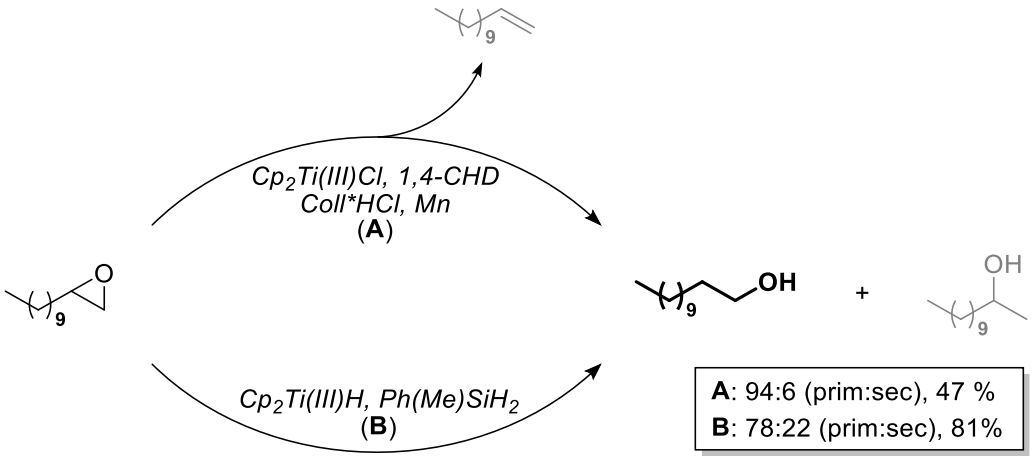

Scheme 66: Transformation of dodecene oxide to the corresponding primary and secondary alcohols *via* route (**A**) and (**B**).[70,131]

The titanocene-catalyzed hydrosilylation is significantly more sustainable and avoids deoxygenation owing to the fast intramolecular HAT. Therefore, despite its lower

regioselectivity, we employed this system in the opening of monoalkyl-substituted epoxides and investigated numerous conditions and catalysts to address this limitation.

As outlined in Chapter 1.8, the activation of the precatalyst Cp_2TiMe_2 is capricious, and due to its light sensitivity, the catalyst must be freshly prepared.[131] Hence, the bench-stable titanocene dichloride (**[Ti]-1**) was employed as the precatalyst and the active species was generated *via* the more reliable allyl- or benzyl activation (Scheme 67). Disappointingly, both methods yielded the alcohol with an even lower regioisomeric ratio. Moreover, both activation procedures afforded the alcohol with essentially the same regioselectivity. This can be attributed to the formation of *Lewis*-acidic Mg-salts in the allyl- and benzyl-activation (Scheme 44/48). They activate the epoxide for nucleophilic ring opening by titanocene hydride (Scheme 67). Consequently, the *Markovnikov* alcohol is formed *via* an S_N2-type reaction. Despite the presence of *Lewis*-acidic Mg-salts in solution, the use of a bench-stable precatalyst **[Ti]-1** along with a simple activation procedure makes this approach significantly more attractive than the previous approach. Therefore, we continued our investigations with this approach and screened numerous conditions with the aim of suppressing this side reaction.

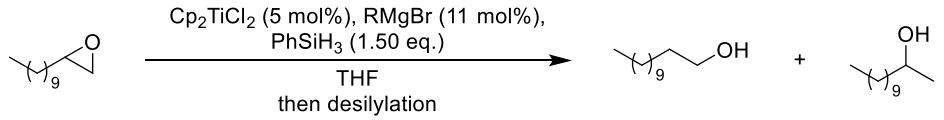

R = allyl (***allyl activation***), THF (0.5M), 16 h[a]	63	:	37
R = benzyl (***benzyl activation***), THF (0.125M), 24 h	64	:	36

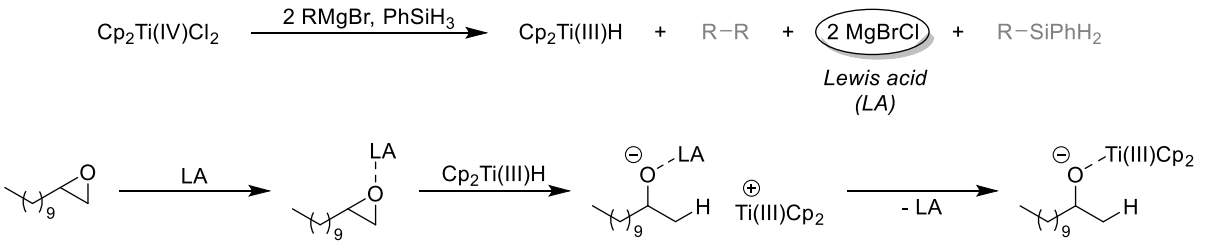

Scheme 67: Titanocene-catalyzed hydrosilylation of dodecene oxide *via* either benzyl- or allyl activation;[177] [a]performed by *Klare*;[178] proposed mechanism by *Höthker* for *Lewis* acid catalyzed nucleophilic opening with titanocene hydride (bottom).[162]

Klare screened numerous bulkier titanocene dichlorides in the opening of dodecene oxide (Table 3). The bulkier ligands should sterically encumber the titanium-bound hydride, resulting in reduced hydricity. However, the favored radical pathway is typically also sensitive to increased steric hindrance.[131] In practice, no common trend was observed when increasing the bulk of the ligands. With the sterically more demanding cyclohexyl-substituted titanocene dichloride (**[Ti]-2**), the regioselectivity further deteriorates (Table 3, Entry 3). On the other hand,

the use of the bulky titanocene precatalyst (tBuC$_5$H$_4$)$_2$TiCl$_2$ (**[Ti]-3**) improved the regioselectivity (Table 3, Entry 2).

Table 3: Screening of bulkier titanocene dichlorides in the titanocene catalyzed hydrosilylation of dodecene oxide; all entries performed by *Klare*.[177,178]

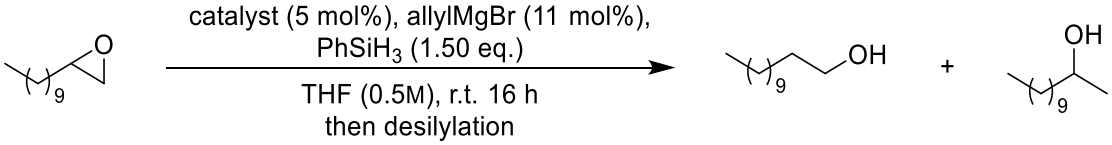

catalyst	conversion/%	*r.r.* (prim:sec)
 **[Ti]-1**	100	63:37
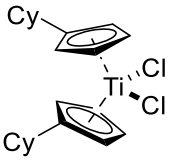 **[Ti]-2** (Cy = cyclohexyl)	92	55:45
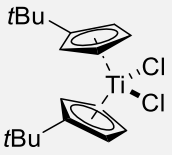 **[Ti]-3**	100	73:27

Further screening experiments by *Klare* investigated the effect of the *Grignard* reagent's halide. He discovered that the use of the respective *Grignard* reagent, including chloride instead of bromide as the counter ion, evidently improves the regioselectivity (Table 4, Entry 1). This is in line with the "HSAB" concept,[179] which suggests that the *Lewis* acidity of $MgCl_2$ is lower than that of MgBrCl. The covalent bond between the "hard" Mg^{2+} cation and the "hard" Cl^- anion is stronger than the bond of the cation to the "softer" Br^- ion. The lower covalent character of the latter is accompanied by a stronger ionic character. Hence, MgBrCl also exhibits increased *Lewis* acidity, favoring the nucleophilic pathway. Notably, with the use of allylMgCl, the regioselectivity (Table 4, Entry 1) is comparable to that obtained with $Cp_2Ti(IV)Me_2$ and $PhSiH_3$, while offering a considerably simpler activation method.

Table 4: Screening of *Grignard* reagent, solvent and catalyst in the titanocene-catalyzed hydrosilylation of dodecene oxide; [a]entries performed by *Klare*.[177,178]

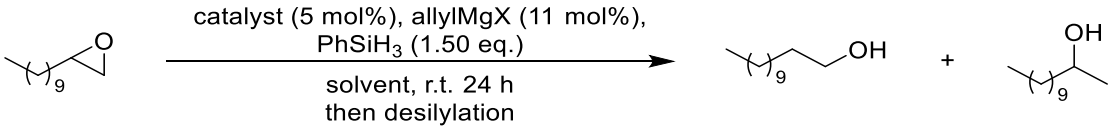

catalyst	X	solvent	conversion/%	*r.r.* (prim:sec)
Cp_2TiCl_2	Cl	THF (0.5M)	100	80:20[a]
$(t\text{BuC}_5H_4)_2TiCl_2$	Cl	THF (0.1M)	100	86:14[a]
Cp_2TiCl_2	Br	THF/1,4-dioxane (1:1, 0.125M)	100	73:27
$(t\text{BuC}_5H_4)_2TiCl_2$	Br	THF/1,4-dioxane (1:1, 0.125M)	100	79:21

By using the superior catalyst **[Ti]-3** according to the screening experiments in Table 3 and the *Grignard* reagent allylMgCl, which leads to Mg-salts with reduced *Lewis* acidity, the regioselectivity of the epoxide opening is further improved, as shown by *Klare* (Table 4, Entry 2).

Earlier studies highlighted the advantageous effect of 1,4-dioxane as a cosolvent in the titanocene-catalyzed reductive opening of epoxides to suppress *Lewis*-acid catalyzed side reactions.[133,153] This can be attributed to the precipitation of the *Lewis*-acidic Mg-salts by 1,4-dioxane through the formation of polymeric chains.[180–182] Therefore, in the context of this work, a THF:1,4-dioxane (1:1) solvent mixture was employed for the opening of dodecene oxide (**44**), using either **[Ti]-1** (Table 4, Entry 3) or **[Ti]-3** (Table 4, Entry 4) in combination with allylMgBr. Rather unexpectedly, the regioselectivity is reduced instead of improved compared to the conditions involving allylMgCl. Nevertheless, even without the presence of *Lewis* acidic Mg-salts, the hydricity of the active species is high enough to open the epoxide according to a nucleophilic mechanism. Thus, it seemed mandatory to attenuate the hydricity of the active species *via* modification of the ligands.

Inspired by previous electron paramagnetic resonance (EPR) studies indicating non-covalent interactions of the employed silanes to the titanium-bound hydride (Scheme 68),[132] silyl substituents were implemented into the ligand sphere. Based on this observation, we proposed that they coordinate intramolecularly to the hydride, thereby reducing the active catalyst's hydricity.

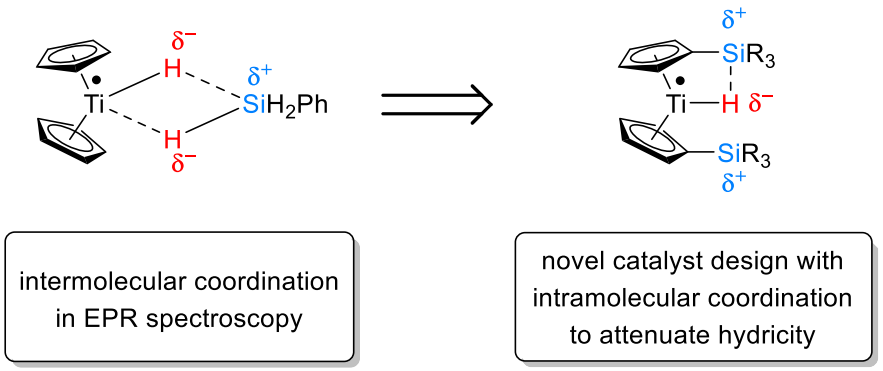

Scheme 68: Novel catalyst design to attenuate hydricity based on coordination of titanium bound hydride and external silane observed in EPR spectroscopy[132,177]

Gratifyingly, the use of trimethylsilyl-substituted (TMS) titanocene dichloride (**[Ti]-4**) confirmed our hypothesis. Despite being the simplest Si-substituted titanocene dichloride, it already significantly improved the regioselectivity (Table 5, Entry 1) compared to the reaction using **[Ti]-1**, as shown by *Klare*. Subsequently, *Klare* replaced allylMgBr with allylMgCl to further improve the regioselectivity (Table 5, Entry 2). Direct comparison of the results obtained with **[Ti]-4** and those with the bulkier catalyst **[Ti]-3** demonstrates that the regioselectivity (Table 5, Entry 1) is governed by electronic rather than steric effects.

Table 5: Screening of *Grignard* and silane reagents employed in the hydrosilylation of dodecene oxide using the Me_3Si-substituted titanocene dichloride; [a]performed by *Klare*; [b]performed by *Schacht*.[177,178]

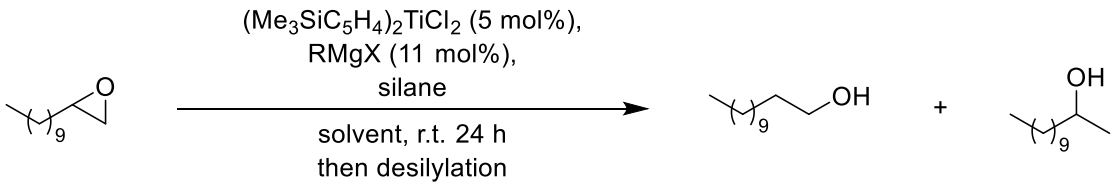

R	X	silane	solvent	*r.r.* (prim:sec)
allyl	Br	$PhSiH_3$ (1.50 eq)	THF (0.5M)	88:12[a]
allyl	Cl	$PhSiH_3$ (1.50 eq)	THF (0.1M)	90:10[a]
benzyl	Br	$PhSiH_3$ (2.50 mol%), PMHS (4.00 eq.)	THF/1,4-dioxane (1:1, 0.125M)	88:12[b]

Schacht tested out the performance of the Si-substituted catalyst using the more sustainable and cost-efficient PMHS as the stoichiometric silane reagent.[133,177] Furthermore, he employed

the benzyl activation procedure, as this activation method is significantly faster.[177] Experimental findings demonstrating that the benzyl activation proceeds at room temperature, whereas the allyl activation requires heating when only substochiometric amounts of phenyl silane are added support this hypothesis. According to *Höthker*, the faster rate of the benzyl activation is associated with a weaker η^3-coordination of the benzyl group to the metal center. He attributed the weaker coordination to the non-equivalent Ti–C^1/T–C^3 bond lengths (Scheme 69), in contrast to the corresponding bonds in the titanium(III) allyl complex. Consequently, the equilibrium is shifted more toward the intermediate in which the benzyl group is η^1-coordinated, leaving a vacant coordination site. As this intermediate undergoes the σ-bond metathesis, the shift toward it accelerates the benzyl activation.[162]

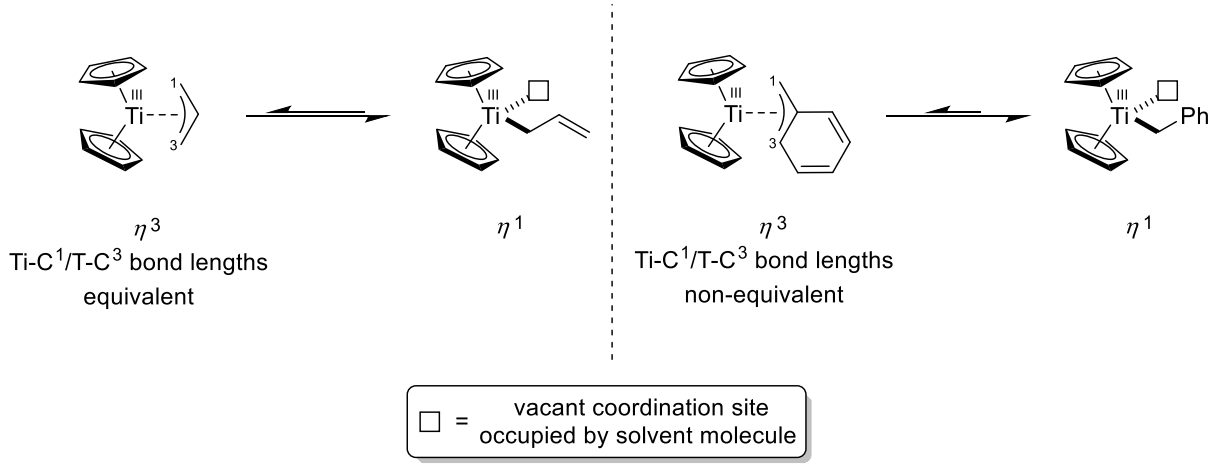

Scheme 69: Equilibrium between η^1- and η^3-coordinated allyl- and benzyl-titanocene(III) complexes; non-equivalent Ti–C bond lengths lead to weaker η^3-coordination, proposed by *Höthker*.[162]

Notably, the more cost-efficient conditions with faster catalyst activation (Table 5, Entry 3) are nearly on par with the other conditions (Table 5, Entry 2) in terms of regioselectivity.

Building on these findings, *Höthker* and *Krebs* designed numerous Si-substituted titanocene dichlorides. Their general procedure started from commercially available chlorosilanes. If the desired substituents were not already bound to the Si-center, all but one chloro substituent were replaced *via* nucleophilic substitution. In the next step, the (remaining) chloro substituent of the synthesized or directly employed silane was substituted with freshly cracked cyclopentadiene (Cp) under basic conditions. Finally, deprotonation of the silyl-bound Cp followed by transmetalation to $TiCl_4$ yielded the respective catalyst. It should be noted that every catalyst discussed in the following is synthesized de novo.[162,177,183]

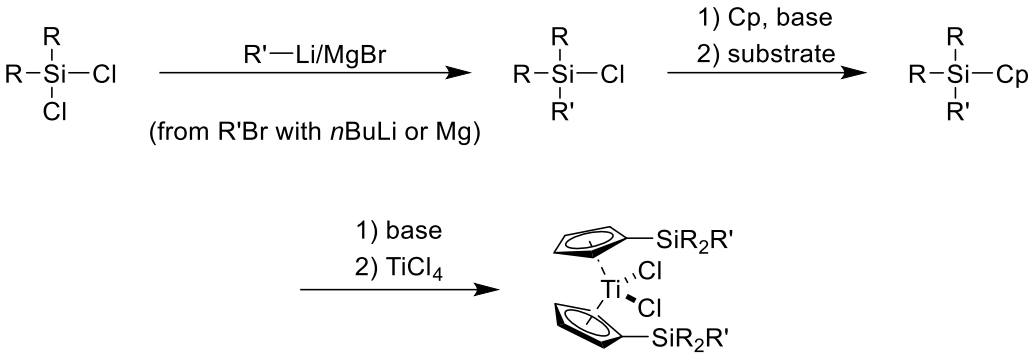

Scheme 70: General procedure for the synthesis of Si-substituted titanocene dichloride from dichlorosilanes by *Höthker* and *Krebs*.[162,183]

These catalysts were applied in the opening of **44** (Scheme 71) to achieve the theoretical limit in terms of regioselectivity (*r.r.* 94:6). In the following, the generally best conditions (**D**) are discussed using the catalysts **[Ti]-4**–**16**.

Replacing the methyl groups of **[Ti]-4** with ethyl groups (**[Ti]-5**) has no impact on selectivity, as the steric and electronic properties remain essentially unchanged. However, the conversion decreases to 76%. Further increasing steric bulk by replacing one methyl group of **[Ti]-4** with a *tert*-butyl substituent (**[Ti]-6**) improves the regioselectivity (*r.r.* 91:9). Yet, introduction of excessively bulky silyl groups, as exemplified by the catalyst bearing triisopropyl-substituted silyl residues (**[Ti]-7**), leads to a pronounced decrease in selectivity (*r.r.* 72:27). This can likely be attributed to the lower accessibility of the Si-centers. In addition, the conversion is substantially reduced.[177]

Modification of only one Cp-ligand with a TMS group (**[Ti]-8**) also negatively affects the selectivity (*r.r.* 82:18). When the catalyst is conformationally locked by a methylene bridge (**[Ti]-9**), the selectivity is similarly low (*r.r.* 81:19). Introduction of a methylene spacer between the Cp-ligand and the Si-center (**[Ti]-10**) results in a regioselectivity (*r.r.* 67:33) comparable to that observed with the use of unmodified titanocene dichloride. Presumably, the distance between the hydride and the silyl groups becomes too large to enable efficient coordination.[177]

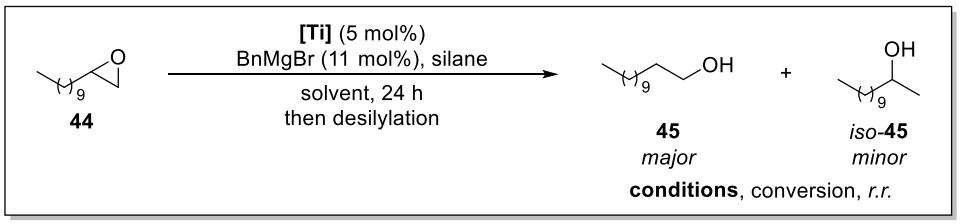

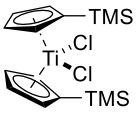

[Ti]-4
A, 100%, *r.r.* 86:14[a]
B, 100%, *r.r.* 88:12[a]
C, 100%, *r.r.* 78:22[a]
D, 100%, *r.r.* 88:12[a]

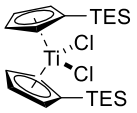

[Ti]-5
A, 100%, *r.r.* 86:14[a]
B, 100%, *r.r.* 84:16[a]
C, 91%, *r.r.* 82:18[a]
D, 76%, *r.r.* 87:13[a]

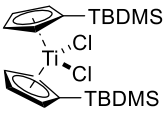

[Ti]-6
A, 100%, *r.r.* 85:15[a]
B, 100%, *r.r.* 86:14[a]
C, 95%, *r.r.* 76:24[a]
D, 100%, *r.r.* 91:9[a]

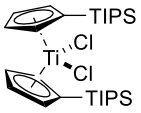

[Ti]-7
A, 94%, *r.r.* 72:28[a]
B, 100%, *r.r.* 86:14[b]
C, 61%, *r.r.* 76:24[c]
D, 37%, *r.r.* 73:27[c]

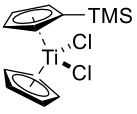

[Ti]-8
A, 100%, *r.r.* 78:22
B, 55%, *r.r.* 80:20[a]
C, 70%, *r.r.* 78:22[a]
D, 63%, *r.r.* 82:18[a]

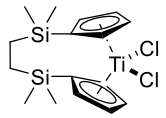

[Ti]-9
A, 100%, *r.r.* 83:17[a]
B, 100%, *r.r.* 83:17[a]
C, 98%, *r.r.* 78:22[a]
D, 81%, *r.r.* 81:19[a]

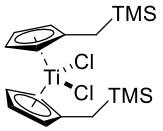

[Ti]-10
A, 60%, *r.r.* 56:44[a]
B, 60%, *r.r.* 74:26[a]
C, 15%, *r.r.* 62:38[c]
D, 16%, *r.r.* 67:33[c]

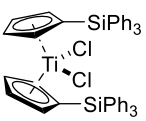

[Ti]-11
A, 100%, *r.r.* 91:9[a]
B, 100%, *r.r.* 87:13[b]
C, 100%, *r.r.* 90:10[a]
D, 64%, *r.r.* 91:9[b]

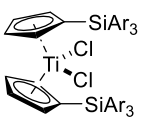

[Ti]-12 (Ar = *p*-F-C_6H_4)
A, 100%, *r.r.* 88:12[a]
B, 100%, *r.r.* 89:11[a]
C, 76%, *r.r.* 87:13
D, 100%, *r.r.* 89:11[a]

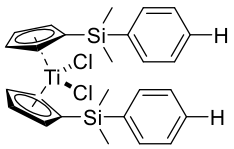

[Ti]-13
A, 100%, *r.r.* 81:19[c]
B, 100%, *r.r.* 88:12[c]
C, 94%, *r.r.* 87:13[a]
D, 99%, *r.r.* 91:9[a]

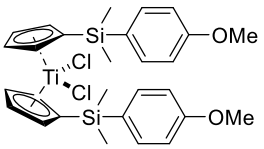

[Ti]-14
A, 100%, *r.r.* 89:11[a]
B, 100%, *r.r.* 87:13[a]
C, 96%, *r.r.* 89:11[a]
D, 100%, *r.r.* 90:10[a]

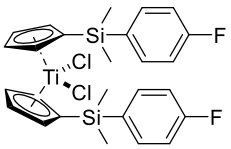

[Ti]-15
A, 100%, *r.r.* 85:15[a]
B, 100%, *r.r.* 88:12[a]
C, 80%, *r.r.* 85:15[a]
D, 80%, *r.r.* 91:9[a]

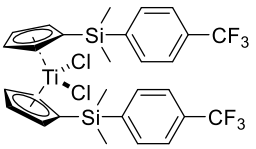

[Ti]-16
A, 100%, *r.r.* 89:11[a]
B, 100%, *r.r.* 89:11[a]
C, 80%, *r.r.* 89:11[a]
D, 31%, *r.r.* 90:10[a]

A: $PhSiH_3$ (1.50 eq.), THF (0.125M)
B: $PhSiH_3$ (1.50 eq.), THF:1,4-dioxane (1:1, 0.125M)
C: $PhSiH_3$ (2.5 mol%), PMHS (4.00 eq.), THF (0.125M)
D: $PhSiH_3$ (2.5 mol%), PMHS (4.00 eq.), THF:1,4-dioxane (1:1, 0.125M)

Scheme 71: Screening of numerous Si-substituted titanocene dichlorides **[Ti]-4**–**16** in the regioselective hydrosilylation of **44** to the *anti-Markovnikov* alcohol **45** under the conditions **A**–**D**; [a]performed by *Schacht*; [b]performed by *Krebs*; [c]performed by *Höthker*.[162,177]

Substitution of the methyl groups of **[Ti]-4** with phenyl groups (**[Ti]-11**) enhances selectivity to the same value observed for **[Ti]-6** (*r.r.* 91:9). This effect can be rationalized by the higher electronegativity of phenyl substituents relative to alkyl groups, arising from their greater *s*-character (sp^2- vs sp^3-hybridization). Implementation of *para*-fluoro-substituted phenyl groups (**[Ti]-12**) results in similar selectivity (*r.r.* 89:11). Replacing only one Me group per Si substituent of **[Ti]-4** with a phenyl group (**[Ti]-13**) again affords the alcohol with an regioisomeric ratio of

91:9. Interestingly, substitution of the *para*-hydrogen atom of the arene with a methoxy group (**[Ti]-14**), a fluorine atom (**[Ti]-15**), or a CF_3 group (**[Ti]-16**) has nearly no impact on the regioselectivity in the opening of **44**.[177] These findings are consistent with studies on relative bond dissociation energies (BDE) of numerous *para*-substituted aryl silanes. Independent of the substitution pattern, many of these have similar BDEs and therefore similar reactivity.[184]

As expected, without using 1,4-dioxane as a cosolvent, the “PMHS conditions” typically yield the alcohol with reduced regioselectivity. Interestingly, when the hydricity of the active species is sufficiently frustrated, the presence of *Lewis*-acidic Mg-salts only has a marginal impact on the selectivity. Therefore, the use of 1,4-dioxane often shows little to no beneficial effect when only using phenyl silane along with the respective electron-deficient catalysts. On the other hand, **[Ti]-7** and **[Ti]-10**, which insufficiently attenuate the hydricity due to the aforementioned reasons, benefit from the use of 1,4-dioxane as a cosolvent.

Because these catalysts still did not afford the alcohol with the desired regioselectivity, *Höthker* and *Krebs* decided to develop even more electron-deficient catalysts. While their general synthetic route provides access to a wide range of Si-substituted titanocenes, it is difficult to avoid complete substitution of all chlorides of the respective chlorosilanes in the first step. This is particularly difficult when electron-deficient aryl groups are introduced, which increase the electron deficiency at the Si-center, and thereby also the rate of substitution for the following chloride. Studies by *Gilman et al.* reporting the reaction of C_6F_5MgBr with dichlorodimethylsilane, which leads to substitution of both chloride groups despite a tenfold excess of the dichlorosilane, highlight this issue.[185]

Therefore, a strategy was established that does not require chloride as a leaving group for the implementation of the cyclopentadienyl group (Scheme 72). Starting from dichloro(methyl)(phenyl)silane, both chlorides were substituted with 3,5-bis(trifluoromethyl)phenyl groups to render the silyl moiety even more electron-deficient than previously employed ones. In this context, electron-withdrawing groups, such as nitro or carbonyl groups, were avoided as they are highly susceptible to the hydrosilylation conditions.[177]

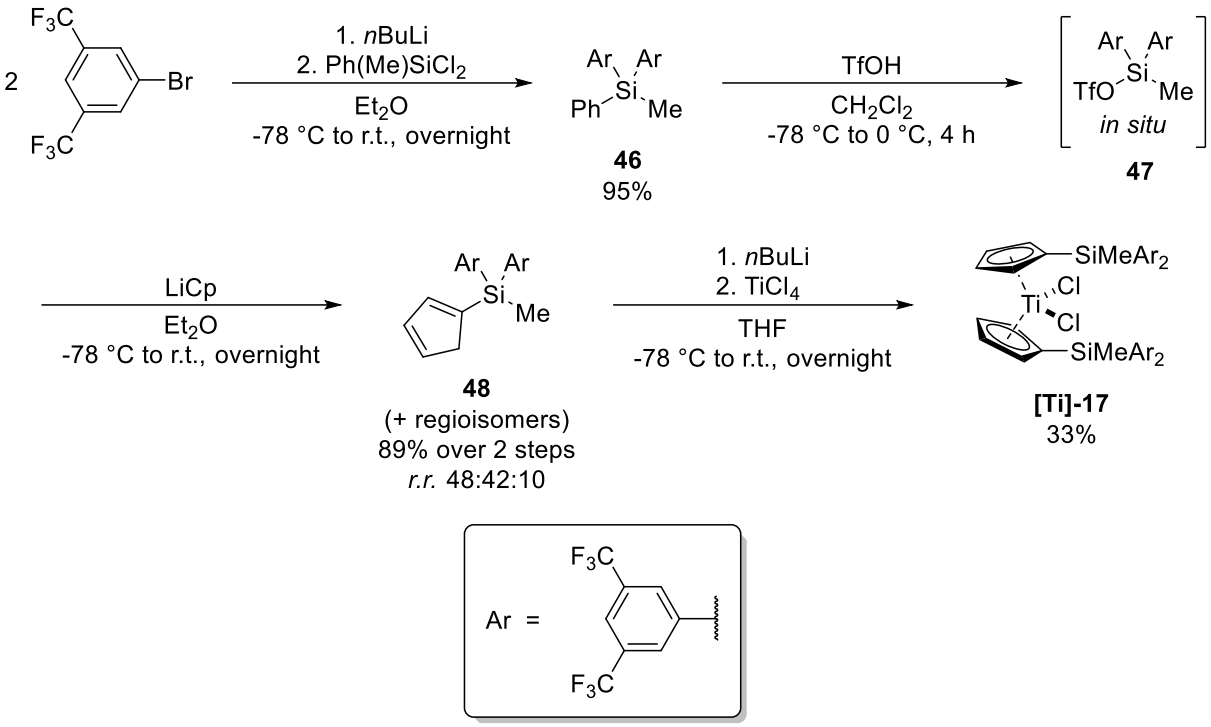

Scheme 72: Synthetic route towards the electron deficient Si-substituted titanocene dichloride **[Ti]-17** starting from chlorosilane and aryl bromide.[177]

By addition of triflic acid in the next step, the most electron-rich arene, the phenyl group, is protonated selectively, resulting in its cleavage. Subsequently, the silyl cation is trapped by triflate, the counterion of the strong acid. After exchanging the phenyl group by a significantly better leaving group, the silane was subjected to the same conditions as in the general approach to afford the respective catalyst (**[Ti]-17**). In summary, we designed the most-electron deficient catalyst **[Ti]-17** among the reported titanocenes (Scheme 71) *via* a more facile route (Scheme 72).[177]

Within the scope of this work, the aryl silane **46** was obtained in excellent yield (95%). Vigorous stirring was essential in this step due to the strong salt formation during the reaction. The crucial steps for achieving a satisfying overall yield are considered to be the formation and subsequent transformation of the most reactive intermediate **47**. Therefore, triflic acid was added at -78 °C to the dissolved intermediate **46**. Furthermore, the mixture was stirred at the same temperature for 30 min before stirring it for another 3.5 h at 0 °C. Due to the high reactivity of the triflate **47**, it was immediately subjected to the next step. Thereby, the Si-substituted Cp **48** was obtained in high yield (89%) over two steps. Finally, transmetallation to $TiCl_4$ at –78 °C yielded the catalyst **[Ti]-17** in acceptable yields (33%).

This catalyst was applied in the opening of **44** to test its performance in terms of regioselectivity. Performing the catalysis only in THF yields the alcohol with the same regioselectivity (*r.r.* 88:12) for both silane reagents (conditions **A** and **D**).[162] As expected, the use of 1,4-dioxane as a

cosolvent only slightly improves the regioselectivity (*r.r.* 90:10) when using $PhSiH_3$ (condition **B**). Gratifyingly, using **[Ti]-17** under condition **D** yields the alcohol with the highest regioselectivity (*r.r.* 93:7) among the screened titanocenes. Considering the experimental error, this catalyst provides the alcohol with the same regioselectivity as the Ti-catalyzed system that uses an external non-nucleophilic HAT donor. Hence, the use of **[Ti]-17** under condition **D** in the titanocene-catalyzed hydrosilylation completely suppresses the nucleophilic pathway.

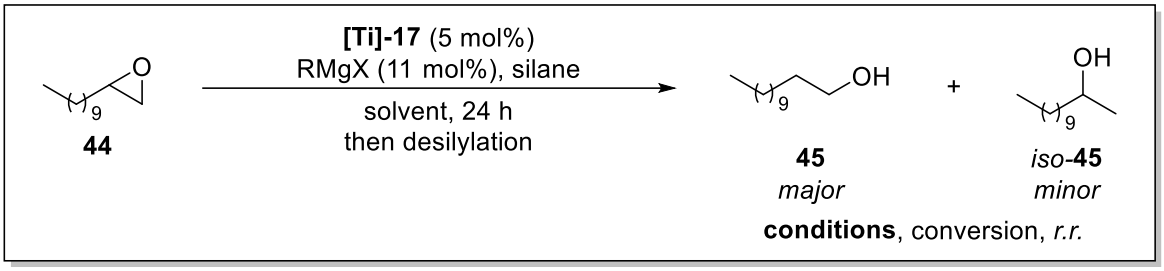

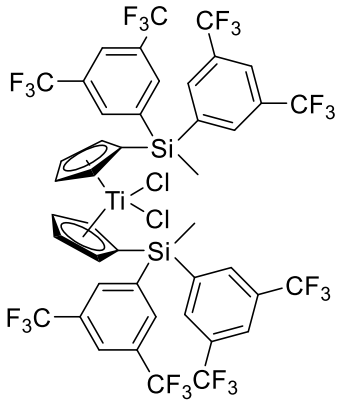

[Ti]-17
A, 75%, *r.r.* 88:12[a]
B, 95%, *r.r.* 90:10
C, 100%, *r.r.* 88:12[a]
D, 100%, *r.r.* 93:7[a]
E, 50%, *r.r.* 77:23

A: BnMgBr, $PhSiH_3$ (1.50 eq.), THF (0.125M)
B: BnMgBr, $PhSiH_3$ (1.50 eq.), THF:1,4-dioxane (1:1, 0.125M)
C: BnMgBr, $PhSiH_3$ (2.5 mol%), PMHS (4.00 eq.), THF (0.125M)
D: BnMgBr, $PhSiH_3$ (2.5 mol%), PMHS (4.00 eq.), THF:1,4-dioxane (1:1, 0.125M)
E: allylMgCl, $PhSiH_3$ (1.50 eq.), THF (0.125M)

Scheme 73: Application of **[Ti]-17** in the hydrosilylation of **44** under the conditions **A**–**E**; [a]entries performed by *Schacht*.[162,177]

To improve the sustainability, the *Grignard* reagent allylMgCl (condition **E**) was tested with the aim of avoiding the carcinogenic solvent 1,4-dioxane. However, the regioselectivity was disappointingly low (*r.r.* 77:23). This is in line with experimental findings, which indicate a slower activation of **[Ti]-17** even with the more facile benzyl activation procedure. Presumably, the allyl activation method is not capable of providing the active species efficiently, resulting in side reactions favoring the *Markovnikov* alcohol. Nevertheless, our present method exhibits significantly improved sustainability compared to the former approach, which uses an external HAT donor, and additionally provides the desired alcohols in high yields and good regioselectivities.

In the context of this work, the catalyst **[Ti]-17** was then applied to other monosubstituted epoxides and compared with the titanocenes ((*t*BuC$_5$H$_4$)$_2$TiCl$_2$ (**[Ti]-3**) and (Me$_3$SiC$_5$H$_4$)$_2$TiCl$_2$ (**[Ti]-4**)) regarding regioselectivity. In agreement with previous results, the regioselectivity increases in the order **[Ti]-3** < **[Ti]-4** < **[Ti]-17**. The length of the alkyl chain does not influence the selectivity. Moreover, silyl protecting groups are stable under our conditions. The improvement in selectivity is particularly pronounced for the opening of **49**. This can be attributed to higher steric repulsion between the catalyst and the substituents in the *β*-position of the epoxide, favoring the TS leading to the secondary radical.

Table 6: Comparison of the top performer **[Ti]-17** to the catalysts **[Ti]-3** and **[Ti]-4** in the regioselective opening of selected monosubstituted alkyl epoxides.[177]

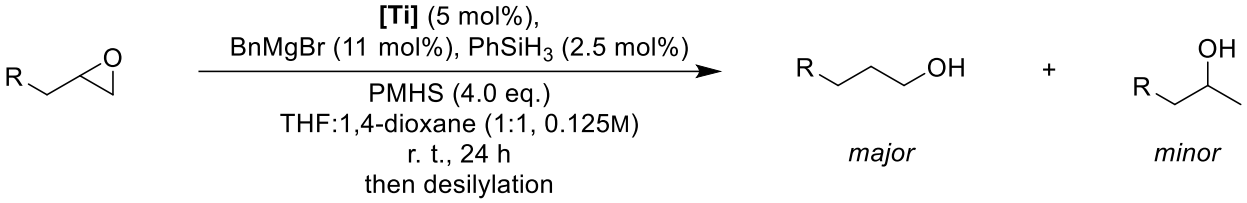

substrate	[Ti]-17	[Ti]-4	[Ti]-3
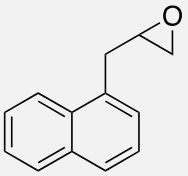 **49**	96/4	92/8	80/20
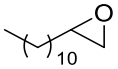 **50**	92/8	86/14	82/18
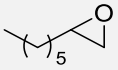 **51**	92/8	86/14	82/18
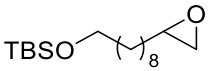 **52**	94/6	89/11	83/17
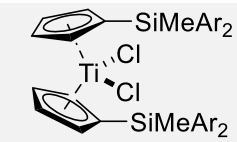 **[Ti]-17** Ar = 3,5-(CF$_3$)$_2$C$_6$H$_3$	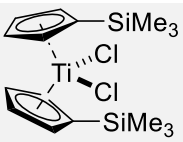 **[Ti]-4**	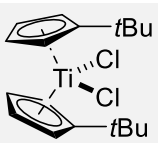 **[Ti]-3**	

After proving the superiority of our catalyst, **[Ti]-17** was applied to a wider range of epoxides (Scheme 74). Generally, the desired alcohols were obtained in high yields with good regioselectivities.

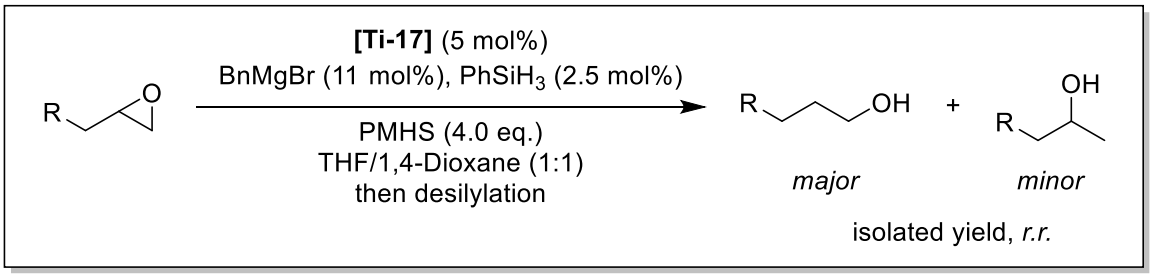

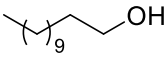

45
74%, *r.r.* 92:8

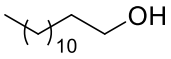

53
74%, *r.r.* 92:8

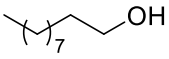

54
76%, *r.r.* 92:8

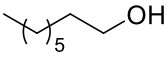

55
74%, *r.r.* 92:8

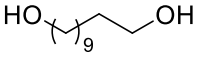

56
73%, *r.r.* 92:8[a]

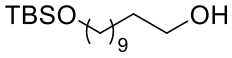

57
71%, *r.r.* 94:6

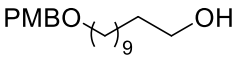

58
63%, *r.r.* 93:7

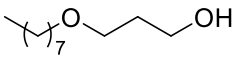

59
74%, *r.r.* 88:12

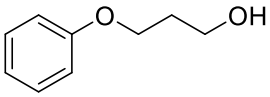

60
71%, *r.r.* 88:12

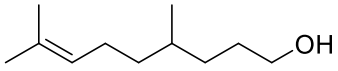

61
77%, *r.r.* >99:1

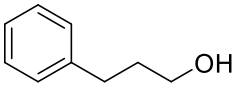

62
74%, *r.r.* 92:8

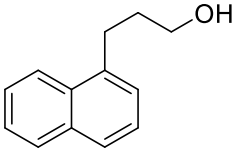

63
82%, *r.r.* 96:4

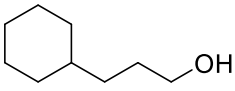

64
77%, *r.r.* >99:1

Scheme 74: Results for the regioselective opening of a wide range of monosubstituted alkyl epoxides using the optimal conditions and the best catalyst in this context **[Ti]-17** according to screening experiments; [a]8.0 equivalents of PMHS employed.[177]

Aside from silyl protecting groups, our conditions also tolerate the *para*-methoxybenzyl (PMB) group (**58**). Notably, even without protecting the alcohol group, the epoxide is opened with high regioselectivity in good yield when employing eight equivalents of PMHS (**56**). The silane reagent is added in higher excess, as the catalyst may also bind to the alcohol. Cleavage of

this bond *via* σ-bond metathesis, accompanied by abstraction of molecular hydrogen, regenerates the active species and protects the alcohol group *in situ via* formation of a silyl ether (Scheme 75).

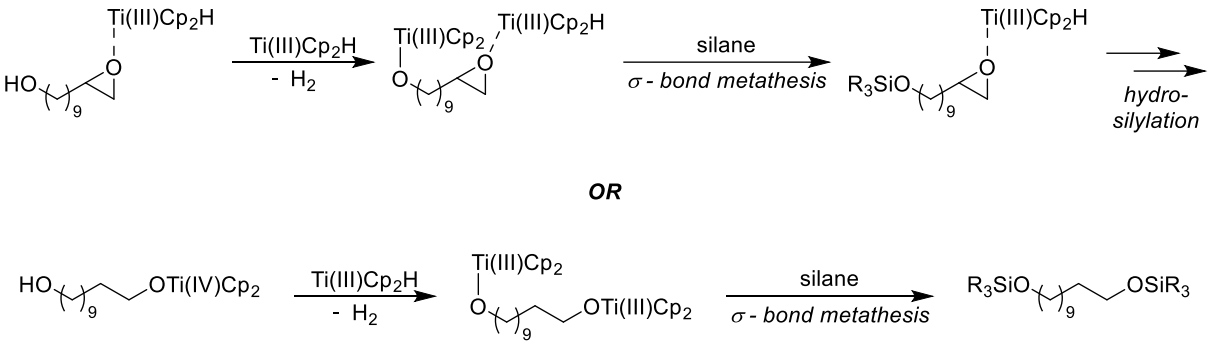

Scheme 75: Postulated mechanisms explaining the requirement of eight equivalents of PMHS in the opening of epoxides with an adjacent alcohol group.

The alcohols **61** and **64** are provided in excellent regioisomeric ratio due to the same reason **63** was obtained with high regioselectivity. The moderate regioselectivity of **59** and **60** arises from electronic destabilization of the *β*-titanoxy radical induced by the oxygen atom in the *β*-position relative to the radical. Previous studies by *Gansäuer et al.* reported the same observation in the titanocene-catalyzed regiodivergent synthesis of 1,2- and 1,3-diols. The formation of the 1,3-diol *via* the secondary radical with the oxygen moiety in the *β*-position was strongly disfavored. Their computational studies confirmed that the electron-withdrawing ability of the oxygen atom destabilized the corresponding transition state aside from steric factors.[186]

Although the regioselectivity is moderate, its increase by using **[Ti]-17** instead of common titanocenes is still significant. This was demonstrated by comparison with the opening of the respective epoxides using commercially available titanocene dichloride (**[Ti]-1**).

Table 7: Comparison of **[Ti]-17** with the commercially available catalyst **[Ti]-1** in the opening of electron-deficient substrates in terms of conversion and regioselectivity.[177]

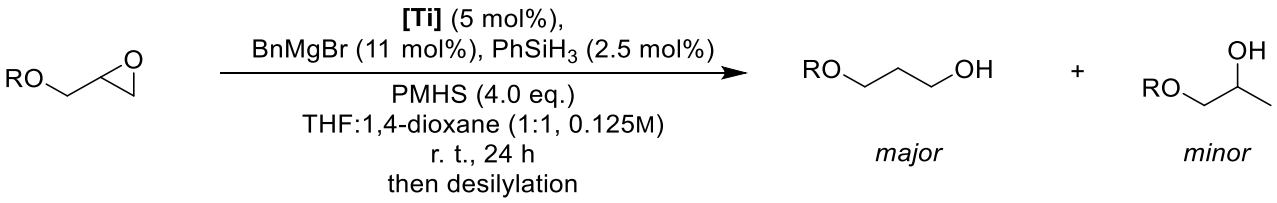

substrate	[Ti]-1	[Ti]-17
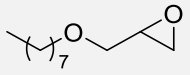 **65**	30% conversion, *r.r.* 60/40	100% conversion, *r.r.* 88/12
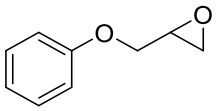 **66**	30% conversion, *r.r.* 60/40	100% conversion, *r.r.* 88/12
	 **[Ti]-1**	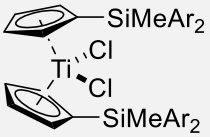 **[Ti]-17** Ar = 3,5-$(CF_3)_2C_6H_3$

The epoxides were generally prepared *via* the *Prilezhae*v-epoxidation using *m*CPBA. Substrate **71** was synthesized from the corresponding aldehyde *via* methylenation according to a literature procedure.[119] The protected epoxyalcohols were produced from the corresponding epoxyalcohol *via* TBS- and PMB-protection following a literature procedure.[187] The yields for these transformations are shown in the following Scheme.

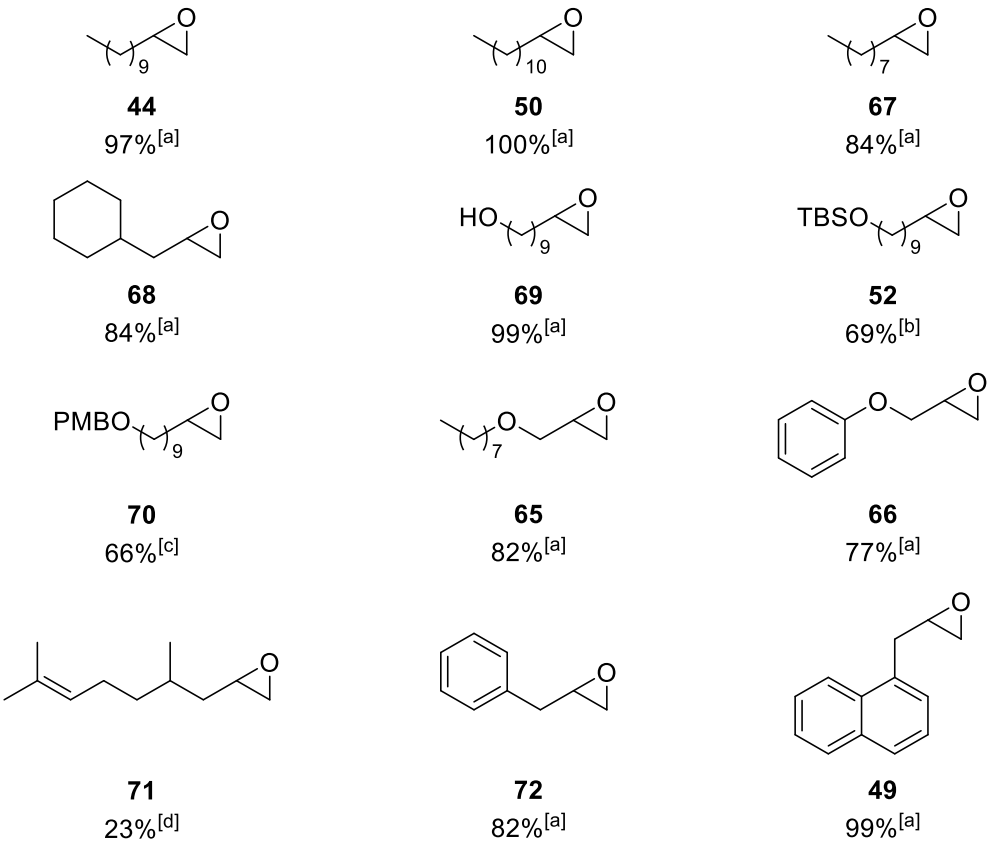

44 97%[a] **50** 100%[a] **67** 84%[a]

68 84%[a] **69** 99%[a] **52** 69%[b]

70 66%[c] **65** 82%[a] **66** 77%[a]

71 23%[d] **72** 82%[a] **49** 99%[a]

Scheme 76: Yields for the synthesis of the epoxide precursors; epoxide **51** was purchased from *Thermo Fisher Scientific*; [a]yields for the *m*CPBA epoxidation; [b]yield for the TBS-protection according to a literature procedure;[187] [c]yield for the PMB-protection according to a literature procedure;[187] [d]yield for the *Corey-Chaykovsky* reaction according to a literature procedure.[119,177]

In conclusion, by employing electron-deficient Si-substituted titanocenes in the titanocene-catalyzed hydrosilylation, we developed an efficient route to fatty alcohols (**45**, **53**–**55**) in high yields under sustainable conditions. While these products are structurally simple, their use in industry is invaluable,[13,14] as briefly described in Chapter 1.1. Fatty alcohols serve as precursors for important surfactants, such as sodium lauryl ether sulfate (SLES) and sodium lauryl sulfate (SLS). Both can be readily synthesized from fatty alcohol **45**. The former is produced *via* ethoxylation under basic conditions, followed by sulfation and neutralization, involving the addition of sulfur trioxide and sodium hydroxide, whereas the latter is directly synthesized by sulfation and neutralization. The long alkyl chain represents the hydrophobic part and the sulfate moiety represents the hydrophilic part. These surfactant properties are exploited in various products, such as detergents, cosmetic products, and emulsifiers.[188–190]

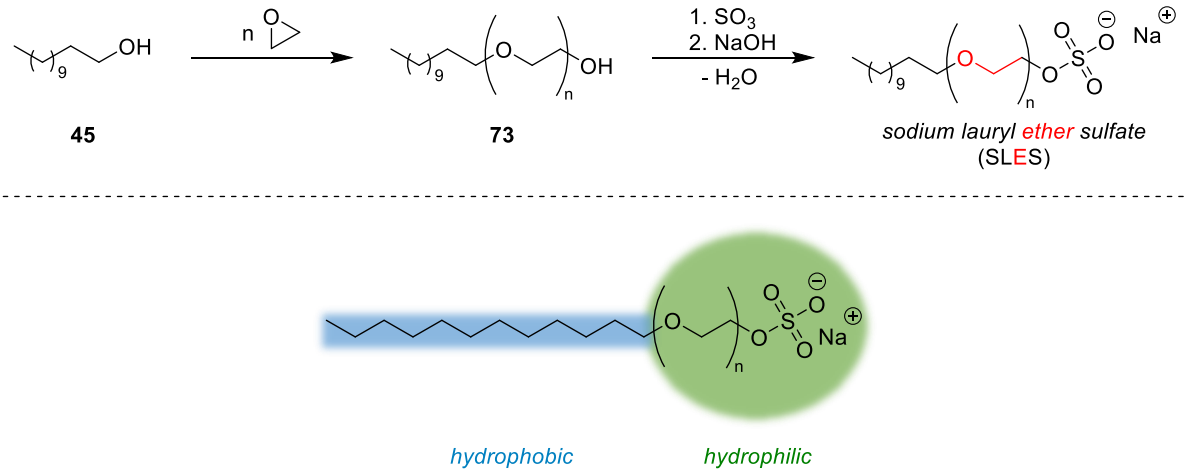

Scheme 77: General approach in the synthesis of the surfactant sodium lauryl ether sulfate (SLES) and properties of the surfactant.[188–190]

3.3 Titanocene-Catalyzed Hydrosilylation of Oxetanes

Epoxides are widely used as substrates for the synthesis of alcohols owing to their facile accessibility and high reactivity, as outlined in Chapter 1.4. However, their high reactivity is both a blessing and a curse, which becomes particularly apparent in the synthesis of fatty alcohols (**45**), as described in the previous Chapter. In this context, the high reactivity of the substrates allows for a competitive nucleophilic pathway because the desired radical mechanism proceeds relatively slow. As a result, an elaborate catalyst design was necessary to reduce the hydricity of the active species and thereby avoid the nucleophilic background reaction (Scheme 72/73). While we screened numerous catalysts and conditions, the use of other substrates in the titanocene-catalyzed hydrosilylation to afford fatty alcohols more efficiently was never considered. One promising substrate may be the structurally similar oxetanes. Their lower reactivity (see Chapter 1.6) may suppress the nucleophilic pathway without the need to reduce the active catalyst's hydricity. However, the lower reactivity may also affect the desired radical pathway.

With the use of the catalytic system described in Chapter 1.7, *Gansäuer et al.* reported difficulties in the reductive opening of oxetanes towards *anti-Markovnikov* alcohols. They failed to produce the desired alcohol in yields comparable to those obtained with the conversion of the corresponding epoxide (Scheme 35/20). This can be attributed to the incomplete conversion and *β*-hydride elimination as a side reaction *via* addition of a second equivalent of the active species. The first drawback presumably arises from the higher stability of oxetanes, and the side reaction may be favored by the slow rate of the HAT with an external donor (1,4-CHD).[101] Furthermore, *γ*-titanoxy radicals are sterically more accessible than *β*-titanoxy radicals due to the larger distance of the radical center to the metals' ligands.[101] Consequently, the addition of a second equivalent of the $Cp_2Ti(III)Cl$ species may be sterically more favored for radicals originating from oxetanes. In summary, this system was not capable of efficiently reducing oxetanes to the desired products due to the slow HAT step combined with the high accessibility of *γ*-titanoxy radicals and the high activation barrier for the oxetane opening by $Cp_2Ti(III)Cl$.[101]

Therefore, we decided to apply the titanocene-catalyzed hydrosilylation to oxetanes. By switching to $Cp_2Ti(III)H$ as the active species, drawbacks associated with the rate of the HAT could be avoided due to the intramolecular nature of this step. Hence, the titanocene-catalyzed hydrosilylation could offer a general and efficient method to reductively open oxetanes towards *anti-Markovnikov* alcohols and thereby also provide an efficient route to fatty alcohols.

In the context of this work, oxetane **74** is used as a screening substrate due to the structural similarity to epoxide **44**, which was used in the previous work. Thereby, the suitability of oxetanes as precursors for fatty alcohols can be evaluated. Furthermore, if the corresponding

anti-Markovnikov alcohol is obtained with the desired yield and regioisomeric ratio, it is reasonable to assume that similar or improved results are obtained for the conversion of disubstituted oxetanes owing to the faster rate of radical ring-opening.

Oxetane **74** was initially synthesized *via* a three-step sequence starting from the corresponding aldehyde. First, the aldehyde was converted into the homoallylic alcohol **75**.[191] Then, the terminal alkene was oxidatively cleaved by ozonolysis and subsequently reduced, forming diol **76**. Finally, *in situ* activation of the terminal alcohol group followed by an intramolecular *Williamson* etherification[192] afforded the oxetane **74** (Scheme 78). In addition to the relatively large number of steps required to access the desired oxetane, the crucial final step consistently gave low yields.

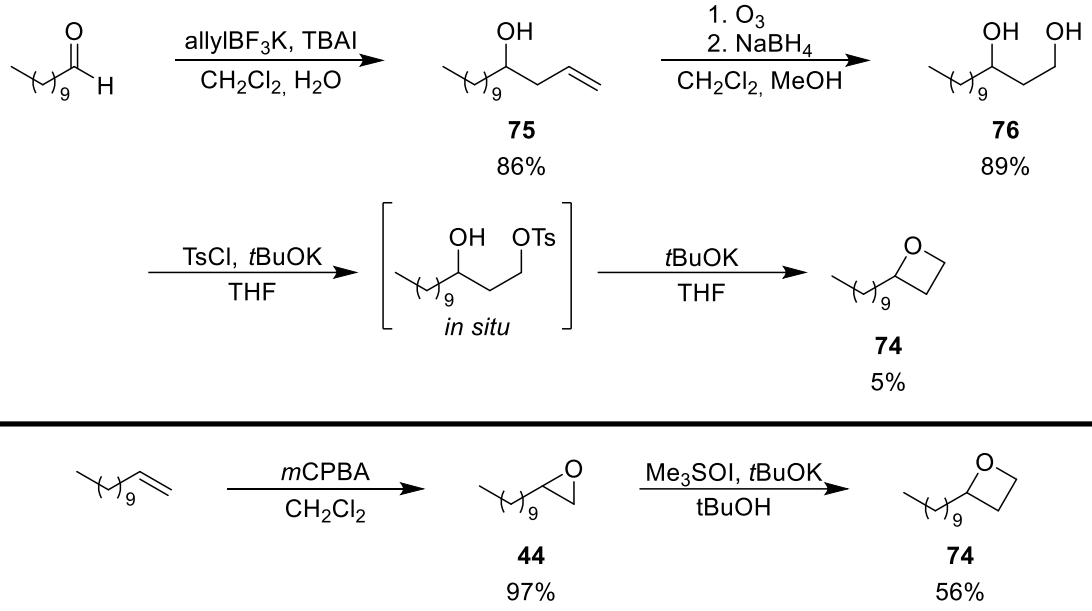

Scheme 78: Two synthetic routes towards oxetane **74**.[119,191,192]

Therefore, we turned to a significantly more straightforward approach based on the *Corey-Chaykovsky* reaction of the corresponding epoxide (Scheme 78).[119] Gratifyingly, oxetane **74** was obtained in much better yield *via* this two-step sequence. Moreover, according to this literature procedure,[119] the oxetane can even be directly prepared from the corresponding aldehyde *via* the *Corey-Chaykovsky* reaction. While we did not test this for oxetane **74**, other structurally similar oxetanes, discussed later, were directly synthesized from the respective carbonyl compounds *via* the *Corey-Chaykovsky* reaction.

For the screening experiments, the most electron-deficient Si-substituted titanocene dichloride **[Ti]-17** among our screened complexes,[177] the simplest Si-substituted catalyst **[Ti]-4**, and the commercially available titanocene dichloride **[Ti]-1** were tested.

Table 8: Screening experiments for the titanocene-catalyzed hydrosilylation of oxetane **74** towards the desired *anti-Markovnikov* alcohol **77** using different titanocenes, catalyst loads, and temperatures; [a]reactions involving **[Ti]-17** and **[Ti]-4** were performed in THF/1,4-dioxane (1:1, 0.125M); [b]performed in THF (0.250M).[193]

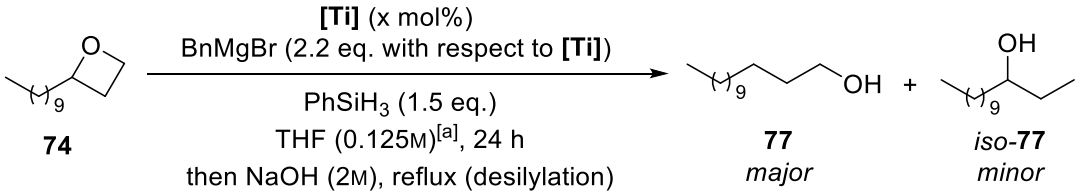

[Ti]	cat. load	temperature	conversion/%	*r.r.*	yield/%
[Ti]-17	5 mol%	r.t.	7	99:1	-
[Ti]-4	5 mol%	r.t.	30	95:5	-
[Ti]-1	5 mol%	r.t.	72	99:1	-
[Ti]-1	10 mol%	r.t.	99	99:1	85
[Ti]-1	5 mol%	reflux	100	99:1	85
[Ti]-1	1 mol%[b]	reflux	100	99:1	78

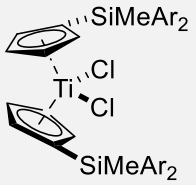

[Ti]-17
Ar = 3,5-$(CF_3)_2C_6H_3$

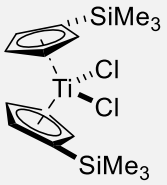

[Ti]-4

[Ti]-1

Surprisingly, catalyst **[Ti]-17**, which performed best in the opening of epoxide **44**,[177] afforded only a low conversion (Table 8, Entry 1) in the opening of the corresponding oxetane **74**. Using the structurally simpler Si-substituted catalyst **[Ti]-4** slightly improved the conversion (Table 8, Entry 2), but it remained low overall. Gratifyingly, the commercially available titanocene dichloride **[Ti]-1** provided a significantly higher conversion while offering excellent regioselectivity (Table 8, Entry 3). In contrast, the opening of epoxide **44** catalyzed by **[Ti]-1** proceeded with markedly lower regioselectivity (*r.r.* 64:36). Notably, despite the low conversions observed with the use of the Si-substituted catalysts, all three catalysts provide the alcohol **77** with a regioisomeric ratio higher than 94:6. Hence, the nucleophilic pathway is completely suppressed in the titanocene-catalyzed hydrosilylation of oxetane **74**, verifying our initial hypothesis. Remarkably, the theoretical regioselectivity limit observed for the opening of

epoxide **44** (*r.r.* 94:6) is even exceeded for the ring-opening reaction of oxetane **74**, as the regioisomeric ratio can reach values up to 99:1. This observation suggests that the steric interactions between the catalyst and oxetane **74** are more pronounced than those involved in the opening of the corresponding epoxide **44**. Consistent with this suggestion, the increased bulk of the catalysts **[Ti]-4** and **[Ti]-17** adversely affects the conversion of the oxetane opening. Given the comparatively high conversion and excellent regioselectivity observed with the readily accessible catalyst **[Ti]-1**, we continued with this catalyst and screened other conditions to further improve the conversion.

Increasing the catalyst load to 10 mol% facilitates the opening of **74** with nearly full conversion in high yield (condition **A**, Table 8, Entry 4). Under reflux conditions, the use of 5 mol% catalyst already provides the desired alcohol **77** with full conversion in the same yield (condition **B**, Table 8, Entry 5). Even with the use of only 1 mol% catalyst under reflux conditions, alcohol **77** was obtained with full conversion, albeit in slightly lower yields (condition **C**, Table 8, Entry 6).

While lower conversions were expected in the screening experiments due to the generally higher stability of oxetanes, the exceptionally high degree of regioselectivity was rather unexpected.

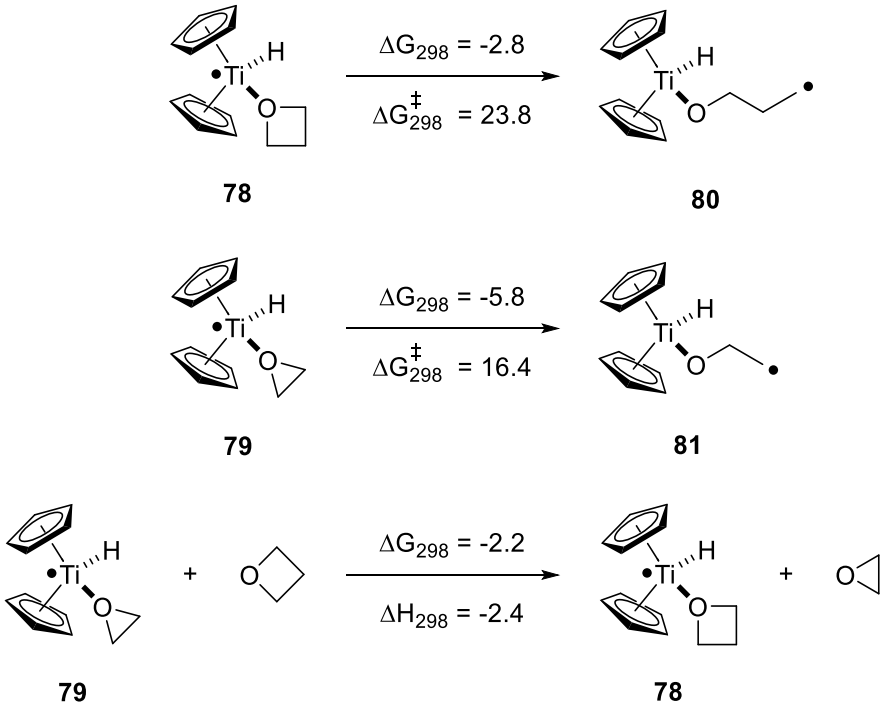

Scheme 79: Free *Gibbs* energies (ΔG) and free activation energies (ΔG‡) for the generation of the titanoxy radicals **80** and **81** from the titanocene complexes **78** and **79** at the PW6B95-D3/def2-QZVP + COSMO-RS // TPSS-D3/def2-TZVP + COSMO level in THF solution and ΔG, ΔH of ligand exchange reactions between **79** and **78** (1M) at 298 K; performed by *Qu*.[193–205]

Therefore, the different reactivity of oxetanes compared to epoxides in the titanocene-catalyzed hydrosilylation was investigated by conducting computational studies at the PW6B95-D3/def2-QZVP + COSMO-RS//TPSS-D3/def2-TZVP + COSMO level in THF solution at 298 K (Scheme 79).[193–205]

We calculated the *Gibbs* free energies (ΔG) and activation energies ($\Delta G^{‡}$) for the opening of both unsubstituted heterocycles to the corresponding titanoxy radicals (**80** and **81**) from the complexed intermediates (**78** and **79**) with $Cp_2Ti(III)H$ at 298 K. Moreover, the difference in free *Gibbs* energy (ΔG) and enthalpy (ΔH) for the binding of the active species to the epoxide (**79**) and the oxetane (**78**) was determined (Scheme 79). Consistent with previous studies discussed in Chapter 1.6,[101] the oxetane opening is 3 kcal/mol less favored due to the slightly lower ring strain (Δ = 2 kcal/mol). Furthermore, the activation barrier is 7.4 kcal/mol higher in energy compared to the corresponding epoxide opening reaction due to the $\sigma \rightarrow \pi$ delocalization[103] involved in the latter reaction. Notably, the binding of the active species to the oxetane is slightly more favored (ΔG = –2.2 kcal/mol, ΔH = –2.4 kcal/mol), primarily due to the enthalpy.

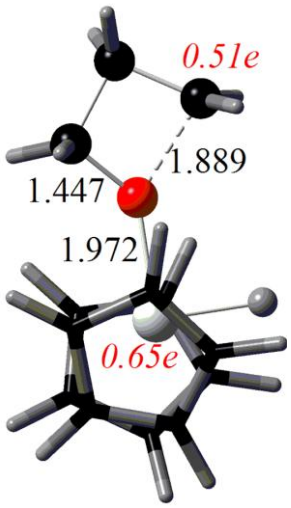

TS-O

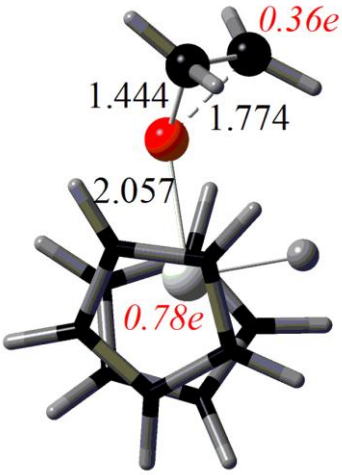

TS-E

Figure 19: Structures of the transition states of oxetane opening **TS-O** and epoxide opening **TS-E**. The C, H, O, and Ti atoms are illustrated as black, grey, red and white balls. Selected bond lengths (in Å) and spin densities are shown in black and red numbers, respectively; measured by *Qu*.[193]

Furthermore, the structures of the transition states were calculated for the epoxide opening (**TS-E**) and oxetane opening (**TS-O**) (Figure 19). The shorter Ti–O bond (1.97 Å (**TS-O**) vs. 2.06 Å (**TS-E**)) and the longer C–O bond (1.89 Å (**TS-O**) vs. 1.77 Å (**TS-E**)), which is broken during the oxidative addition, in **TS-O**, indicate that this transition state is “later” than **TS-E**.

Accordingly, the spin density of carbon in the C–O bond is higher in **TS-O** (0.51) than in **TS-E** (0.36). The computational studies are in line with experimental findings and previous studies.[101]

The higher activation barrier for the titanocene-catalyzed hydrosilylation of oxetanes supports our hypothesis that nucleophilic side reactions, responsible for the generation of the other regioisomer, are suppressed by the lower reactivity of oxetanes. For the same reason, higher temperatures are necessary for the full conversion of the substrate. Nevertheless, only 1 mol% catalyst is required under reflux conditions. Remarkably, subjecting the catalysis to higher temperatures does not deteriorate the regioselectivity.

The shorter Ti–O bond and longer C–O bond within the late **TS-O** result in a stronger contact between the catalyst's ligands and the substrate. Consequently, the steric interactions between those two are more pronounced, thereby increasing the energetic difference between the transition state leading to the primary radical and that leading to the secondary radical. Therefore, higher regioselectivity is achieved in the opening of oxetanes. In conclusion, by employing monosubstituted oxetanes in the titanocene-catalyzed hydrosilylation under the optimized conditions, the desired alcohol is obtained without the need for elaborate catalyst design, and with even better results.

We proposed a mechanism for the titanocene-catalyzed hydrosilylation of oxetanes similar to the corresponding epoxide opening reaction (Scheme 80). After generating the active species *via* benzyl activation, the oxetane is opened in a single-electron oxidative addition towards the corresponding *γ*-titanoxy radical. Subsequent intramolecular HAT followed by *σ*-bond metathesis using phenyl silane yields a silyl ether and regenerates the titanocene(III) hydride.

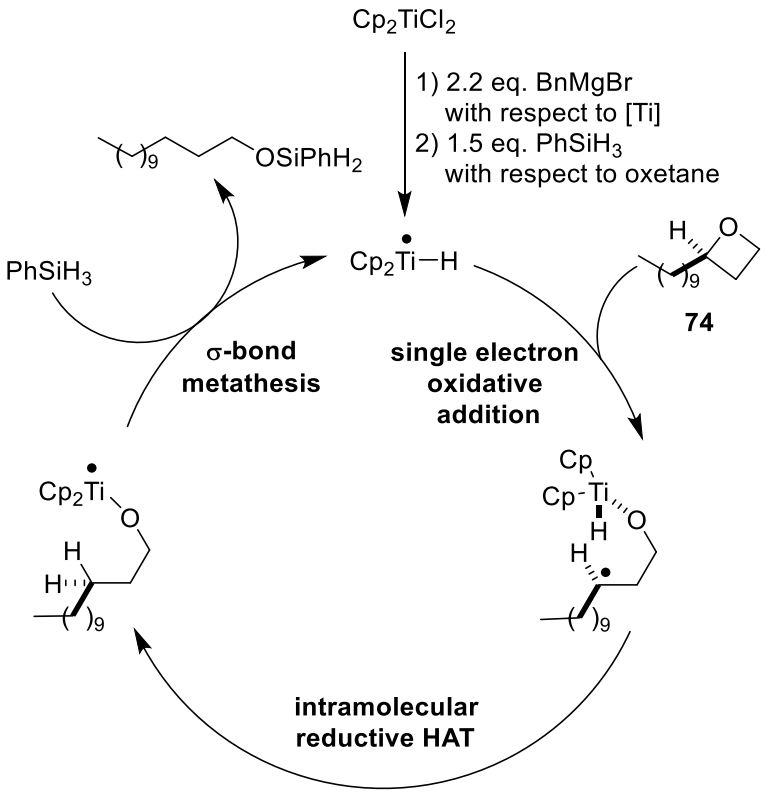

Scheme 80: Catalytic cycle for the titanocene-catalyzed hydrosilylation of oxetanes employing the benzyl activation and using phenyl silane.[193]

After establishing suitable conditions for the hydrosilylation of oxetanes and gaining a fundamental mechanistic understanding, a wide range of oxetanes were prepared. In this work, not only 2-substituted, but also 2,2-disubstituted and 3-substituted oxetanes were synthesized.

As mentioned before, the substrates were generally prepared *via* the *Corey-Chaykovsky* reaction from the corresponding ketones or epoxides.[119] The yields of the 2-substituted and 2,2-disubstituted substrates are shown in Scheme 81. The 3-substituted oxetanes were prepared by *Kilic* from diethyl phenylmalonate *via* the formation of the corresponding diols and subsequent intramolecular *Williamson* etherification,[192] similar to our initial synthetic route described in Scheme 78.

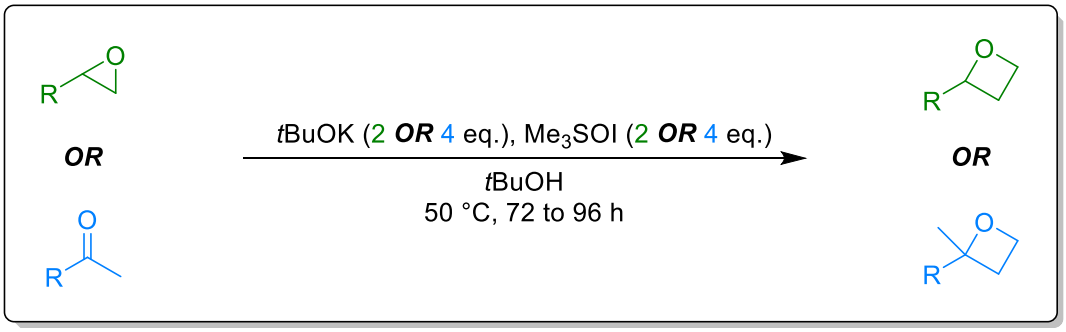

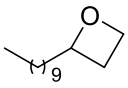

74
56%

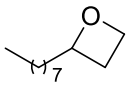

82
58%[a]

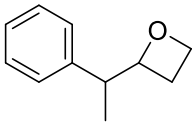

83
54%[a]

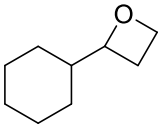

84
49%[a]

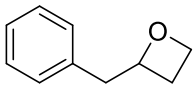

85
37%

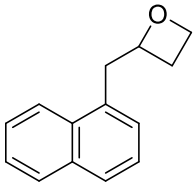

86
32%

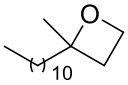

87
31%[a]

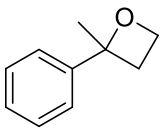

88
60%[a]

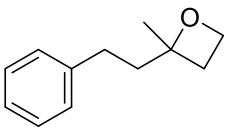

89
69%

Scheme 81: Methylenation of numerous epoxides and ketones towards the respective oxetanes *via Corey-Chaykovksy* reaction; [a]performed by *Kilic*.[193]

To examine the scope of our method, the titanocene-catalyzed hydrosilylation was then applied to these oxetanes under the optimized conditions (**A**, **B**, or **C**) using **[Ti]-1** (Scheme 82).

Gratifyingly, independent of the substitution pattern, the desired alcohols were obtained with high yields and excellent regioisomeric ratios. When the more energy-efficient conditions **A** were sufficient to achieve full conversion to the desired alcohol, no further optimization was pursued. In cases where full conversion was not obtained, the slightly superior conditions **B** were employed, to ensure complete conversion. Gratifyingly, applying the more sustainable conditions **C** to oxetane **89**, afforded alcohol **96** in identical yield and regioisomeric ratio as observed for conditions **A**. Notably, the opening of oxetane **89** with the previous system, discussed in Chapter 1.7, required excessive amounts of Mn and 1,4-CHD as well as large

quantities of Coll*HCl and 20 mol% of titanocene dichloride. Even then, the desired product was only obtained in 50% yield along with 15% of homoallylic alcohol as a side product (Scheme 35). Hence, we significantly improved the sustainability while simultaneously increasing the yield with our method.

By producing the alcohols **53**, **64**, **90**, **91**, **92**, and **93** essentially as single isomers in high yields, we proved the superiority of oxetanes as substrates in the synthesis of fatty alcohols *via* the titanocene-catalyzed hydrosilylation. As expected, the opening of 2,2-disubstituted oxetanes (**94**–**96**) exclusively affords the *anti-Markovnikov* alcohol, which is consistent with the corresponding opening reactions of 1,1-disubstituted epoxides reported in previous studies.[131] With the opening of 3-substituted oxetanes (**97**–**98**), we demonstrated that the hydrosilylation mechanism can even proceed *via* primary radicals instead of undergoing an unwanted side reaction. Furthermore, *Kilic* demonstrated the scalability of this method by performing the titanocene-catalyzed hydrosilylation of **82** on a gram-scale with good yield. Because the reaction generally proceeds without the formation of greater impurities, a simple bulb-to-bulb distillation was sufficient to purify the product.

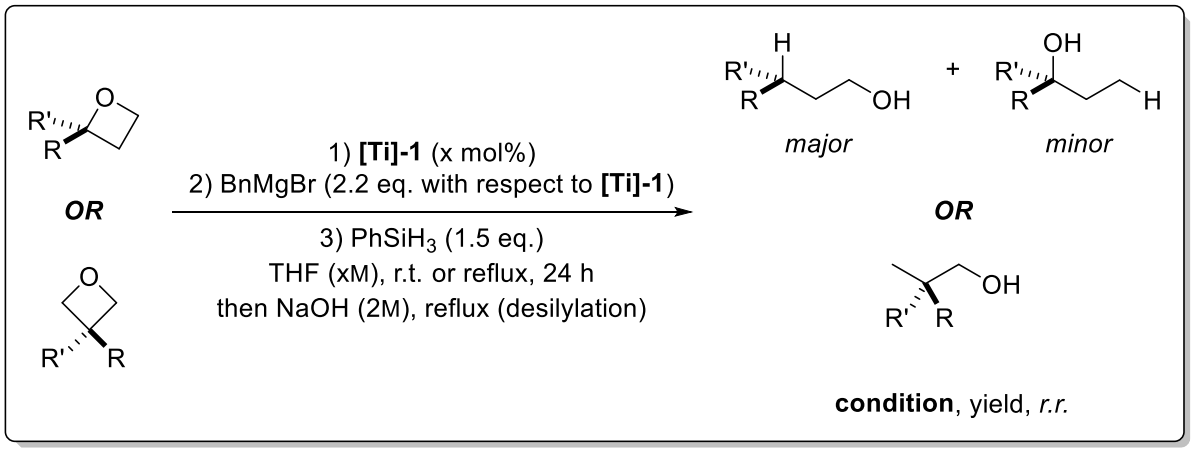

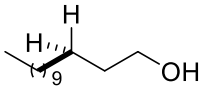

53
A, 85%, *r.r.* 99:1
B, 85%, *r.r.* 99:1
C, 78%, *r.r.* 99:1

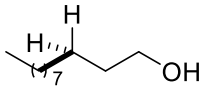

90
A, 89%, *r.r.* 99:1[a]
A, 69% (1.0 g scale), *r.r.* 99:1[a]

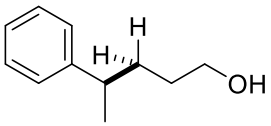

91
B, 76%, *r.r.* 99:1[a]

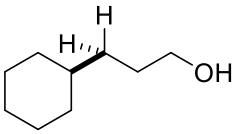

64
B, 80%, *r.r.* 99:1[a]

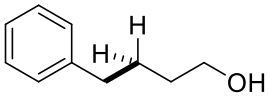

92
B, 86%, *r.r.* 98:2

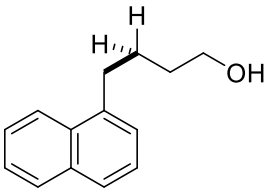

93
A, 69%, *r.r.* 98:2

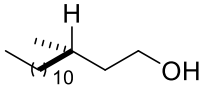

94
A, 86%, *r.r.* >99:1[a]

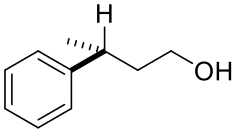

95
A, 70%, *r.r.* >99:1[a]

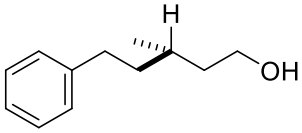

96
A, 86%, *r.r.* >99:1
C, 85%, *r.r.* >99:1

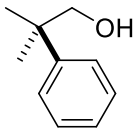

97
B, 74%[a]

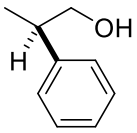

98
B, 71%[a]

Scheme 82: Substrate scope of the titanocene-catalyzed hydrosilylation of oxetanes using phenyl silane; condition **A**: 10 mol% **[Ti]**, THF (0.125M), room temperature; condition **B**: 5 mol% **[Ti]**, THF (0.125M), reflux temperature; condition **C**: 1 mol% **[Ti]**, THF (0.250M), reflux; the regioisomeric ratios were determined from NMR spectra of the crude products, after flash chromatography the minor isomers were completely absent; [a]performed by *Kilic*.[193]

To further improve the sustainability of our method, the PMHS conditions were employed under reflux. Analogously to the hydrosilylation of epoxides, substoichiometric amounts of $PhSiH_3$ were used as a “kick-starter”. However, we omitted the addition of 1,4-dioxane as a cosolvent, as the *Lewis*-acidic Mg-salts seem to pose no problem in the regioselective opening of oxetanes. Gratifyingly, applying these conditions to oxetane **74** also resulted in an excellent regioisomeric ratio of 99:1 (**53**), confirming our assumption. By avoiding the carcinogenic solvent 1,4-dioxane and employing the more sustainable and cost-efficient PMHS, the overall sustainability was improved noticeably. Satisfyingly, reducing the catalyst load from 5 mol% to 1 mol% afforded alcohol **53** with a similarly high yield. After establishing the optimal conditions in terms of sustainability, these were applied to the oxetanes **95**, **96**, **97**, and **98** with either 5 or 1 mol% catalyst load to demonstrate the generality of our method (Scheme 83).

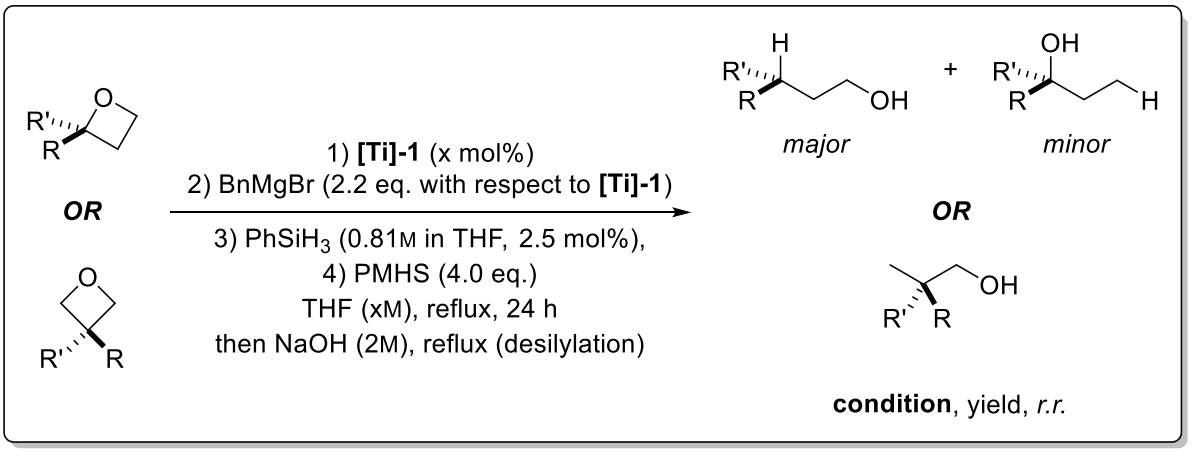

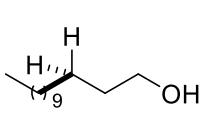

53
B, 73%, *r.r.* 99:1
C, 75%, *r.r.* 99:1

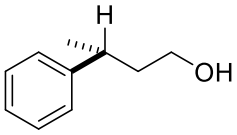

95
C, 64%, *r.r.* >99:1[a]

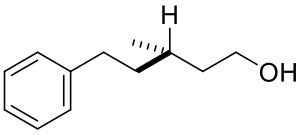

96
C, 70%, *r.r.* >99:1

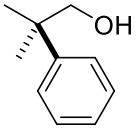

97
B, 76%[a]

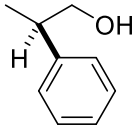

98
B, 79%[a]

Scheme 83: Substrate scope of the titanocene-catalyzed hydrosilylation of oxetanes using phenyl silane and PMHS; condition **B**: 5 mol% **[Ti]**, THF (0.125M), reflux temperature; condition **C**: 1 mol% **[Ti]**, THF (0.250M), reflux temperature; [a]performed by *Kilic*.[193]

Although *Takekoshi et al.* already reported a method for the titanium-catalyzed opening of oxetanes towards *anti-Markovnikov* alcohols in 2012,[206] the overall sustainability of their system is lower than that of our approach. They require stoichiometric amounts of Mg powder, Me_3SiCl, and often a large excess (10 eq.) of 1,4-CHD.[206] Furthermore, they commonly rely on a Ti-complex (**[Ti]-18**) that requires a multi-step synthesis,[206,207] whereas our approach exclusively employs the commercially available **[Ti]-1** to achieve the desired outcome. They subjected oxetane **99**, which is structurally similar to oxetane **85**, to their conditions (Scheme 84).[206] Albeit our approach affords the structurally similar alcohol **92** in lower yields, it is superior in terms of sustainability and operational simplicity.

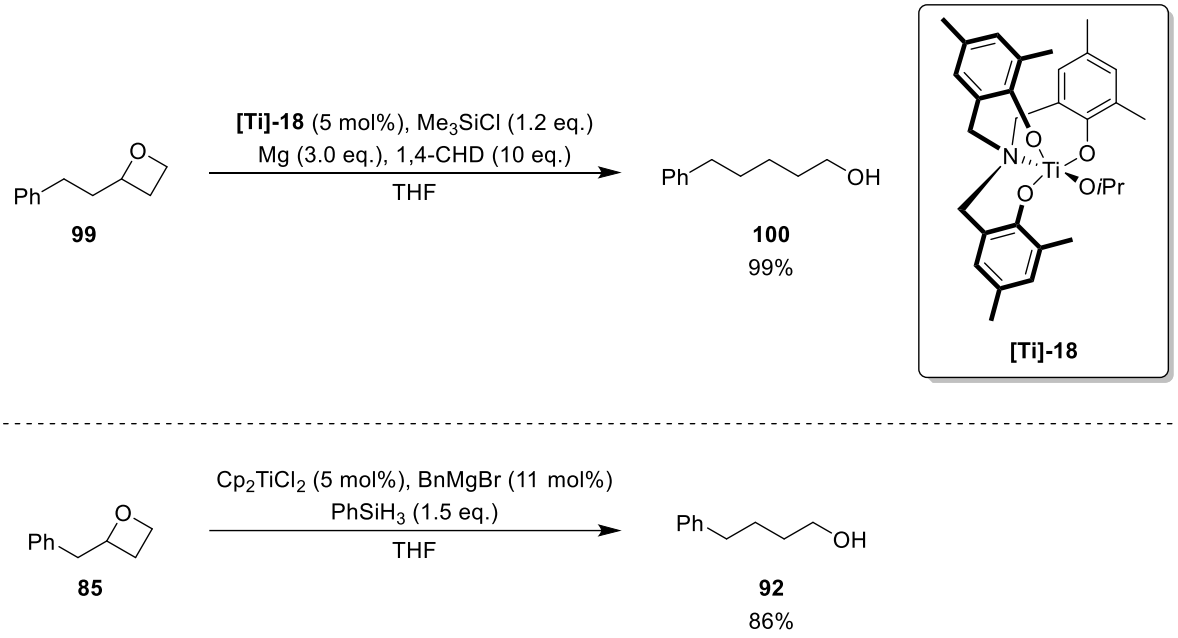

Scheme 84: Comparison of the titanium-catalyzed opening of oxetane **99** by *Takekoshi et al.* (top)[206] to the titanocene-catalyzed hydrosilylation of the structurally similar oxetane **85** (bottom)[193], performed in this work.

In conclusion, we developed a highly sustainable method to transform oxetanes, independent of the substitution pattern, into the corresponding *anti-Markovnikov* alcohols with excellent regioselectivity and good yields. Furthermore, we provided a more efficient synthetic route to fatty alcohols than epoxide hydrosilylation. Moreover, the titanocene-catalyzed hydrosilylation of oxetanes affords the desired alcohols with substitution patterns that are more difficult to access *via* the corresponding epoxide opening reactions.

4. Summary

In this work, novel aspects of the titanocene-catalyzed hydrosilylation were investigated. We developed a straightforward approach to synthesize enantiomerically and diastereomerically enriched *anti-Markovnikov* alcohols from a diastereomeric mixture of trisubstituted olefins. Our approach does not require the prior separation of olefins due to the diastereoconverging course of the Ti-catalyzed hydrosilylation.[131] To achieve control over the absolute configuration of the generated stereocenters, in addition to the relative control provided by the hydrosilylation, a suitable enantioselective epoxidation method was required. In this context, the *Shi*-epoxidation[86] fulfilled all our requirements. First, it controls the absolute configuration of the less-substituted stereocenter regardless of the olefin's geometry. Second, the *Shi*-epoxidation transforms both olefin stereoisomers with high enantioselectivity. Because the subsequent titanocene-catalyzed hydrosilylation ablates the initial configuration at the higher substituted stereocenter and introduces new stereochemical information relative to the other stereocenter, the *anti-Markovnikov* alcohol is obtained almost as a single enantiomer. We employed numerous trisubstituted olefins as an (*E*)/(*Z*)-mixture to prove our concept (Scheme 85). The resulting epoxides were amenable to diastereoselective hydrosilylation using phenyl silane or the more sustainable PMHS as the terminal HAT reagent.[148]

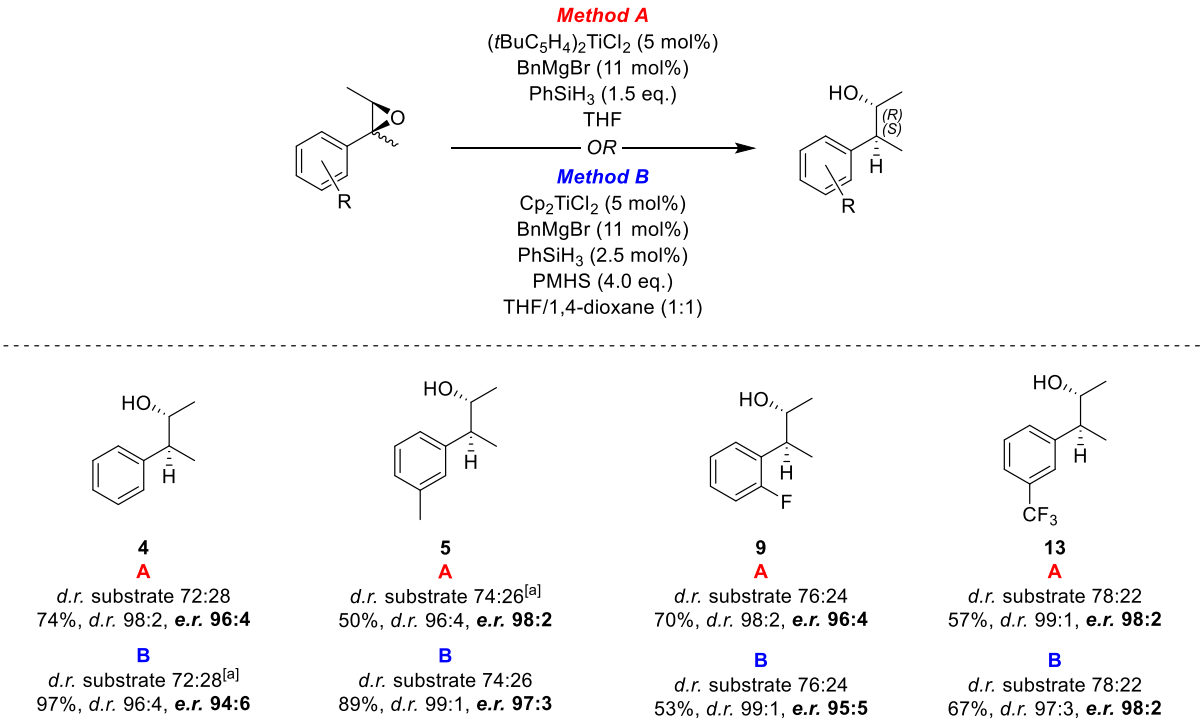

4
A
d.r. substrate 72:28
74%, *d.r.* 98:2, ***e.r.* 96:4**
B
d.r. substrate 72:28[a]
97%, *d.r.* 96:4, ***e.r.* 94:6**

5
A
d.r. substrate 74:26[a]
50%, *d.r.* 96:4, ***e.r.* 98:2**
B
d.r. substrate 74:26
89%, *d.r.* 99:1, ***e.r.* 97:3**

9
A
d.r. substrate 76:24
70%, *d.r.* 98:2, ***e.r.* 96:4**
B
d.r. substrate 76:24
53%, *d.r.* 99:1, ***e.r.* 95:5**

13
A
d.r. substrate 78:22
57%, *d.r.* 99:1, ***e.r.* 98:2**
B
d.r. substrate 78:22
67%, *d.r.* 97:3, ***e.r.* 98:2**

Scheme 85: Selected enantiomerically enriched (*anti*:*syn*) epoxide mixtures, synthesized from the olefins *via* *Shi*-epoxidation, reductively opened *via* the diastereoconverging titanocene-catalyzed hydrosilylation according to conditions **A** and **B**; [a]performed by *Mika*.[148]

In the second project, i focused on optimizing the regioselectivity of the titanocene-catalyzed hydrosilylation of monosubstituted alkyl epoxides. Previous studies demonstrated that the transformation of dodecene oxide results in a regioisomeric mixture (*r.r.* 78:22) of the *anti-Markovnikov* (major) and *Markovnikov* (minor) alcohol.[131] This can be rationalized by the hydricity of the active species, which enables the opening of the epoxide according to a nucleophilic mechanism, leading to the unwanted *Markovnikov* alcohol. Therefore, we screened numerous conditions and catalysts for the titanocene-catalyzed hydrosilylation in order to completely suppress the nucleophilic pathway. After extensive screening, we discovered that the use of more electron-deficient titanocenes significantly improves the regioselectivity. The design of these titanocenes was inspired by previous EPR studies[132] demonstrating the non-covalent interaction between the employed silane and the titanium-bound hydride. In cooperation with *Höthker* and *Krebs*, numerous Si-substituted titanocenes were designed exhibiting attenuated hydricity arising from the intramolecular coordination between the silyl groups and the titanium-bound hydride. Eventually, we designed a sufficiently electron-deficient complex (**[Ti]-17**) that affords the *anti-Markovnikov* alcohol **45** with essentially the same regioselectivity (*r.r.* 92:8) as observed in the opening of dodecene oxide (**44**) with $Cp_2Ti(III)Cl$ and a non-nucleophilic HAT reagent. Subsequently, we subjected a wide range of monosubstituted alkyl epoxides to our conditions using the novel catalyst **[Ti]-17** (Scheme 86).[177]

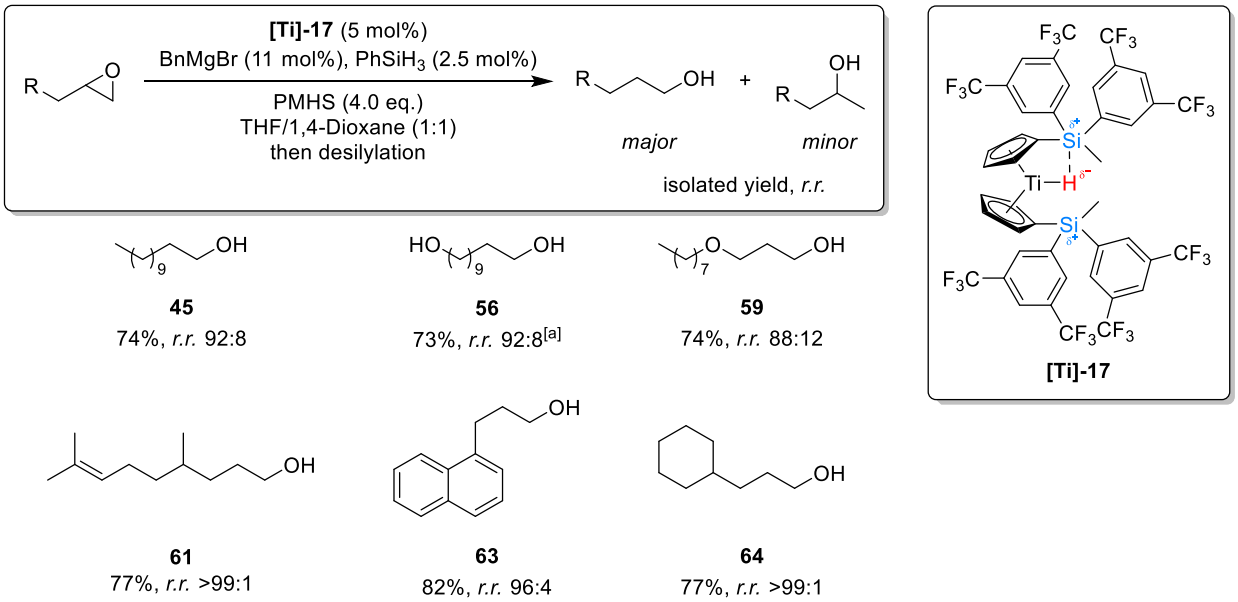

Scheme 86: Regioselective opening of monosubstituted alkyl epoxides to the desired *anti-Markovnikov* alcohols *via* the titanocene-catalyzed hydrosilylation using the electron deficient complex **[Ti]-17**; [a]8.0 equivalents of PMHS employed.[177]

In the final part of my work, the titanocene-catalyzed opening of oxetanes was investigated. With $Cp_2Ti(III)Cl$ as the active species and an external HAT reagent (1,4-CHD), oxetane

opening had previously been shown to occur sluggishly at best due to *β*-hydride elimination as a side reaction, initiated by the addition of a second equivalent of the active species (Scheme 35).[101] Therefore, we applied the titanocene-catalyzed hydrosilylation to oxetanes to suppress unwanted radical trapping, as the HAT step is significantly faster due to the intramolecular nature. Gratifyingly, the desired *anti-Markovnikov* alcohols were obtained in high yields without the formation of the elimination side product (Scheme 87). In contrast to epoxide hydrosilylation, the transformation of monosubstituted alkyl oxetanes leads to excellent regioisomeric ratios without the need of elaborate catalyst design. We investigated this surprisingly different reactivity of oxetanes compared to epoxides with DFT studies. They demonstrated the higher activation barrier and a “later” transition state for the opening of oxetanes, which is consistent with experimental findings. The higher activation barrier obviates the need for elaborate catalyst design to suppress the nucleophilic pathway, and the “later” TS leads to improved regioselectivity than in the corresponding optimized epoxide opening reaction.[193] We demonstrated the efficiency of oxetane hydrosilylation by applying the system to a wide range of oxetanes with different substitution patterns. We proposed a mechanism similar to the epoxide hydrosilylation (Scheme 87).[193]

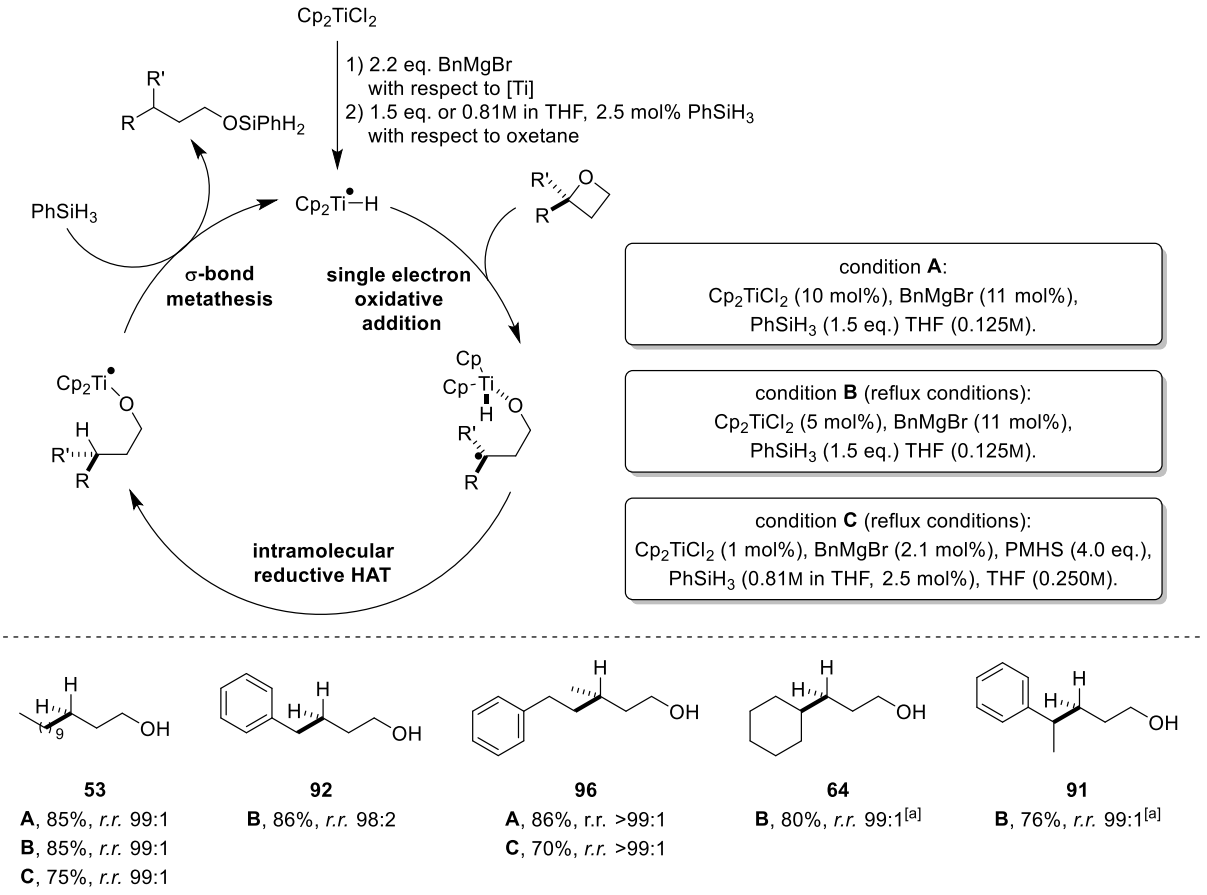

Scheme 87: Proposed mechanism of the titanocene-catalyzed hydrosilylation of oxetanes and the substrate scope of the system according to conditions **A**, **B**, or **C**; [a]performed by *Kilic*.[193]

5. Experimental Part

5.1 General Information

All moisture- or oxygen-sensitive reactions were carried out under inert atmosphere (argon) using standard *Schlenk* and vacuum line techniques. The solvents used were purified and deoxygenated by distillation (THF over Na for reactions involving Ti(III)), by an *MBraun MB-SPS-800* system (THF, Et_2O, CH_2Cl_2). Other solvents were either distilled under air (petroleum ether 40/65 (PE), cyclohexane (CH), ethyl acetate (EA)) or used without further purification (dimethoxymethane (DMM), CH_2Cl_2, CH_3CN, Et_2O, NEt_3). All reactions were monitored by thin-layer chromatography (TLC) on *Merck* silica gel 60 F254 plates using UV light as visualizing agent (if applicable) or a solution of ammoniummolybdate tetrahydrate (25 g/L) and $Ce(SO_4)_2$*4 H_2O (10 g/L) in 10% aqueous H_2SO_4 followed by heating. The products were purified by flash chromatography on *Merck* silica gel 60 (0.035–0.070 mm).

^{1}H-, ^{13}C-, ^{19}F- and ^{29}Si-NMR spectra were recorded on *Bruker Avance I 300 MHz* (^{1}H-base frequency: 300.13 MHz), *Bruker Avance I 300 MHz* (*Oxford Magnet*) (^{1}H-base frequency: 300.13 MHz), *Bruker Avance I 400 MHz* (^{1}H-base frequency: 400.13 MHz), *Bruker Avance I 500 MHz* (^{1}H-base frequency: 499.13 MHz), *Bruker Avance III HD Ascend 500 MHz* (^{1}H-base frequency: 500.13 MHz) or *Bruker Avance III 700 MHz Cryo* (^{1}H-base frequency: 700.41 MHz) at 298 K. Chemical shifts are denoted in ppm (δ), and calibrated by using residual nondeuterated solvent [$CHCl_3$ (7.26 ppm) or C_6H_6 (7.16 ppm)] as internal reference for ^{1}H-NMR and the deuterated solvent [$CDCl_3$ (77.2 ppm) or C_6D_6 (128.1 ppm)] as internal standard for ^{13}C-NMR.[208] Overlapping signals of different diastereomers are indicated with an asterisk. ^{19}F-spectra are recorded without an internal standard. In order to distinguish diastereoisomers by ^{19}F-NMR spectroscopy, their shift is reported with two decimals. High resolution mass spectra analysis was performed on a *Thermoquest MAT 95 CL* instrument (*Thermo Finnigan*, EI/ESI) or an *Orbitrap XL* mass spectrometer (*Thermo Fisher Scientific*, APCI/ESI). Melting points were measured on the *DigiMelt MPA* 160. IR spectra were recorded on the ATR-IR spectrometers *NicoletTM 380* or *Shimadzu IRSpirit.* Optical rotations were measured on an *Anton Paar MCP 150 polarimeter* and are given as specific rotations. MPLC was performed on a *Teledyne* Combi*Flash*® Rf^+ chromatography system. Enantiomeric excesses were determined by chiral HPLC by *Schneider*. In the case of unsatisfactory separation of enantiomers, the enantiomeric excess was determined using ^{19}F-NMR following esterification using (*S*)-*Mosher*-acid chloride and comparison of the corresponding (*R*)-MTPA ester obtained from a racemic alcohol sample.[209] These racemic alcohols were obtained by titanocene catalyzed hydrosilylation of racemic epoxides, which were prepared by *Prilezhaev* epoxidation.

5.2 Synthesis of *Grignard* Solutions and Titanocene Dichlorides

5.2.1 BnMgBr Solution

Magnesium turnings (5.83 g, 240 mmol, 6.00 eq.) were dry stirred in an argon-flushed heat-dried *Schlenk* tube for two days until the magnesium was finely divided. Dry Et_2O (10 mL) was added to cover the magnesium and the suspension was cooled to 0 °C. A solution of benzyl bromide (4.75 mL, 40.0 mmol, 1.00 eq.) in dry Et_2O (40 mL) was added dropwise over a period of 2 h. Stirring was continued at 0 °C for another 4 h before the solution was filtered *via* cannula into another *Schlenk* tube. The concentration was determined according to *Love*.[210]

5.2.2 Titanocene Dichlorides

[Ti]-3, **[Ti]-4**, **[Ti]-8**, and **[Ti]-12** were synthesized by the work group according to a literature procedure,[177,211] while **[Ti]-1** was acquired from *Sigma-Aldrich*.

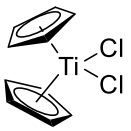

[Ti]-1

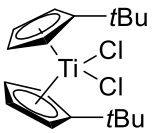

[Ti]-3

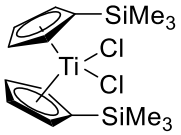

[Ti]-4

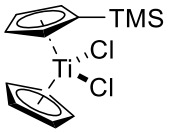

[Ti]-8

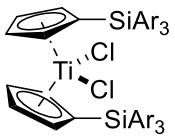

[Ti]-12
(Ar = *p*-F-C_6H_4)

5.3 General Procedures

5.3.1 *Wittig*-Olefination (GP I)

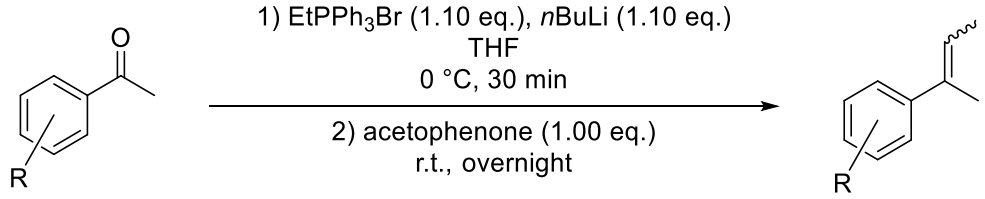

The reaction is performed under argon. $EtPPh_3Br$ (1.10 eq.) is dissolved in dry THF (40 mL) before cooling the solution to 0 °C. Then, *n*BuLi (2.5M in hexanes, 1.10 eq.) is slowly added, and the mixture is stirred for 30 min. at 0 °C. Subsequently, the respective ketone (1.00 eq.) is added before stirring the mixture at room temperature for the indicated amount of time. The reaction mixture is washed with sat. aq. NH_4Cl-solution and H_2O. Afterwards, the aqueous phase is extracted three times with Et_2O. The combined organic layers are washed with brine and dried over $MgSO_4$. Following the removal of solvents under reduced pressure, an excess of PE is added until no more solids precipitate from the solution. Filtration is followed by concentration of the filtrate and subsequent purification by flash chromatography. The desired olefins are obtained as a mixture of (*E*)- and (*Z*)-isomers. The diastereomers are identified by comparison with literature values. In case of new compounds, the (*E*)-geometry is assumed for the isomer with a smaller difference in shift for the benzylic- and homobenzylic methyl groups in the ^1H- and ^{13}C-NMR spectra. This assignment is based on a comparison with literature values for various (*E*)- and (*Z*)-*α*,*β*-dimethyl styrenes. Overlapping NMR signals of (*E*)- and (*Z*)-isomers are denoted with asterisks.

5.3.2 *Prilezhaev*-Epoxidation (GP II)

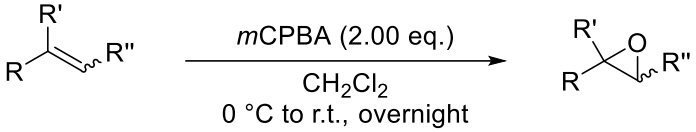

In an open round bottom flask, the respective olefin (1.00 eq.) is dissolved in CH_2Cl_2 (10 mL/mmol olefin), and the mixture is cooled to 0 °C. Then, *meta*-chloroperoxybenzoic acid (≤77% in H_2O, 2.00 eq.) is added portionwise and the mixture is stirred overnight. Afterwards, the reaction is quenched by addition of aq. NaOH (2M in H_2O) before separating the layers and extracting the aqueous layer three times with CH_2Cl_2. Subsequent washing of the combined organic layers with brine is followed by drying over $MgSO_4$ and removal of solvents under reduced pressure. Flash chromatography yields the desired epoxide. Trisubstituted epoxides are obtained as a mixture of *anti*- and *syn*-isomers. The diastereomers

are assigned by ^{1}H- and ^{13}C-NMR spectroscopy in analogy to the assignment of their respective olefins, with the more similar CH_3-shifts being attributed to the *anti*-isomer. Overlapping NMR signals of *anti*- and *syn*-isomers are denoted with asterisks.

5.3.3 *Shi*-Epoxidation (GP III)

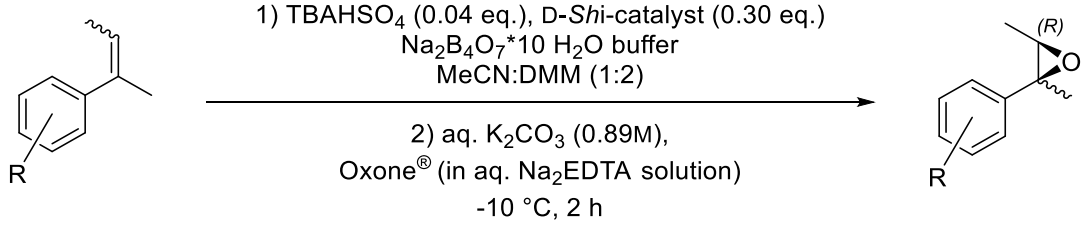

To a stirred solution of the respective olefin (1.00 eq.) in MeCN-DMM (1:2, 15 mL/mmol olefin), a buffer solution (0.05M $Na_2B_4O_7$*10 H_2O in 4*10^{-4}M aq. Na_2(EDTA), 10 mL/mmol olefin), $TBAHSO_4$ (0.04 eq.), and D-*Shi*-catalyst **1** (0.30 eq.) are added. After cooling the mixture to -10 °C, an Oxone® solution (0.85 g in 6.5 mL 4*10^{-4}M aq. Na_2(EDTA)/mmol olefin, 1.38 eq.) and aq. K_2CO_3 solution (0.89M, 6.5 mL/mmol olefin) are added simultaneously dropwise over a period of 2 h at the indicated temperature. After stirring for the indicated amount of time at the given temperature, PE and H_2O are added. The aqueous layer is extracted three times with PE before washing the combined organic layers with brine and drying them over $MgSO_4$. Removal of the solvents under reduced pressure followed by purification *via* flash chromatography yields the desired epoxides as *syn*/*anti*-mixtures. *Anti*- and *syn*-diastereomers are assigned by ^{1}H- and ^{13}C-NMR spectroscopy in analogy to the assignment of their respective olefins, with the more similar CH_3-shifts being attributed to the *anti*-isomer. Overlapping NMR signals of *anti*- and *syn*-isomers are denoted with asterisks.

5.3.4 *Corey-Chaykovsky* Reaction (GP IV)

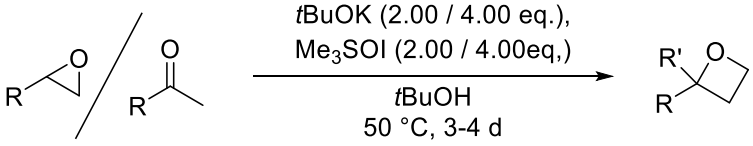

The following procedure is inspired by a method reported by *Okuma et al.*[119] The reaction is performed under argon. In a heat-dried *Schlenk* flask, a suspension of *t*BuOK (2.00 or 4.00 eq.) and trimethylsulfoxonium iodide (2.00 or 4.00 eq.) in dry *t*BuOH (2.40 or 3.00 mL/mmol substrate) is stirred for 1 h at 50 °C. Then, a solution of the respective epoxide or ketone (1.00 eq.) in dry *t*BuOH (1.20 or 0.60 mL/mmol substrate) is added, and the mixture is stirred for 3-4 days at 50 °C. Upon completion, the reaction is quenched by addition of H_2O.

The layers are separated, and the aqueous layer is extracted three times with EA. The combined organic layers are washed with brine, dried over sodium sulfate, and the solvent is removed under reduced pressure. The crude product is purified by flash chromatography to obtain the corresponding oxetane.

5.3.5 Hydrosilylation of Trisubstituted Epoxides Using $PhSiH_3$ as a Terminal HAT Reagent (GP V)

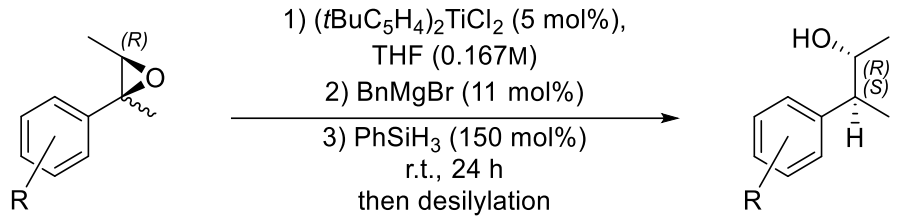

The reaction is performed under argon. In a heat-dried *Schlenk* tube, $(t\text{BuC}_5\text{H}_4)_2\text{TiCl}_2$ (5 mol%) is dissolved in freshly distilled THF (6 mL/mmol epoxide). Then, BnMgBr (11 mol%) is added, and the mixture is stirred until the color of the solution changes from red to deep purple. After subsequent addition of $PhSiH_3$ (1.50 eq.), the color turns green, indicating the activation of the titanocene catalyst. At last, the respective epoxide (1.00 eq.) is added, and the reaction mixture is stirred for 24 h at room temperature. Afterwards, THF (40 mL/mmol epoxide) and NaOH-solution (2M in H_2O, 40 mL/mmol epoxide) are added before heating the mixture to reflux overnight. After cooling to room temperature, the layers are separated, and the aqueous layer is extracted three times with Et_2O. The combined organic layers are washed with brine and dried over magnesium sulfate. After removal of solvents under reduced pressure and flash chromatography, the desired alcohol is obtained. The *d.r.* values are determined from the crude ^{1}H-NMR spectra, while the *e.r.* values of the products are determined from ^{19}F-NMR spectroscopy after esterification according to **GP XI**.

5.3.6 Hydrosilylation of Trisubstituted Epoxides Using PMHS as a Terminal HAT Reagent (GP VI)

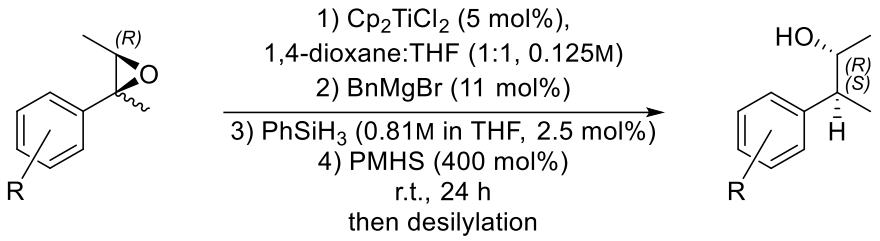

The reaction is performed under argon. In a heat-dried *Schlenk* tube, Cp_2TiCl_2 (5 mol%) is dissolved in freshly distilled THF (8 mL/mmol epoxide). Then, BnMgBr (11 mol%) is added and the mixture is stirred until the color of the solution changes from red to deep purple. After subsequent addition of $PhSiH_3$ (0.81M in THF, 2.5 mol%) the color turns green, indicating the activation of the titanocene catalyst. Subsequently, 1,4-dioxane (4 mL/mmol epoxide) and PMHS (4.00 eq.) are added. At last, the respective epoxide (1.00 eq.) is added, and the reaction mixture is stirred for 24 h at room temperature. Afterwards, THF (40 mL/mmol epoxide) and NaOH solution (2M in H_2O, 40 mL/mmol epoxide) are added before heating the mixture to reflux overnight. After cooling to room temperature, the layers are separated, and the aqueous layer is extracted three times with Et_2O. The combined organic layers are washed with brine and dried over magnesium sulfate. After removal of solvents under reduced pressure and flash chromatography, the desired alcohol is obtained. The *d.r.* values are determined from the crude ^{1}H-NMR spectra, while the *e.r.* values of the products are determined from ^{19}F-NMR spectroscopy after esterification according to **GP XI**.

5.3.7 Hydrosilylation of Monosubstituted Epoxides Using $PhSiH_3$ as a Terminal HAT Reagent (GP VII)

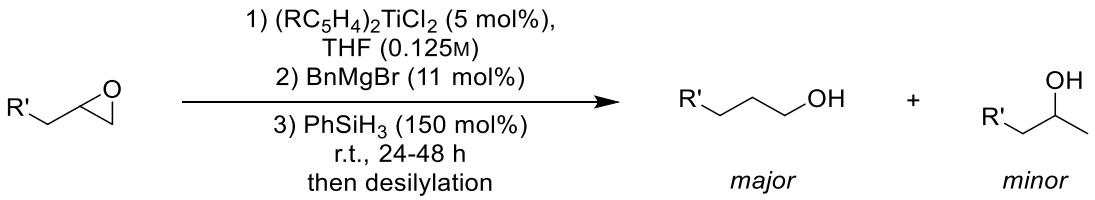

The reaction is performed under argon. In a heat-dried *Schlenk* tube, the respective titanocene (5 mol%) is dissolved in freshly distilled THF (8 mL/mmol epoxide). Then, BnMgBr (11 mol%) is added, and the mixture is stirred until the color of the solution changes from red to deep purple. After subsequent addition of $PhSiH_3$ (1.50 eq.), the color turns green, indicating the activation of the titanocene catalyst. At last, the respective epoxide (1.00 eq.) is added, and the reaction mixture is stirred for the indicated amount of time at room temperature. Afterwards, THF (40 mL/mmol epoxide) and NaOH-solution (2M in H_2O, 40 mL/mmol epoxide) are added

before heating the mixture to reflux overnight. After cooling to room temperature, the layers are separated, and the aqueous layer is extracted three times with Et_2O. The combined organic layers are washed with brine and dried over magnesium sulfate. After removal of solvents under reduced pressure and flash chromatography, the desired alcohol is obtained as a mixture of regioisomers. The NMR data are only shown for the major isomer. The *r.r.* values are determined from the crude ^{1}H-NMR spectra by integration of the characteristic signals indicated below.

5.3.8 Hydrosilylation of Monosubstituted Epoxides Using PMHS as a Terminal HAT Reagent (GP VIII)

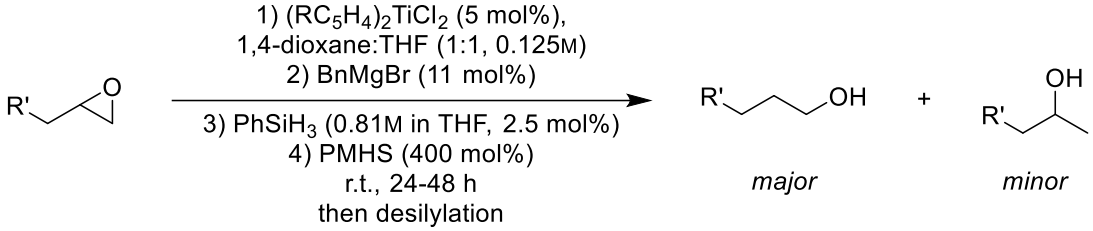

The reaction is performed under argon. In a heat-dried *Schlenk* tube, the respective titanocene (5 mol%) is dissolved in freshly distilled THF (4 mL/mmol epoxide). Then, BnMgBr (11 mol%) is added, and the mixture is stirred until the color of the solution changes from red to deep purple. After subsequent addition of $PhSiH_3$ (0.81M in THF, 2.5 mol%), the color turns green, indicating the activation of the titanocene catalyst. Subsequently, 1,4-dioxane (4 mL/mmol epoxide) and PMHS (4.00 eq.) are added. At last, the respective epoxide (1.00 eq.) is added, and the reaction mixture is stirred for the indicated amount of time at room temperature. Afterwards, THF (40 mL/mmol epoxide) and NaOH solution (2M in H_2O, 40 mL/mmol epoxide) are added before heating the mixture to reflux overnight. After cooling to room temperature, the layers are separated, and the aqueous layer is extracted three times with Et_2O. The combined organic layers are washed with brine and dried over magnesium sulfate. After removal of solvents under reduced pressure and flash chromatography, the desired alcohol is obtained as a mixture of regioisomers. The NMR data are only shown for the major isomer. The *r.r.* values are determined from the crude ^{1}H-NMR spectra by integration of the characteristic signals indicated below.

5.3.9 Hydrosilylation of Oxetanes Using $PhSiH_3$ as a Terminal HAT Reagent (GP IX)

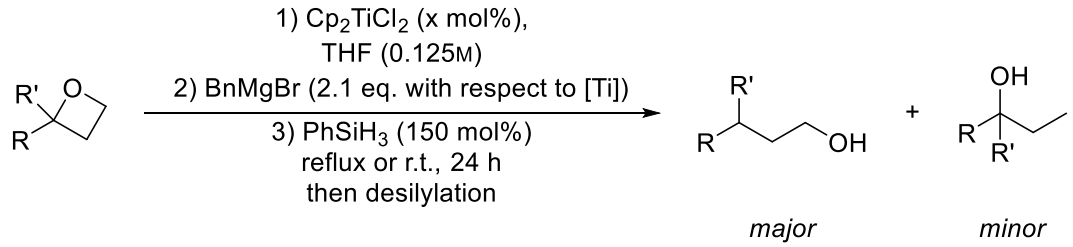

The reaction is performed under argon. In a heat-dried *Schlenk* tube, Cp_2TiCl_2 (x mol%) is dissolved in freshly distilled THF (8 mL/mmol oxetane). Then, BnMgBr (2.1 eq. with respect to [Ti]) is added, and the mixture is stirred until the color of the solution changes from red to deep purple. After subsequent addition of $PhSiH_3$ (1.50 eq.), the color turns green, indicating the activation of the titanocene catalyst. At last, the respective oxetane (1.00 eq.) is added, and the reaction mixture is stirred for 24 h under reflux conditions or at room temperature. Afterwards, THF (40 mL/mmol oxetane) and NaOH-solution (2M in H_2O, 40 mL/mmol oxetane) are added before heating the mixture to reflux overnight. After cooling to room temperature, the layers are separated, and the aqueous layer is extracted three times with Et_2O. The combined organic layers are washed with brine and dried over sodium sulfate. After removal of solvents under reduced pressure, the crude product is obtained either as a mixture of regioisomers or as the predominant isomer (the primary alcohol) in pure form. The *r.r.* values are determined from the crude ^{1}H-NMR spectra by integration of the characteristic signals indicated below.

5.3.10 Hydrosilylation of Oxetanes Using PMHS as a Terminal HAT Reagent (GP X)

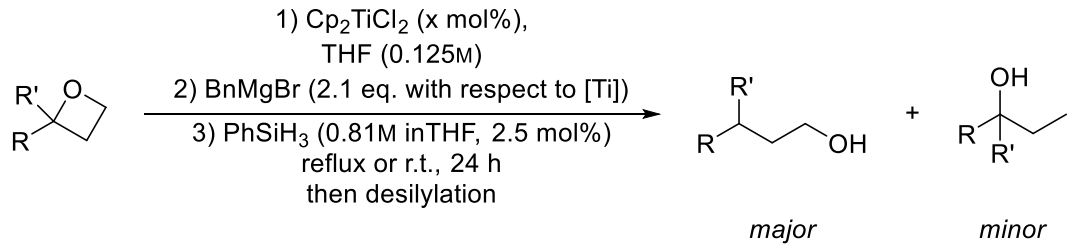

The reaction is performed under argon. In a heat-dried *Schlenk* tube, Cp_2TiCl_2 (x mol%) is dissolved in freshly distilled THF (8 mL/mmol oxetane). Then, BnMgBr (2.1 eq. with respect to [Ti]) is added and the mixture is stirred until the color of the solution changes from red to deep purple. After subsequent addition of $PhSiH_3$ (0.81M in THF, 2.5 mol%), the color turns green, indicating the activation of the titanocene catalyst. Subsequently, PMHS (4.00 eq.) is added. At last, the respective oxetane (1.00 eq.) is added, and the reaction mixture is stirred for 24 h under reflux conditions or at room temperature. Afterwards, THF (40 mL/mmol oxetane) and NaOH-solution (2M in H_2O, 40 mL/mmol oxetane) are added before heating the mixture to

reflux overnight. After cooling to room temperature, the layers are separated, and the aqueous layer is extracted three times with Et_2O. The combined organic layers are washed with brine and dried over sodium sulfate. After removal of solvents under reduced pressure, the crude product is obtained either as a mixture of regioisomers or as the predominant isomer (the primary alcohol) in pure form. The *r.r.* values are determined from the crude ^{1}H-NMR spectra by integration of the characteristic signals indicated below.

5.3.11 Esterification of Alcohols Using *Mosher* Acid Chloride (GP XI)

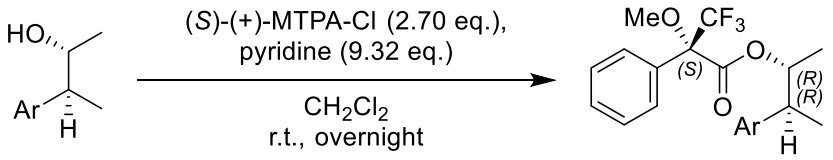

The reaction is performed under argon. In a heat-dried *Schlenk* tube, the respective alcohol (2-5 mg) is dissolved in dry DCM (0.5 mL) before adding dry pyridine (15 µL) and (*S*)-*Mosher* acid chloride (10 µL). After stirring the mixture overnight at r.t., the reaction is quenched by addition of H_2O, and the layers are separated. The aqueous phase is extracted three times with Et_2O, and the combined organic phases are dried over $MgSO_4$. After removal of solvents under reduced pressure and purification by MPLC (*RediSep* R_f Gold, CH:EA 100:0-80:20), the desired ester is obtained.

5.4 Synthesis of Catalysts

5.4.1 D-*Shi*-catalyst (2)

(3a'*R*,4*S*,7'*S*,7a'*S*)-2,2,2',2'-Tetramethyltetrahydrospiro[[1,3]dioxolane-4,6'-[1,3]dioxolo[4,5-c]pyran]-7'-ol (1)

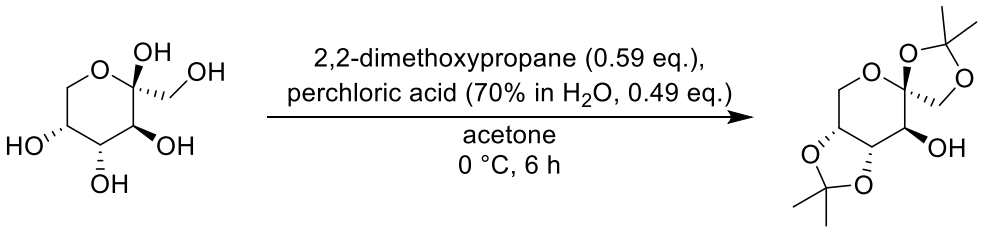

The reaction was performed under argon. To a suspension of D-fructose (36.8 g, 204 mmol, 1.00 eq.) and 2,2-dimethoxypropane (14.8 mL, 120 mmol, 0.59 eq.) in acetone (740 mL), perchloric acid (70% in H_2O, 8.60 mL, 100 mmol, 0.49 eq.) was added at 0 °C before stirring the mixture for 6 h. After quenching the reaction by addition of ammonium hydroxide solution until a pH of 8–9 was reached, the solvent was removed under reduced pressure. The residue was recrystallized from *n*-Pentane:CH_2Cl_2 (1:1), yielding the desired alcohol **1** (23.9 g, 91.8 mmol, 45%) as a colorless solid.

^{1}H-NMR (400 MHz, $CDCl_3$) *δ*/ppm: 4.24–4.09 (m, 4H), 4.04–3.96 (m, 2H), 3.70–3.63 (m, 1H), 1.53 (s, 3H), 1.52 (s, 3H), 1.44 (s, 3H), 1.37 (s, 3H).

^{13}C-NMR (126 MHz, $CDCl_3$) *δ*/ppm: 112.0, 109.6, 104.7, 77.4[a], 73.5, 72.5, 70.6, 60.9, 28.1, 26.6, 26.4, 26.1.

[a]signal overlapping with solvent signal.

The analytical data are in agreement with the literature.[86]

(3a'*R*,4*S*,7a'*R*)-2,2,2',2'-Tetramethyldihydrospiro[[1,3]dioxolane-4,6'-[1,3]dioxolo[4,5-c]pyran]-7'(4'H)-one (2)

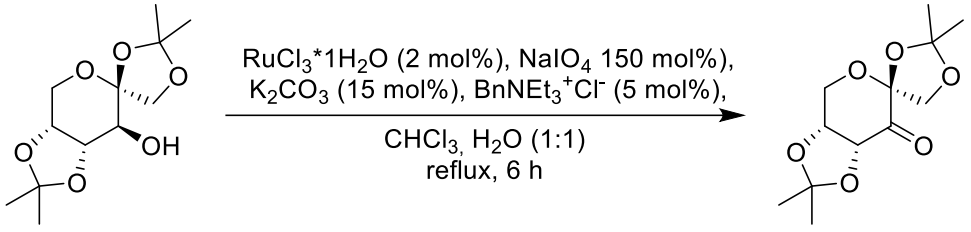

$RuCl_3$*1H_2O (414 mg, 1.84 mmol, 0.02 eq.) was added to a suspension of alcohol **1** (23.9 g, 91.8 mmol, 1.00 eq.), $NaIO_4$ (29.5 g, 137.7 mmol, 1.50 eq.), benzyltriethylammonium chloride

(1.05 g, 4.60 mmol, 0.05 eq.), and K_2CO_3 (1.90 g, 13.8 mmol, 0.15 eq.) in H_2O (105 mL) and $CHCl_3$ (105 mL). The mixture was stirred under reflux conditions for 6 h. Then, the suspension was cooled to r.t., *i*PrOH (25 mL) was added, and the suspension was stirred for an additional hour. Afterwards, the mixture was filtered through a Celite® plug and the layers were separated. The aqueous layer was extracted three times with CH_2Cl_2, and the combined organic phases were washed with sat. aq. Na_2SO_3, H_2O, and brine (100 mL), before drying it over $MgSO_4$ and removing the solvent under reduced pressure. The crude product was purified by flash chromatography (SiO_2, CH:EA 8:2–1:1), yielding the desired ketone **2** (7.82 g, 30.3 mmol, 33%) as a colorless solid.

^{1}H-NMR (400 MHz, $CDCl_3$): δ/ppm: 4.72 (d, J = 5.2 Hz, 1H), 4.60 (d, J = 9.5 Hz, 1H), 4.54 (ddd, J = 5.6, 2.2, 1.0 Hz, 1H), 4.38 (dd, J = 13.5, 2.2 Hz, 1H), 4.11 (dt, J = 13.5, 0.8 Hz, 1H), 3.98 (d, J = 9.5 Hz, 1H), 1.54 (s, 3H), 1.45 (s, 3H), 1.40–1.38 (m, 6H).

^{13}C-NMR (101 MHz, $CDCl_3$): δ/ppm: 197.1, 114.0, 110.8, 104.3, 78.1, 76.0, 70.1, 60.2, 27.3, 27.0, 26.6, 26.1.

The spectroscopic data agree with the literature.[86]

5.4.2 Bis-[η^5-(((bis(3,5-bis(trifluoromethyl)phenyl)(methyl)silane)cyclopentadienyl)] Titanium Dichloride ([Ti]-17)

Bis(3,5-bis(trifluoromethyl)phenyl)(methyl)(phenyl)silane (46)

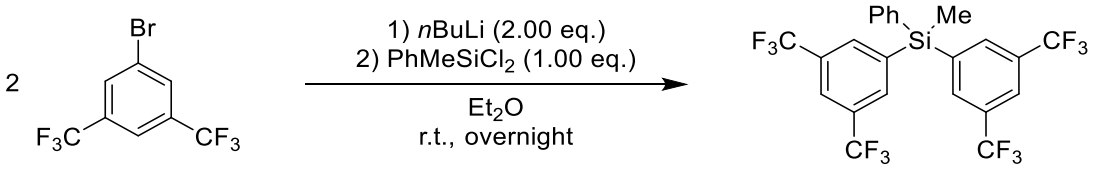

The reaction was performed under argon. 1-bromo-3,5-bis(trifluoromethyl)benzene (30.5 g, 104 mmol, 2.08 eq.) was dissolved in dry Et_2O (100 mL) and cooled to –78 °C before slowly adding *n*BuLi (2.5M in hexanes, 41 mL, 103 mmol, 2.03 eq.) and stirring the mixture for 1 h. Afterwards, dichloro(methyl)(phenyl)silane (9.56 g, 50.0 mmol, 1.00 eq.) was added and the mixture was allowed to warm to ambient temperature while stirring for 17 h. The reaction was quenched with H_2O and the layers were separated. The aqueous phase was extracted three times with Et_2O and the combined organic phases were washed with brine. Drying over $MgSO_4$ followed by removal of solvents under reduced pressure and flash chromatography (SiO_2, CH 100%) yielded the desired silane **46** as a colorless, crystalline solid (25.9 g, 47.3 mmol, 95%).

^{1}H-NMR (499 MHz, $CDCl_3$) *δ*/ppm: 7.98–7.93 (m, 2H), 7.90–7.83 (m, 4H), 7.55–7.49 (m, 1H), 7.48–7.41 (m, 4H), 0.99 (s, 3H).

^{13}C-NMR (126 MHz, $CDCl_3$) *δ*/ppm: 138.3, 135.1, 134.9–134.8 (m), 131.7, 131.6 (q, *J* = 33.5 Hz), 131.1, 128.9, 124.2 (hept, *J* = 3.6 Hz), 123.4 (q, *J* = 272.6 Hz), –3.5.

^{19}F-NMR (470 MHz, $CDCl_3$) *δ*/ppm: –63.0.

IR *ν*/cm^{-1}: 3078, 1838, 1815, 1616, 1600, 1593, 1432, 1362, 1330, 1324, 1277, 1168, 1121, 1095, 999, 970, 940, 921, 918, 900, 844, 832, 822, 786, 778, 736, 706, 697, 679, 619, 604, 572, 547, 541, 515, 508.

HRMS (EI): exp. 546.0664

calc. 546.0668 ($C_{23}H_{14}F_{12}Si^{+\bullet}$ = $[M]^{+\bullet}$)

m.p.: 83 °C

Bis(3,5-bis(trifluoromethyl)phenyl)(methyl)silyl trifluoromethanesulfonate (47)

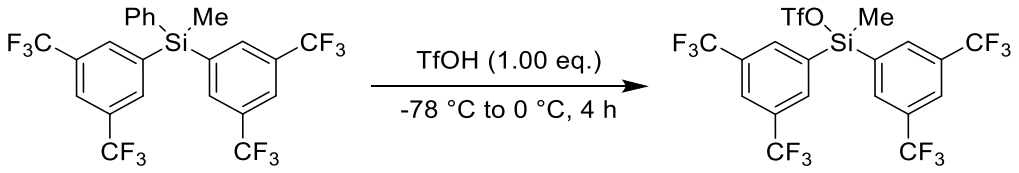

The reaction was performed under argon. In a heat-dried *Schlenk* flask, **46** (25.9 g, 47.3 mmol, 1.00 eq.) was dissolved in dry CH_2Cl_2 (200 mL) and cooled to –78 °C before slowly adding HOTf (4.3 mL, 48.7 mmol, 1.03 eq.). The mixture was stirred for 30 min at –78 °C and 3.5 h at 0 °C. Finally, the solvent was removed under reduced pressure to yield the silyltriflate **47** as a yellow oil. Owing to its instability, neither a yield nor extensive analytical data were recorded. Instead, the triflate was immediately employed in the next step. Its formation can be monitored by the appearance of its characteristic methyl shift of 1.25 ppm in the ^{1}H-NMR spectroscopy (499 MHz, $CDCl_3$) and the disappearance of its precursor's phenyl signals.

Bis(3,5-bis(trifluoromethyl)phenyl)(cyclopenta-2,4-dien-1-yl)(methyl)silane (48)

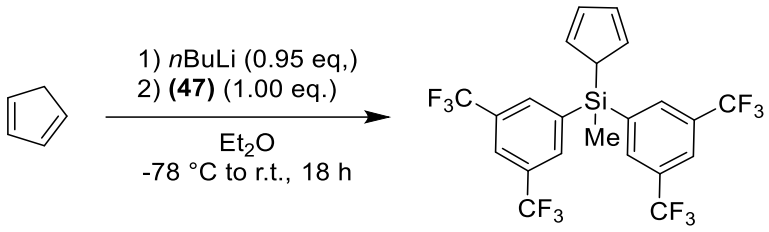

The reaction was performed under argon. In a heat-dried *Schlenk* flask, *n*BuLi (2.5M in hexanes, 15.0 mL, 37.5 mmol, 0.95 eq.) was slowly added to freshly cracked cyclopentadiene (3.40 mL, 41.1 mmol, 1.03 eq.) in dry Et_2O (250 mL) at –78 °C and stirred for 30 min. Then, **47** (29.3 g, 47.3 mmol, 1.00 eq. (*assuming quantitative conversion from **47***)) was added very slowly. The mixture was warmed to ambient temperature and stirred for 18 h. The resulting suspension was filtered and washed with cyclohexane to yield the desired product **48** as a colorless oil as a mixture of regioisomers (22.5 g, 42.1 mmol, 89%, *r.r.* 48:41:10). The product was used without further purification.

^{1}H-NMR (500 MHz, $CDCl_3$) *δ*/ppm: 7.98–7.87 (m, 6H), 7.05–6.49 (m, 4H), 3.93 (bs, 1H), 0.57 (s, 3H).
The regioisomeric ratio was determined by comparison of CH- and CH_2-signals at 3.93 (*major*), 3.12 (*minor* 1) and 3.20 ppm (*minor* 2).

^{13}C-NMR (126 MHz, $CDCl_3$) *δ*/ppm: 137.7, 134.1–134.0 (m), 133.5 (bs), 132.1 (bs), 131.5 (q, *J* = 33.2 Hz), 124.1–123.9 (m), 123.5 (q, *J* = 273.4 Hz), 47.9, –5.6.

^{19}F-NMR (470 MHz, $CDCl_3$) *δ*/ppm: –63.0.

^{29}Si-NMR (99 MHz, $CDCl_3$) *δ*/ppm: –15.0.

IR *ν*/cm^{-1}: 1615, 1359, 1275, 1172, 1122, 1095, 997, 952, 919, 897, 843, 831, 818, 775, 749, 728, 706, 681, 605, 515.

HRMS (EI): exp. 534.0668

calc. 534.0668 ($C_{22}H_{14}F_{12}Si^{\bullet+}$ = $[M]^{\bullet+}$)

Bis-[η^5-(((bis(3,5-bis(trifluoromethyl)phenyl)(methyl)silane)cyclopentadienyl)] Titanium Dichloride ([Ti]-17)

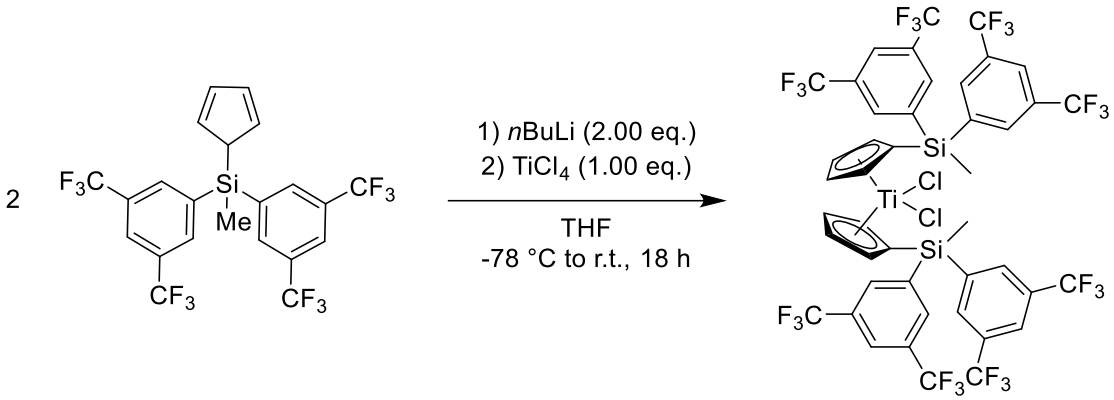

The reaction was performed under argon. In a heat-dried *Schlenk* flask, **48** (22.5 g, 42.1 mmol, 2.04 eq.) was dissolved in dry THF (75 mL), and cooled to –78 °C before slowly adding *n*BuLi (2.5M in hexanes, 17.5 mL, 43.8 mmol, 2.12 eq.). The mixture was stirred for 30 min. Separately, in another heat-dried *Schlenk* flask, THF (75 mL) was cooled to 0 °C before slowly adding $TiCl_4$ (2.26 mL, 20.6 mmol, 1.00 eq.) and vigorously stirring the suspension for 30 min. Then, the $TiCl_4$ solution was transferred to the lithium cyclopentadienide solution at –78 °C before letting the mixture warm to ambient temperature and stir for 18 h. The solvent was removed under reduced pressure. Subsequently, the residue was filtered through a Celite® plug and washed with *n*-pentane. The solvent was removed under reduced pressure and the resulting crude product was purified by size exclusion chromatography (BioBeads®, CH_2Cl_2). Finally, the obtained solid was washed with cold *n*-pentane to yield the desired titanocene **[Ti]-17** as a red-bown solid (8.07 g, 6.81 mmol, 33%).

^{1}H-NMR (500 MHz, $CDCl_3$) δ/ppm: 7.95–7.92 (m, 8H), 7.86–7.82 (m, 16H), 6.68 (t, J = 2.5 Hz, 8H), 6.50 (t, J = 2.5 Hz, 8H), 1.10 (s, 6H).

^{13}C-NMR (126 MHz, $CDCl_3$) δ/ppm: 138.0, 135.3–134.9 (m), 132.4, 131.5 (q, J = 33.2 Hz), 126.1, 124.3–124.0 (m), 123.4 (q, J = 273.2 Hz), 117.1, 0.1.

^{19}F-NMR (470 MHz, $CDCl_3$) δ/ppm: –63.0.

^{29}Si-NMR (99 MHz, $CDCl_3$) δ/ppm: –13.0.

IR ν/cm^{-1}: 3102, 3079, 1616, 1600, 1412, 1360, 1324, 1276, 1172, 1122, 1106, 1095, 1050, 1001, 946, 923, 900, 834, 821, 776, 733, 706, 682, 605, 574, 547, 514.

HRMS (APCI): exp. 1190.0620

calc. 1190.0618 ($C_{46}H_{29}ClF_{24}NSi_2Ti^+$ = $[M+CH_3CN-Cl]^+$)

5.5 Synthesis of Alkenes

5.5.1 1-(But-2-en-2-yl)-3-methylbenzene (101)

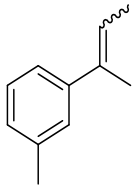

According to **GP I**, *n*BuLi (2.5M solution in hexanes, 8.8 mL, 22.0 mmol, 1.10 eq.), 1-(*m*-tolyl)ethan-1-one (2.68 g, 20.0 mmol, 1.00 eq.) and $EtPPh_3Br$ (8.17 g, 22.0 mmol, 1.10 eq.) in THF (40 mL) were stirred for 24 h. Work-up and flash chromatography (SiO_2, PE) yielded olefin **101** (2.24 g, 15.3 mmol, 77%, 56:44 (*E*):(*Z*)) as a colorless oil.

^{1}H-NMR (499 MHz, $CDCl_3$) *δ*/ppm: major (*E*):

7.25–7.15 (m, 4H), 5.84 (qq, *J* = 6.8, 1.4 Hz, 1H), 2.36* (d, *J* = 4.4 Hz, 3H), 2.02* (dp, *J* = 3.2, 1.4 Hz, 3H), 1.79 (dt, *J* = 6.8, 1.3 Hz, 3H).

minor (*Z*):

7.08–6.97 (m, 4H), 5.55 (qq, *J* = 6.8, 1.6 Hz, 1H), 2.36* (d, *J* = 4.4 Hz, 3H), 2.02* (dp, *J* = 3.2, 1.4 Hz, 3H), 1.60 (dq, *J* = 6.9, 1.6 Hz, 3H).

^{13}C-NMR (126 MHz, $CDCl_3$) *δ*/ppm: major (*E*):

144.1, 137.6, 135.6, 128.1, 127.2, 126.4, 122.7, 122.3, 25.5, 21.5, 14.9.

minor (*Z*):

141.9, 137.6, 136.9, 128.7, 127.9, 127.1, 125.2, 121.4, 21.5, 15.6, 14.3.

The analytical data are in agreement with the literature.[212]

5.5.2 1-(But-2-en-2-yl)-4-methylbenzene (102)

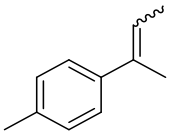

According to **GP I**, *n*BuLi (2.5M solution in hexanes, 8.8 mL, 22.0 mmol, 1.08 eq.), 1-(*p*-tolyl)ethan-1-one (2.74 g, 20.4 mmol, 1.00 eq.) and $EtPPh_3Br$ (8.17 g, 22.0 mmol, 1.08 eq.) in THF (40 mL) were stirred for 24 h. Work-up and flash chromatography (SiO_2, PE) yielded olefin **102** (2.00 g, 13.7 mmol, 67%, 55:45 (*E*):(*Z*)) as a colorless oil.

^{1}H-NMR (499 MHz, $CDCl_3$) *δ*/ppm: major (*E*):

7.29–7.27 (m, 2H), 7.14–7.10* (m, 2H), 5.84 (dt, *J* = 6.9, 1.4 Hz, 1H), 2.34 (s, 3H), 2.03–2.01* (m, 3H), 1.80 (dq, *J* = 6.8, 1.2 Hz, 3H).

minor (*Z*):

7.16 (d, *J* = 7.8 Hz, 2H), 7.14–7.10* (m, 2H), 5.55 (dd, *J* = 6.9, 1.5 Hz, 1H), 2.36 (s, 3H), 2.03–2.01* (m, 3H), 1.62 (dq, *J* = 6.9, 1.5 Hz, 3H).

^{13}C-NMR (126 MHz, $CDCl_3$) *δ*/ppm: major (*E*):

141.3, 136.1, 135.4, 128.9, 125.5, 121.8, 21.1, 15.6, 14.4.

minor (*Z*):

139.0, 136.8, 136.0, 129.0, 128.1, 121.4, 25.6, 21.3, 15.0.

The analytical data are in agreement with the literature.[212]

5.5.3 1-(But-2-en-2-yl)-4-fluorobenzene (103)

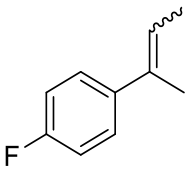

According to **GP I**, *n*BuLi (2.5M solution in hexanes, 8.80 mL, 22.0 mmol, 1.10 eq.), 1-(4-fluorophenyl)ethan-1-one (2.76 g, 20.0 mmol, 1.00 eq.) and $EtPPh_3Br$ (8.17 g, 22.0 mmol, 1.10 eq.) in THF (40 mL) were stirred for 24 h. Work-up and flash chromatography (SiO_2, PE) yielded olefin **103** (2.04 g, 13.6 mmol, 68%, 63:37 (*E*):(*Z*)) as a colorless oil.

^{1}H-NMR (499 MHz, $CDCl_3$) δ/ppm: major (*E*):

7.34–7.29 (m, 2H), 7.06–6.94* (m, 2H), 5.80 (qq, *J* = 6.8, 1.4 Hz, 1H), 2.02–1.99* (m, 3H), 1.79 (dq, *J* = 6.8, 1.1 Hz, 3H).

minor (*Z*):

7.19–7.12 (m, 2H), 7.06–6.94* (m, 2H), 5.56 (qq, *J* = 6.9, 1.5 Hz, 1H), 2.02–1.99* (m, 3H), 1.58 (dq, *J* = 6.9, 1.6 Hz, 3H).

^{13}C-NMR (126 MHz, $CDCl_3$) δ/ppm: major (*E*):

161.7* (d, *J* = 244.8 Hz), 140.1 (d, *J* = 3.3 Hz), 134.5, 126.9 (d, *J* = 7.7 Hz), 122.3 (d, *J* = 1.5 Hz), 114.8 (d, *J* = 21.1 Hz), 15.6, 14.3.

minor (*Z*):

161.4* (d, *J* = 244.6 Hz), 137.7 (d, *J* = 3.2 Hz), 135.8, 129.6 (d, *J* = 7.8 Hz), 121.9, 114.8 (d, *J* = 21.2 Hz), 25.4, 14.8.

The analytical data are in agreement with the literature.[153]

5.5.4 1-(But-2-en-2-yl)-4-chlorobenzene (104)

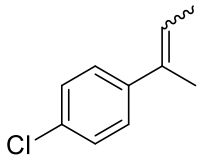

According to **GP I**, *n*BuLi (2.5M solution in hexanes, 17.6 mL, 44.0 mmol, 1.10 eq.), 1-(4-chlorophenyl)ethan-1-one (6.18 g, 40.0 mmol, 1.00 eq.) and $EtPPh_3Br$ (16.3 g, 44.0 mmol, 1.10 eq.) in THF (80 mL) were stirred for 24 h. Work-up and flash chromatography (SiO_2, PE) yielded olefin **104** (5.44 g, 32.6 mmol, 82%, 65:35 (*E*):(*Z*)) as a colorless oil.

^{1}H-NMR (499 MHz, $CDCl_3$) δ/ppm: major (*E*):

7.37–7.24* (m, 3H), 7.17–7.11* (m, 1H), 5.86 (qq, *J* = 6.9, 1.4 Hz, 1H), 2.01* (hept, *J* = 1.9 Hz, 3H), 1.81 (dq, *J* = 6.9, 1.1 Hz, 3H).

minor (*Z*):

7.37–7.24* (m, 3H), 7.17–7.11* (m, 1H), 5.59 (qq, *J* = 7.0, 1.5 Hz, 1H), 2.01* (hept, *J* = 1.9 Hz, 3H), 1.59 (dq, *J* = 7.0, 1.6 Hz, 2H).

^{13}C-NMR (126 MHz, $CDCl_3$) *δ*/ppm: major (*E*):

142.4, 134.5, 129.5, 128.2, 123.1*, 122.3*, 25.2, 14.9.

minor (*Z*):

140.3, 135.7, 132.1, 126.8, 123.1*, 122.3*, 15.4, 14.4.

The analytical data are in agreement with the literature.[212]

5.6 Synthesis of Epoxides

5.6.1 (3*R*)-2,3-Dimethyl-2-(*m*-tolyl)oxirane (24)

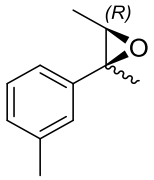

***Shi*-Epoxidation of (101) towards enantiomerically enriched epoxide:**

According to **GP III**, Oxone® solution (4.25 g in 4 x 10^{-4}M aq. Na_2(EDTA) (35 mL), 6.90 mmol, 1.38 eq.) and aq. K_2CO_3-solution (4.00 g in water (35 mL), 28.9 mmol, 5.79 eq.) were simultaneously added dropwise to a solution of olefin **101** (0.73 g, 5.00 mmol, 1.00 eq., 56:44 (*E*):(*Z*)), $TBAHSO_4$ (0.08 g, 0.22 mmol, 0.04 eq.) and D-*Shi*-catalyst (**2**) (0.73 g, 2.70 mmol, 0.30 eq.) in acetonitrile (50 mL), dimethoxymethane (100 mL) and a borate-buffer-solution (100 mL, 0.05M $Na_2B_4O_7$*10 H_2O in 4 x 10^{-4}M aq. Na_2(EDTA)) at –10 °C over the course of 1 h. Following stirring for 24 h at the same temperature, work-up and flash chromatography (SiO_2, PE:Et_2O 95:5 + 1% NEt_3) yielded epoxide **24** (1.08 g, 5.89 mmol, 65%, 74:26 *anti:syn*) as a colorless liquid.

***Prilezhaev*-Epoxidation of (101) towards racemic epoxide:**

In a slight variation of **GP II**, *m*CPBA (70% in H_2O, 1.11 g, 4.50 mmol, 1.50 eq.) was added to a solution of olefin **101** (0.61 g, 3.00 mmol, 1.00 eq., 56:44 (*E*):(*Z*)) in CH_2Cl_2 (30 mL), before stirring the mixture overnight. Work-up and flash chromatography (SiO_2, 95:5 PE:Et_2O + 1% NEt_3) yielded epoxide ***rac*-24** (0.16 g, 0.96 mmol, 32%, 99:1 *anti*:*syn*).

^{1}H-NMR (499 MHz, $CDCl_3$) *δ*/ppm: major (*anti*):

7.20–7.08 (m, 4H), 2.97 (q, *J* = 5.5 Hz, 1H), 2.38* (d, *J* = 4.9 Hz, 3H), 1.67* (d, *J* = 6.1 Hz, 3H), 1.45 (d, *J* = 5.5 Hz, 3H).

minor (*syn*):

7.28–7.23 (m, 4H), 3.19 (q, *J* = 5.4 Hz, 1H), 2.38* (d, *J* = 4.9 Hz, 3H), 1.67* (d, *J* = 6.1 Hz, 3H), 1.02 (d, *J* = 5.4 Hz, 3H).

^{13}C-NMR (126 MHz, $CDCl_3$) *δ*/ppm: major (*anti*):

43.0, 138.0, 128.2, 127.9, 125.7, 122.2, 62.4, 60.4, 21.5, 17.5, 14.4.

	minor (*syn*):
	139.6, 137.7, 127.9, 127.9, 127.2, 123.6, 62.7, 61.3, 24.7, 21.5, 14.6.
IR $\tilde{\nu}$/cm^{-1}:	2966, 2926, 1609, 1489, 1456, 1381, 1070, 888, 782, 701.
HRMS (APCI):	exp. 163.1118
	calc. 163.1117 ($C_{11}H_{15}O^+ = [M+H]^+$)
$[\alpha]_D^{20}$:	+19.1° (CH_2Cl_2)

5.6.2 (3*R*)-2,3-Dimethyl-2-(*p*-tolyl)oxirane (25)

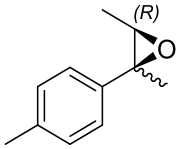

***Shi*-Epoxidation of (102) towards enantiomerically enriched epoxide:**

According to **GP III**, Oxone® solution (8.54 g in 4 x 10^{-4}M aq. Na_2(EDTA) (67 mL), 14.7 mmol, 1.38 eq.) and aq. K_2CO_3-solution (8.04 g in water (67 mL), 61.7 mmol, 5.79 eq.) were simultaneously added dropwise to a solution of olefin **102** (1.47 g, 10.1 mmol, 1.00 eq., 55:45 (*E*):(*Z*)), $TBAHSO_4$ (0.15 g, 0.44 mmol, 0.04 eq.) and D-*Shi*-catalyst (**2**) (0.78 g, 3.01 mmol, 0.30 eq.) in acetonitrile (50 mL), dimethoxymethane (100 mL) and a borate-buffer-solution (100 mL, 0.05M $Na_2B_4O_7$*10 H_2O in 4 x 10^{-4}M aq. Na_2(EDTA)) at –10 °C over the course of 1 h. Following stirring for 24 h at the same temperature, work-up and flash chromatography (SiO_2, PE:Et_2O 95:5 + 1% NEt_3) yielded epoxide **25** (1.19 mg, 7.34 mmol, 73%, 53:47 *anti:syn*) as a colorless liquid.

***Prilezhaev*-Epoxidation of (102) towards racemic epoxide:**

According to **GP II**, *m*CPBA (70% in H_2O, 1.21 g, 4.89 mmol, 1.50 eq.) was added to a solution of olefin **102** (0.48 g, 3.26 mmol, 1.00 eq., 55:45 (*E*):(*Z*)) in CH_2Cl_2 (30 mL), before stirring the mixture overnight. Work-up and flash chromatography (SiO_2, 95:5 PE:Et_2O + 1% NEt_3) yielded epoxide ***rac*-25** (0.20 g, 1.25 mmol, 38%, 72:28 *anti*:*syn*).

^{1}H-NMR (499 MHz, $CDCl_3$) *δ*/ppm: major (*anti*):

7.25–7.20* (m, 2H), 7.17–7.12* (m, 2H), 2.94 (q, *J* = 5.4 Hz, 1H), 2.34 (s, 3H), 1.64 (s, 3H), 1.42 (d, *J* = 5.5 Hz, 3H).

minor (*syn*):

7.25–7.20* (m, 2H), 7.18–7.12* (m, 2H), 3.15 (q, *J* = 5.4 Hz, 1H), 2.35 (s, 4H), 1.63 (s, 3H), 0.99 (d, *J* = 5.3 Hz, 3H).

^{13}C-NMR (126 MHz, $CDCl_3$) *δ*/ppm: major (*anti*):

140.2, 137.0, 129.1, 125.1, 62.6, 60.4, 21.2, 17.6, 14.6*.

minor (*syn*):

136.8, 136.8, 128.9, 126.6, 62.7, 61.4, 24.8, 21.2, 14.6*.

$[\alpha]_D^{20}$: +21.7° (CH_2Cl_2)

The analytical data are in agreement with the literature.[153]

5.6.3 (3*R*)-2-(4-Fluorophenyl)-2,3-dimethyloxirane (30)

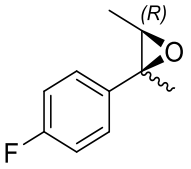

Shi-Epoxidation of (103) towards enantiomerically enriched epoxide:

According to **GP III**, Oxone® solution (9.05 g in 4 x 10^{-4}M aq. Na_2(EDTA) (67 mL), 14.7 mmol, 1.38 eq.) and aq. K_2CO_3-solution (8.52 g in water (67 mL), 61.7 mmol, 5.79 eq.) were simultaneously added dropwise to a solution of olefin **103** (1.60 g, 10.7 mmol, 1.00 eq., 63:37 (*E*):(*Z*)), $TBAHSO_4$ (0.16 g, 0.47 mmol, 0.04 eq.) and D-*Shi*-catalyst (**2**) (0.82 g, 3.19 mmol, 0.30 eq.) in acetonitrile (50 mL), dimethoxymethane (100 mL) and a borate-buffer-solution (80 mL, 0.05M $Na_2B_4O_7$*10 H_2O in 4 x 10^{-4}M aq. Na_2(EDTA)) at –10 °C over the course of 2 h. Following stirring for 24 h at the same temperature, work-up and flash chromatography (SiO_2, PE:Et_2O 97:3 + 1% NEt_3) yielded epoxide **30** (1.53 g, 5.53 mmol, 52%, 77:23 *anti:syn*) as a colorless solid.

***Prilezhaev*-Epoxidation of (103) towards racemic epoxide:**

According to **GP II**, *m*CPBA (70% in H_2O, 0.98 g, 4.00 mmol, 1.50 eq.) was added to a solution of olefin **103** (0.40 g, 2.66 mmol, 1.00 eq., 63:37 (*E*):(*Z*)) in CH_2Cl_2 (30 mL), before stirring the mixture overnight. Work-up and flash chromatography (SiO_2, 95:5 PE:Et_2O + 1% NEt_3) yielded epoxide ***rac*-30** (0.13 g, 0.78 mmol, 43%, 70:30 *anti*:*syn*).

^{1}H-NMR (499 MHz, $CDCl_3$) *δ*/ppm: major (*anti*):

7.33–7.28* (m, 2H), 7.06–6.97* (m, 2H), 2.91 (q, *J* = 5.5 Hz, 1H), 1.63 (s, 3H), 1.42 (d, *J* = 5.4 Hz, 3H).

minor (*syn*):

7.34–7.28* (m, 2H), 7.07–6.97* (m, 2H), 3.16 (q, *J* = 5.4 Hz, 1H), 1.62 (s, 3H), 0.97 (d, *J* = 5.4 Hz, 3H).

^{13}C-NMR (126 MHz, $CDCl_3$) *δ*/ppm: major (*anti*):

162.2* (d, *J* = 245.2 Hz), 139.0 (d, *J* = 3.0 Hz), 126.9 (d, *J* = 8.0 Hz), 115.2* (d, *J* = 21.3 Hz), 62.7, 60.1, 17.6, 14.5*.

minor (*syn*):

162.1* (d, *J* = 245.3 Hz), 135.6 (d, *J* = 3.1 Hz), 128.3 (d, *J* = 8.0 Hz), 115.1* (d, *J* = 21.5 Hz), 62.4, 61.4, 24.7, 14.5*.

$[\alpha]_D^{20}$: +18.3° (CH_2Cl_2)

The analytical data are in agreement with the literature.[153]

5.6.4 (3*R*)-2-(4-Chlorophenyl)-2,3-dimethyloxirane (35)

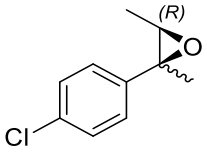

***Shi*-Epoxidation of (104) towards enantiomerically enriched epoxide:**

According to **GP III**, Oxone® solution (8.54 g in 4 x 10^{-4}M aq. Na_2(EDTA) (67 mL), 14.7 mmol, 1.38 eq.) and aq. K_2CO_3-solution (8.04 g in water (67 mL), 61.7 mmol, 5.79 eq.) were simultaneously added dropwise to a solution of olefin **104** (1.70 g, 10.2 mmol, 1.00 eq., 65:35 (*E*):(*Z*)), $TBAHSO_4$ (0.15 g, 0.44 mmol, 0.04 eq.) and D-*Shi*-catalyst (**2**) (0.82 g,

3.19 mmol, 0.31 eq.) in acetonitrile (50 mL), dimethoxymethane (100 mL) and a borate-buffer-solution (100 mL, 0.05M $Na_2B_4O_7$*10 H_2O in 4 x 10^{-4}M aq. Na_2(EDTA)) at –10 °C over the course of 1 h. Following stirring for 24 h at the same temperature, work-up and flash chromatography (SiO_2, PE:Et_2O 95:5 + 1% NEt_3) yielded epoxide **35** (1.20 g, 6.60 mmol, 65%, 75:25 *anti:syn*) as a colorless liquid.

***Prilezhaev*-Epoxidation of (104) towards racemic epoxide:**

According to **GP II**, *m*CPBA (70% in H_2O, 1.11 g, 4.50 mmol, 1.50 eq.) was added to a solution of olefin **104** (0.49 mL, 3.00 mmol, 1.00 eq., 65:35 (*E*):(*Z*)) in CH_2Cl_2 (30 mL) before stirring the mixture overnight. After work-up and flash chromatography (SiO_2, 95:5 PE:Et_2O + 1% NEt_3), epoxide ***rac*-35** (0.41 g, 2.24 mmol, 74%, 62:38 *anti*:*syn*).

^{1}H-NMR (400 MHz, $CDCl_3$) *δ*/ppm: major (*anti*):

7.34–7.26* (m, 4H), 2.91 (q, *J* = 5.5 Hz, 1H), 1.63* (d, *J* = 3.8 Hz, 3H), 1.43 (d, *J* = 5.5 Hz, 3H).

minor (*syn*):

7.34–7.26* (m, 4H), 3.18 (q, *J* = 5.4 Hz, 1H), 1.63* (d, *J* = 3.8 Hz, 3H), 0.98 (d, *J* = 5.4 Hz, 1H).

^{13}C-NMR (101 MHz, $CDCl_3$) *δ*/ppm: major (*anti*):

141.6, 133.0*, 128.4, 126.5, 62.6, 59.9, 17.3, 14.4.

minor (*syn*):

138.2, 133.0*, 128.3, 128.0, 62.2, 61.3, 24.3, 14.4.

IR *ν*/cm^{-1}: 2967, 2930, 1600, 1492, 1456, 1413, 1400, 1382, 1330, 1284, 1092, 1072, 1031, 1013, 977, 901, 849, 819, 762, 723, 631, 603, 577, 544.

HRMS (APCI): exp. 183.0567

calc. 183.0571 ($C_{10}H_{12}ClO^+$ = $[M+H]^+$)

$[\alpha]_D^{20}$: +22.1° (CH_2Cl_2)

5.6.5 2-Undecyloxirane (50)

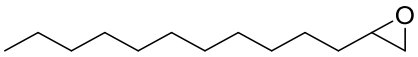

According to **GP II**, tridec-1-ene (2.40 mL, 10.1 mmol, 1.00 eq.) and *m*CPBA (≥77% in H_2O, 4.93 g, 22.0 mmol, 2.18 eq.) were mixed in CH_2Cl_2 (100 mL) and stirred for 18 h. After work-up, the epoxide **50** was obtained as a light-yellow oil (2.00 g, 10.1 mmol, 100%).^{1}H-NMR (500 MHz, $CDCl_3$) *δ*/ppm: 2.90 (tdd, *J* = 5.6, 3.9, 2.7 Hz, 1H), 2.74 (dd, *J* = 5.0, 4.0 Hz, 1H), 2.46 (dd, *J* = 5.1, 2.7 Hz, 1H), 1.56–1.20 (m, 20H), 0.88 (t, *J* = 6.9 Hz, 3H).

^{13}C-NMR (126 MHz, $CDCl_3$) *δ*/ppm: 52.6, 47.3, 32.6, 32.1, 29.8, 29.8, 29.7 (2C), 29.6, 29.5, 26.1, 22.8, 14.3.

The analytical data are in good agreement with the literature.[213]

5.6.6 2-Decyloxirane (44)

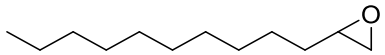

According to **GP II**, dodec-1-ene (4.40 mL, 20.0 mmol, 1.00 eq.) and *m*CPBA (70% in H_2O, 9.86 g, 40.0 mmol, 2.00 eq.) were mixed in CH_2Cl_2 (200 mL) and stirred for 16 h. After work-up, epoxide **44** (3.59 g, 19.5 mmol, 97%) was obtained as a colorless oil.

^{1}H-NMR (700 MHz, $CDCl_3$) *δ*/ppm: 2.94–2.87 (m, 1H), 2.74 (dd, *J* = 5.1, 4.0 Hz, 1H), 2.46 (dd, *J* = 5.1, 2.7 Hz, 1H), 1.54–1.49 (m, 2H), 1.49–1.39 (m, 2H), 1.37–1.21 (m, 14H), 0.88 (t, *J* = 7.1 Hz, 3H).

^{13}C-NMR (176 MHz, $CDCl_3$) *δ*/ppm: 52.5, 47.3, 32.6, 32.0, 29.7, 29.7, 29.6, 29.5, 26.1, 22.8, 14.2.

The analytical data are consistent with the literature.[214]

5.6.7 2-Octyloxirane (67)

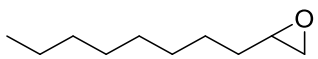

According to **GP II**, dec-1-ene (3.80 mL, 20.0 mmol, 1.00 eq.) and *m*CPBA (70% in H_2O, 9.86 g, 40.0 mmol, 2.00 eq.) were mixed in CH_2Cl_2 (200 mL) and stirred for 16 h. After work-up, epoxide **67** (2.63 g, 16.8 mmol, 84%) was obtained as a colorless oil.

^{1}H-NMR (700 MHz, $CDCl_3$) δ/ppm: 2.90 (tdd, J = 5.6, 4.0, 2.7 Hz, 1H), 2.74 (dd, J = 5.1, 3.9 Hz, 1H), 2.46 (dd, J = 5.1, 2.7 Hz, 1H), 1.55–1.39 (m, 4H), 1.37–1.23 (m, 10H), 0.88 (t, J = 7.1 Hz, 3H).

^{13}C-NMR (176 MHz, $CDCl_3$) δ/ppm: 52.5, 47.3, 32.7, 32.0, 29.7, 29.6, 29.4, 26.1, 22.8, 14.2.

The analytical data are consistent with the literature.[215]

5.6.8 2-Cyclohexyloxirane (68)

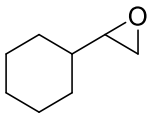

According to **GP II**, vinylcyclohexane (2.74 mL, 20.0 mmol, 1.00 eq.) and *m*CPBA (70% in H_2O, 9.86 g, 40.0 mmol, 2.00 eq.) were mixed in CH_2Cl_2 (200 mL) and stirred for 23 h. After work-up, epoxide **68** (2.63 g, 16.8 mmol, 84%) was obtained as a colorless oil.

^{1}H-NMR (500 MHz, $CDCl_3$) δ/ppm: 2.71 (dd, J = 4.2, 2.3 Hz, 2H), 2.56–2.50 (m, 1H), 1.92–1.84 (m, 1H), 1.79–1.63 (m, 4H), 1.31–1.03 (m, 6H).

^{13}C-NMR (126 MHz, $CDCl_3$) δ/ppm: 56.8, 46.2, 40.5, 29.9, 29.0, 26.5, 25.8, 25.7.

The analytical data are consistent with the literature.[216]

5.6.9 2-Benzyloxirane (72)

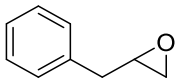

According to **GP II**, allylbenzene (2.70 mL, 20.0 mmol, 1.00 eq.) and *m*CPBA (70% in H_2O, 9.86 g, 40.0 mmol, 2.00 eq.) were mixed in CH_2Cl_2 (200 mL) and stirred for 23 h. After work-up, epoxide **72** (2.20 g, 16.4 mmol, 82%) was obtained as a colorless oil.

^{1}H-NMR (700 MHz, $CDCl_3$) δ/ppm: 7.36–7.30 (m, 2H), 7.27 (d, J = 7.3 Hz, 3H), 3.17 (tdd, J = 5.5, 3.8, 2.7 Hz, 1H), 2.94 (dd, J = 14.5, 5.6 Hz, 1H), 2.85 (d, J = 5.4 Hz, 1H), 2.83–2.79 (m, 1H), 2.57 (dd, J = 5.0, 2.7 Hz, 1H).

^{13}C-NMR (176 MHz, $CDCl_3$) δ/ppm: 137.3, 129.1, 128.7, 126.8, 52.6, 47.0, 38.9.

The analytical data are consistent with the literature.[217]

5.6.10 2-(Naphthalen-1-ylmethyl)oxirane (49)

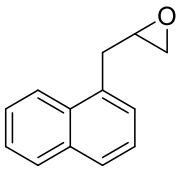

According to **GP II**, 1-allylnaphthalene (3.30 mL, 20.0 mmol, 1.00 eq.) and *m*CPBA (70% in H_2O, 9.86 g, 40.0 mmol, 2.00 eq.) were mixed in CH_2Cl_2 (200 mL) and stirred for 18 h. After work-up and purification *via* flash chromatography (SiO_2, *n*-Pentane:Et_2O 9:1 + 1% NEt_3), epoxide **49** (3.65 g, 19.8 mmol, 99%) was obtained as a yellow oil.

^{1}H NMR (400 MHz, $CDCl_3$) *δ*/ppm: 8.07 (d, *J* = 8.3 Hz, 1H), 7.88 (dd, *J* = 8.0, 1.6 Hz, 1H), 7.79 (dd, *J* = 6.6, 2.9 Hz, 1H), 7.60–7.48 (m, 2H), 7.48–7.40 (m, 2H), 3.44 (dd, *J* = 14.3, 5.0 Hz, 1H), 3.34 (ddd, *J* = 8.9, 4.7, 2.8 Hz, 1H), 3.28 (dd, *J* = 14.3, 5.0 Hz, 1H), 2.83 (dd, *J* = 4.9, 3.8 Hz, 1H), 2.61 (dd, *J* = 5.0, 2.6 Hz, 1H).

^{13}C NMR (126 MHz, $CDCl_3$) *δ*/ppm: 134.0, 133.7, 132.4, 128.9, 127.6, 127.0, 126.3, 125.8, 125.7, 123.9, 52.2, 47.4, 35.8.

The analytical data are in good agreement with the literature.[218]

5.6.11 2-((Octyloxy)methyl)oxirane (65)

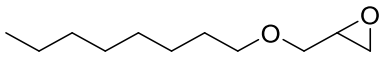

According to **GP II**, 1-(allyloxy)octane (2.10 mL, 9.99 mmol, 1.00 eq.) and *m*CPBA (70% in H_2O, 4.93 g, 22.0 mmol, 2.20 eq.) were mixed in CH_2Cl_2 (100 mL) and stirred for 18 h. After work-up and purification *via* flash chromatography (SiO_2, PE:Et_2O 97:3 + 1% NEt_3), epoxide **65** was obtained as a colorless oil (1.52 g, 8.16 mmol, 82%).

^{1}H-NMR (500 MHz, $CDCl_3$) *δ*/ppm: 3.70 (dd, *J* = 11.5, 3.1 Hz, 1H), 3.48 (qt, *J* = 9.2, 6.7 Hz, 2H), 3.39 (dd, *J* = 11.5, 5.8 Hz, 1H), 3.15 (ddt, *J* = 5.8, 4.2, 2.9 Hz, 1H), 2.80 (dd, *J* = 5.1, 4.1 Hz, 1H), 2.61 (dd, *J* = 5.0, 2.7 Hz, 1H), 1.63–1.53 (m, 2H), 1.39–1.21 (m, 10H), 0.92–0.83 (m, 3H).

^{13}C-NMR (126 MHz, $CDCl_3$) *δ*/ppm: 71.9, 71.6, 51.1, 44.5, 32.0, 29.8, 29.6, 29.4, 26.2, 22.8, 14.2.

The analytical data are in good agreement with the literature.[219]

5.6.12 2-(Phenoxymethyl)oxirane (66)

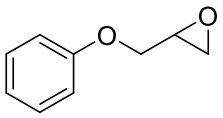

According to **GP II**, (allyloxy)benzene (1.34 g, 9.99 mmol, 1.00 eq.) and *m*CPBA (70% in H_2O, 4.93 g, 22.0 mmol, 2.20 eq.) were mixed in CH_2Cl_2 (100 mL) and stirred for 48 h. After work-up and purification *via* flash chromatography (SiO_2, PE:Et_2O 7:3 + 1% NEt_3) the epoxide **66** was obtained as a light-yellow oil (1.16 g, 7.72 mmol, 77%).

^{1}H-NMR (500 MHz, $CDCl_3$) *δ*/ppm: 7.35–7.24 (m, 2H), 7.01–6.90 (m, 3H), 4.22 (dd, *J* = 11.0, 3.2 Hz, 1H), 3.98 (dd, *J* = 11.0, 5.6 Hz, 1H), 3.36 (dddd, *J* = 5.8, 4.1, 3.3, 2.7 Hz, 1H), 2.91 (dd, *J* = 5.0, 4.1 Hz, 1H), 2.76 (dd, *J* = 4.9, 2.7 Hz, 1H).

^{13}C-NMR (126 MHz, $CDCl_3$) *δ*/ppm: 158.6, 129.7, 121.4, 114.8, 68.8, 50.3, 44.9.

The analytical data are in good agreement with the literature.[220]

5.6.13 9-(Oxiran-2-yl)nonan-1-ol (69)

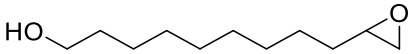

According to **GP II**, 10-undecen-1-ol (2.00 mL, 9.96 mmol, 1.00 eq.) and *m*CPBA (70% in H_2O, 4.93 g, 22.0 mmol, 2.21 eq.) were mixed in CH_2Cl_2 (100 mL) and stirred for 18 h. After work-up, the epoxide **69** was obtained as a colorless oil (1.84 g, 9.90 mmol, 99%).

^{1}H-NMR (500 MHz, $CDCl_3$) *δ*/ppm: 3.64 (t, *J* = 6.6 Hz, 2H), 2.90 (tdd, *J* = 5.5, 3.9, 2.7 Hz, 1H), 2.74 (dd, *J* = 5.0, 4.0 Hz, 1H), 2.46 (dd, *J* = 5.0, 2.7 Hz, 1H), 1.64–1.22 (m, 17H).

^{13}C-NMR (126 MHz, $CDCl_3$) *δ*/ppm: 63.2, 52.6, 47.3, 32.9, 32.6, 29.6, 29.6, 29.5, 29.5, 26.1, 25.9.

The analytical data are in good agreement with the literature.[221]

5.6.14 2-(2,6-Dimethylhept-5-en-1-yl)oxirane (71)

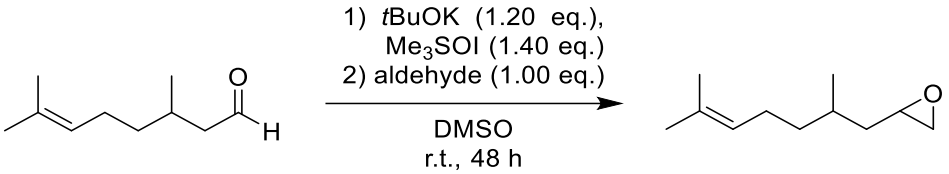

The reaction was performed under argon. In a heat-dried *Schlenk* flask, *t*BuOK (1.35 g, 12.0 mmol, 1.20 eq.) was added to a suspension of trimethylsulfoxonium iodide (3.10 g, 14.1 mmol, 1.41 eq.) in DMSO (10 mL) at room temperature. After stirring the mixture for 30 min., 3,7-dimethyloct-6-enal (1.84 g, 10.0 mmol, 1.00 eq.) was added over a period of 30 min. The resulting yellow solution was stirred for 48 h. Then, the mixture was washed with water and the phases were separated. The aqueous phase was extracted with Et_2O (3 x 20 mL) and the combined organic phases washed with brine (50 mL) and dried over $MgSO_4$. Removal of solvents under reduced pressure and flash chromatography (SiO_2, PE:Et_2O 95:5 + 1% NEt_3) yielded the desired epoxide **71** as a yellow oil (380 mg, 2.26 mmol, 23%, *d.r.* 55:45).

^{1}H-NMR (500 MHz, $CDCl_3$) *δ*/ppm: 5.09 (tdd, *J* = 5.7, 2.8, 1.4 Hz, 1H), 2.93 (ddddd, *J* = 6.4, 5.0, 3.8, 2.7, 1.0 Hz, 1H), 2.77 (ddd, *J* = 5.2, 4.0, 0.6 Hz, 1H), 2.45 (dd, *J* = 5.1, 2.7 Hz, 1H), 2.08–1.90 (m, 2H), 1.68 (s, 3H) 1.60 (s, 3H), 1.57–1.15 (m, 5H), 0.97 (d, *J* = 6.7 Hz, 3H) (*only major isomer shown*).

The *d.r.* was determined by comparison of CH-signals at 2.45 (*major*) and 2.42 ppm (minor).

^{13}C-NMR (126 MHz, $CDCl_3$) *δ*/ppm: 131.5, 124.7, 51.3, 47.7, 40.0, 37.5, 30.7, 25.9, 25.6, 19.7, 17.8 (*only major isomer shown*).

The analytical data are in good agreement with the literature.[222]

5.7 Synthesis of Oxetanes

5.7.1 2-Decyloxetane (74)

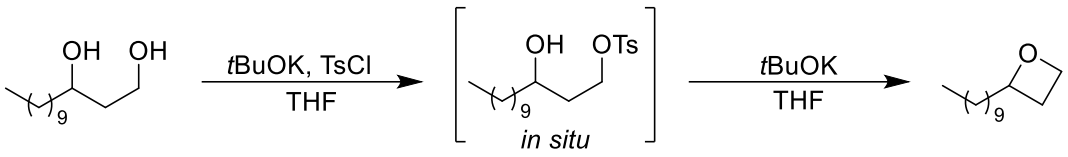

The following procedure is inspired by a method reported by *Dussault et al.*[192] The reaction was performed under argon. A solution of the diol **76** (860 mg, 4.00 mmol, 1.00 eq.) in THF (40 mL) was cooled to 0 °C before adding *t*BuOK (448 mg, 4.00 mmol, 1.00 eq.) in one portion. Then, tosyl chloride (777 mg, 4.40 mmol, 1.10 eq.) was added over 30 min at the same temperature. After stirring the mixture for 2 h at 0 °C, a second portion of *t*BuOK (440 mg, 4.00 mmol, 1.00 eq.) was added. Subsequently the mixture was allowed to warm to r.t. and stirred overnight. The mixture was then quenched with water before separating the layers. The aqueous layer was extracted three times with Et_2O. Then, the combined organic layers were washed with brine and dried over magnesium sulfate. After removal of the solvent under reduced pressure and purification by flash chromatography (SiO_2, *n*-Pentane:Et_2O 9:1 + 1% NEt_3), oxetane **74** (39.7 mg, 0.20 mmol, 5%) was obtained as a colorless oil.

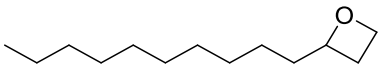

According to **GP IV**, epoxide **44** (0.90 mL, 4.00 mmol, 1.00 eq.), *t*BuOK (897 mg, 8.00 mmol, 2.00 eq.) and trimethylsulfoxonium iodide (1.76 g, 8.00 mmol, 2.00 eq.) were mixed in dry *t*BuOH (15 mL) and stirred for 3 days at 50 °C. After work-up and purification by flash chromatography (SiO_2, *n*-Pentane:Et_2O 9:1 + 1% NEt_3), oxetane **74** (264 mg, 1.63 mmol, 56%) was obtained as a colorless oil.

^{1}H NMR (500 MHz, $CDCl_3$) δ/ppm: 4.80 (p, J = 6.9 Hz, 1H), 4.65 (td, J = 7.9, 5.7 Hz, 1H), 4.48 (dt, J = 9.2, 5.7 Hz, 1H), 2.64 (dtd, J = 10.9, 7.9, 5.8 Hz, 1H), 2.31 (dq, J = 10.3, 7.6 Hz, 1H), 1.79 (ddd, J = 13.0, 9.2, 6.2 Hz, 1H), 1.64 (dq, J = 13.8, 5.2, 3.8 Hz, 1H), 1.37–1.21 (m, 16H), 0.88 (t, J = 6.8 Hz, 3H).

^{13}C NMR (126 MHz, $CDCl_3$) δ/ppm: 83.0, 68.2, 38.2, 32.0, 29.7, 29.7, 29.6, 29.5, 27.9, 24.2, 22.8, 14.2.

IR $\tilde{\nu}$/cm^{-1}: 2989, 2955, 2922, 2873, 2853, 1466, 1377, 1225, 980, 924, 721, 433, 403.

HRMS (APCI): exp. 199.2056

calc. 199.2062 ($C^{13}H^{27}O^+$ = $[M+H]^+$)

5.7.2 2-Benzyloxetane (85)

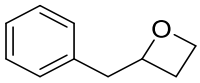

According to **GP IV**, epoxide **72** (0.70 mL, 5.00 mmol, 1.00 eq.), *t*BuOK (1.12 g, 10.0 mmol, 2.00 eq.) and trimethylsulfoxonium iodide (2.20 g, 10.0 mmol, 2.00 eq.) were mixed in dry *t*BuOH (18 mL) and stirred for 3 days at 50 °C. After work-up and purification by flash chromatography (SiO_2, *n*-Pentane:Et_2O 8:2 + 1% NEt_3), oxetane **85** (274 mg, 1.85 mmol, 37%) was obtained as a colorless oil.

^{1}H NMR (700 MHz, $CDCl_3$) *δ*/ppm: 7.32–7.28 (m, 2H), 7.24–7.21 (m, 3H), 5.07–5.01 (m, 1H), 4.65 (ddd, *J* = 8.4, 7.6, 5.8 Hz, 1H), 4.48 (dt, *J* = 9.1, 5.8 Hz, 1H), 3.09 (dd, *J* = 13.8, 6.3 Hz, 1H), 2.98 (dd, *J* = 13.8, 6.6 Hz, 1H), 2.64 (dddd, *J* = 11.0, 8.4, 7.4, 5.8 Hz, 1H), 2.43 (dddd, *J* = 11.0, 9.1, 7.6, 6.8 Hz, 1H).

^{13}C NMR (176 MHz, $CDCl_3$) *δ*/ppm: 137.2, 129.3, 128.5, 126.5, 82.8, 68.1, 44.2, 27.2.

IR $\tilde{\nu}$/cm^{-1}: 3027, 2880, 1737, 1604, 1496, 1453, 1365, 1229, 1103, 1077, 1030, 945, 843, 699, 627, 584, 498.

HRMS (APCI): exp. 148.0887

calc. 148.0888 ($C_{10}H_{12}O$ = $[M]^+$)

5.7.3 2-(Naphthalen-1-ylmethyl)oxetane (86)

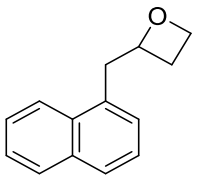

According to **GP IV**, epoxide **49** (787 mg, 4.27 mmol, 1.00 eq.), *t*BuOK (958 mg, 8.54 mmol, 2.00 eq.) and trimethylsulfoxonium iodide (1.88 g, 8.54 mmol, 2.00 eq.) were mixed in dry *t*BuOH (15 mL) and stirred for 3 days at 50 °C. After work-up and purification by flash chromatography (SiO_2, *n*-Pentane:Et_2O 9:1 + 1% NEt_3), oxetane **86** (271 mg, 1.37 mmol, 32%) was obtained as a colorless oil.

^{1}H NMR (400 MHz, $CDCl_3$) δ/ppm: 8.07 (dq, J = 8.7, 0.9 Hz, 1H), 7.90–7.83 (m, 1H), 7.76 (dt, J = 8.2, 1.2 Hz, 1H), 7.58–7.46 (m, 2H), 7.42 (dd, J = 8.1, 7.0 Hz, 1H), 7.36 (dd, J = 7.0, 1.3 Hz, 1H), 5.31–5.20 (m, 1H), 4.68 (td, J = 8.0, 5.9 Hz, 1H), 4.57 (dt, J = 9.1, 5.8 Hz, 1H), 3.65 (dd, J = 14.2, 6.2 Hz, 1H), 3.43 (dd, J = 14.2, 7.0 Hz, 1H), 2.65 (dddd, J = 11.0, 8.3, 7.3, 5.8 Hz, 1H), 2.52 (dddd, J = 11.0, 9.0, 7.7, 6.8 Hz, 1H).

^{13}C NMR (101 MHz, $CDCl_3$) δ/ppm: 134.0, 133.2, 132.3, 128.9, 127.4, 127.1, 126.1, 125.7, 125.6, 123.9, 82.1, 68.2, 41.1, 27.8.

IR $\tilde{\nu}$/cm^{-1}: 3044, 2993, 2930, 2876, 1595, 1509, 1363, 1225, 1014, 945, 840, 637, 552, 513, 431, 409.

HRMS (ESI): exp. 199.1117

calc. 199.1123 ($C_{14}H_{15}O^+$ = $[M+H]^+$)

5.7.4 2-Methyl-2-phenethyloxetane (89)

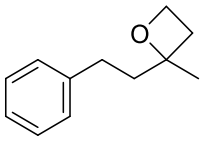

According to **GP IV**, 4-phenylbutan-2-one (1.50 mL, 10.0 mmol, 1.00 eq.), *t*BuOK (4.49 g, 40.0 mmol, 4.00 eq.) and trimethylsulfoxonium iodide (8.80 g, 40.0 mmol, 4.00 eq.) were mixed in dry *t*BuOH (36 mL) and stirred for 4 days at 50 °C. After work-up and purification by flash chromatography (SiO_2, *n*-Pentane:Et_2O 100:0–97:3 + 1% NEt_3), oxetane **89** (1.21 g, 6.90 mmol, 69%) was obtained as a light yellow oil.

^{1}H NMR (700 MHz, $CDCl_3$) δ/ppm: 7.30 (td, J = 7.5, 1.6 Hz, 2H), 7.25–7.22 (m, 2H), 7.20 (td, J = 7.2, 1.4 Hz, 1H), 4.56–4.52 (m, 1H), 4.50–4.46 (m, 1H), 2.73 (dt, J = 8.9, 6.1 Hz, 2H), 2.51 (dddd, J = 10.9, 8.9, 6.8, 1.4 Hz, 1H), 2.40–2.35 (m, 1H), 2.03–1.98 (m, 2H), 1.49 (d, J = 1.5 Hz, 3H).

^{13}C NMR (176 MHz, $CDCl_3$) δ/ppm: 142.3, 128.5, 125.9, 86.4, 64.4, 44.1, 32.4, 30.1, 27.4.

The analytical data are consistent with the literature.[101]

5.8 Employing Protecting Groups

5.8.1 *tert*-Butyldimethyl((9-(oxiran-2-yl)nonyl)oxy)silane (52)

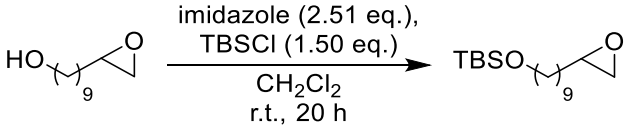

The reaction was performed under argon. In a heat-dried *Schlenk* flask, imidazole (1.76 g, 25.9 mmol, 2.51 eq.) and TBSCl (2.33 g, 15.5 mmol, 1.50 eq.) were dissolved in CH_2Cl_2 (25 mL) before slowly adding alcohol **69** (1.92 g, 10.3 mmol, 1.00 eq.). The mixture was stirred for 20 h at room temperature. Then, the reaction was quenched with H_2O and the layers were separated. The aqueous layer was extracted three times with Et_2O and the combined organic phases were washed with H_2O and aq. NaOH (2M in H_2O) and dried over $MgSO_4$. Removal of solvents under reduced pressure and purification *via* flash chromatography (SiO_2, PE:Et_2O 9:1) yielded the product **52** as a colorless oil (2.15 g, 7.15 mmol, 69%).

^{1}H-NMR (500 MHz, $CDCl_3$) δ/ppm: 3.59 (t, J = 6.6 Hz, 2H), 2.90 (tdd, J = 5.6, 3.9, 2.7 Hz, 1H), 2.74 (dd, J = 5.1, 3.9 Hz, 1H), 2.46 (dd, J = 5.0, 2.7 Hz, 1H), 1.56–1.24 (m, 16H), 0.89 (s, 9H), 0.04 (s, 6H).

^{13}C-NMR (126 MHz, $CDCl_3$) δ/ppm: 63.5, 52.5, 47.3, 33.0, 32.6, 29.7, 29.6, 29.6, 29.5, 26.1, 26.1, 25.9, 18.5, –5.1, –5.1.

The analytical data are in good agreement with the literature.[223]

5.8.2 2-(9-((4-Methoxybenzyl)oxy)nonyl)oxirane (70)

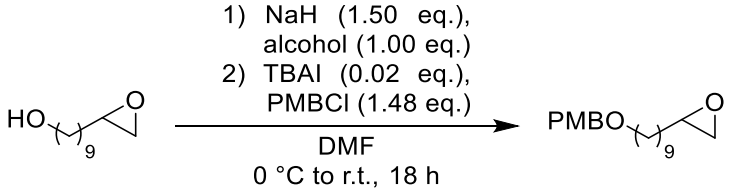

The reaction was performed under argon. In a heat-dried *Schlenk* flask, NaH (60% in mineral oil, 162 mg, 6.75 mmol, 1.50 eq.) was suspended in DMF (7.5 mL) before cooling the mixture to 0 °C. Then, alcohol **69** (838 mg, 4.50 mmol, 1.00 eq.) was added and the suspension was stirred for 30 min at the same temperature. Finally, tetra-*n*-butylammonium iodide (TBAI, 33.2 mg, 0.09 mmol, 0.02 eq.) and PMBCl (0.90 mL, 6.67 mmol, 1.48 eq.) were added before allowing the mixture warm to ambient temperature and stir for 18 h. Subsequently, the mixture

was washed with saturated aqueous NH_4Cl solution and the phases were separated. The aqueous phase was extracted three times with Et_2O and the combined organic phases were washed with brine and dried over $MgSO_4$. After removal of solvents under reduced pressure, the crude product was purified *via* flash chromatography (SiO_2, PE:Et_2O 8:2) to yield the product **70** as a colorless oil (910 mg, 2.97 mmol, 66%).

^{1}H-NMR (500 MHz, $CDCl_3$) *δ*/ppm: 7.31–7.23 (m, 2H), 6.92–6.84 (m, 2H), 4.44 (d, *J* = 15.5 Hz, 2H), 3.80 (d, *J* = 0.8 Hz, 3H), 3.43 (t, *J* = 6.6 Hz, 2H), 2.90 (tdd, *J* = 5.3, 3.9, 2.7 Hz, 1H), 2.74 (dd, *J* = 5.0, 3.9 Hz, 1H), 2.46 (dd, *J* = 5.1, 2.7 Hz, 1H), 1.64–1.25 (m, 16H).

^{13}C-NMR (126 MHz, $CDCl_3$) *δ*/ppm: 159.1, 130.8, 129.2, 113.8, 72.5, 70.2, 55.3, 52.4, 47.1, 32.5, 29.8, 29.5, 29.5, 29.4, 26.2, 26.0.

The analytical data are in good agreement with the literature.[223]

5.9 Synthesis of Alcohols

5.9.1 (2*R*,3*S*)-3-Phenylbutan-2-ol (4)

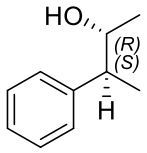

Hydrosilylation of enantiomerically enriched epoxide using $PhSiH_3$:

According to **GP V**, **[Ti]-3** (18.5 mg, 50.0 *µ*mol, 5 mol%), BnMgBr (0.61M in Et_2O, 0.18 mL, 0.11 mmol, 11 mol%), $PhSiH_3$ (0.19 mL, 1.50 mmol, 1.50 eq.) and epoxide **3**,[148] (147.4 mg, 0.99 mmol, 1.00 eq., *d.r.* 72:28) in THF (6 mL) were stirred for 20 h at room temperature. Desilylation, followed by work-up and flash chromatography (SiO_2, CH:EA 9:1) yielded alcohol **4** (0.111 g, 0.74 mmol, 74%, *d.r.* 98:2, *e.r.* 96:4) as a pale yellow oil.

Hydrosilylation of enantiomerically enriched epoxide using PMHS perfomed by *Mika*.

Hydrosilylation of racemic epoxide using $PhSiH_3$ performed by *Höthker*.

^{1}H-NMR (499 MHz, $CDCl_3$) *δ*/ppm: 7.38–7.28 (m, 2H), 7.28–7.19 (m, 3H) 3.85 (dq, *J* = 7.5 Hz, 6.2 Hz, 1H), 2.68 (p, *J* = 7.2 Hz, 1H), 1.27 (d, *J* = 7.1 Hz, 3H), 1.23 (d, *J* = 6.2 Hz, 3H).
The *d.r.* was determined by comparison with a CH_3 signal of the minor diastereomer at 1.09 ppm (d, $CDCl_3$).

^{13}C-NMR (126 MHz, $CDCl_3$) *δ*/ppm: 143.7, 128.8, 128.2, 126.9, 72.5, 48.1, 20.8, 18.0.

$[\alpha]_D^{20}$: –24.2° (CH_2Cl_2)

The alcohol's *e.r.* was determined by ^{19}F-NMR spectroscopy following esterification with (*S*)-MTPA chloride ($CDCl_3$, 470 MHz, major: –71.37 ppm; minor: –71.60 ppm).

The analytical data are in agreement with the literature.[153]

5.9.2 (2*R*,3*S*)-3-(*m*-Tolyl)butan-2-ol (5)

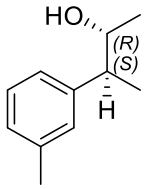

Hydrosilylation of enantiomerically enriched epoxide using $PhSiH_3$:

According to **GP V**, **[Ti]-3** (9.0 mg, 24.9 *µ*mol, 5 mol%), BnMgBr (0.68M in Et_2O, 80 *µ*L, 54.4 *µ*mol, 11 mol%), $PhSiH_3$ (90 *µ*L, 0.73 mmol, 1.46 eq.) and epoxide **24** (81.1 mg, 0.50 mmol, 1.00 eq., *d.r.* 74:26) in THF (3 mL) were stirred for 24 h at room temperature. Desilylation, followed by work-up and flash chromatography (SiO_2, CH:EA 9:1) yielded alcohol **5** (41.1 mg, 0.25 mmol, 50%, *d.r.* 96:4, *e.r.* 98:2) as a pale yellow oil.

Hydrosilylation of enantiomerically enriched epoxide using PMHS:

According to **GP VI**, **[Ti]-1** (6.8 mg, 27.3 *µ*mol, 6 mol%), BnMgBr (0.74M in Et_2O, 70 *µ*L, 51.8 *µ*mol, 11 mol%), $PhSiH_3$ (0.81M in THF, 20 *µ*L, 16.2 *µ*mol, 3.0 mol%), PMHS (0.12 mL, 2.01 mmol, 4.34 eq.) and epoxide **24** (75.1 mg, 0.46 mmol, 1.00 eq., *d.r.* 74:26) in THF (2 mL) and 1,4-dioxane (2 mL) were stirred for 24 h at room temperature. Desilylation, followed by work-up and flash chromatography (SiO_2, PE:Et_2O 9:1) yielded alcohol **5** (68.0 mg, 0.41 mmol, 89%, *d.r.* 99:1, *e.r.* 97:3) as a pale yellow oil.

Hydrosilylation of racemic epoxide using $PhSiH_3$:

According to **GP V**: **[Ti]-3** (9.00 mg, 25.0 *µ*mol, 5 mol%), BnMgBr (0.74M in Et_2O, 74.3 *µ*L, 55.0 *µ*mol, 11 mol%), $PhSiH_3$ (92.5 *µ*L, 0.75 mmol, 1.5 eq.) and epoxide ***rac*-24** (81.1 mg, 0.50 mmol, 1.00 eq., *d.r.* 99:1) in THF (3 mL) were stirred for 24 h at room temperature. Desilylation, followed by work-up and flash chromatography (SiO_2, PE:Et_2O 9:1) yielded alcohol ***rac*-5** (63.0 mg, 0.38 mmol, 76%, *d.r.* 99:1).

^{1}H-NMR (499 MHz, $CDCl_3$) *δ*/ppm: 7.27–7.23 (m, 1H), 7.11–7.04 (m, 3H), 3.86 (dq, *J* = 7.7, 6.2 Hz, 1H), 2.66 (p, *J* = 7.2 Hz, 1H), 2.38 (s, 3H), 1.27 (t, *J* = 6.9 Hz, 6H).
The *d.r.* was determined by comparison with a CH_3 signal of the minor diastereomer at 1.10 ppm (d, $CDCl_3$).

^{13}C-NMR (126 MHz, $CDCl_3$) *δ*/ppm: 143.6, 138.3, 128.8, 128.6, 127.6, 125.0, 72.4, 48.0, 21.5, 20.6, 18.0.

$[\alpha]_D^{20}$: –28.4° (CH_2Cl_2)

The alcohol's *e.r.* was determined by ^{19}F-NMR spectroscopy following esterification with (*S*)-MTPA chloride according to **GP XI** ($CDCl_3$, 470 MHz, major: –71.36 ppm; minor: –71.64 ppm).

The analytical data are in agreement with the literature.[133]

5.9.3 (2*R*,3*S*)-3-(*p*-Tolyl)butan-2-ol (6)

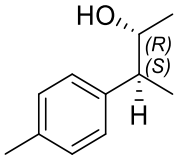

Hydrosilylation of enantiomerically enriched epoxide using $PhSiH_3$:

According to **GP V**, **[Ti]-3** (19.0 mg, 52.6 *µ*mol, 5 mol%), BnMgBr (0.61M in Et_2O, 0.18 mL, 110 *µ*mol, 11mol%), $PhSiH_3$ (0.18 mL, 1.46 mmol, 1.47 eq.) and epoxide **25** (161.0 mg, 0.99 mmol, 1.00 eq., *d.r.* 53:47) in THF (6 mL) were stirred for 24 h at room temperature. Desilylation, followed by work-up and flash chromatography (SiO_2, PE:Et_2O 9:1) yielded alcohol **6** (124.0 mg, 0.75 mmol, 76%, *d.r.* 98:2, *e.r.* 95:5) as a pale yellow oil.

Hydrosilylation of enantiomerically enriched epoxide using PMHS:

According to **GP VI**, **[Ti]-1** (6.6 mg, 26.5 *µ*mol, 5mol%), BnMgBr (0.74M solution in Et_2O, 70 *µ*L, 51.8 *µ*mol, 10 mol%), $PhSiH_3$ (0.81M in THF, 20 *µ*L, 16.2 *µ*mol, 3.0 mol%), PMHS (0.12 mL, 2.01 mmol, 4.05 eq.) and epoxide **25** (80.4 mg, 0.50 mmol, 1.00 eq., *d.r.* 53:47) in THF (2 mL) and 1,4-dioxane (2 mL) were stirred for 24 h at room temperature. Desilylation, followed by work-up and flash chromatography (SiO_2, PE:Et_2O 9:1) yielded alcohol **6** (65.0 mg, 0.40 mmol, 80%, *d.r.* 95:5, *e.r.* 93:7) as a pale yellow oil.

Hydrosilylation of racemic epoxide using $PhSiH_3$:

According to **GP V**, **[Ti]-3** (17.9 mg, 51.0 *µ*mol, 5 mol%), BnMgBr (0.61M in Et_2O, 0.18 mL, 110 *µ*mol, 11mol%), $PhSiH_3$ (0.19 mL, 1.50 mmol, 1.50 eq.) and ***rac*-25** (160.2 mg, 0.99 mmol, 1.00 eq., *d.r.* 72:28) in THF (6 mL) were stirred for 24 h at room temperature. Desilylation, followed by work-up and flash chromatography (SiO_2, CH:EA 9:1) yielded ***rac*-6** (120 mg, 0.73 mmol, 73%, *d.r.* 98:2) as a pale yellow oil.

^{1}H-NMR (499 MHz, $CDCl_3$) *δ*/ppm: 7.18–7.07 (m, 4H), 3.82 (dq, *J* = 7.6, 6.2 Hz, 1H), 2.64 (p, *J* = 7.2 Hz, 1H), 2.33 (s, 3H), 1.24 (dd, *J* = 10.1, 6.6 Hz, 6H).
The *d.r.* was determined by comparison with a CH_3 signal of the minor diastereomer at 1.09 ppm (d, $CDCl_3$).

^{13}C-NMR (126 MHz, $CDCl_3$) δ/ppm: 140.5, 136.3, 129.4, 127.9, 72.4, 47.6, 21.0, 20.6, 18.0.

$[\alpha]_D^{20}$: –16.8°(CH_2Cl_2)

The alcohol's *e.r.* was determined by ^{19}F-NMR spectroscopy following esterification with (*S*)-MTPA chloride according to **GP XI** ($CDCl_3$, 470 MHz, major: –71.34 ppm; minor: –71.62 ppm).

The analytical data are in agreement with the literature.[153]

5.9.4 (2*R*,3*S*)-3-(4-Fluorophenyl)butan-2-ol (11)

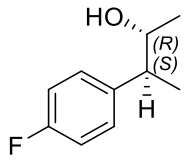

Hydrosilylation of enantiomerically enriched epoxide using $PhSiH_3$:

According to **GP V**, **[Ti]-3** (18.1 mg, 50.1 *µ*mol, 5 mol%), BnMgBr (0.61M in Et_2O, 0.18 mL, 110 *µ*mol, 11 mol%), $PhSiH_3$ (0.18 mL, 1.46 mmol, 1.45 eq.) and epoxide **30** (167.8 mg, 1.01 mmol, 1.00 eq., *d.r.* 77:23) in THF (6 mL) were stirred for 24 h at room temperature. Desilylation, followed by work-up and flash chromatography (SiO_2, PE:Et_2O 9:1) yielded alcohol **11** (129.0 mg, 0.77 mmol, 76%, *d.r.* 97:3, *e.r.* 96:4) as a pale yellow oil.

Hydrosilylation of enantiomerically enriched epoxide using PMHS:

According to **GP VI**, **[Ti]-1** (6.17 mg, 25.0 *µ*mol, 5 mol%), BnMgBr (74.3 *µ*L, 55.0 *µ*mol, 0.74M in Et_2O, 11 mol%), $PhSiH_3$ (15.4 *µ*L, 12.5 *µ*mol, 2.5 mol%), PMHS (0.12 mL, 2.01 mmol, 4.05 eq.) and epoxide **30** (83.1 mg, 0.50 mmol, 1.00 eq., *d.r.* 77:23) in THF (2 mL) and 1,4-dioxane (2 mL) were stirred for 24 h at room temperature. Desilylation, followed by work-up and flash chromatography (SiO_2, PE:Et_2O 9:1) yielded alcohol **11** (51.0 mg, 0.30 mmol, 60%, *d.r.* 94:6, *e.r.* 95:5) as a pale yellow oil.

Hydrosilylation of racemic epoxide using $PhSiH_3$:

According to **GP V**, **[Ti]-3** (9.00 mg, 25.0 *µ*mol, 5 mol%), BnMgBr (0.61M in Et_2O, 0.09 mL, 55 *µ*mol, 11 mol%), $PhSiH_3$ (0.09 mL, 0.75 mmol, 1.50 eq.) and ***rac*-30** (86.3 mg, 0.52 mmol, 1.00 eq., *d.r.* 70:30) in THF (3 mL) were stirred for 24 h at room temperature. Desilylation, followed by work-up and flash chromatography (SiO_2, PE:Et_2O 9:1) yielded ***rac*-11** (50.0 mg, 0.30 mmol, 58%, *d.r.* 95:5) as a pale yellow oil.

^{1}H-NMR (499 MHz, $CDCl_3$) δ/ppm: 7.24–7.18 (m, 2H), 7.05–6.98 (m, 2H), 3.82 (dq, *J* = 7.3, 6.2 Hz, 1H), 2.67 (p, *J* = 7.1 Hz, 1H), 1.25 (d, *J* = 7.2 Hz, 3H), 1.21 (d, *J* = 6.2 Hz, 3H).

The *d.r.* was determined by comparison with a CH_3 signal of the minor diastereomer at 1.09 ppm (d, $CDCl_3$).

^{13}C-NMR (126 MHz, $CDCl_3$) δ/ppm: 161.8 (d, J = 244.5 Hz), 139.3 (d, J = 3.2 Hz), 129.6 (d, J = 7.8 Hz), 115.5 (d, J = 21.0 Hz), 72.5, 47.3, 20.9, 18.2.

$[\alpha]_D^{20}$: –16.5° (CH_2Cl_2)

The alcohol's *e.r.* was determined by ^{19}F-NMR spectroscopy following esterification with (*S*)-MTPA chloride according to **GP XI** ($CDCl_3$, 470 MHz, major: –71.26 ppm; minor: –71.50 ppm).

The analytical data are in agreement with the literature.[153]

5.9.5 (2*R*,3*S*)-3-(4-Chlorophenyl)butan-2-ol (16)

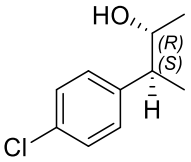

Hydrosilylation of enantiomerically enriched epoxide using $PhSiH_3$:

According to **GP V**, **[Ti]-3** (18.7 mg, 51.8 μmol, 5 mol%), BnMgBr (0.70M in Et_2O, 0.16 mL, 112 μmol, 11 mol%), $PhSiH_3$ (0.18 mL, 1.46 mmol, 1.46 eq.) and epoxide **35** (183.1 mg, 1.00 mmol, 1.00 eq., *d.r.* 75:25) in THF (6 mL) were stirred for 24 h at room temperature. Desilylation, followed by work-up and flash chromatography (SiO_2, PE:Et_2O 9:1) yielded alcohol **16** (130.0 mg, 0.70 mmol, 70%, *d.r.* 98:2, *e.r.* 97:3) as a pale yellow oil.

Hydrosilylation of enantiomerically enriched epoxide using PMHS:

According to **GP IV**, **[Ti]-1** (6.5 mg, 26.1 μmol, 5 mol%), BnMgBr (0.74M solution in Et_2O, 70 μL, 51.8 μmol, 10mol%), $PhSiH_3$ (0.81M in THF, 20 μL, 16.2 μmol, 3.0 mol%), PMHS (0.12 mL, 2.01 mmol, 4.06 eq.) and epoxide **35** (90.4 mg, 0.49 mmol, 1.00 eq., *d.r.* 75:25) in THF (2 mL) and 1,4-dioxane (2 mL) were stirred for 24 h at room temperature. Desilylation, followed by work-up and flash chromatography (SiO_2, PE:Et_2O 9:1) yielded alcohol **16** (58.0 mg, 0.31 mmol, 63%, *d.r.* 99:1, *e.r.* 96:4) as a pale yellow oil.

Hydrosilylation of racemic epoxide using $PhSiH_3$:

According to **GP V**, **[Ti]-3** (18.1 mg, 50.0 μmol, 0.05 eq.), BnMgBr (0.16 mL, 0.11 mmol, 0.70M in Et_2O, 0.11 eq.), $PhSiH_3$ (0.19 mL, 1.50 mmol, 1.50 eq.) and epoxide ***rac*-35** (181.7 mg, 0.99 mmol, 1.00 eq., *d.r.* 62:38) in THF (6 mL) were stirred for 24 h at room temperature. Desilylation, followed by work-up and flash chromatography (SiO_2, PE:Et_2O 9:1) yielded alcohol ***rac*-16** (0.13 g, 0.70 mmol, 70%, *d.r.* 96:4).

^{1}H-NMR (499 MHz, $CDCl_3$) δ/ppm: 7.34–7.26 (m, 2H), 7.22–7.15 (m, 2H), 3.83 (dq, J = 7.2, 6.2 Hz, 1H), 2.67 (p, J = 7.1 Hz, 1H), 1.25 (d, J = 7.1 Hz, 3H), 1.21 (d, J = 6.2 Hz, 3H).
The *d.r.* was determined by comparison with a CH_3 signal of the minor diastereomer at 1.11 ppm (d, $CDCl_3$).

^{13}C-NMR (126 MHz, $CDCl_3$) δ/ppm: 142.1, 132.4, 129.4, 128.7, 72.2, 47.2, 20.8, 17.9.

$[\alpha]_D^{20}$: –30.2° (CH_2Cl_2)

The alcohol's *e.r.* was determined by ^{19}F-NMR spectroscopy following esterification with (*S*)-MTPA chloride according to **GP XI** ($CDCl_3$, 470 MHz, major: –71.22 ppm; minor: –71.52 ppm).

The analytical data are in agreement with the literature.[133]

5.9.6 (2*R*,3*S*)-3-(2-Fluorophenyl)butan-2-ol (9)

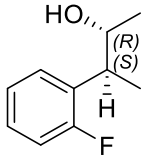

Hydrosilylation of enantiomerically enriched epoxide using $PhSiH_3$:

According to **GP V**, **[Ti]-3** (9.0 mg, 24.9 µmol, 5mol%), BnMgBr (0.74M in Et_2O, 70 µL, 51.8 µmol, 10 mol%), $PhSiH_3$ (90 µL, 0.73 mmol, 1.46 eq.) and epoxide **28**,[148] (83.1 mg, 0.50 mmol, 1.00 eq., *d.r.* 76:24) in THF (3 mL) were stirred for 24 h at room temperature. Desilylation, followed by work-up and flash chromatography (SiO_2, PE:Et_2O 9:1) yielded alcohol **9** (59.0 mg, 0.35 mmol, 70%, *d.r.* 98:2, *e.r.* 96:4) as a pale yellow oil.

Hydrosilylation of enantiomerically enriched epoxide using PMHS:

According to **GP VI**, **[Ti]-1** (6.2 mg, 24.9 µmol, 5 mol%), BnMgBr (0.74M in Et_2O, 70 µL, 51.8 µmol, 11 mol%), $PhSiH_3$ (0.81M in THF, 20 µL, 16.2 µmol, 3.0 mol%), PMHS (0.12 mL, 2.01 mmol, 4.33 eq.) and epoxide **28**,[148] (77.1 mg, 0.46 mmol, 1.00 eq., *d.r.* 76:24) in THF (2 mL) and 1,4-dioxane (2 mL) were stirred for 24 h at room temperature. Desilylation, followed by work-up and flash chromatography (SiO_2, PE:Et_2O 9:1) yielded alcohol **9** (41.0 mg, 0.24 mmol, 53%, *d.r.* 99:1, *e.r.* 95:5) as a pale yellow oil.

Hydrosilylation of racemic epoxide using $PhSiH_3$:

According to **GP V**, **[Ti]-3** (9.00 mg, 25.0 µmol, 0.05 eq.), BnMgBr (74.3 µL, 55.0 µmol, 0.74M in Et_2O, 0.11 eq.), $PhSiH_3$ (92.5 µL, 0.75 mmol, 1.50 eq.) and ***rac*-28**,[148] (83.1 mg, 0.50 mmol,

1.00 eq., *d.r.* 70:30) in THF (3 mL) were stirred for 24 h at room temperature. Desilylation, followed by work-up and flash chromatography (SiO_2, PE:Et_2O 9:1) yielded alcohol ***rac*-9** (55.0 mg, 0.33 mmol, 66%, *d.r.* 98:2).

^{1}H-NMR (499 MHz, $CDCl_3$) δ/ppm: 7.30 (td, J = 7.5, 1.9 Hz, 1H), 7.21 (dddd, J = 8.1, 7.2, 5.2, 1.9 Hz, 1H), 7.12 (td, J = 7.5, 1.4 Hz, 1H), 7.04 (ddd, J = 10.4, 8.1, 1.3 Hz, 1H), 4.03–3.91 (m, 1H), 3.11 (p, J = 7.1 Hz, 1H), 1.29 (dd, J = 7.2, 0.7 Hz, 3H), 1.26–1.16 (m, 3H).
The *d.r.* was determined by comparison with a CH_3 signal of the minor diastereomer at 1.13 ppm (d, $CDCl_3$).

^{13}C-NMR (126 MHz, $CDCl_3$) δ/ppm: 161.1 (d, J = 244.7 Hz), 130.2 (d, J = 14.6 Hz), 129.1 (d, J = 5.0 Hz), 127.9 (d, J = 8.4 Hz), 124.2 (d, J = 3.5 Hz), 115.5 (d, J = 23.3 Hz), 71.3 (d, J = 1.4 Hz), 40.3 (d, J = 1.0 Hz), 20.9, 16.8 (d, J = 1.2 Hz).

$[\alpha]_D^{20}$: –22.4° (CH_2Cl_2)

The alcohol's *e.r.* was determined by ^{19}F-NMR spectroscopy following esterification with (*S*)-MTPA chloride according to **GP XI** ($CDCl_3$, 470 MHz, major: –71.40 ppm; minor: –71.64 ppm).

The analytical data are in agreement with the literature.[224]

5.9.7 (2*R*,3*S*)-3-(2-Chlorophenyl)butan-2-ol (14)

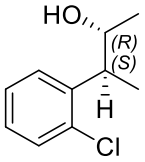

Hydrosilylation of enantiomerically enriched epoxide using $PhSiH_3$:

According to **GP V**, **[Ti]-3** (9.3 mg, 25.8 µmol, 5 mol%), BnMgBr (0.74M in Et_2O, 70 µL, 51.8 µmol, 10 mol%), $PhSiH_3$ (90 µL, 0.73 mmol, 1.46 eq.) and epoxide **33**,[148] (91.3 mg, 0.50 mmol, 1.00 eq., *d.r.* 32:68) in THF (3 mL) were stirred for 24 h at room temperature. Desilylation, followed by work-up and flash chromatography (SiO_2, PE:Et_2O 9:1) yielded alcohol **14** (62.0 mg, 0.34 mmol, 67%, *d.r.* 93:7, *e.r.* 96:4) as a pale yellow oil.

Hydrosilylation of enantiomerically enriched epoxide using PMHS:

According to **GP IV**, **[Ti]-1** (6.8 mg, 27.3 µmol, 5mol%), BnMgBr (0.74M in Et_2O, 70 µL, 51.8 µmol, 11 mol%), $PhSiH_3$ (0.81M in THF, 20 µL, 16.2 µmol, 3.0mol%), PMHS (0.12 mL,

2.01 mmol, 4.03 eq.) and epoxide **33**,[148] (91.1 mg, 0.50 mmol, 1.00 eq., *d.r.* 32:68) in THF (2 mL) and 1,4-dioxane (2 mL) were stirred for 24 h at room temperature. Desilylation, followed by work-up and flash chromatography (SiO_2, PE:Et_2O 9:1) yielded alcohol **14** (68.0 mg, 0.37 mmol, 74%, *d.r.* 96:4, *e.r.* 96:4) as a pale yellow oil.

Hydrosilylation of racemic epoxide using PMHS:

According to **GP VI**, **[Ti]-1** (12.5 mg, 50.0 *µ*mol, 5 mol%), BnMgBr (0.15 mL, 0.11 mmol, 0.74M in Et_2O, 11 mol%), $PhSiH_3$ (0.81M in THF, 30 *µ*L, 25.0 *µ*mol, 2.5 mol%), PMHS (0.24 mL, 4.02 mmol, 4.00 eq.) and ***rac*-33**,[148] (182.7 mg, 1.00 mmol, 1.00 eq., *d.r.* 62:38) in 1,4-dioxane (4 mL) and THF (4 mL) were stirred for 24 h at room temperature. Desilylation, followed by work-up and flash chromatography (SiO_2, PE/Et_2O 9:1) yielded alcohol ***rac*-14** (135.0 mg, 0.74 mmol, 74%, *d.r.* 96:4).

^{1}H-NMR (499 MHz, $CDCl_3$) *δ*/ppm: 7.37 (ddd, *J* = 9.5, 7.9, 1.6 Hz, 2H), 7.26 (dd, *J* = 15.1, 1.4 Hz, 1H), 7.20–7.10 (m, 1H), 4.07–3.93 (m, 1H), 3.39 (p, *J* = 7.0 Hz, 1H), 1.24 (dd, *J* = 12.3, 6.7 Hz, 6H). The *d.r.* was determined by comparison with a CH_3 signal of the minor diastereomer at 1.17 ppm (d, $CDCl_3$).

^{13}C-NMR (126 MHz, $CDCl_3$) *δ*/ppm: 141.2, 134.8, 129.9, 128.4, 127.7, 127.2, 71.6, 43.0, 20.7, 17.2.

IR *v*/cm^{-1}: 3383, 2973, 1475, 1440, 1378, 1097, 1037, 1013, 914, 748, 689, 460.

HRMS (APCI): exp. 167.0622

calc. 167.0622 ($C_{10}H_{12}Cl^+ = [M+H–H_2O]^+$)

$[\alpha]_D^{20}$: –24.0° (CH_2Cl_2)

The alcohol's *e.r.* was determined by ^{19}F-NMR spectroscopy following esterification with (*S*)-MTPA chloride according to **GP XI** ($CDCl_3$, 470 MHz, major: –71.38 ppm; minor: –71.71 ppm).

5.9.8 (2*R*,3*S*)-3-(3-(Trifluoromethyl)phenyl)butan-2-ol (13)

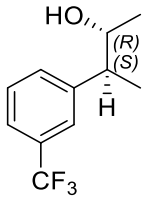

Hydrosilylation of enantiomerically enriched epoxide using $PhSiH_3$:

According to **GP V**, **[Ti]-3** (9.0 mg, 24.9 *µ*mol, 5 mol%), BnMgBr (0.74M in Et_2O, 70 *µ*L, 51.8 *µ*mol, 10 mol%), $PhSiH_3$ (90 *µ*L, 0.73 mmol, 1.46 eq.) and epoxide **32**,[148] (108.1 mg, 0.50 mmol, 1.00 eq., *d.r.* 78:22) in THF (3 mL) were stirred for 24 h at room temperature. Desilylation, followed by work-up and flash chromatography (SiO_2, PE:Et_2O 9:1) yielded alcohol **13** (62.0 mg, 0.28 mmol, 57%, *d.r.* 99:1, *e.r.* 98:2) as a pale yellow oil.

Hydrosilylation of enantiomerically enriched epoxide using PMHS:

According to **GP VI**, **[Ti]-1** (6.2 mg, 24.9 *µ*mol, 5 mol%), BnMgBr (0.74M in Et_2O, 70 *µ*L, 51.8 *µ*mol, 10 mol%), $PhSiH_3$ (0.81M in THF, 20 *µ*L, 16.2 *µ*mol, 3.0 mol%), PMHS (0.12 mL, 2.01 mmol, 4.02 eq.) and epoxide **32**,[148] (108.1 mg, 0.50 mmol, 1.00 eq., *d.r.* 78:22) in THF (2 mL) and 1,4-dioxane (2 mL) were stirred for 24 h at room temperature. Desilylation, followed by work-up and flash chromatography (SiO_2, PE:Et_2O 9:1) yielded alcohol **13** (73.0 mg, 0.33 mmol, 67%, *d.r.* 97:3, *e.r.* 98:2) as a pale yellow oil.

Hydrosilylation of racemic epoxide using PMHS:

According to **GP VI**, **[Ti]-1** (6.17 mg, 25.0 *µ*mol, 5 mol%), BnMgBr (74.3 *µ*L, 55.0 *µ*mol, 0.74M in Et_2O, 11 mol%), $PhSiH_3$ (15.4 *µ*L, 12.5 *µ*mol, 2.5 mol%), PMHS (0.12 mL, 2.01 mmol, 4.02 eq.) and ***rac*-32**,[148] (108.1 mg, 0.50 mmol, 1.00 eq., *d.r.* 69:31) in THF (2 mL) and 1,4-dioxane (2 mL) were stirred for 24 h at room temperature. Desilylation, followed by work-up and flash chromatography (SiO_2, PE:Et_2O 9:1) yielded alcohol ***rac*-13** (88.0 mg, 0.40 mmol, 80%, *d.r.* 97:3).

^{1}H-NMR (499 MHz, $CDCl_3$) *δ*/ppm: 7.56–7.42 (m, 4H), 3.92 (dq, *J* = 7.1, 6.2 Hz, 1H), 2.79 (p, *J* = 7.1 Hz, 1H), 1.32 (d, *J* = 7.1 Hz, 3H), 1.24 (d, *J* = 6.2 Hz, 3H).
The *d.r.* was determined by comparison with the CH_3 signal of the minor diastereomer at 1.10 (d, $CDCl_3$).

^{13}C-NMR (126 MHz, $CDCl_3$) *δ*/ppm: 144.7, 131.6 (q, *J* = 1.4 Hz), 130.8 (q, *J* = 31.9 Hz), 128.9, 124.8 (q, *J* = 3.9 Hz), 124.2 (q, *J* = 272.4 Hz), 123.5 (q, *J* = 3.9 Hz), 72.1, 47.6, 20.9, 17.8.

IR $\tilde{\nu}$/cm^{-1}: 3380, 2975, 1325, 1161, 1119, 1073, 917, 801, 703.

HRMS (APCI): exp. 201.0885

calc. 201.0886 ($C_{10}H_{12}CF_3^+$ = $[M+H-H_2O]^+$)

$[\alpha]_D^{20}$: –16.3° (CH_2Cl_2)

The alcohol's *e.r.* was determined by ^{19}F-NMR spectroscopy following esterification with (*S*)-MTPA chloride according to **GP XI** ($CDCl_3$, 470 MHz, major: –71.22 ppm; minor: –71.46 ppm).

5.9.9 Tridecan-1-ol (53)

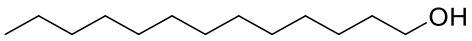

Screening Experiment according to Table 6, Entry 2:

According to **GP VIII**, **[Ti]-3** (9.1 mg, 25.2 µmol, 5 mol%), BnMgBr (1.03M in Et_2O, 50 µL, 51.5 µmol, 10 mol%), $PhSiH_3$ (0.81M in THF, 20 µL, 16.2 µmol, 3.0 mol%), PMHS (0.12 mL, 2.01 mmol, 3.99 eq.) and epoxide **50** (100.1 mg, 505 µmol, 1.00 eq.) were mixed in THF:1,4-dioxane (1:1, 4 mL) and stirred for 24 h at room temperature. Desilylation, followed by work-up and flash chromatography (SiO_2, PE:Et_2O 6:4) yielded the desired alcohol **53** as a light-yellow oil as a mixture of regioisomers (72.0 mg, 359 µmol, 71%, *r.r.* 82:18).

Screening Experiment according to Table 6, Entry 2:

According to **GP VIII**, **[Ti]-4** (10.0 mg, 25.4 µmol, 5 mol%), BnMgBr (1.03M in Et_2O, 50 µL, 51.5 µmol, 10 mol%), $PhSiH_3$ (0.81M in THF, 20 µL, 16.2 µmol, 3.0 mol%), PMHS (0.12 mL, 2.01 mmol, 3.95 eq.) and epoxide **50** (100.9 mg, 509 µmol, 1.00 eq.) were mixed in THF:1,4-dioxane (1:1, 4 mL) and stirred for 24 h at room temperature. Desilylation, followed by work-up and flash chromatography (SiO_2, PE:Et_2O 6:4) yielded the desired alcohol **53** as a light-yellow oil as a mixture of regioisomers (61.0 mg, 304 µmol, 60%, *r.r.* 86:14).

Screening Experiment according to Table 6, Entry 2:

According to **GP VIII**, **[Ti]-17** (31.5 mg, 26.6 µmol, 5 mol%), BnMgBr (0.67M in Et_2O, 80 µL, 53.6 µmol, 11 mol%), $PhSiH_3$ (0.81M in THF, 20 µL, 16.2 µmol, 3.0 mol%), PMHS (0.12 mL, 2.01 mmol, 3.99 eq.) and epoxide **50** (99.7 mg, 503 µmol, 1.00 eq.) were mixed in THF:1,4-dioxane (1:1, 4 mL) and stirred for 24 h at room temperature. Desilylation, followed by work-up and flash chromatography (SiO_2, PE:Et_2O 6:4) yielded the desired alcohol **53** as a light-yellow oil as a mixture of regioisomers (74.6 mg, 372 µmol, 74%, *r.r.* 92:8).

Screening Experiment according to Table 8, Entry 1:

According to a modification of **GP IX**, **[Ti]-17** (30.1 mg, 25.4 *µ*mol, 5 mol%), BnMgBr (0.62M in Et_2O, 90 *µ*L, 55.8 *µ*mol, 11 mol%), $PhSiH_3$ (90 *µ*L, 730 *µ*mol, 1.50 eq.) and oxetane **74** (99.0 mg, 499 *µ*mol, 1.00 eq.) were mixed in THF:1,4-dioxane (1:1, 4 mL) and stirred for 24 h at room temperature. Desilylation, followed by work-up yielded the desired alcohol **53** as a light-yellow oil as a mixture of regioisomers (conversion 7%, *r.r.*> 99:1). Owing to the low conversion, isolation was omitted.

Screening Experiment according to Table 8, Entry 2:

According to a modification of **GP IX**, **[Ti]-4** (10.0 mg, 25.4 *µ*mol, 5 mol%), BnMgBr (0.62M in Et_2O, 90 *µ*L, 55.8 *µ*mol, 11 mol%), $PhSiH_3$ (90 *µ*L, 730 *µ*mol, 1.50 eq.) and oxetane **74** (100 mg, 504 *µ*mol, 1.01 eq.) were mixed in THF:1,4-dioxane (1:1, 4 mL) and stirred for 24 h at room temperature. Desilylation, followed by work-up yielded the desired alcohol **53** as a light-yellow oil as a mixture of regioisomers (conversion 30%, *r.r.*> 99:1). Owing to the low conversion, isolation was omitted.

Screening Experiment according to Table 8, Entry 3:

According to **GP IX**, **[Ti]-1** (7.5 mg, 30.1 *µ*mol, 6 mol%), BnMgBr (0.75M in Et_2O, 70 *µ*L, 52.5 *µ*mol, 11 mol%), $PhSiH_3$ (90 *µ*L, 730 *µ*mol, 1.50 eq.) and oxetane **74** (101 mg, 509 *µ*mol, 1.02 eq.) were mixed in THF (4 mL) and stirred for 24 h at room temperature. Desilylation, followed by work-up yielded the desired alcohol **53** as a light-yellow oil as a mixture of regioisomers (conversion 72%, *r.r.*> 99:1). Owing to the low conversion, isolation was omitted.

Screening Experiment according to Table 8, Entry 4:

According to **GP IX**, **[Ti]-1** (12.2 mg, 50.0 *µ*mol, 10 mol%), BnMgBr (0.75M in Et_2O, 150 *µ*L, 113 *µ*mol, 0.22 eq.), $PhSiH_3$ (90 *µ*L, 730 *µ*mol, 1.50 eq.) and oxetane **74** (99.3 mg, 501 *µ*mol, 1.00 eq.) were mixed in THF (4 mL) and stirred for 24 h at room temperature. Desilylation followed by work-up and purification by flash chromatography (SiO_2, *n*-Pentane:Et_2O 6:4) yielded the desired alcohol **53** as a colorless oil as a mixture of regioisomers (85.2 mg, 425 *µ*mol, 85%, *r.r.* 99:1).

Screening Experiment according to Table 8, Entry 5:

According to **GP IX**, **[Ti]-1** (6.5 mg, 26.1 *µ*mol, 5 mol%), BnMgBr (0.75M in Et_2O, 70 *µ*L, 52.5 *µ*mol, 11 mol%), $PhSiH_3$ (90 *µ*L, 730 *µ*mol, 1.50 eq.) and oxetane **74** (100 mg, 504 *µ*mol, 1.01 eq.) were mixed in THF (4 mL) and stirred for 24 h under reflux conditions. Desilylation followed by work-up and purification by flash chromatography (SiO_2, *n*-Pentane:Et_2O 6:4) yielded the desired alcohol **53** as a colorless oil as a mixture of regioisomers (84.9 mg, 424 *µ*mol, 85%, *r.r.* 99:1).

Screening Experiment according to Table 8, Entry 6:

In a slight variation of **GP IX**, **[Ti]-1** (6.4 mg, 25.7 *µ*mol, 1 mol%), BnMgBr (0.77M in Et_2O, 70 *µ*L, 53.9 *µ*mol, 2.1 mol%), $PhSiH_3$ (0.40 mL, 3.25 mmol, 1.50 eq.) and oxetane **74** (438 mg, 2.21 mmol, 1.00 eq.) were mixed in THF (10 mL) and stirred for 24 h under reflux conditions. Desilylation followed by work-up and purification by flash chromatography (SiO_2, *n*-Pentane:Et_2O 6:4) yielded the desired alcohol **53** as a colorless oil as a mixture of regioisomers (344 mg, 1.72 mmol, 78%, *r.r.* 99:1).

Screening Experiment according to Scheme 83:

According to **GP X**, **[Ti]-1** (6.1 mg, 24.5 *µ*mol, 5 mol%), BnMgBr (0.77M in Et_2O, 70 *µ*L, 53.9 *µ*mol, 12 mol%), $PhSiH_3$ (0.81M in THF, 20 *µ*L, 16.2 *µ*mol, 3.5 mol%), PMHS (0.12 mL, 2.01 mmol, 4.38 eq.) and oxetane **74** (90.7 mg, 457 *µ*mol, 1.00 eq.) were mixed in THF (4 mL) and stirred for 24 h under reflux conditions. Desilylation, followed by work-up and flash chromatography (SiO_2, PE:Et_2O 6:4) yielded the desired alcohol **53** as a light-yellow oil as a mixture of regioisomers (73.1 mg, 365 *µ*mol, 73%, *r.r.* 99:1).

Screening Experiment according to Scheme 83:

According to a slight variation of **GP X**, **[Ti]-1** (6.2 mg, 25.0 *µ*mol, 1 mol%), BnMgBr (0.77M in Et_2O, 70 *µ*L, 53.9 *µ*mol, 2.1 mol%), $PhSiH_3$ (0.81M in THF, 80 *µ*L, 64.8 *µ*mol, 2.5 mol%), PMHS (0.60 mL, 10.0 mmol, 4.00 eq.) and oxetane **74** (496 mg, 2.50 mmol, 1.00 eq.) were mixed in THF (10 mL) and stirred for 24 h under reflux conditions. Desilylation, followed by work-up and flash chromatography (SiO_2, PE:Et_2O 6:4) yielded the desired alcohol **53** as a light-yellow oil as a mixture of regioisomers (376 mg, 1.88 mmol, 75%, *r.r.* 99:1).

^{1}H-NMR (500 MHz, $CDCl_3$) *δ*/ppm: 3.64 (t, *J* = 6.6 Hz, 2H), 1.56 (dt, *J* = 8.0, 6.5 Hz, 2H), 1.38–1.22 (m, 20H), 0.88 (t, *J* = 6.9 Hz, 3H).
The regioisomeric ratio was determined by comparison of CH_2- and CH_3-signals at 3.64 (*major*), and 1.18 ppm (*minor*).

^{13}C-NMR (126 MHz, $CDCl_3$) *δ*/ppm: 63.1, 32.8, 31.9, 29.7, 29.6, 29.6, 29.6, 29.6, 29.4, 29.3, 25.7, 22.7, 14.1.

The analytical data are in good agreement with the literature.[225]

5.9.10 Dodecan-1-ol (45)

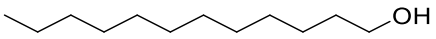

Screening Experiment according to Scheme 66:

According to **GP VII**, **[Ti]-1** (8.30 mg, 33.3 *µ*mol, 6.77 mol%), BnMgBr (0.70 M in Et_2O, 80 *µ*L, 56.0 *µ*mol, 0.11 eq.) $PhSiH_3$ (90 *µ*L, 730 *µ*mol, 1.50 eq.) and epoxide **44** (91.1 mg, 494 *µ*mol, 1.00 eq.) were mixed in THF (4 mL) and stirred for 24 h at room temperature. Desilylation, followed by work-up yielded the desired alcohol **45** as a light-yellow oil as a mixture of regioisomers (100% conversion, *r.r.* 64:36). The isolated yield was not determined, as the reaction was performed for screening purposes only.

Screening Experiment according to Table 4, Entry 3:

The reaction was performed under argon. In a heat-dried *Schlenk* tube, **[Ti]-1** (8.00 mg, 32.1 *µ*mol, 6.40 mol%) was dissolved in freshly distilled THF (2 mL). Then, allylMgBr (0.91 M in Et_2O, 60 *µ*L, 55.0 *µ*mol, 11.0 mol%) was added and the mixture was stirred until the color of the solution changed from red to deep purple. After subsequent addition of $PhSiH_3$ (90 *µ*L, 730 *µ*mol, 1.50 eq.) the color turned green indicating the activation of the titanocene catalyst. Subsequently, dry 1,4-dioxane (2 mL) was added. At last, epoxide **44** (92.0 mg, 499 *µ*mol, 1.00 eq.) was added and the reaction mixture was stirred for 24 h at room temperature. Afterwards, THF (20 mL) and NaOH solution (2M in H_2O, 20 mL) were added before heating the mixture to reflux overnight. After cooling to room temperature, the layers were separated and the aqueous layer was extracted three times with Et_2O. The combined organic layers were washed with brine and dried over magnesium sulfate. After removal of solvents under reduced pressure, the crude alcohol **45** (100% conversion, *r.r.* 73/27) was yielded. The isolated yield was not determined, as the reaction was performed for screening purposes only.

Screening Experiment according to Table 4, Entry 4:

The reaction was performed under argon. In a heat-dried *Schlenk* tube, **[Ti]-3** (10.3 mg, 28.5 *µ*mol, 5.70 mol%) was dissolved in freshly distilled THF (2 mL). Then, allylMgBr (0.91M in Et_2O, 60 *µ*L, 55.0 *µ*mol, 11.0 mol%) was added and the mixture was stirred until the color of the solution changed from red to deep purple. After subsequent addition of $PhSiH_3$ (90 *µ*L, 730 *µ*mol, 1.50 eq.) the color turned green indicating the activation of the titanocene catalyst. Subsequently, dry 1,4-dioxane (2 mL) was added. At last, epoxide **44** (92.0 mg, 499 *µ*mol, 1.00 eq.) was added and the reaction mixture was stirred for 24 h at room temperature. Afterwards, THF (20 mL) and NaOH solution (2M in H_2O, 20 mL) were added before heating the mixture to reflux overnight. After cooling to room temperature, the layers were separated and the aqueous layer was extracted three times with Et_2O. The combined organic layers were washed with brine and dried over magnesium sulfate. After removal of solvents under reduced

pressure, the crude alcohol **45** (100% conversion, *r.r.* 79/21) was yielded. The isolated yield was not determined, as the reaction was performed for screening purposes only.

Screening Experiment according to Scheme 71:

According to **GP VII**, **[Ti]-8** (8.60 mg, 26.8 *µ*mol, 5 mol%), BnMgBr (0.82 M in Et_2O, 70 *µ*L, 57.5 *µ*mol, 11 mol%), $PhSiH_3$ (90 *µ*L, 730 *µ*mol, 1.50 eq.) and epoxide **44** (93.5 mg, 507 *µ*mol, 1.00 eq.) were mixed in THF (4 mL) and stirred for 24 h at room temperature. Desilylation, followed by work-up yielded the desired alcohol **45** as a light-yellow oil as a mixture of regioisomers (100% conversion, *r.r.* 78:22). The isolated yield was not determined, as the reaction was performed for screening purposes only.

Screening Experiment according to Scheme 71:

According to a modification of **GP VIII**, **[Ti]-12** (21.8 mg, 25.0 *µ*mol, 5 mol%), BnMgBr (0.82M in Et_2O, 70 *µ*L, 55.0 *µ*mol, 11 mol%), $PhSiH_3$ (0.81M in THF, 20 *µ*L, 16.2 *µ*mol, 3.0 mol%), PMHS (0.12 mL, 2.01 mmol, 4.09 eq.), and epoxide **44** (91.7 mg, 498 *µ*mol, 1.00 eq.) were mixed in THF (4 mL) and stirred for 24 h at room temperature. Desilylation, followed by work-up yielded the desired alcohol **45** as a light-yellow oil as a mixture of regioisomers (76% conversion, *r.r.* 87:13). Owing to the low conversion, isolation was omitted.

Screening Experiment according to Scheme 73:

According to a modification of **GP VII**, **[Ti]-17** (28.6 mg, 24.1 *µ*mol, 4.82 mol%), allylMgCl (1.51 M in Et_2O, 40 *µ*L, 55.0 *µ*mol, 11 mol%), $PhSiH_3$ (90 *µ*L, 730 *µ*mol, 1.50 eq.), and epoxide **44** (91.1 mg, 494 *µ*mol, 1.00 eq.) were mixed in THF (4 mL) and stirred for 24 h at room temperature. Desilylation, followed by work-up yielded the desired alcohol **45** as a light-yellow oil as a mixture of regioisomers (50% conversion, *r.r.* 77:23). Owing to the low conversion, isolation was omitted.

Screening Experiment according to Scheme 73:

According to a modification of **GP VIII**, **[Ti]-17** (28.2 mg, 23.8 *µ*mol, 5 mol%), BnMgBr (0.82M in Et_2O, 70 *µ*L, 55.0 *µ*mol, 11 mol%), $PhSiH_3$ (90 *µ*L, 730 *µ*mol, 1.50 eq.), and epoxide **44** (91.8 mg, 498 *µ*mol, 1.00 eq.) were mixed in THF:1,4-dioxane (1:1, 4 mL) and stirred for 24 h at room temperature. Desilylation, followed by work-up and flash chromatography (SiO_2, PE:Et_2O 6:4) yielded the desired alcohol **45** as a light-yellow oil as a mixture of regioisomers (70.0 mg, 380 *µ*mol, 75%, *r.r.* 90:10).

The remaining catalyst screening experiments were performed analogously by *Krebs*, *Höthker*, *Klare* and *Schacht*.

^{1}H-NMR (500 MHz, $CDCl_3$) δ/ppm: 3.64 (t, J = 6.6 Hz, 2H), 1.60–1.53 (m, 2H), 1.27 (d, J = 11.7 Hz, 18H), 0.88 (t, J = 6.9 Hz, 3H).
The regioisomeric ratio was determined by comparison of CH_2- and CH_3-signals at 3.64 (*major*), and 1.18 ppm (*minor*).

^{13}C-NMR (126 MHz, $CDCl_3$) δ/ppm: 63.3, 33.0, 32.1, 29.8, 29.8, 29.8, 29.7, 29.6, 29.5, 25.9, 22.8, 14.3.

The analytical data are in good agreement with the literature.[226]

5.9.11 Decan-1-ol (54)

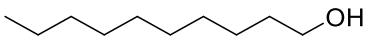

According to **GP VIII**, **[Ti]-17** (29.3 mg, 24.7 µmol, 5 mol%), BnMgBr (0.93M in Et_2O, 60 µL, 55.8 µmol, 11 mol%), $PhSiH_3$ (0.81M in THF, 20 µL, 16.2 µmol, 3.0 mol%), PMHS (0.12 mL, 2.01 mmol, 4.09 eq.) and epoxide **67** (76.8 mg, 491 µmol, 1.00 eq.) were mixed in THF:1,4-dioxane (1:1, 4 mL) and stirred for 24 h at room temperature. Desilylation, followed by work-up and flash chromatography (SiO_2, PE:Et_2O 7:3) yielded the desired alcohol **54** as a light-yellow oil as a mixture of regioisomers (59.1 mg, 373 µmol, 76%, *r.r.* 92:8).

^{1}H-NMR (500 MHz, $CDCl_3$) δ/ppm: 3.63 (t, J = 6.6 Hz, 2H), 1.55 (dt, J = 8.4, 6.5 Hz, 2H), 1.38–1.21 (m, 14H), 0.88 (t, J = 6.9 Hz, 3H).
The regioisomeric ratio was determined by comparison of CH_2- and CH_3-signals at 3.63 (*major*), and 1.18 ppm (*minor*).

^{13}C-NMR (126 MHz, $CDCl_3$) δ/ppm: 63.2, 33.0, 32.0, 29.8, 29.7, 29.6, 29.5, 25.9, 22.8, 14.2.

The analytical data are in good agreement with the literature.[226]

5.9.12 Octan-1-ol (55)

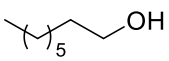

Screening Experiment according to Table 6, Entry 3:

According to **GP VIII**, **[Ti]-3** (9.4 mg, 26.0 µmol, 5 mol%), BnMgBr (1.03M in Et_2O, 50 µL, 51.5 µmol, 10 mol%), epoxide **51** (65.5 mg, 511 µmol, 1.00 eq.), $PhSiH_3$ (0.81M in THF, 20 µL, 16.2 µmol, 3 mol%) and PMHS (0.12 mL, 2.01 mmol, 3.93 eq.) were mixed in THF:1,4-

dioxane (1:1, 4 mL) and stirred for 24 h. After work-up and flash chromatography (SiO_2, PE:Et_2O 4:6), the desired alcohol **55** was obtained as a light-yellow oil as a mixture of regioisomers (16.0 mg, 123 *µ*mol, 24%, *r.r.* 82:18).

Screening Experiment according to Table 6, Entry 3:

According to **GP VIII**, **[Ti]-4** (10.5 mg, 26.7 *µ*mol, 5 mol%), BnMgBr (1.03M in Et_2O, 50 *µ*L, 51.5 *µ*mol, 10 mol%), epoxide **51** (62.9 mg, 491 *µ*mol, 1.00 eq.), $PhSiH_3$ (0.81M in THF, 20 *µ*L, 16.2 *µ*mol, 3 mol%) and PMHS (0.12 mL, 2.01 mmol, 4.09 eq.) were mixed in THF:1,4-dioxane (1:1, 4 mL) and stirred for 24 h. After work-up and flash chromatography (SiO_2, PE:Et_2O 4:6), the desired alcohol **55** was obtained as a light-yellow oil as a mixture of regioisomers (35.2 mg, 270 *µ*mol, 55%, *r.r.* 86:14).

Screening Experiment according to Table 6, Entry 3:

According to **GP VIII**, **[Ti]-17** (31.1 mg, 26.2 *µ*mol, 5 mol%), BnMgBr (0.67M in Et_2O, 80 *µ*L, 53.6 *µ*mol, 11 mol%), epoxide **51** (64.3 mg, 502 *µ*mol, 1.00 eq.), $PhSiH_3$ (0.81M in THF, 20 *µ*L, 16.2 *µ*mol, 3 mol%) and PMHS (0.12 mL, 2.01 mmol, 4.00 eq.) were mixed in THF:1,4-dioxane (1:1, 4 mL) and stirred for 24 h. After work-up and flash chromatography (SiO_2, PE:Et_2O 4:6), the desired alcohol **55** was obtained as a light-yellow oil as a mixture of regioisomers (48.4 mg, 372 *µ*mol, 74%, *r.r.* 92:8).

^{1}H-NMR (500 MHz, $CDCl_3$) *δ*/ppm: 3.64 (t, *J* = 6.6 Hz, 2H), 1.56 (dq, *J* = 7.8, 6.5 Hz, 2H), 1.39–1.23 (m, 10H), 0.91–0.85 (m, 3H).
The regioisomeric ratio was determined by comparison of CH_2- and CH_3-signals at 3.64 (*major*), and 1.18 ppm (*minor*).

^{13}C-NMR (126 MHz, $CDCl_3$) *δ*/ppm: 63.2, 33.0, 32.0, 29.5, 29.4, 25.9, 22.8, 14.2.

The analytical data are in good agreement with the literature.[226]

5.9.13 2-Cyclohexylethan-1-ol (64)

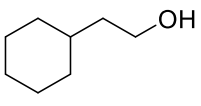

According to **GP VIII**, **[Ti]-17** (31.3 mg, 26.4 *µ*mol, 5 mol%), BnMgBr (1.03M in Et_2O, 50 *µ*L, 51.5 *µ*mol, 10 mol%), $PhSiH_3$ (0.81M in THF, 20 *µ*L, 16.2 *µ*mol, 3.0 mol%), PMHS (0.12 mL, 2.01 mmol, 3.99 eq.) and epoxide **68** (70.6 mg, 503 *µ*mol, 1.00 eq.) were mixed in THF:1,4-dioxane (1:1, 4 mL) and stirred for 24 h at room temperature. Desilylation, followed by work-

up and flash chromatography (SiO_2, PE:Et_2O 4:6) yielded the desired alcohol **64** as a light-yellow oil as a mixture of regioisomers (55.1 mg, 387 *µ*mol, 77%, *r.r.* >99:1).

^{1}H-NMR (500 MHz, $CDCl_3$) *δ*/ppm: 3.62 (t, *J* = 6.7 Hz, 2H), 1.75–1.62 (m, 5H), 1.57 (dq, *J* = 9.5, 6.7 Hz, 2H), 1.28–1.08 (m, 7H), 0.95–0.82 (m, 2H).

The regioisomeric ratio was determined by comparison of CH_2- and CH-signals at 3.62 (*major*), and 3.96–3.86 ppm (*minor*).

^{13}C-NMR (126 MHz, $CDCl_3$) *δ*/ppm: 63.6, 37.6, 33.6, 33.5, 30.3, 26.8, 26.5.

The analytical data are in good agreement with the literature.[227]

5.9.14 3-Phenylpropan-1-ol (62)

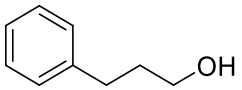

According to **GP VIII**, **[Ti]-17** (31.0 mg, 26.2 *µ*mol, 5 mol%), BnMgBr (0.67M in Et_2O, 80 *µ*L, 53.6 *µ*mol, 11 mol%), $PhSiH_3$ (0.81M in THF, 20 *µ*L, 16.2 *µ*mol, 3.0 mol%), PMHS (0.12 mL, 2.01 mmol, 4.06 eq.) and epoxide **72** (66.4 mg, 495 *µ*mol, 1.00 eq.) were mixed in THF:1,4-dioxane (1:1, 4 mL) and stirred for 24 h at room temperature. Desilylation, followed by work-up and flash chromatography (SiO_2, PE:Et_2O 4:6) yielded the desired alcohol **62** as a light-yellow oil as a mixture of regioisomers (49.9 mg, 366 *µ*mol, 74%, *r.r.* 92:8).

^{1}H-NMR (500 MHz, $CDCl_3$) *δ*/ppm: 7.29 (td, *J* = 7.2, 1.5 Hz, 2H), 7.24–7.17 (m, 3H), 3.68 (t, *J* = 6.4 Hz, 2H), 2.74–2.70 (m, 2H), 1.95–1.87 (m, 2H).
The regioisomeric ratio was determined by comparison of CH_2- and CH_3-signals at 3.68 (*major*), and 1.26 ppm (*minor*).

^{13}C-NMR (126 MHz, $CDCl_3$) *δ*/ppm: 141.9, 128.6, 128.5, 126.0, 62.4, 34.4, 32.2.

The analytical data are in good agreement with the literature.[228]

5.9.15 3-(Naphthalen-1-yl)propan-1-ol (63)

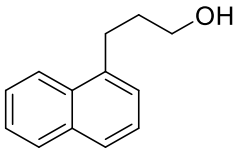

Screening Experiment according to Table 6, Entry 1:

According to **GP VII**, **[Ti]-3** (9.3 mg, 25.8 *µ*mol, 5 mol%), BnMgBr (1.03M in Et_2O, 50 *µ*L, 51.5 *µ*mol, 10 mol%), $PhSiH_3$ (0.81M in THF, 20 *µ*L, 16.2 *µ*mol, 3.0 mol%), PMHS (0.12 mL, 2.01 mmol, 4.01 eq.) and epoxide **49** (92.3 mg, 501 *µ*mol, 1.00 eq.) were mixed in THF:1,4-dioxane (1:1, 4 mL) and stirred for 24 h at room temperature. Desilylation, followed by work-up and flash chromatography (SiO_2, PE:Et_2O 4:6) yielded the desired alcohol **63** as a light-yellow oil as a mixture of regioisomers (70.9 mg, 381 *µ*mol, 76%, *r.r.* 80:20).

Screening Experiment according to Table 6, Entry 1:

According to **GP VII**, **[Ti]-4** (9.6 mg, 24.4 *µ*mol, 5 mol%), BnMgBr (1.03M in Et_2O, 50 *µ*L, 51.5 *µ*mol, 10 mol%), $PhSiH_3$ (0.81M in THF, 20 *µ*L, 16.2 *µ*mol, 3.0 mol%), PMHS (0.12 mL, 2.01 mmol, 4.06 eq.) and epoxide **49** (91.0 mg, 494 *µ*mol, 1.00 eq.) were mixed in THF:1,4-dioxane (1:1, 4 mL) and stirred for 24 h at room temperature. Desilylation, followed by work-up and flash chromatography (SiO_2, PE:Et_2O 4:6) yielded the desired alcohol **63** as a light-yellow oil as a mixture of regioisomers (75.4 mg, 405 *µ*mol, 82%, *r.r.* 92:8).

Screening Experiment according to Table 6, Entry 1:

According to **GP VII**, **[Ti]-17** (29.3 mg, 24.7 *µ*mol, 5 mol%), BnMgBr (0.67M in Et_2O, 80 *µ*L, 53.6 *µ*mol, 11 mol%), $PhSiH_3$ (0.81M in THF, 20 *µ*L, 16.2 *µ*mol, 3.0 mol%), PMHS (0.12 mL, 2.01 mmol, 4.06 eq.) and epoxide **49** (91.2 mg, 495 *µ*mol, 1.00 eq.) were mixed in THF:1,4-dioxane (1:1, 4 mL) and stirred for 24 h at room temperature. Desilylation, followed by work-up and flash chromatography (SiO_2, PE:Et_2O 4:6) yielded the desired alcohol **63** as a light-yellow oil as a mixture of regioisomers (75.6 mg, 406 *µ*mol, 82%, *r.r.* 96:4).

^{1}H-NMR (500 MHz, $CDCl_3$) *δ*/ppm: 8.11–8.03 (m, 1H), 7.86 (dd, *J* = 7.5, 1.8 Hz, 1H), 7.72 (d, *J* = 8.0 Hz, 1H), 7.50 (dddd, *J* = 16.1, 8.2, 6.9, 1.5 Hz, 2H), 7.44–7.33 (m, 2H), 3.76 (t, *J* = 6.3 Hz, 2H), 3.23–3.15 (m, 2H), 2.09–1.99 (m, 2H).
The regioisomeric ratio was determined by comparison of CH_2- and CH_3-signals at 3.76 (*major*), and 1.34 ppm (*minor*).

^{13}C-NMR (126 MHz, $CDCl_3$) *δ*/ppm: 138.1, 134.1, 132.0, 128.9, 126.9, 126.0, 125.7, 125.6, 123.9, 62.7, 33.7, 29.3.

The analytical data are in good agreement with the literature.[229]

5.9.16 3-(Octyloxy)propan-1-ol (59)

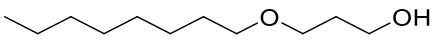

Screening Experiment according to Table 7, Entry 1:

According to **GP VIII**, **[Ti]-1** (8.2 mg, 32.9 *µ*mol, 6.6 mol%), BnMgBr (0.82M in Et_2O, 70 *µ*L, 55.0 *µ*mol, 11 mol%), $PhSiH_3$ (0.81M in THF, 20 *µ*L, 16.2 *µ*mol, 3.0 mol%), PMHS (0.12 mL, 2.01 mmol, 3.97 eq.) and epoxide **65** (93.4 mg, 501 *µ*mol, 1.00 eq.) were mixed in THF:1,4-dioxane (1:1, 4 mL) and stirred for 72 h at room temperature. Desilylation, followed by work-up yielded the desired alcohol **59** as a light-yellow oil as a mixture of regioisomers (30% conversion, *r.r.* 60:40). Owing to the low conversion, isolation was omitted.

Screening Experiment according to Table 7, Entry 1:

According to **GP VIII**, **[Ti]-17** (29.0 mg, 24.5 *µ*mol, 5 mol%), BnMgBr (0.67M in Et_2O, 80 *µ*L, 53.6 *µ*mol, 11 mol%), $PhSiH_3$ (0.81M in THF, 20 *µ*L, 16.2 *µ*mol, 3.0 mol%), PMHS (0.12 mL, 2.01 mmol, 3.97 eq.) and epoxide **65** (94.3 mg, 506 *µ*mol, 1.00 eq.) were mixed in THF:1,4-dioxane (1:1, 4 mL) and stirred for 48 h at room temperature. Desilylation, followed by work-up and flash chromatography (SiO_2, PE:Et_2O 4:6) yielded the desired alcohol **59** as a light-yellow oil as a mixture of regioisomers (70.4 mg, 374 *µ*mol, 74%, *r.r.* 88:12).

^{1}H-NMR (500 MHz, $CDCl_3$) *δ*/ppm: 3.77 (t, *J* = 5.5 Hz, 2H), 3.61 (t, *J* = 5.7 Hz, 2H), 3.42 (t, *J* = 6.7 Hz, 2H), 1.83 (p, *J* = 5.6 Hz, 2H), 1.55 (dt, *J* = 8.0, 6.5 Hz, 2H), 1.35–1.22 (m, 10H), 0.87 (t, *J* = 6.9 Hz, 3H). The regioisomeric ratio was determined by comparison of CH_2- and CH_3-signals at 3.77 (*major*), and 1.14 ppm (*minor*).

^{13}C-NMR (126 MHz, $CDCl_3$) *δ*/ppm: 71.7, 70.6, 62.6, 32.1, 32.0, 29.8, 29.6, 29.4, 26.3, 22.8, 14.2.

The analytical data are in good agreement with the literature.[230]

5.9.17 3-Phenoxypropan-1-ol (60)

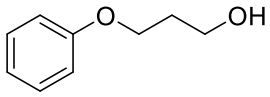

Screening Experiment according to Table 7, Entry 2:

According to **GP VIII**, **[Ti]-1** (8.0 mg, 32.1 *µ*mol, 6.4 mol%), BnMgBr (0.82M in Et_2O, 70 *µ*L, 55.0 *µ*mol, 11 mol%), $PhSiH_3$ (0.81M in THF, 20 *µ*L, 16.2 *µ*mol, 3.0 mol%), PMHS (0.12 mL, 2.01 mmol, 4.07 eq.) and epoxide **66** (74.1 mg, 493 *µ*mol, 1.00 eq.) were mixed in THF:1,4-dioxane (1:1, 4 mL) and stirred for 72 h at room temperature. Desilylation, followed by work-up yielded the desired alcohol **60** as a light-yellow oil as a mixture of regioisomers (100% conversion, *r.r.* 60:40). The isolated yield was not determined, as the reaction was performed for screening purposes only.

Screening Experiment according to Table 7, Entry 2:

According to **GP VIII**, **[Ti]-17** (28.9 mg, 24.4 *µ*mol, 5 mol%), BnMgBr (1.03M in Et_2O, 50 *µ*L, 51.5 *µ*mol, 10 mol%), $PhSiH_3$ (0.81M in THF, 20 *µ*L, 16.2 *µ*mol, 3.0 mol%), PMHS (0.12 mL, 2.01 mmol, 4.07 eq.) and epoxide **66** (74.0 mg, 493 *µ*mol, 1.00 eq.) were mixed in THF:1,4-dioxane (1:1, 4 mL) and stirred for 48 h at room temperature. Desilylation, followed by work-up and flash chromatography (SiO_2, PE:Et_2O 4:6) yielded the desired alcohol **60** as a light-yellow oil as a mixture of regioisomers (53.3 mg, 350 *µ*mol, 71%, *r.r.* 88:12).

^{1}H-NMR (500 MHz, $CDCl_3$) *δ*/ppm: 7.31–7.27 (m, 2H), 6.98–6.90 (m, 3H), 4.13 (t, *J* = 5.9 Hz, 2H), 3.87 (t, *J* = 5.9 Hz, 2H), 2.08–2.02 (m, 2H).
The regioisomeric ratio was determined by comparison of CH_2- and CH_3-signals at 4.13 (*major*), and 1.29 ppm (*minor*).

^{13}C-NMR (126 MHz, $CDCl_3$) *δ*/ppm: 158.8, 129.6, 121.0, 114.6, 65.8, 60.7, 32.1.

The analytical data are in good agreement with the literature.[231]

5.9.18 4,8-Dimethylnon-7-en-1-ol (61)

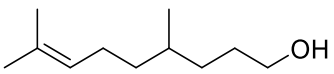

According to **GP VIII**, **[Ti]-17** (29.2 mg, 24.6 *µ*mol, 5 mol%), BnMgBr (1.03M in Et_2O, 50 *µ*L, 51.5 *µ*mol, 10 mol%), $PhSiH_3$ (0.81M in THF, 20 *µ*L, 16.2 *µ*mol, 3.0 mol%), PMHS (0.12 mL, 2.01 mmol, 3.97 eq.) and epoxide **71** (85.2 mg, 506 *µ*mol, 1.00 eq.) were mixed in THF:1,4-dioxane (1:1, 4 mL) and stirred for 48 h at room temperature. Desilylation, followed by work-

up and flash chromatography (SiO_2, PE:Et_2O 7:3) yielded the desired alcohol **61** as a light-yellow oil as a mixture of regioisomers (66.4 mg, 390 *µ*mol, 77%, *r.r.* >99:1).

^{1}H-NMR (500 MHz, $CDCl_3$) *δ*/ppm: 5.09 (ddq, *J* = 8.6, 5.7, 1.5 Hz, 1H), 3.63 (t, *J* = 6.7 Hz, 2H), 2.05–1.90 (m, 2H), 1.68 (q, *J* = 1.3 Hz, 3H), 1.60 (d, *J* = 1.3 Hz, 3H), 1.59–1.30 (m, 5H), 1.20–1.11 (m, 2H), 0.89 (d, *J* = 6.5 Hz, 3H).
The regioisomeric ratio was determined by comparison of CH_2- and CH-signals at 3.63 (*major*), and 4.00–3.82ppm (*minor*).

^{13}C-NMR (126 MHz, $CDCl_3$) *δ*/ppm: 131.3, 125.0, 63.6, 37.2, 33.0, 32.4, 30.5, 25.9, 25.7, 19.7, 17.8.

The analytical data are in good agreement with the literature.[232]

5.9.19 Undecane-1,11-diol (56)

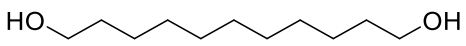

According to **GP VII**, **[Ti]-17** (29.1 mg, 24.5 *µ*mol, 5 mol%), BnMgBr (0.67M in Et_2O, 80 *µ*L, 53.6 *µ*mol, 11 mol%), epoxide **69** (95.0 mg, 510 *µ*mol, 1.00 eq.), $PhSiH_3$ (0.81M in THF, 20 *µ*L, 16.2 *µ*mol, 3 mol%) and PMHS (0.24 mL, 4.02 mmol, 7.87 eq.) were mixed in THF:1,4-dioxane (1:1, 4 mL) and stirred for 48 h. After work-up and flash chromatography (SiO_2, 100% Et_2O), the desired alcohol **56** was obtained as a light-yellow oil as a mixture of regioisomers (70.1 mg, 372 *µ*mol, 73%, *r.r.* 92:8).

^{1}H-NMR (500 MHz, $CDCl_3$) *δ*/ppm: 3.64 (t, *J* = 6.6 Hz, 4H), 1.56 (dq, *J* = 8.0, 6.5 Hz, 4H), 1.38–1.24 (m, 14H).

The regioisomeric ratio was determined by comparison of CH_2- and CH_3-signals at 3.64 (*major*), and 1.18 ppm (*minor*).

^{13}C-NMR (126 MHz, $CDCl_3$) *δ*/ppm: 63.1, 32.8, 29.6, 29.5, 29.4, 25.7.

The analytical data are in good agreement with the literature.[233]

5.9.20 11-((*tert*-Butyldimethylsilyl)oxy)undecan-1-ol (57)

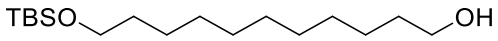

Screening Experiment according to Table 6, Entry 4:

According to **GP VIII**, **[Ti]-3** (9.6 mg, 26.6 *µ*mol, 5 mol%), BnMgBr (1.03M in Et_2O, 50 *µ*L, 51.5 *µ*mol, 10 mol%), $PhSiH_3$ (0.81M in THF, 20 *µ*L, 16.2 *µ*mol, 3.0 mol%), PMHS (0.12 mL, 2.01 mmol, 4.02 eq.) and epoxide **52** (150 mg, 499 *µ*mol, 1.00 eq.) were mixed in THF:1,4-dioxane (1:1, 4 mL) and stirred for 24 h at room temperature. Desilylation, followed by work-up and flash chromatography (SiO_2, PE:Et_2O 4:6) yielded the desired alcohol **57** as a light-yellow oil as a mixture of regioisomers (81.4 mg, 269 *µ*mol, 54%, *r.r.* 83:17).

Screening Experiment according to Table 6, Entry 4:

According to **GP VIII**, **[Ti]-4** (10.6 mg, 27.0 *µ*mol, 5 mol%), BnMgBr (1.03M in Et_2O, 50 *µ*L, 51.5 *µ*mol, 10 mol%), $PhSiH_3$ (0.81M in THF, 20 *µ*L, 16.2 *µ*mol, 3.0 mol%), PMHS (0.12 mL, 2.01 mmol, 3.97 eq.) and epoxide **52** (152 mg, 506 *µ*mol, 1.00 eq.) were mixed in THF:1,4-dioxane (1:1, 4 mL) and stirred for 24 h at room temperature. Desilylation, followed by work-up and flash chromatography (SiO_2, PE:Et_2O 4:6) yielded the desired alcohol **57** as a light-yellow oil as a mixture of regioisomers (88.6 mg, 293 *µ*mol, 58%, *r.r.* 89:11).

Screening Experiment according to Table 6, Entry 4:

According to **GP VIII**, **[Ti]-17** (30.6 mg, 25.8 *µ*mol, 5 mol%), BnMgBr (1.03M in Et_2O, 50 *µ*L, 51.5 *µ*mol, 10 mol%), $PhSiH_3$ (0.81M in THF, 20 *µ*L, 16.2 *µ*mol, 3.0 mol%), PMHS (0.12 mL, 2.01 mmol, 4.00 eq.) and epoxide **52** (151 mg, 502 *µ*mol, 1.00 eq.) were mixed in THF:1,4-dioxane (1:1, 4 mL) and stirred for 48 h at room temperature. Desilylation, followed by work-up and flash chromatography (SiO_2, PE:Et_2O 4:6) yielded the desired alcohol **57** as a light-yellow oil as a mixture of regioisomers (108 mg, 356 *µ*mol, 71%, *r.r.* 94:6).

^{1}H-NMR (500 MHz, $CDCl_3$) *δ*/ppm: 3.64 (t, *J* = 6.6 Hz, 2H), 3.59 (t, *J* = 6.7 Hz, 2H), 1.60–1.47 (m, 4H), 1.38–1.24 (m, 14H), 0.89 (s, 9H), 0.05 (s, 6H).
The regioisomeric ratio was determined by comparison of CH_2- and CH_3-signals at 3.64 (*major*), and 1.18 ppm (*minor*).

^{13}C-NMR (126 MHz, $CDCl_3$) *δ*/ppm: 63.5, 63.2, 33.0, 33.0, 29.8, 29.7, 29.7, 29.6, 29.6, 26.1, 25.9, 25.9, 18.5, –5.1.

The analytical data are in good agreement with the literature.[234]

5.9.21 11-((4-Methoxybenzyl)oxy)undecan-1-ol (58)

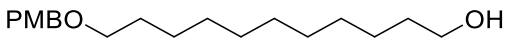

According to **GP VIII**, **[Ti]-17** (28.0 mg, 23.6 µmol, 5 mol%), BnMgBr (1.03M in Et_2O, 50 µL, 51.5 µmol, 11 mol%), $PhSiH_3$ (0.81M in THF, 20 µL, 16.2 µmol, 3.0 mol%), PMHS (0.12 mL, 2.01 mmol, 4.05 eq.) and epoxide **70** (152 mg, 496 µmol, 1.00 eq.) were mixed in THF:1,4-dioxane (1:1, 4 mL) and stirred for 48 h at room temperature. Desilylation, followed by work-up and flash chromatography (SiO_2, PE:Et_2O 4:6) yielded the desired alcohol **58** as a light-yellow oil as a mixture of regioisomers (96.6 mg, 313 µmol, 63%, *r.r.* 93:7).

^{1}H-NMR (500 MHz, $CDCl_3$) *δ*/ppm: 7.29–7.24 (m, 2H), 6.90–6.86 (m, 2H), 4.43 (s, 2H), 3.80 (s, 3H), 3.64 (td, *J* = 6.7, 2.0 Hz, 2H), 3.43 (t, *J* = 6.7 Hz, 2H), 1.57 (ddt, *J* = 14.6, 8.5, 6.6 Hz, 4H), 1.39–1.24 (m, 14H).
The regioisomeric ratio was determined by comparison of CH_2- and CH_3-signals at 3.43 (*major*), and 1.18 ppm (*minor*).

^{13}C-NMR (126 MHz, $CDCl_3$) *δ*/ppm: 159.2, 131.0, 129.4, 113.9, 72.7, 70.4, 63.2, 55.4, 33.0, 29.9, 29.7, 29.7, 29.6, 29.6, 26.3, 25.9.

The analytical data are in good agreement with the literature.[235]

5.9.22 4-Phenylbutan-1-ol (92)

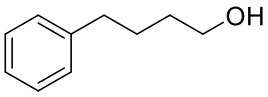

According to **GP IX**, **[Ti]-1** (6.10 mg, 24.5 µmol, 5 mol%), BnMgBr (0.75M in Et_2O, 70 µL, 52.5 µmol, 11 mol%), $PhSiH_3$ (90 µL, 730 µmol, 1.50 eq.) and oxetane **85** (77.1 mg, 520 µmol, 1.04 eq.) were mixed in THF (4 mL) and stirred for 24 h under reflux conditions. Desilylation, followed by work-up and purification by flash chromatography (SiO_2, *n*-Pentane:Et_2O 6:4) yielded the desired alcohol **92** as a yellow oil as a mixture of regioisomers (67.2 mg, 447 µmol, 86%, *r.r.* 98:2).

^{1}H NMR (700 MHz, $CDCl_3$) *δ*/ppm: 7.30–7.27 (m, 2H), 7.20–7.17 (m, 3H), 3.66 (t, *J* = 6.6 Hz, 2H), 2.65 (t, *J* = 7.7 Hz, 2H), 1.74–1.68 (m, 2H), 1.64–1.59 (m, 2H).
The regioisomeric ratio was determined by comparison of CH_2- and CH_3-signals in ^{1}H-NMR at 3.66 (*major*) and 1.01 ppm (*minor*).

^{13}C NMR (176 MHz, $CDCl_3$) δ/ppm: 142.5, 128.5, 128.4, 125.9, 63.0, 35.8, 32.5, 27.7.

The analytical data are consistent with the literature.[236,237]

5.9.23 4-(Naphthalen-1-yl)butan-1-ol (93)

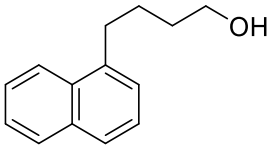

According to **GP IX**, **[Ti]-1** (11.5 mg, 46.2 *µ*mol, 9 mol%), BnMgBr (0.75M in Et_2O, 150 *µ*L, 113 *µ*mol, 22 mol%), $PhSiH_3$ (90 *µ*L, 730 *µ*mol, 1.50 eq.) and oxetane **86** (102 mg, 513 *µ*mol, 1.03 eq.) were mixed in THF (4 mL) and stirred for 24 h at room temperature. Desilylation, followed by work-up and purification *via* flash chromatography (SiO_2, *n*-Pentane:Et_2O 6:4) yielded the desired alcohol **93** as a light yellow oil as a mixture of regioisomers (69.1 mg, 345 *µ*mol, 69%, *r.r.* 98:2).

^{1}H NMR (400 MHz, $CDCl_3$) δ/ppm: 8.05 (dq, *J* = 8.6, 1.0 Hz, 1H), 7.90–7.82 (m, 1H), 7.72 (dt, *J* = 8.1, 1.1 Hz, 1H), 7.50 (dddd, *J* = 16.0, 8.1, 6.8, 1.5 Hz, 2H), 7.40 (dd, *J* = 8.1, 7.0 Hz, 1H), 7.33 (dd, *J* = 7.0, 1.3 Hz, 1H), 3.69 (t, *J* = 6.5 Hz, 2H), 3.16–3.08 (m, 2H), 1.91–1.79 (m, 2H), 1.78–1.65 (m, 2H).

The regioisomeric ratio was determined by comparison of CH_2- and CH_3-signals in ^{1}H-NMR at 3.69 (*major*) and 1.01 ppm (*minor*). The minor isomer, which was used as a reference, is the opening side product of **85** due to structural similarity.

^{13}C NMR (126 MHz, $CDCl_3$) δ/ppm: 138.5, 134.0, 132.0, 128.9, 126.7, 126.1, 125.9, 125.6, 125.5, 123.9, 63.0, 32.9, 27.0.

The analytical data are consistent with the literature.[237,238]

5.9.24 3-Methyl-5-phenylpentan-1-ol (96)

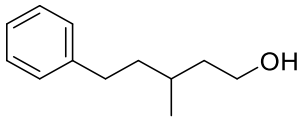

Screening Experiment according to Scheme 82:

In a slight variation of **GP IX**, **[Ti]-1** (6.50 mg, 26.1 *µ*mol, 1 mol%), BnMgBr (0.70 M in Et_2O, 80 *µ*L, 56.0 *µ*mol, 2.1 mol%), $PhSiH_3$ (0.47 mL, 3.81 mmol, 1.50 eq.) and oxetane **89** (444 mg, 2.52 mmol, 1.00 eq.) were mixed in THF (10 mL) and stirred for 24 h under reflux conditions. Desilylation, followed by work-up and purification *via* flash chromatography (SiO_2, *n*-Pentane:Et_2O 7:3) yielded the desired alcohol **96** as a light yellow oil as a mixture of regioisomers (379 mg, 2.13 mmol, 85%, *r.r.* >99:1).

Screening Experiment according to Scheme 82:

According to **GP IX**, **[Ti]-1** (11.9 mg, 47.8 *µ*mol, 10 mol%), BnMgBr (0.85 M in Et_2O, 130 *µ*L, 111 *µ*mol, 22 mol%), $PhSiH_3$ (90 *µ*L, 730 *µ*mol, 1.50 eq.) and oxetane **89** (89.2 mg, 506 *µ*mol, 1.01 eq.) were mixed in THF (4 mL) and stirred for 24 h at room temperature. Desilylation, followed by work-up and purification by flash chromatography (SiO_2, *n*-Pentane:Et_2O 7:3) yielded the desired alcohol **96** as a light yellow oil as a mixture of regioisomers (76.3 mg, 428 *µ*mol, 86%, *r.r.* >99:1).

Screening Experiment according to Scheme 83:

According to **GP X**, **[Ti]-1** (4.3 mg, 17.3 *µ*mol, 1 mol%), BnMgBr (0.77 M in Et_2O, 50 *µ*L, 38.5 *µ*mol, 3 mol%), $PhSiH_3$ (0.81M in THF, 50 *µ*L, 40.5 *µ*mol, 3 mol%), PMHS (0.37 mL, 6.16 mmol, 4.53 eq.) and oxetane **89** (240 mg, 1.36 mmol, 1.00 eq.) were mixed in THF (5.80 mL) and stirred for 24 h under reflux conditions. Desilylation, followed by work-up and flash chromatography (SiO_2, PE:Et_2O 6:4) yielded the desired alcohol **96** as a light-yellow oil as a mixture of regioisomers (73.1 mg, 365 *µ*mol, 73%, *r.r.* 99:1).

^{1}H NMR (400 MHz, $CDCl_3$) *δ*/ppm: 7.30–7.25 (m, 2H), 7.19 (d, *J* = 7.3 Hz, 3H), 3.77–3.62 (m, 2H), 2.74–2.53 (m, 2H), 1.73–1.55 (m, 3H), 1.55–1.38 (m, 2H), 0.98 (d, *J* = 6.2 Hz, 3H).
The regioisomeric ratio was determined by comparison of CH_2- and CH_3-signals in ^{1}H-NMR at 3.77–3.62 (*major*) and 0.93 ppm (*minor*).

^{13}C NMR (126 MHz, $CDCl_3$) *δ*/ppm: 143.0, 128.5, 128.4, 125.8, 61.3, 40.0, 39.1, 33.5, 29.4, 19.7.

The analytical data are consistent with the literature.[101,239]

5.10 Miscellaneous Reactions

5.10.1 Tetradec-1-en-4-ol (75)

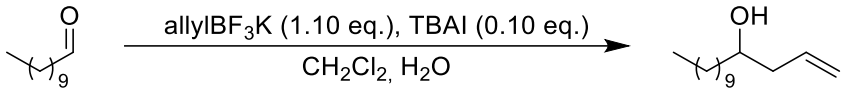

The following procedure is inspired by a method reported by *Thadani et al*.[191] In a round-bottom flask, undecanal (4.10 mL, 20.0 mmol, 1.00 eq.) and tetra-*n*-butylammonium iodide (739 mg, 2.00 mmol, 0.10 eq.) were dissolved in CH_2Cl_2 (60 mL). Subsequently, H_2O (60 mL) and potassium allyltrifluoroborate (3.26 g, 22.0 mmol, 1.10 eq.) were added. The biphasic reaction mixture was vigorously stirred for 3 hours at room temperature. Upon completion, the layers were separated and the aqueous layer was extracted three times with CH_2Cl_2. The combined organic layers were washed with brine, dried over magnesium sulfate and the solvent was removed under reduced pressure. After purification by column chromatography (SiO_2, *n*-Pentane:Et_2O 8:2) the allyl alcohol **75** (3.87 g, 18.2 mmol, 91%) was obtained as a colorless oil.

^{1}H NMR (400 MHz, $CDCl_3$) *δ*/ppm: 5.91–5.76 (m, 1H), 5.18–5.09 (m, 2H), 3.64 (dq, *J* = 9.2, 3.9 Hz, 1H), 2.30 (dddd, *J* = 13.8, 6.8, 3.5, 1.4 Hz, 1H), 2.13 (dt, *J* = 14.6, 7.9 Hz, 1H), 1.75–1.51 (m, 2H), 1.27 (d, *J* = 8.2 Hz, 16H), 0.88 (t, *J* = 6.7 Hz, 3H).

^{13}C NMR (126 MHz, $CDCl_3$) *δ*/ppm: 134.8, 118.0, 70.8, 41.8, 36.5, 32.0, 29.6, 29.5, 29.3, 25.7, 22.1, 14.1.

The analytical data are consistent with the literature.[240]

5.10.2 Tridecane-1,3-diol (76)

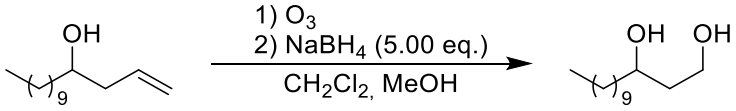

In a round-bottom three-necked flask, allylic alcohol **75** (2.12 g, 10.0 mmol, 1.00 eq.) was dissolved in a mixture of CH_2Cl_2 (140 mL) and methanol (10 mL). Subsequently, an ozone stream generated with oxygen from the ozone generator was bubbled into the reaction mixture at –78 °C under vigorous stirring. The process was carried out until the color of the solution turned deep blue. Then, $NaBH_4$ (1.89 g, 50.0 mmol, 5.00 eq.) was added in one portion at -78 °C. The cooling was removed and the reaction mixture was stirred overnight at room temperature. Afterwards the mixture was quenched with a saturated ammonium chloride solution. Subsequently, the layers were separated and the aqueous layer was extracted three

times with CH_2Cl_2. The combined organic layers were washed with brine, dried over sodium sulfate and the solvent was removed under reduced pressure. After purification by column chromatography (SiO_2, *n*-Pentane:Et_2O 1:1 to 0:100) the diol **76** (1.52 g, 8.08 mmol, 81%) was obtained as colorless solid.

^{1}H NMR (500 MHz, $CDCl_3$) *δ*/ppm: 4.11–3.59 (m, 3H), 1.90–1.39 (m, 4H), 1.27 (d, *J* = 6.7 Hz, 16H), 0.88 (t, *J* = 6.9 Hz, 3H).

^{13}C NMR (126 MHz, $CDCl_3$) *δ*/ppm: 72.5, 62.1, 38.5, 38.0, 37.1, 32.1, 29.8, 29.7, 29.5, 25.7, 25.2, 22.8, 14.2.

IR $\tilde{\nu}$/cm^{-1}: 3372, 2921, 2852, 1487, 1419, 1378, 1331, 1280, 1157, 1156, 721, 691, 665.

HRMS (APCI): exp. 217.2162

calc. 217.2167 ($C_{13}H_{29}O_2^+$ = $[M+H]^+$)

6. Appendix

6.1 List of Schemes, Figures, and Tables

6.1.1 Schemes

6.1.2 Figures

6.1.3 Tables

6.2 Abbreviations

σ-CAM	sigma bond metathesis
Ac	acetyl
Ad	adamantyl
AML	acute myeloid leukemia
APCI	atmospheric-pressure chemical ionization
aq	aqueous
Ar	aryl
BDE	bond dissociation energy
Bn	benzyl
Bu	butyl
calc	calculated
CH	cyclohexane
CHAT	catalytic hydrogen atom transfer
CHD	cyclohexadiene
Coll	2,4,6-collidine
Cp	cyclopentadienyl
CSA	camphor sulfonic acid
Cy	cyclohexyl
d	doublet
d.r.	diastereomeric ratio
DAT	deuterium atom transfer
DET	diethyl tartrate
DFT	density functional theory
DG	directing group
DI	deuterium incorporation
DIPAMP	ethylenebis[(2-methoxyphenyl)phenylphosphine]
DMF	dimethylformamide
DMM	dimethoxymethane
DMSO	dimethylsulfoxide
e.g.	for example (Latin: exempli gratia)
e.r.	enantiomeric ratio
E_a	activation energy
EA	ethyl acetate

EDTA	ethylenediaminetetraacetic acid
ee	enantiomeric excess
EI	electron ionization
EPR	electron paramagnetic resonance
eq	equivalent(s)
ESI	electrospray ionization
Et	ethyl
ET	electron transfer
et al.	et alia (= and others)
exp	experimental
g	gram
gem	geminal
GP	general procedure
h	hour
HAT	hydrogen atom transfer
hept	heptet
HPLC	high-performance liquid chromatography
HRMS	high-resolution mass spectrometry
HSAB	hard and soft acids and bases
Hz	hertz
*i*Pr	*iso*-propyl
IR	infrared
K	Kelvin
kcal	kilocalories
kg	kilogram
LA	*Lewis* acid
L-Dopa	3,4-dihydroxy-L-phenylalanine
m	meta
m	multiplet
m.p.	melting point
*m*CPBA	*meta*-chloroperoxybenzoic acid
Me	methyl
mg	milligram
MHz	megahertz

min	minute(s)
MPLC	medium-pressure liquid chromatography
MS	multiple sclerosis
MTPA	*α*-methoxy-*α*-trifluoromethylphenylacetic acid
NMR	nuclear magnetic resonance
o	ortho
ox.	oxidative
p	*para*
p	pentet
PCC	pyridinium chlorochromate
PE	petroleum ether
pH	potential of hydrogen
Ph	phenyl
Piv	pivaloyl
PMB	*para*-methoxybenzyl
PMHS	polymethylhydrosiloxane
ppm	parts per million
PPNO	phenylpyridine-*N*-oxide
Pr	propyl
py	pyridine
q	quartet
r.r.	regioisomeric ratio
r.t.	room temperature
rac	racemic
s	singlet
sat	saturated
SET	single electron transfer
sext	sextet
SLES	sodium lauryl ether sulfate
SLS	sodium lauryl sulfate
S_N2	second-order nucleophilic substitution
t	triplet
TBA	tetrabutyl ammonium
TBDMS	*tert*-butyldimethylsilyl

TBS	*tert*-butyldimethylsilyl
*t*Bu	*tert*-butyl
TES	triethylsilyl
Tf	triflyl
THF	tetrahydrofuran
TIPS	triisopropylsilyl
TLC	thin-layer chromatography
TMS	trimethylsilyl
TS	transition state
UV	ultraviolet
vs	versus

6.3 References

[1] I. Zohar, N. Alperson-Afil, N. Goren-Inbar, M. Prévost, T. Tütken, G. Sisma-Ventura, I. Hershkovitz, J. Najorka, *Nat. Ecol. Evol.* **2022**, *6*, 2016–2028.

[2] A. Fletcher, D. Baird, M. Spataro, A. Fairbairn, *Cambridge Archaeological Journal* **2017**, *27*, 351–369.

[3] Z. Lin, J. M. Natoli, J. C. Picuri, S. E. Shaw, W. J. Bowyer, *J. Archaeol. Sci. Rep.* **2021**, *39*, 103134.

[4] M. Radivojević, B. W. Roberts, *J. World Prehist.* **2021**, *34*, 195–278.

[5] S. Seetharaman, *Fundamentals of Metallurgy*, Woodhead Publishing, Cambridge, **2005**.

[6] Z. A. Szydło, *Pure Appl. Chem.* **2022**, *94*, 869–888.

[7] American Chemical Society International Historic Chemical Landmarks, "Antoine-Laurent Lavoisier: The Chemical Revolution", available at http://www.acs.org/content/acs/en/education/whatischemistry/landmarks/lavoisier.html, (accessed: 16.12.2025).

[8] Y. Yang, K. Raipala, L. Holappa in *Treatise on Process Metallurgy* (Editor S. Seetharaman, R. Guthrie, A. McLean, S. Seetharaman, H. Y. Sohn), Elsevier, Amsterdam, **2014**, 2–88.

[9] M. S. Kenevisi, F. S. Gobber, P. Fino, M. Lombardi, F. Bondioli, S. Biamino, D. Ugues, *Mater. Des.* **2025**, *258*, 114639.

[10] M. C. Moynihan, J. M. Allwood, *Proc. R. Soc. A* **2014**, *470*, 20140170.

[11] J. Galán, L. Samek, P. Verleysen, K. Verbeken, Y. Houbaert, *Rev. Metal.* **2012**, *48*, 118–131.

[12] Z. Gholami, F. Gholami, Z. Tišler, M. Vakili, *Energies* **2021**, *14*, 8190.

[13] Z. Wang in *Comprehensive Organic Name Reactions and Reagents*, Wiley, Hoboken, NJ, **2010**, 3134–3138.

[14] D. Bajpai, V. K. Tyagi, *J. Oleo Sci.* **2007**, *56*, 327–340.

[15] C. Kennes, *Front. Environ. Eng.* **2023**, *2*, 1–4.

[16] C. K. Swain, *Discover Environ.* **2024**, *2*, 1–14.

[17] A. Ivanković, *Int. J. Sustainable Green Energy* **2017**, *6*, 39.

[18] P. T. Anastas, J. C. Warner, *Green Chemistry,* 1. Ed., Oxford University Press, Oxford, **2000**.

[19] B. H. Kreps, *Am. J. Econ. Sociol.* **2020**, *79*, 695–717.

[20] V. Pace, P. Hoyos, L. Castoldi, P. Domínguez de María, A. R. Alcántara, *ChemSusChem* **2012**, *5*, 1369–1379.

[21] G. Ertl, H.-J. Freund, *Phys. Today* **1999**, *52*, 32–38.

[22] R. Tesser, E. Santacesaria in *The Chemical Reactor from Laboratory to Industrial Plant*, Springer Nature Switzerland, Cham, **2025**, 133–211.

[23] N. Pal, A. Bhaumik, *RSC Adv.* **2015**, *5*, 24363–24391.

[24] A. Z. Fadhel, P. Pollet, C. L. Liotta, C. A. Eckert, *Molecules* **2010**, *15*, 8400–8424.

[25] R. A. Sheldon, I. Arends, U. Hanefeld, *Green Chemistry and Catalysis*, Wiley-VCH, Weinheim, **2008**.

[26] K. Kaneda, T. Mizugaki, T. Mitsudome, *Encyclopedia of Catalysis*, John Wiley & Sons, Hoboken, NJ, **2010**.

[27] K. Cavell, S. Golunski, D. Miller, *Platinum Met. Rev.* **2010**, *54*, 233–238.

[28] M.-W. Ha, S.-M. Paek, *Molecules* **2021**, *26*, 4792.

[29] A. C. Muresan, *Ann. "Dunarea Jos" Univ. Galati Fascicle IX* **2018**, *41*, 30–34.

[30] J. Humphreys, R. Lan, S. Tao, *Adv. Energy Sustainability Res.* **2021**, *2*, 2000043.

[31] V. Palma, C. Ruocco, M. Cortese, S. Renda, E. Meloni, G. Festa, M. Martino, *Metals* **2020**, *10*, 866.

[32] V. V. Gande, N. C. Kani, I. Goyal, R. Chauhan, Y. Qi, S. A. Olusegun, J. A. Gauthier, M. R. Singh, *EES Catal.* **2025**, *3*, 883–920.

[33] K. H. R. Rouwenhorst, F. Jardali, A. Bogaerts, L. Lefferts, *Energy Environ. Sci.* **2021**, *14*, 2520–2534.

[34] Y. G. Shelke, A. Yashmeen, A. V. A. Gholap, S. J. Gharpure, A. R. Kapdi, *Chem. Asian J.* **2018**, *13*, 2991–3013.

[35] W. H. Brooks, W. C. Guida, K. G. Daniel, *Curr. Top. Med. Chem.* **2011**, *11*, 760–770.

[36] W. S. Knowles, *J. Chem. Educ.* **1986**, *63*, 222.

[37] P. Tang, H. Wang, W. Zhang, F.-E. Chen, *Green Synth. Catal.* **2020**, *1*, 26–41.

[38] A. Klein, B. Goldfuss, J.-I. van der Vlugt, *Inorganics* **2018**, *6*, 19.

[39] D. R. Hartline, K. Meyer, *JACS Au* **2021**, *1*, 698–709.

[40] T. Chu, G. I. Nikonov, *Chem. Rev.* **2018**, *118*, 3608–3680.

[41] J. A. Osborn, F. H. Jardine, J. F. Young, G. Wilkinson, *J. Chem. Soc. A* **1966**, 1711–1732.

[42] H. Takaya, T. Ohta, N. Sayo, H. Kumobayashi, S. Akutagawa, S. Inoue, I. Kasahara, R. Noyori, *J. Am. Chem. Soc.* **1987**, *109*, 1596–1597.

[43] T. Ohkuma, M. Koizumi, H. Doucet, T. Pham, M. Kozawa, K. Murata, E. Katayama, T. Yokozawa, T. Ikariya, R. Noyori, *J. Am. Chem. Soc.* **1998**, *120*, 13529–13530.

[44] R. Noyori, M. Kitamura, T. Ohkuma, *Proc. Natl. Acad. Sci. U.S.A.* **2004**, *101*, 5356–5362.

[45] G. Helmchen, *Chem. Eur. J.* **2023**, *29*, e202301488.

[46] S. Munnuri, A. M. Adebesin, M. P. Paudyal, M. Yousufuddin, A. Dalipe, J. R. Falck, *J. Am. Chem. Soc.* **2017**, *139*, 18288–18294.

[47] S. Krehl, D. Geißler, S. Hauke, O. Kunz, L. Staude, B. Schmidt, *Beilstein J. Org. Chem.* **2010**, *6*, 1188–1198.

[48] P. G. Andersson, I. J. Munslow, *Modern Reduction Methods*, Wiley-VCH, Weinheim, **2008**.

[49] P. Devendar, R.-Y. Qu, W.-M. Kang, B. He, G.-F. Yang, *J. Agric. Food Chem.* **2018**, *66*, 8914–8934.

[50] S. Wang, X. Li, C. Lai, Y. Zhang, X. Lin, S. Ding, *RSC Adv.* **2024**, *14*, 30566–30581.

[51] C. S. Horbaczewskyj, I. J. S. Fairlamb, *Org. Process Res. Dev.* **2022**, *26*, 2240–2269.

[52] R. J. M. Gebbink, M.-E. Moret, *Non-Noble Metal Catalysis*, Wiley-VCH, Weinheim, **2019**.

[53] "Abundance in Earth's Crust of the elements", available at https://periodictable.com/Properties/A/CrustAbundance.html, (accessed: 14.11.2025).

[54] M. Najafizadeh, S. Yazdi, M. Bozorg, M. Ghasempour-Mouziraji, M. Hosseinzadeh, M. Zarrabian, P. Cavaliere, *J. Alloys Compd.* **2024**, *3*, 100019.

[55] A. J. Haider, Z. N. Jameel, I. H. Al-Hussaini, *Energy Procedia* **2019**, *157*, 17–29.

[56] S. L. Schneider, H. W. Lim, *Photodermatol. Photoimmunol. Photomed.* **2019**, *35*, 442–446.

[57] J. R. de Laeter, J. K. Böhlke, P. de Bièvre, H. Hidaka, H. S. Peiser, K. J. R. Rosman, P. D. P. Taylor, *Pure Appl. Chem.* **2003**, *75*, 683–800.

[58] A. Klaue, M. Kruck, N. Friederichs, F. Bertola, H. Wu, M. Morbidelli, *Ind. Eng. Chem. Res.* **2019**, *58*, 886–896.

[59] A. Biffis, P. Centomo, A. Del Zotto, M. Zecca, *Chem. Rev.* **2018**, *118*, 2249–2295.

[60] C. Daniel, N. Koga, J. Han, X. Y. Fu, K. Morokuma, *J. Am. Chem. Soc.* **1988**, *110*, 3773–3787.

[61] X. Wu, Y. Chang, S. Lin, *Chem* **2022**, *8*, 1805–1821.

[62] A. Shamiri, M. H. Chakrabarti, S. Jahan, M. A. Hussain, W. Kaminsky, P. V. Aravind, W. A. Yehye, *Materials* **2014**, *7*, 5069–5108.

[63] L. L. Böhm, *Angew. Chem. Int. Ed.* **2003**, *42*, 5010–5030.

[64] N. Bahri-Laleh, A. Correa, S. Mehdipour-Ataei, H. Arabi, M. N. Haghighi, G. Zohuri, L. Cavallo, *Macromolecules* **2011**, *44*, 778–783.

[65] P. N. Khanam, M. A. A. AlMaadeed, *Adv. Manuf. Polym. Compos. Sci.* **2015**, *1*, 63–79.

[66] N. Chandimali, S. G. Bak, E. H. Park, H.-J. Lim, Y.-S. Won, E.-K. Kim, S.-I. Park, S. J. Lee, *Cell Death Discovery* **2025**, *11*, 19.

[67] A. Gansäuer, H. Bluhm, *Chem. Rev.* **2000**, *100*, 2771–2788.

[68] A. Gansäuer, *Synlett* **1998**, *1998*, 801–809.

[69] A. Gansäuer, M. Moschioni, D. Bauer, *Eur. J. Org. Chem.* **1998**, *1998*, 1923–1927.

[70] A. Gansäuer, H. Bluhm, M. Pierobon, *J. Am. Chem. Soc.* **1998**, *120*, 12849–12859.

[71] T. V. RajanBabu, W. A. Nugent, *J. Am. Chem. Soc.* **1994**, *116*, 986–997.

[72] G. L. Cunningham, A. W. Boyd, R. J. Myers, W. D. Gwinn, W. I. Le Van, *J. Chem. Phys.* **1951**, *19*, 676–685.

[73] G. L. Cunningham, A. W. Boyd, W. D. Gwinn, W. I. LeVan, *J. Chem. Phys.* **1949**, *17*, 211–212.

[74] J. A. Bull, R. A. Croft, O. A. Davis, R. Doran, K. F. Morgan, *Chem. Rev.* **2016**, *116*, 12150–12233.

[75] S. Höthker, A. Gansäuer, *Global Challenges* **2023**, *7*, 2200240.

[76] N. N. Schwartz, J. H. Blumbergs, *J. Org. Chem.* **1964**, *29*, 1976–1979.

[77] H. Hussain, A. Al-Harrasi, I. R. Green, I. Ahmed, G. Abbas, N. U. Rehman, *RSC Adv.* **2014**, *4*, 12882–12917.

[78] T. Katsuki, K. B. Sharpless, *J. Am. Chem. Soc.* **1980**, *102*, 5974–5976.

[79] T. Sawano, H. Yamamoto, *Eur. J. Org. Chem.* **2020**, *2020*, 2369–2378.

[80] Y. Gao, J. M. Klunder, R. M. Hanson, H. Masamune, S. Y. Ko, K. B. Sharpless, *J. Am. Chem. Soc.* **1987**, *109*, 5765–5780.

[81] W. Zhang, J. L. Loebach, S. R. Wilson, E. N. Jacobsen, *J. Am. Chem. Soc.* **1990**, *112*, 2801–2803.

[82] K. Srinivasan, P. Michaud, J. K. Kochi, *J. Am. Chem. Soc.* **1986**, *108*, 2309–2320.

[83] E. N. Jacobsen, W. Zhang, A. R. Muci, J. R. Ecker, L. Deng, *J. Am. Chem. Soc.* **1991**, *113*, 7063–7064.

[84] R. Irie, Y. Ito, T. Katsuki, *Synlett* **1991**, *1991*, 265–266.

[85] L. Deng, E. N. Jacobsen, *J. Org. Chem.* **1992**, *57*, 4320–4323.

[86] Z.-X. Wang, Y. Tu, M. Frohn, J.-R. Zhang, Y. Shi, *J. Am. Chem. Soc.* **1997**, *119*, 11224–11235.

[87] G. Pappenberger, H.-P. Hohmann, *Adv. Biochem. Eng./Biotechnol.* **2014**, *143*, 143–188.

[88] J. C. Chao, D. T. Huibers, US 4322569A, **1982**.

[89] L. F. Moreno, *J. Chem. Educ.* **2012**, *89*, 175–176.

[90] M. Hanif, A. F. Zahoor, M. J. Saif, U. Nazeer, K. G. Ali, B. Parveen, A. Mansha, A. R. Chaudhry, A. Irfan, *RSC Adv.* **2024**, *14*, 13100–13128.

[91] E. Bartmann, *Angew. Chem. Int. Ed.* **1986**, *25*, 653–654.

[92] T. Cohen, I. H. Jeong, B. Mudryk, M. Bhupathy, M. M. A. Awad, *J. Org. Chem.* **1990**, *55*, 1528–1536.

[93] T. V. RajanBabu, W. A. Nugent, M. S. Beattie, *J. Am. Chem. Soc.* **1990**, *112*, 6408–6409.

[94] H. C. Brown, B. C. S. Rao, *J. Am. Chem. Soc.* **1956**, *78*, 5694–5695.

[95] J. Guo, P. Teo, *Dalton Trans.* **2014**, *43*, 6952–6964.

[96] A. Gansäuer, A. Barchuk, F. Keller, M. Schmitt, S. Grimme, M. Gerenkamp, C. Mück-Lichtenfeld, K. Daasbjerg, H. Svith, *J. Am. Chem. Soc.* **2007**, *129*, 1359–1371.

[97] K. Daasbjerg, H. Svith, S. Grimme, M. Gerenkamp, C. Mück-Lichtenfeld, A. Gansäuer, A. Barchuk, F. Keller, *Angew. Chem. Int. Ed.* **2006**, *45*, 2041–2044.

[98] A. Gansäuer, D. von Laufenberg, C. Kube, T. Dahmen, A. Michelmann, M. Behlendorf, R. Sure, M. Seddiqzai, S. Grimme, D. V. Sadasivam, G. D. Fianu, R. A. Flowers, *Chem. Eur. J.* **2015**, *21*, 280–289.

[99] A. Gansäuer, M. Behlendorf, D. von Laufenberg, A. Fleckhaus, C. Kube, D. V. Sadasivam, R. A. Flowers, *Angew. Chem. Int. Ed.* **2012**, *51*, 4739–4742.

[100] A. Gansäuer, S. Narayan, *Adv. Synth. Catal.* **2002**, *344*, 465.

[101] A. Gansäuer, N. Ndene, T. Lauterbach, J. Justicia, I. Winkler, C. Mück-Lichtenfeld, S. Grimme, *Tetrahedron Lett.* **2008**, *64*, 11839–11845.

[102] J. L. Wolk, T. Hoz, H. Basch, S. Hoz, *J. Org. Chem.* **2001**, *66*, 915–918.

[103] A. J. Sterling, R. C. Smith, E. A. Anderson, F. Duarte, *J. Org. Chem.* **2024**, *89*, 9979–9989.

[104] C. Huynh, F. Derguini-Boumechal, G. Linstrumelle, *Tetrahedron Lett.* **1979**, *20*, 1503–1506.

[105] S. Searles, *J. Am. Chem. Soc.* **1951**, *73*, 124–125.

[106] R. N. Loy, E. N. Jacobsen, *J. Am. Chem. Soc.* **2009**, *131*, 2786–2787.

[107] J. A. Burkhard, G. Wuitschik, M. Rogers-Evans, K. Müller, E. M. Carreira, *Angew. Chem. Int. Ed.* **2010**, *49*, 9052–9067.

[108] G. Wuitschik, E. M. Carreira, B. Wagner, H. Fischer, I. Parrilla, F. Schuler, M. Rogers-Evans, K. Müller, *J. Med. Chem.* **2010**, *53*, 3227–3246.

[109] J. J. Rojas, J. A. Bull, *J. Med. Chem.* **2023**, *66*, 12697–12709.

[110] G. Wuitschik, M. Rogers-Evans, A. Buckl, M. Bernasconi, M. Märki, T. Godel, H. Fischer, B. Wagner, I. Parrilla, F. Schuler, J. Schneider, A. Alker, W. B. Schweizer, K. Müller, E. M. Carreira, *Angew. Chem. Int. Ed.* **2008**, *47*, 4512–4515.

[111] G. Wuitschik, M. Rogers-Evans, K. Müller, H. Fischer, B. Wagner, F. Schuler, L. Polonchuk, E. M. Carreira, *Angew. Chem. Int. Ed.* **2006**, *45*, 7736–7739.

[112] S.-R. Wang, C.-G. Yang, P. A. Sánchez-Murcia, J. P. Snyder, N. Yan, G. Sáez-Calvo, J. F. Díaz, F. Gago, W.-S. Fang, *Org. Lett.* **2015**, *17*, 6098–6101.

[113] P. Gabko, M. Kalník, M. Bella, *Beilstein J. Org. Chem.* **2025**, *21*, 1324–1373.

[114] S. Searles, R. G. Nickerson, W. K. Witsiepe, *J. Org. Chem.* **1959**, *24*, 1839–1844.

[115] A. Di Martino, C. Galli, P. Gargano, L. Mandolini, *J. Chem. Soc., Perkin Trans. 2* **1985**, 1345.

[116] M. Oelgemöller, N. Hoffmann, *Org. Biomol. Chem.* **2016**, *14*, 7392–7442.

[117] M. D'Auria, R. Racioppi, *Molecules* **2013**, *18*, 11384–11428.

[118] G. Büchi, C. G. Inman, E. S. Lipinsky, *J. Am. Chem. Soc.* **1954**, *76*, 4327–4331.

[119] K. Okuma, Y. Tanaka, S. Kaji, H. Ohta, *J. Org. Chem.* **1983**, *48*, 5133–5134.

[120] E. D. Butova, A. V. Barabash, A. A. Petrova, C. M. Kleiner, P. R. Schreiner, A. A. Fokin, *J. Org. Chem.* **2010**, *75*, 6229–6235.

[121] K. Soai, S. Niwa, T. Yamanoi, H. Hikima, M. Ishizaki, *J. Chem. Soc. Chem. Commun.* **1986**, 1018–1019.

[122] A. Gansäuer, A. Fleckhaus, M. A. Lafont, A. Okkel, K. Kotsis, A. Anoop, F. Neese, *J. Am. Chem. Soc.* **2009**, *131*, 16989–16999.

[123] A. Gansäuer, M. Otte, F. Piestert, C.-A. Fan, *Tetrahedron Lett.* **2009**, *65*, 4984–4991.

[124] J. A. M. Simoes, J. L. Beauchamp, *Chem. Rev.* **1990**, *90*, 629–688.

[125] A. Gansäuer, L. Shi, M. Otte, I. Huth, A. Rosales, I. Sancho-Sanz, N. M. Padial, J. E. Oltra, *Top. Curr. Chem.* **2012**, *320*, 93–120.

[126] M. T. Reding, S. L. Buchwald, *J. Org. Chem.* **1995**, *60*, 7884–7890.

[127] J. Yun, S. L. Buchwald, *J. Am. Chem. Soc.* **1999**, *121*, 5640–5644.

[128] N. E. Lee, S. L. Buchwald, *J. Am. Chem. Soc.* **1994**, *116*, 5985–5986.

[129] R. Walsh, *Acc. Chem. Res.* **1981**, *14*, 246–252.

[130] M. D. Allendorf, C. F. Melius, P. Ho, M. R. Zachariah, *J. Phys. Chem.* **1995**, *99*, 15285–15293.

[131] A. Gansäuer, M. Klatte, G. M. Brändle, J. Friedrich, *Angew. Chem. Int. Ed.* **2012**, *51*, 8891–8894.

[132] D. S. G. Henriques, K. Zimmer, S. Klare, A. Meyer, E. Rojo-Wiechel, M. Bauer, R. Sure, S. Grimme, O. Schiemann, R. A. Flowers, A. Gansäuer, *Angew. Chem. Int. Ed.* **2016**, *55*, 7671–7675.

[133] J. H. Schacht, S. Wu, S. Klare, S. Höthker, N. Schmickler, A. Gansäuer, *ChemCatChem* **2022**, *14*.

[134] K. Hans Wedepohl, *Geochim. Cosmochim. Acta* **1995**, *59*, 1217–1232.

[135] K. Senapati, *Synlett* **2005**, *2005*, 1960–1961.

[136] J. Pesti, G. L. Larson, *Org. Process Res. Dev.* **2016**, *20*, 1164–1181.

[137] N. Gürler, S. Paşa, H. Temel, *J. Taiwan Inst. Chem. Eng.* **2021**, *123*, 261–271.

[138] M. H. BinSabt, F. A. Azeez, N. Suleiman, *ACS Omega* **2023**, *8*, 12886–12898.

[139] Z. Lin, *Coord. Chem. Rev.* **2007**, *251*, 2280–2291.

[140] R. Waterman, *Organometallics* **2013**, *32*, 7249–7263.

[141] P. L. Watson, *J. Am. Chem. Soc.* **1983**, *105*, 6491–6493.

[142] T. D. Tilley, *Acc. Chem. Res.* **1993**, *26*, 22–29.

[143] T. Ziegler, E. Folga, A. Berces, *J. Am. Chem. Soc.* **1993**, *115*, 636–646.

[144] G. S. Hammond, *J. Am. Chem. Soc.* **1955**, *77*, 334–338.

[145] R. P. Bell, *Proc. R. Soc. A* **1936**, *154*, 414–429.

[146] M. G. Evans, M. Polanyi, *Trans. Faraday Soc.* **1936**, *32*, 1333.

[147] M. G. Evans, M. Polanyi, *Trans. Faraday Soc.* **1938**, *34*, 11.

[148] S. Höthker, R. Mika, H. Goli, A. Gansäuer, *Chem. Eur. J.* **2023**, *29*, e202301031.

[149] H. A. Martin, F. Jellinek, *Angew. Chem. Int. Ed.* **1964**, *3*, 311.

[150] H. A. Martin, F. Jellinek, *J. Organomet. Chem.* **1966**, *6*, 293–296.

[151] H. A. Martin, F. Jellinek, *J. Organomet. Chem.* **1967**, *8*, 115–128.

[152] E. Klei, J. H. Teuben, H. J. de Liefde Meijer, E. J. Kwak, A. P. Bruins, *J. Organomet. Chem.* **1982**, *224*, 327–339.

[153] D. S. G. Henriques, E. Rojo-Wiechel, S. Klare, R. Mika, S. Höthker, J. H. Schacht, N. Schmickler, A. Gansäuer, *Angew. Chem. Int. Ed.* **2022**, *61*, e202114198.

[154] W. J. Teo, X. Yang, Y. Y. Poon, S. Ge, *Nat. Commun.* **2020**, *11*, 5193.

[155] C. Matt, C. Kern, J. Streuff, *ACS Catal.* **2020**, *10*, 6409–6413.

[156] J. Weweler, S. L. Younas, J. Streuff, *Angew. Chem. Int. Ed.* **2019**, *58*, 17700–17703.

[157] B. G. Das, A. Chirila, M. Tromp, J. N. H. Reek, B. de Bruin, *J. Am. Chem. Soc.* **2016**, *138*, 8968–8975.

[158] J. Chen, S. Wang, J. Zhang, H. Ying, H. Zheng, X. Dong, J. Che, X. Chen, G. Cheng, *ChemistrySelect* **2020**, *5*, 10924–10927.

[159] T. Pirali, M. Serafini, S. Cargnin, A. A. Genazzani, *J. Med. Chem.* **2019**, *62*, 5276–5297.

[160] M. Dean, V. W. Sung, *Drug Des. Dev. Ther.* **2018**, *12*, 313–319.

[161] Z. Zhang, W. Tang, *Acta Pharm. Sin. B* **2018**, *8*, 721–732.

[162] S. Höthker, *Dissertation*, Rheinische Friedrich-Wilhelms-Universität, Bonn, **2024**.

[163] X. Liu, L. Longwitz, B. Spiegelberg, J. Tönjes, T. Beweries, T. Werner, *ACS Catal.* **2020**, *10*, 13659–13667.

[164] J. Meinwald, S. S. Labana, M. S. Chadha, *J. Am. Chem. Soc.* **1963**, *85*, 582–585.

[165] Z. Wang in *Comprehensive Organic Name Reactions and Reagents*, Wiley, Hoboken, NJ, **2009**, 1880–1882.

[166] N. M. Hein, Y. Seo, S. J. Lee, M. R. Gagné, *Green Chem.* **2019**, *21*, 2662–2669.

[167] F. Zhou, L. Zhu, B.-W. Pan, Y. Shi, Y.-L. Liu, J. Zhou, *Chem. Sci.* **2020**, *11*, 9341–9365.

[168] B. E. Maryanoff, A. B. Reitz, *Chem. Rev.* **1989**, *89*, 863–927.

[169] H. C. Kolb, M. S. VanNieuwenhze, K. B. Sharpless, *Chem. Rev.* **1994**, *94*, 2483–2547.

[170] U. Nookaraju, E. Begari, P. Kumar, *Org. Biomol. Chem.* **2014**, *12*, 5973–5980.

[171] B. D. Brandes, E. N. Jacobsen, *J. Org. Chem.* **1994**, *59*, 4378–4380.

[172] P. Fristrup, B. B. Dideriksen, D. Tanner, P.-O. Norrby, *J. Am. Chem. Soc.* **2005**, *127*, 13672–13679.

[173] R. D. Bach, J. L. Andres, A. L. Owensby, H. B. Schlegel, J. J. W. McDouall, *J. Am. Chem. Soc.* **1992**, *114*, 7207–7217.

[174] S. Mio, Y. Kumagawa, S. Sugai, *Tetrahedron Lett.* **1991**, *47*, 2133–2144.

[175] W. P. Griffith, S. V. Ley, G. P. Whitcombe, A. D. White, *J. Chem. Soc. Chem. Commun.* **1987**, 1625.

[176] T. J. Michnick, D. S. Matteson, *Synlett* **1991**, *1991*, 631–632.

[177] S. Höthker, H. Goli, S. Klare, T. Krebs, J. H. Schacht, A. Gansäuer, *Chem. Eur. J.* **2024**, *30*, e202402694.

[178] S. Klare, *Dissertation*, Rheinische Friedrich-Wilhelms-Universität, Bonn, **2019**.

[179] T.-L. Ho, *Chem. Rev.* **1975**, *75*, 1–20.

[180] A. C. Cope, *J. Am. Chem. Soc.* **1935**, *57*, 2238–2240.

[181] R. Fischer, H. Görls, P. R. Meisinger, R. Suxdorf, M. Westerhausen, *Chem. Eur. J.* **2019**, *25*, 12830–12841.

[182] W. Schlenk, W. Schlenk, *Ber. Dtsch. Chem. Ges. A/B* **1929**, *62*, 920–924.

[183] T. Krebs, *Dissertation*, Rheinische Friedrich-Wilhelms-Universität, Bonn, **2022**.

[184] Y.-H. Cheng, X. Zhao, K.-S. Song, L. Liu, Q.-X. Guo, *J. Org. Chem.* **2002**, *67*, 6638–6645.

[185] I. Haiduc, H. Gilman, *J. Organomet. Chem.* **1968**, *13*, 257–258.

[186] A. Gansäuer, P. Karbaum, D. Schmauch, M. Einig, L. Shi, A. Anoop, F. Neese, *Chem. Asian J.* **2014**, *9*, 2289–2294.

[187] R. Mika, *Dissertation*, Rheinische Friedrich-Wilhelms-Universität, Bonn, **2024**.

[188] D. Myers, *Surfactant Science and Technology,* 3. Ed., John Wiley & Sons, Hoboken, NJ, **2006**.

[189] C. Ade-Browne, M. Mirzamani, A. Dawn, S. Qian, R. G. Thompson, R. W. Glenn, H. Kumari, *Colloids Surf. A* **2020**, *595*, 124704.

[190] K. Noweck, W. Grafahrend in *Ullmann's Encyclopedia of Industrial Chemistry* (Editor M. Bohnet, F. Ullmann), Wiley-VCH, Weinheim, **2003**, 117–141.

[191] A. N. Thadani, R. A. Batey, *Org. Lett.* **2002**, *4*, 3827–3830.

[192] P. H. Dussault, T. K. Trullinger, F. Noor-e-Ain, *Org. Lett.* **2002**, *4*, 4591–4593.

[193] H. Goli, U. Kilic, S. Grimme, Z.-W. Qu, A. Gansäuer, *ACS Catal.* **2026**, *16*, 2628–2635.

[194] *TURBOMOLE* V7.4, a development of University of Karlsruhe and Forschungszentrum Karlsruhe GmbH, 1989-2007, TURBOMOLE GmbH, **2019,** available at http://www.turbomole.com, (accessed: 2025).

[195] J. Tao, J. P. Perdew, V. N. Staroverov, G. E. Scuseria, *Phys. Rev. Lett.* **2003**, *91*, 146401.

[196] F. Weigend, R. Ahlrichs, *Phys. Chem. Chem. Phys.* **2005**, *7*, 3297–3305.

[197] S. Grimme, J. Antony, S. Ehrlich, H. Krieg, *J. Chem. Phys.* **2010**, *132*, 154104.

[198] S. Grimme, S. Ehrlich, L. Goerigk, *J. Comput. Chem.* **2011**, *32*, 1456–1465.

[199] A. Klamt, G. Schüürmann, *J. Chem. Soc., Perkin Trans. 2* **1993**, 799–805.

[200] F. Eckert, A. Klamt, *AIChE J.* **2002**, *48*, 369–385.

[201] F. Weigend, *Phys. Chem. Chem. Phys.* **2006**, *8*, 1057–1065.

[202] S. Grimme, *Chem. Eur. J.* **2012**, *18*, 9955–9964.

[203] Y. Zhao, D. G. Truhlar, *J. Phys. Chem. A* **2005**, *109*, 5656–5667.

[204] L. Goerigk, A. Hansen, C. Bauer, S. Ehrlich, A. Najibi, S. Grimme, *Phys. Chem. Chem. Phys.* **2017**, *19*, 32184–32215.

[205] F. Eckert, A. Klamt, *COSMOtherm* Version C3.0, Release 16.01, COSMOlogic GmbH & Co. KG, Leverkusen, Germany, **2015**.

[206] N. Takekoshi, K. Miyashita, N. Shoji, S. Okamoto, *Adv. Synth. Catal.* **2013**, *355*, 2151–2157.

[207] G. Licini, M. Mba, C. Zonta, *Dalton Trans.* **2009**, 5265–5277.

[208] G. R. Fulmer, A. J. M. Miller, N. H. Sherden, H. E. Gottlieb, A. Nudelman, B. M. Stoltz, J. E. Bercaw, K. I. Goldberg, *Organometallics* **2010**, *29*, 2176–2179.

[209] J. A. Dale, D. L. Dull, H. S. Mosher, *J. Org. Chem.* **1969**, *34*, 2543–2549.

[210] B. E. Love, E. G. Jones, *J. Org. Chem.* **1999**, *64*, 3755–3756.

[211] R. A. Howie, G. P. McQuillan, D. W. Thompson, G. A. Lock, *J. Org. Chem.* **1986**, *303*, 213–220.

[212] J. Zhao, B. Cheng, C. Chen, Z. Lu, *Org. Lett.* **2020**, *22*, 837–841.

[213] L. Balas, J. Bertrand-Michel, F. Viars, J. Faugere, C. Lefort, S. Caspar-Bauguil, D. Langin, T. Durand, *Org. Biomol. Chem.* **2016**, *14*, 9012–9020.

[214] P. Villo, L. Toom, E. Eriste, L. Vares, *Eur. J. Org. Chem.* **2013**, *2013*, 6886–6899.

[215] D. Limnios, C. G. Kokotos, *J. Org. Chem.* **2014**, *79*, 4270–4276.

[216] K. Bojaryn, S. Fritsch, C. Hirschhäuser, *Org. Lett.* **2019**, *21*, 2218–2222.

[217] A. G. Dalling, T. Yamauchi, N. G. McCreanor, L. Cox, J. F. Bower, *Angew. Chem. Int. Ed.* **2019**, *58*, 221–225.

[218] T. Nakagiri, M. Murai, K. Takai, *Org. Lett.* **2015**, *17*, 3346–3349.

[219] E. Molnár, E. Barbu, C.-F. Lien, D. C. Górecki, J. Tsibouklis, *Biomacromolecules* **2010**, *11*, 2880–2889.

[220] M. D. Nikalje, M. Sasikumar, M. Muthukrishnan, *Tetrahedron Asymmetry* **2010**, *21*, 2825–2829.

[221] D. Yang, Y.-C. Yip, G.-S. Jiao, M.-K. Wong, *J. Org. Chem.* **1998**, *63*, 8952–8956.

[222] D. F. Taber, P. Guo, *J. Org. Chem.* **2008**, *73*, 9479–9481.

[223] J. R. Vyvyan, J. A. Meyer, K. D. Meyer, *J. Org. Chem.* **2003**, *68*, 9144–9147.

[224] D. Méndez-Sánchez, J. Mangas-Sánchez, E. Busto, V. Gotor, V. Gotor-Fernández, *Adv. Synth. Catal.* **2016**, *358*, 122–131.

[225] Z. Li, M. K. Gupta, T. S. Snowden, *Eur. J. Org. Chem.* **2015**, *2015*, 7009–7019.

[226] T. Osako, K. Torii, S. Hirata, Y. Uozumi, *ACS Catal.* **2017**, *7*, 7371–7377.

[227] Z. Jiao, K. W. Chee, J. S. Zhou, *J. Am. Chem. Soc.* **2016**, *138*, 16240–16243.

[228] T. Toyao, S. M. A. H. Siddiki, A. S. Touchy, W. Onodera, K. Kon, Y. Morita, T. Kamachi, K. Yoshizawa, K.-I. Shimizu, *Chem. Eur. J.* **2017**, *23*, 1001–1006.

[229] J. A. Gurak, K. M. Engle, *ACS Catal.* **2018**, *8*, 8987–8992.

[230] K. Miura, M. Tomita, Y. Yamada, A. Hosomi, *J. Org. Chem.* **2007**, *72*, 787–792.

[231] J. A. Murphy, F. Schoenebeck, N. J. Findlay, D. W. Thomson, S. Zhou, J. Garnier, *J. Am. Chem. Soc.* **2009**, *131*, 6475–6479.

[232] H. Lebel, C. Ladjel, *J. Org. Chem.* **2005**, *690*, 5198–5205.

[233] N. Soga, T. Yoshiki, A. Sato, T. Kawamoto, I. Ryu, H. Matsubara, *Tetrahedron Lett.* **2021**, *69*, 152977.

[234] M. Petermichl, C. Steinert, R. Schobert, *Synthesis* **2019**, *51*, 730–738.

[235] M. A. Márquez-Cadena, J. Ren, W. Ye, P. Qian, R. Tong, *Org. Lett.* **2019**, *21*, 9704–9708.

[236] M. G. Mura, L. de Luca, G. Giacomelli, A. Porcheddu, *Adv. Synth. Catal.* **2012**, *354*, 3180–3186.

[237] W. Liu, T. Leischner, W. Li, K. Junge, M. Beller, *Angew. Chem. Int. Ed.* **2020**, *59*, 11321–11324.

[238] X.-B. Yan, C.-L. Li, W.-J. Jin, P. Guo, X.-Z. Shu, *Chem. Sci.* **2018**, *9*, 4529–4534.

[239] I. Dokli, M. Gredičak, *Eur. J. Org. Chem.* **2015**, *2015*, 2727–2732.

[240] T. P. Blaisdell, T. C. Caya, L. Zhang, A. Sanz-Marco, J. P. Morken, *J. Am. Chem. Soc.* **2014**, *136*, 9264–9267.

7. Abstract

Titanocene-Catalyzed Hydrosilylation of Cyclic Ethers to Stereochemically Enriched *Anti-Markovnikov* Alcohols and Fatty Alcohols

Keywords: Catalysis ● Radicals ● Epoxides ● Oxetanes ● Hydrosilylation

In this thesis, titanocene-catalyzed hydrosilylations are investigated as tools towards pharmaceutically relevant motifs. First, this work establishes a straightforward approach to stereochemically enriched *anti-Markovnikov* alcohols from a diastereomeric mixture of trisubstituted olefins *via* enantioselective epoxidation followed by the diastereoconverging Ti-catalyzed hydrosilylation. Central to this strategy is the use of a suitable enantioselective epoxidation method. In this context, the *Shi*-epoxidation fulfilled all requirements. It controls the absolute configuration of the less-substituted stereocenter regardless of the olefin's geometry. Moreover, it transforms both olefin isomers into their respective epoxides with high enantioselectivity. The subsequent titanocene-catalyzed hydrosilylation erases the stereochemical information at the higher-substituted carbon and establishes a new relative configuration with respect to the less-substituted stereocenter, resulting in a single stereoisomer of the desired *anti-Markovnikov* alcohol.

Second, this work focuses on optimizing the regioselectivity for the titanocene-catalyzed hydrosilylation of monosubstituted alkyl epoxides. The relatively slow radical opening of these substrates by $Cp_2Ti(III)H$ allows the hydricity of the active species to promote a competing nucleophilic pathway, yielding unwanted *Markovnikov* alcohols. To suppress this nucleophilic mechanism, the hydricity of the active species is reduced by modifying the cyclopentadienyl ligands of titanocene dichloride with strongly *Lewis*-acidic silyl groups, which intramolecularly coordinate to the titanium-bound hydride. By additionally using 1,4-dioxane as a cosolvent to precipitate *Lewis*-acidic Mg salts, the regioselectivity of epoxide opening is improved from a regioisomeric ratio of 63:37 to 93:7.

Finally, in this work, the titanocene-catalyzed hydrosilylation was applied to oxetanes. In contrast to the previous approach using $Cp_2Ti(III)Cl$ as the active species and an external HAT reagent, the hydrosilylation system efficiently reduces oxetanes towards the *anti-Markovnikov* alcohols without the formation of an elimination side product. The *β*-hydride elimination is avoided due to the fast intramolecular HAT step. Moreover, the higher stability of oxetanes suppresses the competing nucleophilic side reaction observed for the opening of monosubstituted epoxides. Therefore, no elaborate catalyst design is necessary to achieve high regioselectivity in the opening of monosubstituted alkyl oxetanes. The regioselectivity (*r.r.* 99:1) is even higher compared to the corresponding optimized epoxide opening reaction (*r.r.* 93:7) due to the stronger contact of the catalyst's ligands with the substrate in the transition state of oxetane opening.